

# FINAL REPORT

Leptospirosis in Endangered Island Foxes and California Sea Lions: Outbreak Prediction and Prevention in a Changing World

SERDP Project RC-2635

SEPTEMBER 2021

James Lloyd-Smith  
Katherine Prager  
University of California, Los Angeles

*Distribution Statement A*

*This document has been cleared for public release*



This report was prepared under contract to the Department of Defense Strategic Environmental Research and Development Program (SERDP). The publication of this report does not indicate endorsement by the Department of Defense, nor should the contents be construed as reflecting the official policy or position of the Department of Defense. Reference herein to any specific commercial product, process, or service by trade name, trademark, manufacturer, or otherwise, does not necessarily constitute or imply its endorsement, recommendation, or favoring by the Department of Defense.

**REPORT DOCUMENTATION PAGE**

Form Approved  
OMB No. 0704-0188

The public reporting burden for this collection of information is estimated to average 1 hour per response, including the time for reviewing instructions, searching existing data sources, gathering and maintaining the data needed, and completing and reviewing the collection of information. Send comments regarding this burden estimate or any other aspect of this collection of information, including suggestions for reducing the burden, to Department of Defense, Washington Headquarters Services, Directorate for Information Operations and Reports (0704-0188), 1215 Jefferson Davis Highway, Suite 1204, Arlington, VA 22202-4302. Respondents should be aware that notwithstanding any other provision of law, no person shall be subject to any penalty for failing to comply with a collection of information if it does not display a currently valid OMB control number.  
**PLEASE DO NOT RETURN YOUR FORM TO THE ABOVE ADDRESS.**

<b>1. REPORT DATE (DD-MM-YYYY)</b> 27/09/2021		<b>2. REPORT TYPE</b> SERDP Final Report		<b>3. DATES COVERED (From - To)</b> 9/30/2016 - 9/30/2021	
<b>4. TITLE AND SUBTITLE</b> Leptospirosis in Endangered Island Foxes and California Sea Lions: Outbreak Prediction and Prevention in a Changing World				<b>5a. CONTRACT NUMBER</b> 16-C-0047	
				<b>5b. GRANT NUMBER</b>	
				<b>5c. PROGRAM ELEMENT NUMBER</b>	
<b>6. AUTHOR(S)</b> James Lloyd-Smith Katherine Prager				<b>5d. PROJECT NUMBER</b> RC-2635	
				<b>5e. TASK NUMBER</b>	
				<b>5f. WORK UNIT NUMBER</b>	
<b>7. PERFORMING ORGANIZATION NAME(S) AND ADDRESS(ES)</b> University of California, Los Angeles 610 Charles E. Young Dr. South Box 723905 Los Angeles, CA 90095-7239				<b>8. PERFORMING ORGANIZATION REPORT NUMBER</b> RC-2635	
<b>9. SPONSORING/MONITORING AGENCY NAME(S) AND ADDRESS(ES)</b> Strategic Environmental Research and Development Program (SERDP) 4800 Mark Center Drive, Suite 16F16 Alexandria, VA 22350-3605				<b>10. SPONSOR/MONITOR'S ACRONYM(S)</b> SERDP	
				<b>11. SPONSOR/MONITOR'S REPORT NUMBER(S)</b> RC-2635	
<b>12. DISTRIBUTION/AVAILABILITY STATEMENT</b> DISTRIBUTION STATEMENT A. Approved for public release: distribution unlimited.					
<b>13. SUPPLEMENTARY NOTES</b>					
<b>14. ABSTRACT</b> Leptospirosis, the disease caused by pathogenic bacteria of the genus <i>Leptospira</i> , is a major health burden for humans and animals worldwide and a recognized risk for military personnel. <i>Leptospira</i> has circulated for decades in California sea lions (CSL: <i>Zalophus californianus</i> ), and an outbreak of a near-identical strain was recently discovered in endangered island foxes ( <i>Urocyon littoralis</i> ) on Santa Rosa Island (SRI), California. This raised concerns about risks to island fox subspecies on three nearby Department of Defense islands. This project studied the ecology of <i>Leptospira</i> in these two species of concern, and built models to analyze how non-stationary conditions affect disease incidence and impacts. Our objectives were: (1) to identify the source of the current <i>Leptospira</i> outbreak on SRI, (2) to understand the drivers of <i>Leptospira</i> dynamics in CSL and build a model to make short- and long-term predictions, and (3) to study the ecology of <i>Leptospira</i> in island foxes and build a model to project its future impacts on SRI and assess management strategies under changing conditions.					
<b>15. SUBJECT TERMS</b> Antibody titer kinetics, biosecurity, California Channel Islands, California sea lion ( <i>Zalophus californianus</i> ), capture-mark-resight analysis, climate change, cross-reactivity, cross-ecosystem transmission, cross-species transmission, demographic reconstruction, disease ecology, El Niño Southern Oscillation, endangered species management, epidemic, epizootic, extrinsic drivers, fadeout, force of infection, host susceptibility, infectious disease dynamics, intrinsic drivers, island fox ( <i>Urocyon littoralis</i> ), island spotted skunk ( <i>Spilogale gracilis</i> ), <i>Leptospira interrogans</i> serovar Pomona, leptospirosis, marine heatwave, marine infectious disease, movement ecology, oceanographic anomalies, outbreak prediction, pathogen outbreak, pathogen control strategies, phylogenetics, population ecology, quantitative serology, radiotelemetry, reintroduction programs, Santa Rosa Island fox, semiparametric models, seroprevalence, spatial models, survival analysis, susceptible reconstruction, transmission dynamics, transmission modeling, whole genome sequencing, zoonosis					
<b>16. SECURITY CLASSIFICATION OF:</b>			<b>17. LIMITATION OF ABSTRACT</b> UNCLASS	<b>18. NUMBER OF PAGES</b> 300	<b>19a. NAME OF RESPONSIBLE PERSON</b> James Lloyd-Smith
<b>a. REPORT</b> UNCLASS	<b>b. ABSTRACT</b> UNCLASS	<b>c. THIS PAGE</b> UNCLASS			<b>19b. TELEPHONE NUMBER (Include area code)</b> 310-206-8207

# Table of Contents

List of Tables .....	ix
List of Figures .....	xii
List of Acronyms .....	xviii
Keywords .....	xx
Acknowledgements.....	xxi
1. Abstract.....	1
2. Executive Summary .....	2
Introduction.....	2
Objectives .....	3
Technical Approach.....	4
Results and Discussion .....	5
Origins of the leptospirosis outbreak on Santa Rosa Island.....	5
<i>Leptospira</i> now circulates endemically in SRI foxes, with fluctuations driven by precipitation.....	7
Risks to other subspecies of island fox .....	7
<i>Leptospira</i> in CSL: decades of endemicity, fadeout, and re-emergence.....	8
Non-stationarities in intrinsic and extrinsic drivers govern <i>Leptospira</i> dynamics in CSL .....	9
Implications for Future Research and Benefits.....	10
3. Objectives .....	12
4. Background.....	14
<i>Leptospira</i> and leptospirosis .....	14
Ecology of <i>Leptospira</i> .....	14
Biological samples and diagnostic assays.....	15
Classification and strain typing, .....	15
The island fox ( <i>Urocyon littoralis</i> ).....	16
Ecology of island foxes .....	16
California sea lions (CSL) .....	18
Ecology of CSL.....	18
Leptospirosis in CSL.....	20
<i>Leptospira</i> in Santa Rosa Island foxes.....	21
Conservation concerns on SRI.....	23
Concerns on other islands .....	24
5. Materials and Methods.....	25
5.1. Origins of the Santa Rosa Island Outbreak.....	25

5.1.1. Reconstruction of the fox outbreak up to 2010 .....	25
Laboratory analysis .....	25
Serology .....	25
Polymerase chain reaction (PCR) .....	26
Immunohistochemistry (IHC) .....	26
Bacterial culture .....	27
Bacterial strain typing and sequencing.....	27
Sample collection and population monitoring: island foxes and spotted skunks.....	27
Timeline of island fox population on Santa Rosa Island .....	27
Island foxes in captivity, 2000-2009 .....	28
Wild island foxes: telemetry and mortality collection .....	29
Island foxes and spotted skunks: trapping and sampling .....	30
Additional sample collection.....	32
Retrospective samples: feral pigs, 1987 .....	32
Retrospective samples: island foxes, 1988.....	32
Other terrestrial mammals: deer mice, 2012-2015 .....	32
Other terrestrial mammals: mule deer, 2012-2013.....	33
Data analysis .....	33
Pedigree analysis of captive foxes .....	33
Survival analysis .....	33
Serological cross-reactivity profiles.....	33
5.1.2. Reconstructing the spatiotemporal origins of the SRI outbreak.....	35
Telemetry of reintroduced foxes .....	35
Trapping and sampling.....	35
Estimating the spatiotemporal origin of the outbreak .....	36
Interpolation of fox location data .....	37
5.1.3. Whole genome sequencing and phylogenetics.....	38
Whole genome sequencing.....	38
Genome assembly .....	38
Isolate selection .....	38
Multi-locus strain typing .....	38
Phylogenetic reconstruction of <i>L. interrogans</i> over time.....	38
5.2. <i>Leptospira</i> in California Sea Lions .....	39
5.2.1. Extend long-term time series of leptospirosis in stranded CSL .....	39
5.2.2. Extend long-term time series of CSL demography .....	40

5.2.3. Understand how intrinsic and extrinsic non-stationarities drive leptospirosis outbreaks in CSL.....	41
5.2.3.1. The endemic period.....	41
Leptospirosis data.....	41
Susceptible reconstruction.....	41
Analysis of sex and age classes associated with <i>Leptospira</i> transmission.....	42
Testing for indirect influence of the environment via demographic processes.....	42
Environmental covariates.....	43
Model fitting and model selection.....	44
Environment and body condition.....	45
Real-time prediction.....	46
Long-term prediction of climate change impacts.....	46
Software.....	47
5.2.3.2. Fadeout and re-emergence.....	47
5.3. Understanding the Santa Rosa Island outbreak.....	47
5.3.1. Long-term surveillance of the leptospirosis outbreak on Santa Rosa Island.....	47
Sample collection and population monitoring: island foxes and spotted skunks.....	47
Trap set-up.....	47
Fox sample and data collection.....	48
Skunk sample and data collection.....	52
Sample processing in the field.....	52
Sample analysis.....	54
Microscopic agglutination test (MAT).....	54
Polymerase chain reaction (PCR).....	54
Bacterial culture.....	54
Immunohistochemistry (IHC).....	54
Calculation of seroprevalence and prevalence.....	54
5.3.2. Analyze data to understand the ecology of leptospirosis in island foxes.....	55
5.3.2.1. Longitudinal data.....	55
Fox sample and data collection.....	55
5.3.2.2. Modeling antibody kinetics to estimate time of infection.....	55
Data collection and sampling.....	57
Candidate models.....	58
Bayesian MCMC model fitting.....	59
Prior distribution of peak antibody time.....	60
Prior distribution of peak antibody level.....	60

Model fitting.....	60
Sensitivity analysis using simulated data .....	61
Software .....	62
5.3.2.3. Risk factors for infection.....	62
Study period and study cohort.....	62
Overview of survival analysis.....	62
Data Imputation.....	63
Counting process formulation.....	64
Candidate risk factors for infection with <i>Leptospira</i> .....	64
Imputation and Hazard modeling.....	65
Variable selection.....	65
5.3.2.4. Analysis of host species effects and laboratory effects on serological reactivity profiles .....	65
Study Animals and Sample Collection.....	66
Sample Analysis.....	66
Data Selection .....	67
5.3.3. Impacts of <i>Leptospira</i> on the demography of island foxes .....	67
Tracking mortality in radio-collared foxes.....	67
Demographic impacts: early phase (2004-2010) .....	68
Demographic impacts: later phase (2009-2020) .....	68
5.3.4. Transmission dynamics model for <i>Leptospira</i> in island foxes on SRI.....	70
Stochastic simulation model for <i>Leptospira</i> transmission .....	70
Dividing SRI into functional patches.....	72
Parameter estimation.....	73
Demographic parameters .....	73
Movement parameters.....	74
Infection parameters.....	75
Invasion, persistence, and monitoring.....	75
5.3.5. Transmission dynamics model for <i>Leptospira</i> in island foxes on San Clemente Island .....	76
5.3.6. Determine when infected CSL are found on the islands, during and after a major outbreak .....	76
5.3.7. Investigation of the declining fox population on San Nicolas Island.....	79
Serology .....	79
Cross-reactivity analysis .....	79
Mortality data.....	79
Comparison of seroprevalance data with mortality data.....	80

Necropsy report analysis .....	80
6. Results and Discussion .....	81
6.1. Origins of the Santa Rosa Island Outbreak .....	81
6.1.1. Reconstruction of the fox outbreak up to 2010 .....	81
Exposure to <i>Leptospira</i> was widespread on Santa Rosa Island in the 1980s .....	81
The founders of the captive fox population were positive for <i>Leptospira</i> exposure .....	83
<i>Leptospira</i> did not persist in the captive population .....	86
The <i>Leptospira</i> outbreak expanded rapidly in the reintroduced fox population .....	88
<i>Leptospira</i> strains from before and after the captive period appear the same .....	92
The pathogen may have persisted on Santa Rosa Island in island spotted skunks while foxes were absent .....	96
6.1.2. Reconstructing the spatiotemporal origins of the SRI outbreak .....	99
Spatial reconstruction .....	99
6.1.3. Whole genome sequencing and phylogenetics .....	100
Data summary .....	100
Multi-locus strain typing (MLST) .....	100
Phylogenetic reconstruction .....	101
6.2. <i>Leptospira</i> in California Sea Lions .....	104
6.2.1. Extend long-term time series of leptospirosis in stranded California sea lions .....	104
Interannual variation and cyclic outbreaks .....	104
Spontaneous fadeout of <i>Leptospira</i> circulation in the CSL population .....	104
6.2.2. Extend long-term time series of CSL demography .....	108
6.2.3. Understand how intrinsic and extrinsic non-stationarities drive leptospirosis outbreaks in CSL .....	113
6.2.3.1. The endemic period .....	113
Intrinsic and extrinsic drivers of disease dynamics .....	113
Population immunity is a key driver of outbreak intensity .....	114
Environmental conditions further modulate outbreak intensity .....	117
Putative mechanisms of environmental influence on leptospirosis outbreaks .....	121
Real-time prediction of leptospirosis outbreaks .....	123
Long-term prediction of climate change impacts on outbreak .....	125
Environmental drivers modulate the natural immunity-driven cycling of <i>Leptospira</i> .....	128
6.2.3.2. Fadeout and re-emergence .....	130
<i>Leptospira</i> re-emergence .....	131
6.3. Understanding the Santa Rosa Island outbreak .....	134
6.3.1. Long-term surveillance of the leptospirosis outbreak on Santa Rosa Island .....	134
The island fox population on SRI has continued to grow .....	135

<i>Leptospira</i> seroprevalence and prevalence in island foxes over time.....	135
Spatial-temporal distribution of <i>Leptospira</i> exposure and infection in foxes.....	139
<i>Leptospira</i> seroprevalence and prevalence in island spotted skunks over time.....	141
6.3.2. Analyze data to understand the ecology of leptospirosis in island foxes.....	145
6.3.2.1. Longitudinal samples .....	145
Analysis of longitudinal serology from individual foxes.....	145
Analysis of longitudinal shedding patterns from island foxes.....	147
6.3.2.2. Modeling antibody kinetics to estimate time of infection.....	150
Model fits .....	150
Posterior estimates.....	151
Correlates of model performance .....	152
Simulation results .....	155
Broader implications .....	155
6.3.2.3. Risk factors for infection.....	158
Univariate models .....	158
Multivariate model .....	159
Time-to-seroconversion curves .....	162
Implications for risk analysis .....	164
6.3.2.4. Analysis of host species effects and laboratory effects on serological reactivity profiles .....	165
Highest MAT titer does not reliably indicate the infecting serovar .....	165
Absolute magnitudes of MAT titers vary among host species.....	166
Both absolute and relative titer magnitudes can vary among certified laboratories ...	168
Implications for <i>Leptospira</i> ecology and epidemiology .....	169
6.3.3. Impacts of <i>Leptospira</i> on the demography of island foxes .....	170
Early mortalities associated with leptospirosis .....	170
Preliminary results on demographic impacts - later phase (2009-2020).....	176
6.3.4. Transmission dynamics model for <i>Leptospira</i> in island foxes on SRI.....	176
Demographic parameters .....	176
Movement parameters.....	177
Infection parameters.....	180
Model transmission parameters.....	182
Invasion, persistence, and monitoring.....	183
6.3.5. Transmission dynamics model for <i>Leptospira</i> in island foxes on San Clemente Island .....	185
6.3.6. Determine when infected CSL are found on the islands, during and after a major outbreak .....	187

6.3.7. Analysis of San Nicolas Island.....	189
Serology results show evidence of low but rising exposure to <i>Leptospira</i> .....	189
MAT reactivity patterns do not match those seen on Santa Rosa Island.....	190
Exploring the association between mortalities and <i>Leptospira</i> exposure .....	192
Spatiotemporal analysis.....	193
Individual-level data on serology before death.....	195
Necropsy Report Analysis.....	196
Comparison to earlier serosurveys on San Nicolas Island and other Channel Islands ....	197
Interpretation of MAT reactivity profile in SNI foxes.....	197
7. Conclusions and Implications for Future Research/Implementation.....	199
Conclusions and Major Findings .....	200
Objective 1 .....	200
Objective 2 .....	201
Objective 3 .....	203
Implications for future research/implementation.....	206
Management implications: Santa Rosa Island .....	206
Management implications: other Channel Islands .....	208
Management implications: CSL population.....	210
Summary .....	212
8. Literature Cited .....	214
9. Appendices.....	246
Appendix A. Supporting Data.....	246
Supporting data for 5.1.2. and 6.1.2.....	246
Supporting data for 5.1.3. and 6.1.3.....	246
Supporting data for 5.3.2.4. and 6.3.2.4.....	249
Supporting data for 5.3.4. and 6.3.4.....	249
Appendix B. List of Scientific/Technical Publications.....	250
Appendix C. Other Supporting Material.....	257
Supplementary information for 5.2.3.1. and 6.2.3.1. ....	257
Environment and body condition .....	257
Environment and sea lion movement .....	257
Supplementary information for 5.3.1 and 6.3.1 .....	259
Supplementary information for 5.3.2.2 and 6.3.2.2 .....	262
Prior distribution of peak antibody level.....	262
Simulations and sensitivity analysis.....	263
Correlations between peak antibody level and covariates .....	269

Peak antibody levels of serovars Pomona and Autumnalis.....	270
Predictors of model performance .....	270
JAGS code.....	272
Supplementary information for 5.3.2.4. and 6.3.2.4 .....	274
Supplementary information for 5.3.4. and 6.3.4. ....	275

## List of Tables

Table 4.1. Summary of results from each aim that would support different hypotheses about outbreak source. ....	23
Table 5.1.1.1. Captive fox population size (N), the number of individual foxes with test results, and the total number of serum samples analyzed in captivity. ....	29
Table 5.1.1.2. Total number of actively-collared foxes during each season (fox-year). ....	30
Table 5.1.1.3. Trapping data and sample collection for island foxes. ....	31
Table 5.1.1.4. Trapping data for island spotted skunks. ....	32
Table 5.1.1.5. Samples collected from island spotted skunks. ....	32
Table 5.3.1.1. Trapping data for Channel Island foxes, including the number of total captures and unique individual wild foxes captured from 2003 to 2020. ....	50
Table 5.3.1.2. Samples from wild Channel Island foxes. ....	51
Table 5.3.1.3. Trapping data for island spotted skunks, 2004-2020. ....	53
Table 5.3.1.4. Samples from island spotted skunks, 2010-2019. ....	53
Table 5.3.2.1. Number of individual foxes with longitudinal data on exposure (MAT) and infection (PCR) status. ....	55
Table 5.3.2.2. Example of a counting process formulation for a single individual's risk time. ....	64
Table 6.1.1.1. MAT titer values from 1987 Santa Rosa Island pig samples. ....	81
Table 6.1.1.2. Serology results from 1988 island foxes. ....	83
Table 6.1.1.3. MAT titer values from 1988 Santa Rosa Island fox samples. ....	83
Table 6.1.1.4. Seroprevalence of reintroduced Channel Island foxes by age class, 2004-2010. ....	89
Table 6.1.1.5. PCR and IHC results for deer mouse kidney samples. ....	96
Table 6.1.1.6. PCR, IHC, and MAT results for deer samples. ....	97
Table 6.1.3.1. Frequency of <i>Leptospira interrogans</i> serovar Pomona isolates by host species and sampling year. ....	101
Table 6.1.3.2. Posterior median estimates of genetic and temporal parameters. ....	103
Table 6.2.1.1. Number of California sea lions stranded 2015-2020 and diagnostic tests performed. ....	107
Table 6.2.2.1. California sea lion pups branded and resighting events of all age classes, 2015-2018. ....	111

Table 6.2.2.2. Number of male and female pups weighed in October and February each year, 2015-2018. ....	112
Table 6.2.2.3. Proportion of the yearling population on San Miguel Island in July of each year by sex, 2015-2018. ....	113
Table 6.2.3.1. Cross-validation and full dataset statistics for models including susceptibles only. ....	117
Table 6.2.3.2. Models and model fit statistics for the top 5 models and the susceptibles-only model. ....	121
Table 6.2.3.3. Importance of the candidate variables (within the top 20 models). ....	122
Table 6.3.1.1. Seroprevalence of anti- <i>Leptospira</i> antibodies in SRI island foxes over time. ....	137
Table 6.3.1.2. Prevalence of infection with <i>Leptospira</i> in SRI island foxes over time. ....	138
Table 6.3.1.3. Prevalence of infection with <i>Leptospira</i> in island spotted skunks over time. ....	143
Table 6.3.1.4. Seroprevalence of anti- <i>Leptospira</i> antibodies in island spotted skunks for samples tested at CDC, 2010-2019. ....	143
Table 6.3.2.1. Distribution of the number of MAT tests per fox of the island foxes that ever tested seropositive. ....	145
Table 6.3.2.2. Distribution of the time interval between first positive test and last MAT test, for individual foxes that were tested multiple times. ....	145
Table 6.3.2.3. Model performance on individual peak antibody time. ....	155
Table 6.3.2.4. Potential factors affecting <i>Leptospira</i> infection risk in 1226 foxes between 2004 and 2019. ....	158
Table 6.3.2.5. Median Akaike information criterion (AIC) for multivariate Cox proportional hazards models across 100 bootstrap runs. ....	160
Table 6.3.2.6. Estimates of median hazard ratios of multivariable Cox proportional hazards model with imputed times of seroconversion. ....	161
Table 6.3.2.7. Median survival times (days) given sex, 24-month cumulative precipitation, and fox abundance. The median survival time is the time corresponding to a 50% probability of seroconverting. ....	163
Table 6.3.2.8. Probability of seroconverting when stratified by sex, fox abundance, and 24-month precipitation after 1 and 2 years at risk. ....	164
Table 6.3.3.1. Fates of foxes released from captivity between 2003-2006. ....	171
Table 6.3.3.2. Table of released and wild born radio collared foxes and of all wild fox mortalities. ....	174

Table 6.3.4.1. DIC values for demographic models. ....	177
Table 6.3.4.2. Probabilities of <i>Leptospira</i> persistence and invasion under different scenarios..	184
Table 6.3.6.1. Shedding and seroprevalence data from free-ranging CSL.....	188
Table 6.3.7.1. Seroprevalence of foxes on San Nicolas island by age class, 2010-2015. ....	190
Table 6.3.7.2. Negative binomial regression results for the analysis of the relationship between fox mortality and seroprevalence, 4-segment model. ....	194
Table 6.3.7.3. Negative binomial regression results for the analysis of the relationship between fox mortality and seroprevalence, 3-segment model. ....	195
Table 6.3.7.4. MAT results for 13 SNI foxes with known mortality between 2010 and 2015...	196
Table 6.3.7.5. Frequency of kidney abnormalities in SNI foxes, by decade of mortality. ....	197
Table A.1. Sequenced genomes from four host species in the Coastal California Ecosystem...	247
Table A.2. Multi-locus strain typing (MLST) results. ....	248
Table A.3. ANOVA statistics for the linear regression of environmental variables vs. number of strands (normalized by dividing by population size of the corresponding demographic groups) in the TMMC range. ....	259
Table A.4. Prevalence of infection with <i>Leptospira</i> in SRI island foxes over time, showing results from the CSU protocol. ....	260
Table A.5. Seroprevalence of anti- <i>Leptospira</i> antibodies in island spotted skunks, comparing results from CDC and ADHC. ....	261
Table A.6. Hyperpriors for the different parameters. ....	263
Table A.7. Model performance on individual seroconversion time .....	269
Table A.8. Statistics for the correlations between outcome variable ‘% peak antibody interval reduction’ and candidate variables.....	271
Table A.9. AIC values for linear regression models including single and multiple variables fitted to outcome variable ‘% peak antibody interval reduction’.....	271
Table A.10. The number of samples chosen per serovar Pomona titer level at Lab A for inter-lab titer comparison. ....	275

## List of Figures

Figure E.1. California sea lion abundance and leptospirosis dynamics as of 2014.....	3
Figure E.2. Summary of island fox population growth and leptospirosis outbreak, on Santa Rosa Island as of 2014.....	3
Figure E.3. Host species presence on Santa Rosa Island and <i>Leptospira</i> test results.....	5
Figure E.4. Spatiotemporal reconstruction of the origin of the outbreak. ....	6
Figure E.5. Fox infection prevalence and seroprevalence over time.....	7
Figure E.6. Simulation of time delay to first detection of an infected fox, for different disease scenarios and sampling designs. ....	8
Figure E.7. Stranding and seroprevalence time series. ....	9
Figure E.8. Fadeout of <i>Leptospira</i> from CSL was associated with simultaneous anomalies in susceptible supply and migratory behavior.....	10
Figure 4.1. Focal species in the project: Island fox ( <i>Urocyon littoralis</i> ), <i>Leptospira interrogans</i> , and California sea lions ( <i>Zalophus californianus</i> ).....	15
Figure 4.2. The California Channel Islands and the stranding response range of The Marine Mammal Center (TMMC).....	16
Figure 4.3. Captive breeding enclosures for island foxes on SRI.....	17
Figure 4.4. NPS biologists released island foxes into the wild on SRI. ....	18
Figure 4.5. CSL sharing a beach with northern elephant seal ( <i>Mirounga angustirostris</i> ) and Northern fur seals ( <i>Callorhinus ursinus</i> ). ....	19
Figure 4.6. Malnourished CSL pups in rehabilitation at TMMC in 2014. ....	20
Figure 4.7. California sea lion abundance and leptospirosis dynamics as of 2014. ....	21
Figure 4.8. Number of CSL stranding per month due to leptospirosis (pink shaded; 2010-14) and semi-annual seroprevalence in stranded CSL (pink line; 2010-13).....	21
Figure 4.9. Summary of island fox population growth and leptospirosis outbreak on Santa Rosa Island as of 2014. ....	22
Figure 5.1.1.1. Timeline of events on Santa Rosa Island, and population trajectories of captive and wild foxes until 2010.      28	
Figure 5.1.1.2. Map of the 18 ladder grids on Santa Rosa Island. ....	31
Figure 5.1.2.1. Spatial polygons converted from telemetry data. ....	36
Figure 5.1.2.2. Foxes with time of infection estimates and location data between 2004 and 2006. ....	37

Figure 5.2.1.1. Map of California sea lion sampling locations.....	39
Figure 5.2.3.1. Map of the US West Coast, the occurrence range of CSL, and buoy locations...	44
Figure 5.3.1.1. Island fox in a Tomahawk trap.....	48
Figure 5.3.1.2. Collecting blood and urine samples from island foxes. ....	49
Figure 5.3.2.1. Schematic of antibody kinetic model and the use of informative data.....	58
Figure 5.3.2.2. Schematic of censored data types in the context of the fox system. ....	63
Figure 5.3.3.1. Decision tree to establish island fox infection status from capture and testing data. .....	69
Figure 5.3.4.1. Schematic of <i>Leptospira</i> transmission model for SRI.....	70
Figure 5.3.4.2. Santa Rosa Island divided into 15 functional patches.....	72
Figure 5.3.6.1. Anesthetizing CSL in the field. ....	78
Figure 5.3.6.2. Collecting urine from an anesthetized CSL by catheterization. ....	79
Figure 5.3.7.1. Spatial subdivision of San Nicolas Island. ....	80
Figure 6.1.1.1. Santa Rosa Island species and testing timeline. ....	82
Figure 6.1.1.2. Individual timelines of locations, sample collections, and test results for all 15 foxes taken from the wild into captivity, 2000-2004.....	85
Figure 6.1.1.3. Pedigree of captive fox population with disease state, birth status, and sex for each individual. ....	87
Figure 6.1.1.4. Seroprevalence of reintroduced Channel Island foxes by age group, 2004-2010.	88
Figure 6.1.1.5. Maps of MAT serology results for adult island foxes on Santa Rosa Island, 2004- 2010.....	89
Figure 6.1.1.6. Individual timelines of locations, sample collections, and test results for all foxes released from captivity or born into the wild between 2003-2007. ....	91
Figure 6.1.1.7. Estimated times of infection for the first infected foxes in the outbreak. ....	92
Figure 6.1.1.8. MAT cross-reactivity profile for island foxes sampled during the outbreak, between 2006 and 2013 Island foxes. ....	94
Figure 6.1.1.9. MAT cross-reactivity profile for 1988 Channel Island foxes. ....	94
Figure 6.1.1.10. MAT cross-reactivity profile for Channel Island foxes taken into captivity in 2000 and 2001.....	95
Figure 6.1.1.11. MAT cross-reactivity profile for 1987 feral pigs on Santa Rosa Island.....	95
Figure 6.1.1.12. Locations of the deer mouse kidney samples. ....	97
Figure 6.1.1.13. Maps of MAT serology results for adult island skunks on Santa Rosa Island, 2010-2012. ....	98
Figure 6.1.1.14. MAT cross-reactivity profile for island spotted skunks, sampled 2010-2012. ..	98
Figure 6.1.1.15. Maps of trapping locations for island spotted skunks, 2004-2010.....	99

Figure 6.1.2.1. Spatiotemporal probability of infection for seven foxes between 2004 and 2006. .....	100
Figure 6.1.3.1. Time-calibrated maximum clade credibility tree. ....	102
Figure 6.2.1.1. Stranding and seroprevalence time series.....	105
Figure 6.2.1.2. Stranding, antibody titer, and infection prevalence time-series. ....	106
Figure 6.2.2.1. Age- and sex-specific survival probabilities in California sea lions, 1976-2018. .....	109
Figure 6.2.2.2. Age- and sex-structured California sea lion population reconstruction. ....	110
Figure 6.2.3.1. Reconstructed number of sea lions susceptible to <i>Leptospira</i> , structured by age and sex. ....	115
Figure 6.2.3.2. Reconstructed proportion of susceptibles for a selection of demographic groups. .....	116
Figure 6.2.3.3. Predicted cases for the models including reconstructed susceptibles based on observed (light blue) vs. smoothed (dark blue) population data.....	118
Figure 6.2.3.4. Outbreak size can be predicted using a combination of intrinsic and extrinsic variables. ....	120
Figure 6.2.3.5. Real-time predictions of outbreak size. ....	124
Figure 6.2.3.6. Prediction of outbreak size using only data available prior to the start of the outbreak year being predicted. ....	125
Figure 6.2.3.7. Predicted cases for different climate change scenarios, effects of altered mean values. ....	126
Figure 6.2.3.8. Predicted cases for different climate change scenarios, effects of increased variation. ....	127
Figure 6.2.3.9. Predicted cases for different climate change scenarios, effects of altered means and increased variation. ....	127
Figure 6.2.3.10. Long-term predictions of outbreak size.....	128
Figure 6.2.3.11. The interplay between intrinsic and extrinsic drivers of transmission. ....	130
Figure 6.2.3.12. Depiction of hypothesized link between age- and sex-specific movement patterns and <i>Leptospira</i> transmission dynamics. ....	132
Figure 6.2.3.13. Fadeout and re-emergence of <i>Leptospira</i> in CSL were associated with simultaneous fluctuations in susceptible supply and migratory behavior. ....	133
Figure 6.2.3.14. Proportion of yearling California sea lions stranding above 36 degrees latitude. .....	134
Figure 6.3.1.1. Fox and skunk population trends on SRI. ....	135
Figure 6.3.1.2. Fox infection prevalence and seroprevalence over time. ....	136
Figure 6.3.1.3. Spatiotemporal patterns of seroprevalence in adult foxes. ....	139

Figure 6.3.1.4. Spatiotemporal patterns of seroprevalence in fox pups.....	140
Figure 6.3.1.5. Spatiotemporal patterns of infection prevalence in island foxes.....	141
Figure 6.3.1.6. Skunk infection prevalence and seroprevalence over time. ....	142
Figure 6.3.1.7. Spatiotemporal patterns of seroprevalence in island spotted skunks (CDC lab results for all years).....	144
Figure 6.3.2.1. Longitudinal patterns in MAT anti- <i>Leptospira</i> antibody titers from individual foxes.....	146
Figure 6.3.2.2. Titer levels over time for all foxes that ever exhibited boosting.....	147
Figure 6.3.2.3. Longitudinal patterns in PCR results from all individual wild foxes that ever tested positive for <i>Leptospira</i> DNA in urine.....	149
Figure 6.3.2.4. Observed duration of shedding of <i>Leptospira</i> by infected island foxes. ....	150
Figure 6.3.2.5. Models for antibody kinetics and fit to island fox data. ....	151
Figure 6.3.2.6. Estimated population-level distributions of peak antibody level (A) and decay rate (B), for serovars Pomona and Autumnalis.....	152
Figure 6.3.2.7. Posterior results for two individual foxes with low (A) and high (B) gain in information about peak antibody time .....	153
Figure 6.3.2.8. Posterior densities of peak antibody time.....	154
Figure 6.3.2.9. Distribution of hazard ratios estimated by univariate Cox proportional hazards model with imputed time of infection estimates.....	159
Figure 6.3.2.10. Distribution of hazard ratios estimated by multivariable Cox proportional hazards model with imputed time of infection estimates.....	161
Figure 6.3.2.11. Time-to-infection curves for low, medium, and high levels of fox abundance and 24-month cumulative precipitation when stratified by sex.....	163
Figure 6.3.2.12. Host-specific patterns of relative MAT antibody titers detected against five <i>Leptospira</i> serovars when the infecting serovar is <i>L. interrogans</i> serovar Pomona.....	166
Figure 6.3.2.13. Pairwise antibody titer levels against <i>Leptospira interrogans</i> serovars Pomona, Djasiman, Autumnalis, Bratislava, and Icterohaemorrhagiae in three host species. ....	167
Figure 6.3.2.14. Selected example of longitudinal antibody titer dynamics in a Channel Island fox. ....	168
Figure 6.3.2.15. Comparison of antibody titer results for fox serum samples evaluated at three testing labs. ....	169
Figure 6.3.3.1. Survival rate and causes of death of collared foxes by season.....	172
Figure 6.3.3.2. Individual timelines of released captive-born foxes or post-reintroduction wild-born foxes with kidney tissue tested via IHC or PCR. ....	175
Figure 6.3.4.1. Posterior estimates (means and 95% credible intervals) of demographic parameters through time. ....	177
Figure 6.3.4.2. Movement probability in different seasons.....	178

Figure 6.3.4.3. Movement distance frequency distribution in different seasons, for different time periods.....	179
Figure 6.3.4.4. Pairwise movement probability showing the relative proportion of movements from an origin patch to all other patches. ....	180
Figure 6.3.4.5. Antibody titer distributions for island foxes with PCR-negative and PCR-positive samples.....	181
Figure 6.3.4.6. Distribution of possible times since infection for PCR-negative (left) and PCR-positive (right) samples.....	182
Figure 6.3.4.7. Posterior estimates for transmission parameters fitted using Approximate Bayesian Computation.....	183
Figure 6.3.4.8. Timing of first detection of an infected fox, for different sampling regimes and simulation scenarios.....	185
Figure 6.3.5.1. Timing of first detection of an infected fox on San Clemente Island, for different sampling regimes and simulation scenarios.....	186
Figure 6.3.6.1. <i>Leptospira</i> exposure and infection prevalence in sea lions on San Miguel Island. ....	187
Figure 6.3.7.1. SNI Adult Fox Seroprevalence Maps.....	190
Figure 6.3.7.2. MAT cross-reactivity profile for SRI foxes sampled during the outbreak, between 2006 and 2013.....	191
Figure 6.3.7.3. MAT cross-reactivity profile for SNI foxes, 2010-2015.....	192
Figure 6.3.7.4. Natural mortalities of island foxes on SNI, 1989-2017.....	193
Figure 6.3.7.5. Maps of natural mortalities of island foxes on SNI, 2010-2015. ....	193
Figure 6.3.7.6. Analysis of relationship between fox mortality and seroprevalence, 4-segment model.....	194
Figure 6.3.7.7. Analysis of relationship between fox mortality and seroprevalence, 3-segment model.....	195
Figure 6.3.7.1. Summary of project goals, as included in our project proposal. ....	199
Figure A.1. Island fox infection prevalence on SRI, 2010-2019, comparing the two PCR protocols.....	259
Figure A.2. Skunk prevalence and seroprevalence over time, showing lab differences. ....	260
Figure A.3. Spatiotemporal patterns of seroprevalence in island spotted skunks (CDC results 2010-2015, ADHC results 2016-2019).....	261
Figure A.4. Antibody levels for a subset of individual foxes that tested negative relatively recently.....	262
Figure A.5. Posterior estimates of peak antibody level for different prior distributions. ....	264
Figure A.6. Effect of prior peak antibody level means.....	265

Figure A.7. Effect of prior peak antibody level standard deviations. ....	266
Figure A.8. Effect of prior peak antibody level standard deviations. ....	267
Figure A.9. Antibody decay curves for different decay rates. ....	268
Figure A.10. The number of days (window size) it takes for antibodies to decay from 8 to 6 log <sub>2</sub> dilution units, for a range of biologically realistic decay rates. ....	269
Figure A.11. Correlation between peak antibody levels for serovars Pomona and Autumnalis. ....	270
Figure A.12. Peak antibody interval reduction (heatmap colors) for key correlates decay rate, peak antibody interval size, and level of the first positive sample. ....	272
Figure A.13. Longitudinal antibody titer dynamics in Channel Island foxes. ....	274
Figure A.14. Differences in antibody titer magnitude for a subset (n=32) of samples that were run to endpoint for serovars Autumnalis and Pomona at all three labs ....	275

## List of Acronyms

AIC	Akaike Information Criterion
ANI	Año Nuevo Island
ANOVA	Analysis of Variance
ARS	Agricultural Research Service
BCE	Before Current Era
BMI	Body Mass Index
CDC	Centers for Disease Control and Prevention
CE	Current Era
CI	Confidence Interval
CSL	California Sea Lion
DF	Degrees of Freedom
DNA	Deoxyribonucleic Acid
DoD	Department of Defense
ENSO	El Niño Southern Oscillation
FM	Feature Matching
GPS	Global Positioning System
HKY	Hasegawa, Kishino, and Yano (substitution model)
IHC	Immunohistochemistry
IBDR	Infectious Bacterial Diseases Research Unit
LOOIC	Leave-One-Out Information Criterion
MAT	Microscopic Agglutination Test
MHC	Major Histocompatibility Complex
MML	Marine Mammal Laboratory
MMPA	Marine Mammal Protection Act
NADC	National Animal Disease Center
NES	Northern Elephant Seal
NMFS	National Marine Fisheries Service
NOAA	National Oceanic and Atmospheric Administration
NPS	National Park Service
NSF	National Science Foundation
PCR	Polymerase Chain Reaction
PFGE	Pulsed Field Gel Electrophoresis
PIT	Passive Integrated Transponder
RCSON	Resource Conservation Statement of Need
SCA	Santa Catalina Island, California
SCL	San Clemente Island, California
SCZ	Santa Cruz Island, California
SMI	San Miguel Island, California
SNI	San Nicolas Island, California
SNP	Single Nucleotide Polymorphism

SP	Seroprevalence
SRI	Santa Rosa Island, California
SST	Sea Surface Temperature
ST	Spring Transition
TMMC	The Marine Mammal Center
TMRCA	Time to Most Recent Common Ancestor
UCLA	University of California, Los Angeles
UCSC	University of California, Santa Cruz
US	United States
USDA	United States Department of Agriculture
VHF	Very High Frequency
VNTR	Variable Number of Tandem Repeats
WGS	Whole Genome Sequencing
WRCC	Western Regional Climate Center

## Keywords

Antibody titer kinetics, biosecurity, California Channel Islands, California sea lion (*Zalophus californianus*), capture-mark-resight analysis, climate change, cross-reactivity, cross-ecosystem transmission, cross-species transmission, demographic reconstruction, disease ecology, El Niño Southern Oscillation, endangered species management, epidemic, epizootic, extrinsic drivers, fadeout, force of infection, host susceptibility, infectious disease dynamics, intrinsic drivers, island fox (*Urocyon littoralis*), island spotted skunk (*Spilogale gracilis*), *Leptospira interrogans* serovar Pomona, leptospirosis, marine heatwave, marine infectious disease, movement ecology, oceanographic anomalies, outbreak prediction, pathogen outbreak, pathogen control strategies, phylogenetics, population ecology, quantitative serology, radiotelemetry, reintroduction programs, Santa Rosa Island fox, semiparametric models, seroprevalence, spatial models, survival analysis, susceptible reconstruction, transmission dynamics, transmission modeling, whole genome sequencing, zoonosis

## Acknowledgements

The research reported here was funded by the Strategic Environmental Research and Development Program (SERDP). Our long-term research program on *Leptospira* in the California coastal ecosystem has also benefited from support from the National Science Foundation, the NOAA John H. Prescott Marine Mammal Rescue Assistance Grant Program, the Hellman Family Foundation, and the UCLA Grand Challenges program.

We thank all members of the UCLA, NOAA/NMFS/Alaska Fisheries Science Center Marine Mammal Laboratory (MML), and USDA ARS Infectious Bacterial Diseases Research Unit teams who were involved in carrying out the work proposed in this grant. We thank UCLA team members Angela Guglielmino who led the field work and empirical analyses of the island fox and spotted skunk data; Riley Mumma who led analyses of *Leptospira* whole genome sequences, fox movement trajectories and risk factors for infection; Benny Borremans who led the work on serologic cross-reactivity, and the modeling analyses of intrinsic and extrinsic drivers, antibody titer kinetics, and *Leptospira* transmission dynamics on SRI; and Caitlin Cox who modeled *Leptospira* invasion scenarios on San Clemente Island. Ana Gomez and Sarah Helman have provided valuable contributions to other components of our group's work on *Leptospira* ecology and modeling, and other members of the Lloyd-Smith lab have provided helpful feedback and suggestions. Also at UCLA, David Haake has provided expert advice on *Leptospira* microbiology, and Sorel FitzGibbon provided early advice on bioinformatics pipelines for analyzing *Leptospira* sequences. We thank MML team members Robert DeLong, Sharon Melin, Tony Orr, Jeff Laake, and Jeff Harris for their work on sea lion demography and movement patterns and for their assistance in the field during California sea lion capture and sampling efforts. We thank USDA team members David Alt, Rick Hornsby and Jarlath Nally for their work on obtaining *Leptospira* isolates from bacterial cultures sent to them, sequencing *Leptospira* isolates and for general advice regarding *Leptospira* epidemiology and microbiology.

We thank the staff and volunteers with the National Parks Service for their tremendous efforts obtaining samples from both the island foxes and the spotted skunks. We also thank them for obtaining and sharing detailed data on fox movement and locations. In particular we would like to thank Tim Coonan, who oversaw SRI fox sampling for many years and who shared data and samples from SRI and contributed his expertise on fox ecology and conservation.

We thank the veterinarians, veterinary technicians, researchers and volunteers with The Marine Mammal Center in Sausalito, California for their hard work collecting, archiving and managing data and samples from stranded California sea lions, and for their assistance in the capture and sampling of California sea lions in the wild. In particular we would like to thank and acknowledge Drs. Frances Gulland, Shawn Johnson, Cara Field, Denise Greig, and Padraig Duignan, as well as Carlos Rios and Sophie Guarasci.

We thank staff, researchers, and biologists with the Año Nuevo State Park for supporting our field efforts there. We also thank biologists and researchers from the University of California Santa Cruz (UCSC) as well as those associated with the UCSC Año Nuevo Reserve for their intellectual contributions regarding California sea lion biology, as well as their logistical support for fieldwork conducted on Año Nuevo Island. In particular we would like to thank Pat Morris, Guy Oliver, and Patrick Robinson for their tremendous contributions.

We thank the biologists, veterinarians, and staff with Oregon and Washington Departments of Fish and Wildlife, as well as Dr. Rebecca Greene for logistical support in field efforts in Oregon and Washington, and for contributing California sea lion samples for

analysis. In particular we thank Drs. Julia Burco, Sheanna Steingass, Bryan Wright and Robin Brown, as well as Mike Brown.

We would like to thank all of our laboratory collaborators. We thank Renee Galloway at the Centers for Disease Control and Prevention for her tremendous efforts in performing thousands of serum MAT analyses on our samples and for isolating *Leptospira* from our cultures. We thank David Wu at the Hollings Marine Laboratory, for performing PCR on our urine and kidney samples. We thank Colleen Duncan at Colorado State University for performing immunohistochemistry on kidney samples, and we thank Kristy Pabilonia for performing PCR on our urine and kidney samples. We also thank Niesa Kettler and her colleagues at the Michigan State University Veterinary Diagnostic Laboratory for providing us with *Leptospira* transport and culture media.

Many colleagues at other institutions have contributed samples, expertise, or advice. We thank Ben Gonzales and Lora Konde at the California Department of Fish and Wildlife for providing us with feral pig samples from SRI, and Robert Wayne at UCLA for sharing serum samples collected from island foxes on SRI in the 1980s. We thank Steven Jeffries and Dyanna Lambourn at Washington Department of Fish and Wildlife for sharing a *Leptospira* isolate from an elephant seal, collected with support of the John H. Prescott Marine Mammal Rescue Assistance Grant Program. We thank Deanna Clifford for providing raw data on island fox serology from her past study. We thank Patricia Gaffney for providing scrolls of archived formalin fixed and paraffin embedded island fox kidney tissues for PCR testing to detect *Leptospira* DNA. We thank UCSD scientists Michael Mattias and Joshua Lefler for their assistance in *Leptospira* whole genome sequence assembly and bioinformatic analyses. We thank Kim Pepin (USDA/APHIS) and Bryan Grenfell (Princeton University) for their collaboration on the sea lion/*Leptospira* outbreak drivers model. We thank Francesca Ferrara of the US Navy and biologists from the Institute for Wildlife Studies for sharing serum samples and data from San Nicolas Island foxes. We thank members of the Channel Island Fox Recovery Group and the Friends of the Island Fox for their tireless efforts to save this unique animal.

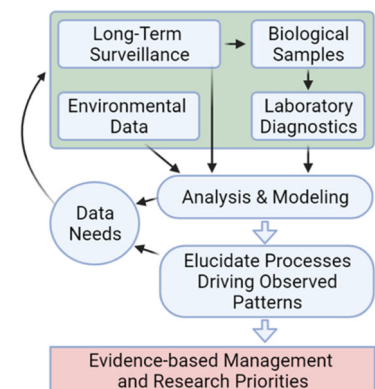
# 1. Abstract

**Introduction and Objectives:** Leptospirosis, the disease caused by pathogenic bacteria of the genus *Leptospira*, is a major health burden for humans and animals worldwide and a recognized risk for military personnel. *Leptospira* has circulated for decades in California sea lions (CSL: *Zalophus californianus*), and an outbreak of a near-identical strain was recently discovered in endangered island foxes (*Urocyon littoralis*) on Santa Rosa Island (SRI), California. This raised concerns about risks to island fox subspecies on three nearby Department of Defense islands. This project studied the ecology of *Leptospira* in these two species of concern, and built models to analyze how non-stationary conditions affect disease incidence and impacts. Our objectives were: (1) to identify the source of the current *Leptospira* outbreak on SRI, (2) to understand the drivers of *Leptospira* dynamics in CSL and build a model to make short- and long-term predictions, and (3) to study the ecology of *Leptospira* in island foxes and build a model to project its future impacts on SRI and assess management strategies under changing conditions.

**Technical Approach:** With our partners, we extended long-term studies of host demography and *Leptospira* spread in both CSL and island foxes. We conducted laboratory analyses on newly collected and archived samples to detect current infections and prior exposure to *Leptospira*. We conducted whole genome sequencing of *Leptospira* isolates from marine and terrestrial hosts and analyzed the sequences to understand transmission routes in the coastal ecosystem. We developed mechanistic and statistical models to reveal underlying processes, project trends under changing conditions, and assess management strategies.

**Results:** The source of the outbreak in reintroduced SRI foxes was spillover from another terrestrial host species on the island, almost certainly island spotted skunks. After an initial epidemic wave in 2006-2007, *Leptospira* has now established endemic circulation in SRI foxes. Our data-driven transmission model projects pathogen persistence under all foreseeable scenarios. Fortunately, the demographic impacts of the disease are moderate, and the fox population has continued to grow. Our models also indicate that island fox populations on other islands are vulnerable to invasion by *Leptospira*, and predict similar impacts. In the CSL system, we analyzed 30 years of annual leptospirosis outbreaks to show that outbreak intensity is driven by the combined effects of susceptible supply and fluctuations in oceanographic conditions. A model capturing these effects could explain 50% of interannual variability and could make real-time predictions of upcoming outbreak intensity. The model also projected that stronger environmental fluctuations under climate change would cause more extreme peaks and troughs in *Leptospira* activity. This prediction was borne out by the spontaneous fadeout of *Leptospira* from 2013-2017 during a marine heatwave, followed by the largest outbreak on record in 2018.

**Benefits:** Our project generated new knowledge and tools to support management of two wildlife species of concern in the California coastal ecosystem. By extending long-term field studies and analyzing the data with mathematical and statistical models to reveal underlying processes, we generated evidence-based guidance for managers and set priorities for future research. Data-driven modeling tools for both systems can be adapted to address future needs of species managers. New insights into *Leptospira* ecology will advance conservation and public health goals, and long-term time series data are priceless assets to study on-going global change.



## 2. Executive Summary

### Introduction

Leptospirosis, the disease caused by pathogenic bacteria of the genus *Leptospira*, is a major health burden for humans and animals worldwide. It causes over 500,000 severe cases annually in humans and has long been recognized as a major threat to US military personnel. Despite its global importance, the ecological dynamics of leptospirosis are understudied. Our study investigated the ecology of *Leptospira* in two wildlife species of concern in California; both species inhabit Department of Defense (DoD) lands, and both have experienced deadly outbreaks of leptospirosis in recent years. Beyond its direct implications for management of wildlife on DoD lands, our study has advanced understanding of *Leptospira* ecology and control in many systems worldwide, and yielded broader insights for population monitoring and species reintroduction programs.

The system includes the pathogen *Leptospira interrogans* serovar Pomona and two major host species: California sea lions (CSL) and island foxes. CSL are an abundant pinniped species that ranges along the western coast of North America. The United States stock of CSL breeds almost entirely on rookery sites on DoD-owned islands in the California Channel Island archipelago. The CSL population has been impacted by leptospirosis (the disease caused by pathogen *Leptospira*) since at least 1984. With collaborators, we have amassed a long-term time series of leptospirosis incidence (since 1983) and seroprevalence (since 1995) from wild CSL that strand on the California coast. Outbreaks occur each year, in the fall, and vary markedly in intensity; from 1984 to 2013, major outbreaks caused mass stranding and mortality every 3-5 years (Figure E.1). Concurrent long-term data on CSL demography, collected via population surveys dating back to the 1970s and a mark-resight program that has operated since 1987, show a pattern of consistent growth over the decades, with substantial perturbations associated with El Niño events and other oceanographic and climatic anomalies (Figure E.1). Together, these long-term datasets present a unique opportunity to study the interaction of disease dynamics and host population dynamics under non-stationary conditions.

Island foxes are an endemic species native to six of the California Channel Islands, with each island home to a unique subspecies. Four subspecies were listed as federally endangered in 2004 after suffering drastic declines in the late 1990s. After intensive population management, including captive breeding programs on SRI and two other islands, all populations are rebounding (and they were de-listed in 2016, after our project began). In fall 2010, evidence of *Leptospira* infection was found in two dead foxes on SRI. Our subsequent investigations revealed evidence of a large outbreak in the foxes (and to a lesser degree, in spotted skunks (*Spilogale gracilis*)). Analysis of banked fox sera from 2009-10 revealed high seroprevalences of anti-*Leptospira* antibodies among adult foxes across SRI, indicating a widespread outbreak (Figure E.2). Sampling of fox and skunk urine identified active infections in both species, with the infecting strain indistinguishable by VNTR genetic typing from *Leptospira* isolates derived from CSL over the period 1970-2010. When we proposed this project, there was no evidence that this strain of *Leptospira* was present on SRI before the fox population crashed, so CSL were the suspected source (possibly via carcass scavenging). Foxes on other islands so far appeared free of the pathogen, though as our proposal underwent final review, concerns arose about the fox population on San Nicolas Island (SNI), which underwent a mysterious decline from 2010-2015.

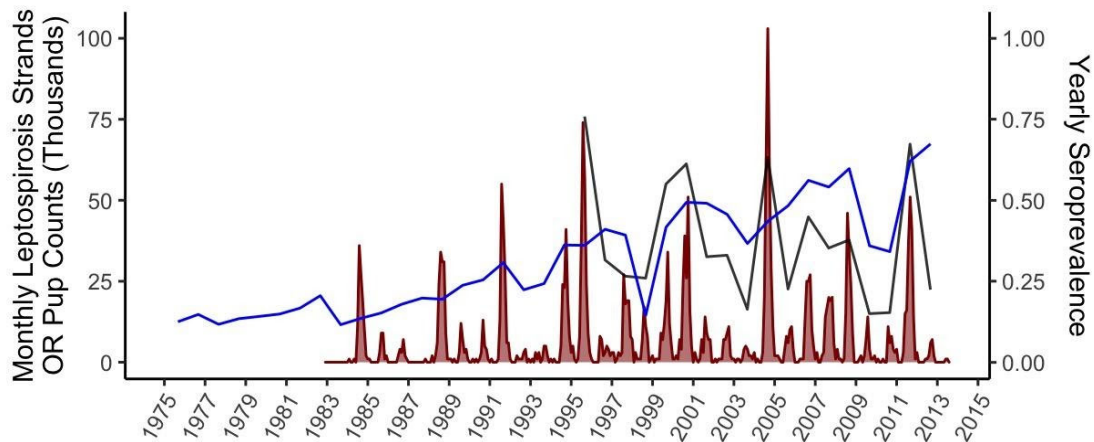


**Figure E.1. California sea lion abundance and leptospirosis dynamics as of 2014**, reflecting knowledge when our proposal was submitted. Number of CSL stranding at TMMC per month due to leptospirosis since 1983 (red filled curve). Seroprevalence of anti-*Leptospira* antibodies in stranded CSL (red line) tracks the patterns seen in the leptospirosis stranding record. The estimated number of CSL pups born each year (blue line) reflects a long-term population growth with sporadic recruitment failures tied to El Niño events and other oceanographic anomalies.

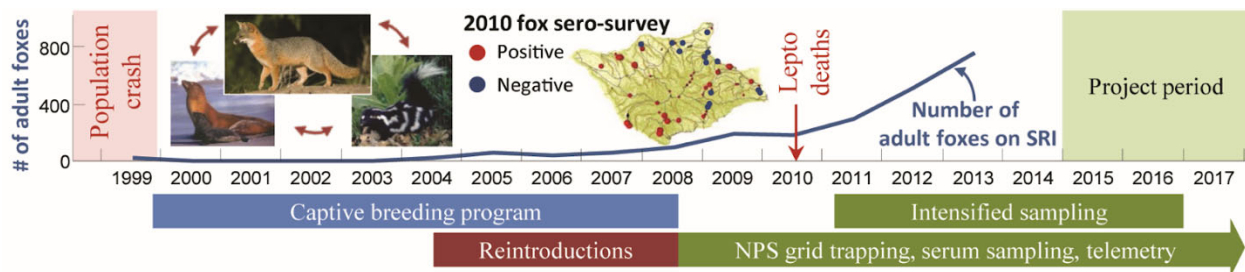


**Figure E.2. Summary of island fox population growth and leptospirosis outbreak, on Santa Rosa Island as of 2014.** This figure reflects our knowledge at the time our proposal was submitted. The growth of the SRI reintroduced wild fox population is shown in blue. The first detection of leptospirosis-affected animals in 2010 is shown by the red arrow, and the inset map shows results from an early survey for evidence of *Leptospira* exposure in foxes sampled in 2010. The inset photographs show the hypothesis, based on pathogen genetic data, that *Leptospira* was transmitting between island foxes, spotted skunks, and California sea lions.

## Objectives

Our project aimed to characterize the ecology of *Leptospira* in the California coastal ecosystem, and to provide evidence-based guidance for management of the pathogen in island fox and sea lion populations. Our work emphasized gathering long-term data sets and building models to characterize processes underlying disease spread, analyze how non-stationary conditions affect disease incidence and impact, and assess needs and future strategies for pathogen control and wildlife management. In addition to generating actionable knowledge on two federally protected species that frequent DoD lands, we aimed to learn general principles of disease transmission in marine and terrestrial systems which could inform species and habitat

management more broadly, improve public health, and reduce disease impacts on future species reintroduction programs.

Given what was known about the system at the outset of our work (summarized above), our study was designed to address three major objectives:

*Objective 1.* To identify the source of the current *Leptospira* outbreak in the endangered Santa Rosa Island fox.

*Objective 2.* To understand how non-stationary drivers shape *Leptospira* dynamics in the CSL population, and formulate a model capable of short-term outbreak prediction and long-term trend projection.

*Objective 3.* To characterize the ecology of *Leptospira* in island foxes, and develop a data-driven model to project impacts and assess prevention and control strategies under changing conditions.

## Technical Approach

Our project comprised an integrative program of field, laboratory, and modeling research. With our partners at the National Park Service, we extended sampling of serum and urine from island foxes and spotted skunks on SRI, via their annual trapping surveys on 18 grids across the island, plus additional target trapping. We also analyzed archived serum and necropsy tissue samples from wild and captive foxes, as well as data from telemetry and trapping studies. We conducted laboratory analyses on prospective and archived samples to detect current *Leptospira* infections (via PCR and culture, from urine or kidney, and IHC of kidney) and prior exposure (via serology) and to assess clinical status (via serum chemistry). Taken together, our efforts have yielded a 15-year record of the leptospirosis outbreak on SRI.

We have also extended long-term studies of CSL demography and *Leptospira* incidence. Our partners at the National Marine Fisheries Service's Marine Mammal Laboratory have continued their program to brand and re-sight sea lions, to extend their demographic study of CSL to 2019. We analyzed these data using capture-mark-resight models to estimate population size and age structure through time, and to estimate the spatial distribution of CSL across resighting sites. With our partners at The Marine Mammal Center we have extended our time series of leptospirosis incidence and seroprevalence in CSL that strand on the California coast, until 2019, using serum, urine, and kidney samples as described above, along with clinical records of CSL in rehabilitation after stranding. These efforts have extended long-term data sets of leptospirosis in CSL to 37 years, and CSL demography to 33 years.

To determine whether CSL carry *Leptospira* to the Channel Islands after big outbreaks, where spillover to foxes could occur, we sampled free-ranging sea lions at San Miguel Island. Combining these efforts with earlier work supported by other funders led to a 10-year time series of *Leptospira* surveillance in wild sea lions on the California coast. Finally, we sequenced the genomes of 49 isolates of *Leptospira* recovered from CSL, elephant seals, island foxes, and spotted skunks, and used phylogenetic tools to analyze these sequences to study transmission linkages in the California coastal ecosystem.

Throughout our project, we developed statistical and mathematical models to integrate lines of evidence, learn about exposure risks, and make projections of future disease impacts under changing conditions. Many modeling approaches were used in the study, including survival analysis, multistate mark-resight models, semiparametric models, and two stochastic spatial models of *Leptospira* transmission dynamics. We also developed novel quantitative methods, including a Bayesian model of antibody titer kinetics to estimate time of infection, and

a resampling-based method to reconstruct movement trajectories from telemetry data. These tools were applied first to learn about the determinants of past patterns, and then to project how disease incidence and impact may change under future non-stationarities.

## Results and Discussion

### *Origins of the leptospirosis outbreak on Santa Rosa Island*

Based on information available before this project, we hypothesized that the *Leptospira* strain causing the outbreak on SRI had been transmitted to island foxes from CSL between 2004 and 2008. Our investigations revealed a very different story. By analyzing archived samples, including some from as far back as the 1980s, we established that *Leptospira* was circulating in SRI foxes (as well as feral pigs then present on the island) before their population crash in the late 1990s (Figure E.3). The last surviving foxes taken into captivity in 2000-2001 had evidence of exposure in the wild, but transmission was halted in the captive population. Captive-born foxes were naïve to the pathogen when they were reintroduced to the wild, but they quickly became infected and some died. In hindsight, it is clear that population managers unknowingly released the captive-bred foxes into a ‘hot’ landscape where undetected *Leptospira* was circulating.

Foxes were functionally extinct from the island landscape for 4-5 years, so another host species must have maintained circulation of the pathogen. By testing archived samples, and collecting new samples where needed, we characterized the roles of other mammal species on the island (Figure E3). Feral swine were exposed in the 1980s, but eradicated from the island in the 1990s. The native deer mice and introduced mule deer (now eradicated) show almost zero signs of exposure. In contrast, we found that island spotted skunks were infected and shedding the same strain of *Leptospira*, and were abundant during the period that foxes were in captivity. Only one species, elk (now eradicated), had no samples available for analysis. These data suggest skunks as the likely source of exposure to the reintroduced fox population.

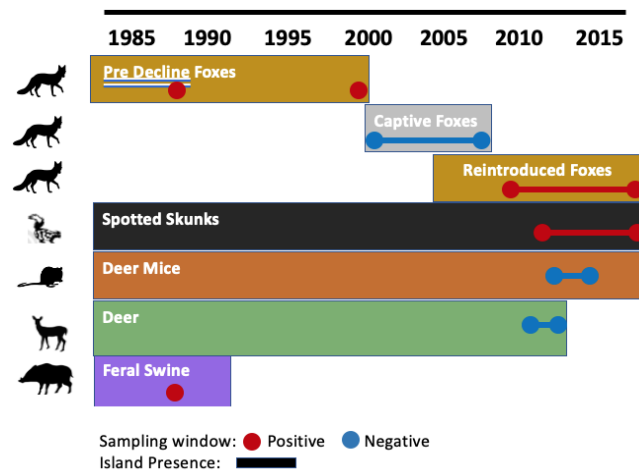


**Figure E.3. Host species presence on Santa Rosa Island and *Leptospira* test results.** Timeline of the presence of species on Santa Rosa Island in colored rectangles, with the sampling window for each species indicated by a dot for a single sampling period or a line for a sampling window. Blue sampling windows indicate negative test results and red indicates positive test results. Spotted skunks are the only species that was present on SRI from 2000-2005 (when foxes were absent from the landscape) that tested positive for *Leptospira*.

We analyzed banked samples and data from reintroduced foxes from 2004-2010 to reconstruct the early phase of the outbreak on SRI. By fall 2006, the first year with a substantial number of serum samples available, signs of exposure to *Leptospira* were present in the majority of adult foxes over most of the island’s area. We estimated the time of infection of the earliest

cases, using a model of serum antibody kinetics calibrated to our later data, pinpointing the first cases to a period in mid-late 2005. We reconstructed the movement trajectories of the early foxes by interpolating telemetry data, and intersected these with the times of infection to map the earliest cases to a region on the northern shore of the island (Figure E.4). These findings tentatively support multiple introductions of *Leptospira* into the fox population, with no signature of proximity to marine mammal haul-outs, lending further support to our conclusion that island skunks were the likely source.

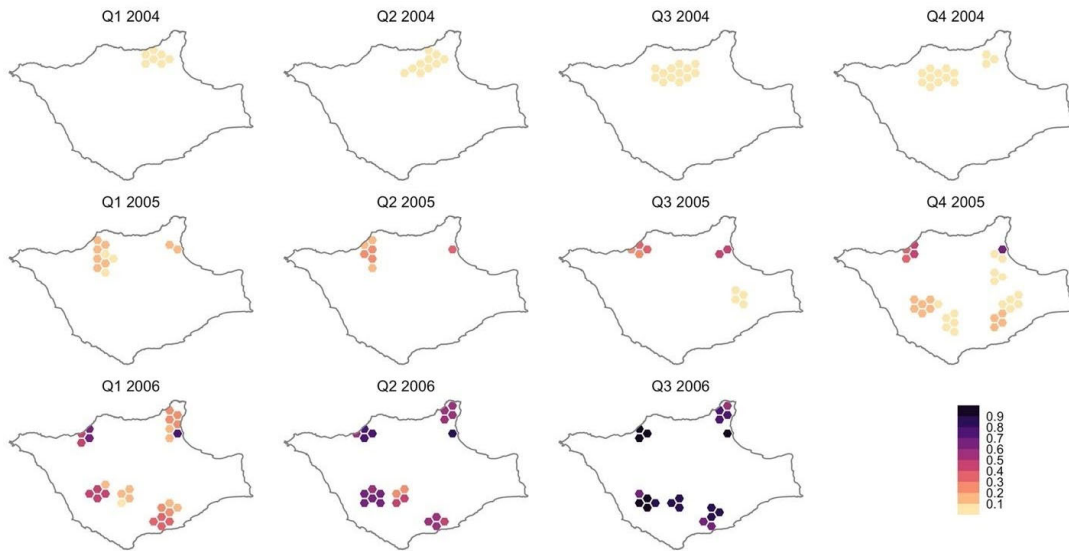


**Figure E.4. Spatiotemporal reconstruction of the origin of the outbreak.** Maps show the locations and cumulative probability of infection for the earliest known cases in the SRI outbreak. Colored grid cells represent the presence of foxes with a non-zero probability of having been infected by that time. The color scale represents the cumulative probability that an individual had been infected by the end of the quarter in question. The darker the color becomes, the higher the probability that an infected fox was present in that cell at that time.

Analysis of whole genome sequences of 49 *Leptospira* isolates taken from island foxes, spotted skunks, CSL, and elephant seals provides independent corroboration of these conclusions. The genome sequence data confirmed that the skunks were carrying the same strain as the foxes, and that the strains carried by sea lions had diverged from the SRI outbreak strain decades before. At the same time, genomic data indicate that *Leptospira* transmission can and does occur between the terrestrial and marine realms – indeed we found direct evidence in the form of a sea lion isolate that nests within the SRI outbreak clade – so spillover between island species and marine mammal species is a continuing possibility (although sea lion to island fox transmission remains a hypothetical risk). The deeper structure of the *Leptospira* phylogeny points to the existence of an as-yet-undiscovered reservoir of *Leptospira*, perhaps in a terrestrial host on the California coast, that has seeded multiple lineages in marine mammal and island communities.

### *Leptospira* now circulates endemically in SRI foxes, with fluctuations driven by precipitation

We extended surveillance of the leptospirosis outbreak on SRI from its origins in 2005 until 2019. The pathogen caused an initial wave of infection from 2006-2007, then settled into an endemic state with ~75% seroprevalence in adults for the last decade (Figure E.5). Since 2011 it has infected 4-27% of island fox pups each year, with similar percentages of foxes testing positive for active shedding, indicating an on-going (if fluctuating) hazard of infection on the island. Skunks have played a declining role in the outbreak since 2010, as their abundance has dropped sharply. Our analysis of risk factors for infection showed that cumulative precipitation over the past 24 months was associated with a marked rise in infection risk, putatively due to better survival (and hence better transmission) of *Leptospira* when the island has more water.

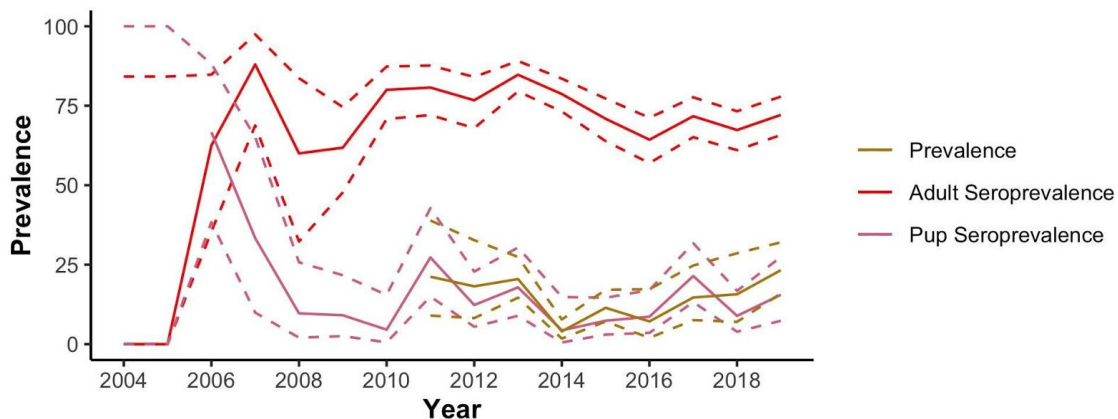


**Figure E.5. Fox infection prevalence and seroprevalence over time.** Adult fox seroprevalence (solid red) and fox pup seroprevalence (solid pink) are from MAT results, and combined pup and adult infection prevalence (solid brown) are from PCR and IHC results, with 95% confidence intervals (dashed lines).

From longitudinal sampling of wild foxes, we determined that island foxes can shed *Leptospira* for up to 3 years after infection, with many individuals shedding more than 1 year. Such chronic shedding plays a key role in enabling the pathogen to maintain an unbroken transmission chain in a small, isolated population like this. We constructed a stochastic, spatial, age-structured model of island fox transmission dynamics on SRI and found that *Leptospira* is predicted to persist on SRI for at least another decade under all foreseeable non-stationary conditions, including a sustained drought or a two-fold drop in island fox population size.

Fortunately, the island fox population on SRI has continued to grow despite the continuing circulation of *Leptospira*, indicating that the demographic impact of the disease is not too severe. By testing archived necropsy samples, we determined that a spike in ‘unknown-cause’ mortalities in 2006-2007 was associated with *Leptospira* infection, so the disease can kill island foxes, but demographic impacts are harder to discern in later data. Potential interactions of *Leptospira* with other stressors, such as drought, are an important avenue for future research.

### *Risks to other subspecies of island fox*

We used our SRI transmission dynamics model, and an independent model developed for San Clemente Island, to assess the risk that *Leptospira* could invade a naïve population of island foxes if the pathogen should be introduced. Both models showed high probability of successful invasion under a range of environmental conditions. We then analyzed the models to characterize

the expected delay before an incipient outbreak was detected, under different surveillance schemes. We found that delays of 12-24 months are likely under the annual passive surveillance schemes used on most islands (Figure E.6), though this could be accelerated with different sampling designs. Detection of endemic circulation would be much more rapid, for sample sizes of 10 or more. Both model findings align with our past experience on SRI.

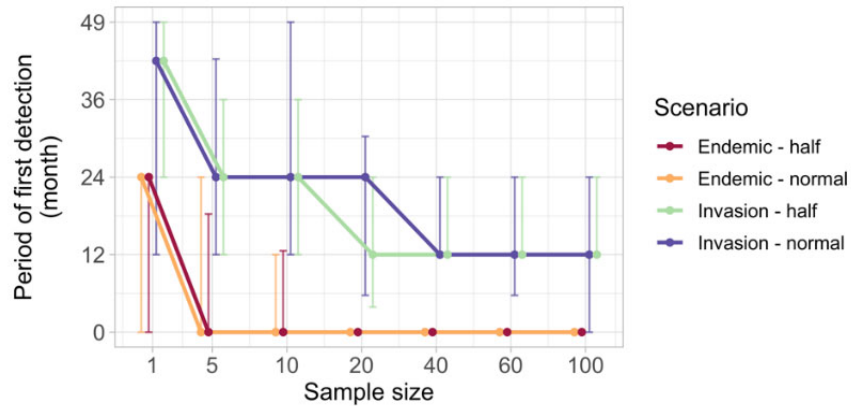


**Figure E.6. Simulation of time delay to first detection of an infected fox, for different disease scenarios and sampling designs.** Using our transmission model of *Leptospira* in SRI foxes, we tested when the first positive test would be obtained for random sampling of foxes with the sample sizes shown. Sampling was conducted for one month at annual intervals (but 3- and 6-month intervals were also modeled). Simulated scenarios were for endemic transmission (starting with 20% infected foxes and 55% recovered foxes) and invasion (starting with 1 infected fox and no recovered foxes), and for fox populations near carrying capacity (‘normal’) and at half of carrying capacity (‘half’). Filled circles show the median time until detection, error bars indicate central 95% quantile range.

#### *Leptospira* in CSL: decades of endemicity, fadeout, and re-emergence

We extended the long-term surveillance of *Leptospira* in the CSL population, and documented an unprecedented 4-year cessation in leptospirosis strands in CSL from early 2013 to mid-2017, followed by reemergence of the disease in a small outbreak in fall 2017, then the largest outbreak on record in 2018 (Figure E.7). We investigated this apparent ‘fadeout’ of the pathogen by testing extensive samples from stranded and wild-captured CSL. All evidence is consistent with a spontaneous break in the endemic circulation of the pathogen after 30 years of uninterrupted annual outbreaks in CSL, followed by reintroduction of the pathogen 4 years later. This period coincided with a series of major oceanographic anomalies, centered on a marine heatwave in the Eastern Pacific Ocean from 2013-2015 (nicknamed “the Blob”) and an ensuing El Niño event in 2015-2016.

We also extended the long-term demographic study of CSL and analyzed mark-resight data to estimate age- and sex-structured survival probabilities each year. We quantified severe impacts to the survival of young CSL during the Blob and El Niño event, as well as the rebound of the CSL population after ocean conditions returned to normal. We developed an algorithm to combine our long-term data on CSL demography and *Leptospira* incidence, to reconstruct the size and age structure of the population of susceptible CSL each year.

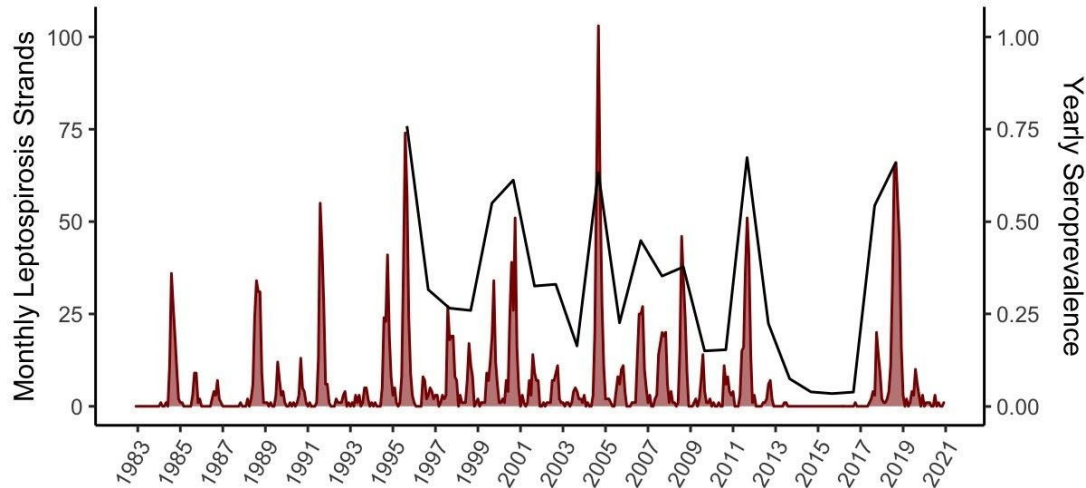


**Figure E.7. Stranding and seroprevalence time series.** Number of California sea lions stranding each month at The Marine Mammal Center (TMMC) with leptospirosis (solid) from 1983 to 2021 and annual seroprevalence of anti-*Leptospira* antibodies in animals stranding at TMMC from 1995 to 2019 (black line). Seroprevalence is excluded for 2020 and 2021 because of small sample sizes.

*Non-stationarities in intrinsic and extrinsic drivers govern *Leptospira* dynamics in CSL*

We modeled 30 years of annual leptospirosis incidence data prior to 2013 (when the fadeout occurred) and found that outbreak intensity is jointly driven by varying susceptible supply and environmental drivers. The supply of susceptible yearling and juvenile CSL was the strongest predictor of outbreak intensity each year, but three markers of oceanographic conditions in the CSL range also had significant influence, which we propose is mediated by CSL foraging and migratory behavior. Our best model explains 50% of variability in outbreak intensity.

We used this model framework to explore how changing conditions can be expected to influence the *CSL/Leptospira* system over short and long timescales. We showed that the model can make real-time predictions of outbreak intensity, using only data that could be gathered months before the outbreak ramps up. These had comparable accuracy to the retrospective model, though the real-time model struggled to predict extreme outbreak sizes. Looking further ahead, we showed that changes in oceanographic drivers predicted under realistic future climate change scenarios are expected to lead to smaller *Leptospira* outbreaks, on average, but with more extreme peaks and troughs.

The fadeout of *Leptospira* from the CSL population was an unexpected demonstration of the extreme outcomes possible when environmental conditions deviate too far from normal. We provide multiple lines of evidence that perturbations in both host demography and seasonal movement patterns – both driven by oceanographic anomalies – caused pathogen fadeout in the system (Figure E.8). When ocean conditions returned to normal after the Blob and 2016 El Niño event, the CSL population recovered and *Leptospira* was reintroduced and reestablished annual outbreaks, including the largest outbreak on record in 2018. This is the first known example of spontaneous fadeout of an endemically circulating pathogen from a large, robust host population. These findings complement the conclusions of our outbreak intensity analysis, demonstrating the powerful influence of non-stationarities in climatic and intrinsic host factors on pathogen transmission and persistence in a natural system.

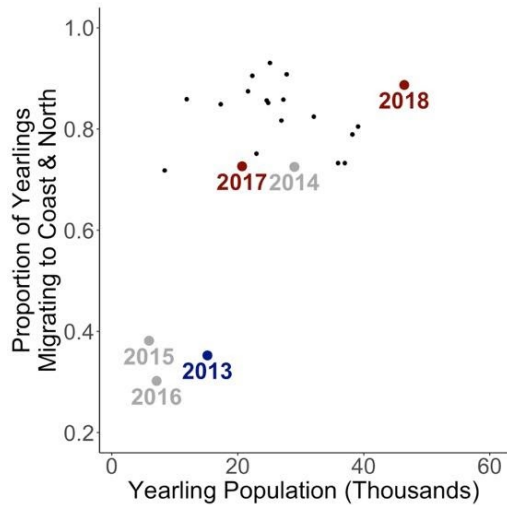


**Figure E.8. Fadeout of *Leptospira* from CSL was associated with simultaneous anomalies in susceptible supply and migratory behavior.** Black points indicate conditions each year from 1996-2012. The year fadeout occurred - 2013 - is marked in blue, the years between fadeout and reemergence are marked in grey, and re-emergence years are red. In 2013, both the size of the yearling population and the proportion leaving the rookery islands to migrate north were anomalously low. By 2017 conditions had returned to ‘normal’ and by 2018 conditions were excellent for *Leptospira* transmission in the sea lion population.

### Implications for Future Research and Benefits

Our project greatly increased our understanding of *Leptospira* ecology in the California coastal ecosystem, revealing new insights and unprecedented phenomena in the long-studied CSL/*Leptospira* system, and shedding important light on the newly discovered island fox/*Leptospira* system. Our work has clear implications for the management of these systems, as well as broader lessons for species management and public health, as well as impacts of climate on disease dynamics. In addition, our project has generated data products and analytic tools and models that will have lasting value.

One straightforward but extremely valuable benefit of our work is the continuation and expansion of several unique long-term studies and their associated time series data. We extended the mark-resight study of CSL demography to 33 years, the time series of *Leptospira* incidence in stranded CSL to 37 years, the time series of seroprevalence in CSL to 25 years, and the time series of sampling free-ranging CSL to 10 years. We also launched analogous long-term data collection for the SRI fox/*Leptospira* system, combining retrospective and prospective studies to create a 15-year record of the leptospirosis outbreak on this island. Each of these long-term studies is a priceless resource, built on years (or decades) of foundational work laid by government scientists and non-profit organizations. These long-term research programs have an irreplaceable role in understanding how complex ecological systems are responding to our changing world; these are crucial lines of inquiry to support management and conservation goals, which simply cannot be addressed from short-term ‘snapshot’ studies. Investment in sustained long-term studies with consistent methodology is essential and can bear fruit in expected and unexpected ways. One example of the latter arose in this project, as our consistent, long-term study of the CSL/*Leptospira* system enabled us to document and understand the spontaneous, climate-driven fadeout of the pathogen after three decades of endemic transmission – an unprecedented observation for any known disease system.

Our work produced concrete guidance to support management of island fox populations on SRI and other Channel Islands, including four island fox subspecies that were listed as endangered until 2016. We have established that the strain of *Leptospira* found on SRI is well adapted to island foxes and will circulate among foxes on SRI for the foreseeable future. Incidence will fluctuate in response to precipitation, but our modeling shows negligible chance that the pathogen will cease to persist. Fortunately, the demographic impacts of the disease are

not severe enough to stall or reverse growth of the SRI fox population, but we did document survival impacts and possible reductions in reproductive success associated with *Leptospira*, and we outlined concerns for possible interaction of this disease with other stressors. The outbreak on SRI does not require active intervention at this point, but continued monitoring is essential.

For the other Channel Islands, we developed best practices to reduce risk of *Leptospira* invasion into naïve fox populations. These include intensive biosecurity measures at mainland ports and island landing sites to prevent introduction by terrestrial wildlife or pet dogs, routine surveillance and (minimally) annual serologic screening for exposure to *L. interrogans* serovar Pomona, and maintenance of collared sentinel fox populations with frequent telemetry ‘life checks’. These strategies could be made stronger and more precise by additional research to identify the unknown reservoir of *Leptospira* that is seeding outbreaks throughout the coastal ecosystem, and by further modeling analyses to optimize surveillance design in response to managers’ needs. We have shared (and will continue to share) our findings and recommendations via the annual meeting of the Island Fox Conservation Working Group, and via direct contacts with population managers.

For the CSL/*Leptospira* system, our project yielded new insights and tools to understand how environmental changes affect the demography and disease dynamics of sea lions. We developed a model framework that can predict the risk of a major seasonal outbreak in CSL each year in real time, given timely provision of data. This advance warning could enable marine mammal stranding centers to expand their capacity to respond, island fox managers to enhance surveillance for *Leptospira* introductions, and public health officials to raise awareness regarding infection risk to humans and their pets. We also projected the range of dynamics to be expected under future climate change scenarios. These capacities and insights will be shared via the NOAA/NMFS West Coast Marine Mammal Stranding Network.

Our project developed numerous modeling and quantitative tools, with applications to our system and to broader understanding of infectious disease ecology and epidemiology. We built stochastic, spatial transmission models for *Leptospira* in island foxes, and demonstrated their utility for predicting future trends and assessing management practices. As a proof of principle, we used our models to produce guidelines for *Leptospira* surveillance on SRI and other islands; we would welcome the opportunity to conduct further work with interested island managers to analyze surveillance designs or other management questions of interest. We developed new tools for disease ecologists, including a method to estimate time of infection from antibody titer kinetics and methods to integrate telemetry data with spatiotemporal risk assessments. Our team applied its skills to the national and global response to COVID-19, making several impactful contributions to support pandemic mitigation efforts.

Long-term, major investments in field work and sample analysis, combined with cutting edge quantitative methods, enabled our project to characterize the ecology of *Leptospira* in the California coastal ecosystem with uncommon depth and precision. Both the island fox and CSL systems are being buffeted by increasingly intense environmental fluctuations. We have laid the foundation in data and knowledge to understand the consequences for disease spread and impact, and have demonstrated a playbook for responding to unforeseen events in these systems. In aggregate, this work puts DoD and other species managers on a stronger footing to anticipate and respond to consequences of future non-stationarities.

### 3. Objectives

This project aimed to characterize the ecology of *Leptospira interrogans* serovar Pomona in two wildlife species of concern – the island fox (*Urocyon littoralis*) and California sea lion (CSL: *Zalophus californianus*) – with emphasis on gathering data and building models to analyze how non-stationary conditions affect disease incidence and impact, and on assessing needs and future strategies for pathogen control and wildlife management. In addition to generating actionable knowledge on two federally protected species that frequent Department of Defense (DoD) lands, we aimed to learn general principles of disease transmission in marine and terrestrial systems which could inform species and habitat management more broadly, and to gain insights to reduce disease impacts on future species reintroduction programs.

The project addressed each of the research priorities in the SERDP Statement of Need RCSON-16-01 (‘Changes in pathogen exposure pathways under non-stationary conditions and their implications for wildlife and human exposure on Department of Defense lands’). It was rooted in understanding the ecology of *Leptospira* in its wildlife hosts and the resulting risks to sensitive wildlife species. Our research took place on DoD lands and the nearby ecosystem on Santa Rosa Island (SRI) that offered a unique opportunity to understand and anticipate challenges on DoD lands. Our project was designed to consider numerous scenarios of future change, including shifts in population dynamics of key wildlife hosts, pathogen introductions to new islands, and direct and indirect effects of our planet’s changing oceans and climate. Mathematical and statistical modeling was integrated throughout our project plan and was central to our scientific approach. Importantly, our findings have direct relevance to present and future pathogen control and wildlife management strategies. For the foxes, we aimed to clarify when pathogen control is warranted, based on health and conservation impacts, as well as whether and how population management and surveillance should be structured to reduce impacts of disease. For the sea lions, we aimed to understand the factors governing outbreak intensity, and hence to develop capacity to anticipate major outbreaks and the risk they may pose to other species, and potentially new sites. We also aimed to build baseline knowledge and long-term data sets to elucidate the causes of mass stranding events and other demographic anomalies in CSL.

When our work began, an outbreak of leptospirosis had been discovered recently in the endangered subspecies of island foxes on SRI, raising fears about conservation impacts to this population and to other endangered island fox subspecies on nearby DoD-owned islands. Preliminary genetic findings indicated that the strain of *Leptospira* causing the outbreak was nearly identical to a strain that had circulated for decades in California sea lions, raising the hypothesis that pathogen spillover from sea lions had sparked the SRI outbreak, and that they could similarly spark outbreaks on DoD-owned islands. Long-term surveillance data from stranded CSL showed major year-to-year variation in *Leptospira* prevalence, indicating that the risk from this reservoir might be mediated by non-stationary factors.

Given this state of knowledge about the system, our study was designed to address three major objectives, each with associated hypotheses:

**Objective 1.** To identify the source of the current *Leptospira* outbreak in the endangered SRI fox.

*Hypothesis 1.* *Leptospira* in SRI foxes originated from CSL between 2004 and 2008.

**Objective 2.** To understand how non-stationary drivers shape *Leptospira* dynamics in the CSL population, and formulate a model capable of short-term outbreak prediction and long-term trend projection.

*Hypothesis 2. The intensity of annual outbreaks in CSL is governed by non-stationary host demography, past disease exposures, and prevailing environmental conditions.*

**Objective 3.** To characterize the ecology of *Leptospira* in island foxes, and develop a data-driven model to project impacts and assess prevention and control strategies under changing conditions.

*Hypothesis 3a. Leptospira can establish persistent circulation in island fox populations, causing significant demographic impacts.*

*Hypothesis 3b. Introduction of Leptospira to naive island fox populations can be anticipated and prevented.*

## 4. Background

The study system includes the pathogen *Leptospira interrogans* serovar Pomona and two host species, island foxes and CSL (Figure 4.1), which have each experienced deadly outbreaks of leptospirosis. Both of these host species are federally protected, under the Endangered Species Act and Marine Mammal Protection Act respectively, and rely on DoD lands for their survival, giving strong incentive for successful species management. Leptospirosis, the disease caused by pathogenic bacteria of the genus *Leptospira*, causes over 500,000 severe cases annually in humans (Haake & Levett, 2015; World Health Organization, 2011) and has long been recognized as a major threat to US military personnel (Corwin et al., 1990; Johnston et al., 1983; Katz et al., 1997; Leggat, 2010; Mackenzie et al., 1966; McCrumb et al., 1957; Russell et al., 2003). Thus, there are substantial reasons, rooted in human health, species conservation, and land management, to understand the routes of *Leptospira* transmission in this system and how they are influenced by non-stationary factors.

In addition to benefits for guiding management of DoD lands and biological resources, this project also aimed to deliver insights on more general problems. These include new methods for studying and managing multi-host pathogens of wildlife, guidelines for managing infectious disease risk in species reintroduction or translocation programs, and new perspectives on infectious disease risks in island systems, including the potential for transmission between marine and terrestrial ecosystems. Finally, despite its global importance, the ecological dynamics of leptospirosis are understudied (Lloyd-Smith et al., 2009). Beyond its particular implications for species of concern in California, our study will advance understanding of *Leptospira* ecology, epidemiology, and control in many systems worldwide, including those where US service members are at immediate risk.

Here we summarize what was known about our system at the time our study began, including pertinent information about the ecology of the pathogen and the two major host species, and the particular history of *Leptospira* on SRI. Further background information is provided at appropriate points in subsequent sections.

### ***Leptospira* and leptospirosis**

#### *Ecology of Leptospira*

*Leptospira* spp. have a complex ecology that can involve multiple host species, environmental reservoirs, and climatic drivers (Adler, 2015; Ellis, 2015; Ko et al., 2009). There are over 300 pathogenic serovars of *Leptospira*, which exhibit variable interactions with different host species, ranging from chronic and asymptomatic infection to acute and fatal disease (Ellis, 2015; Faine et al., 1999; Heath & Johnson, 1994; Ko et al., 2009). The serovar identified in our system, *L. interrogans* serovar Pomona, has been associated with pigs, skunks, foxes, and CSL (Burnstein & Baker, 1954; Campagnolo et al., 2000; Dierauf et al., 1985; Gerber et al., 1993; Gulland et al., 1996; Hathaway et al., 1984; Kingscote, 1986; Lloyd-Smith et al., 2007; Tabel & Karstad, 1967; Vedros et al., 1971). *Leptospira* infects the kidneys and transmits via urine, directly or via contamination of fresh water bodies or moist soil, where the organism can survive and remain infectious for weeks or months (Faine et al., 1999). Trophic transmission (by eating an infected host) has been postulated but not confirmed.



**Figure 4.1. Focal species in the project: Island fox (*Urocyon littoralis*), *Leptospira interrogans*, and California sea lions (*Zalophus californianus*).**

*Biological samples and diagnostic assays.*

Serum and urine are the standard samples used to test live animals for evidence of *Leptospira* infection. Serum is typically analyzed using the microscopic agglutination test (MAT), which detects anti-*Leptospira* antibodies that indicate past exposure (Faine et al., 1999; Lloyd-Smith et al., 2007). Serum chemistry analyses can be run to assess renal compromise caused by the infection. Current infection status and potential infectivity can be tested from urine samples, using real-time polymerase chain reaction (PCR) to detect *L. interrogans* DNA (Wu et al., 2014) or by attempting to culture leptospires to confirm live and infectious pathogen. If kidney tissue can be collected from a fresh carcass, then PCR, culture, immunohistochemistry (IHC), and histopathology can be used to assess infection, kidney pathology characteristic of *Leptospira* infection, and extent of kidney damage.

*Classification and strain typing.*

Historically, *Leptospira* was classified into serovars based on serological reactivity and clustered into serogroups based on antigenically-related serovars (Levett, 2001). However, MAT reactions exhibit cross-reactivity among serovars and are not a reliable indicator of the serovar responsible for a given infection. Reliable strain typing requires isolation through culture of live leptospires to conduct genetic analyses, including pulsed-field gel electrophoresis (PFGE) to determine the infecting serovar. This is a significant challenge, since pathogenic *Leptospira* are notoriously fastidious and slow-growing, making them difficult to culture from field samples. Consequently, serological classification of leptospires remains the dominant approach, despite its shortcomings (Faine et al., 1999; Levett, 2001).

Further delineation of strains within a serovar is not commonly attempted for *Leptospira*, though one pioneering study used variable number of tandem repeat (VNTR) analysis to delineate distinct strains of *L. interrogans* serovar Pomona (Zuerner & Alt, 2009). Before our project, whole genome sequencing (WGS) and phylogenetics had not yet been used to examine the fine structure of *Leptospira* lineages within a serovar.

A more comprehensive overview of diagnostic assays and strain typing for *Leptospira* is provided in section 5.1.1.

### The island fox (*Urocyon littoralis*)

The California Channel Islands are a chain of eight islands off the coast of southern California ranging in size from 2.25 km<sup>2</sup> to 245.8 km<sup>2</sup> (Figure 4.2) (Kinlan et al., 2003). Island foxes are endemic to six of the Channel Islands, with each island home to a unique subspecies. Four subspecies (on SRI, San Miguel Island (SMI), Santa Cruz Island (SCZ), and Santa Catalina Island (SCA)) were listed as federally endangered in 2004 after suffering drastic declines in the late 1990s. After intensive population management, including captive breeding programs on each island, all four populations are rebounding (Coonan et al., 2010, 2014) and were delisted after our project began. However, island fox populations are naturally small and prone to fluctuations (Bakker et al., 2009; Bakker & Doak, 2008), so all six populations are monitored closely.

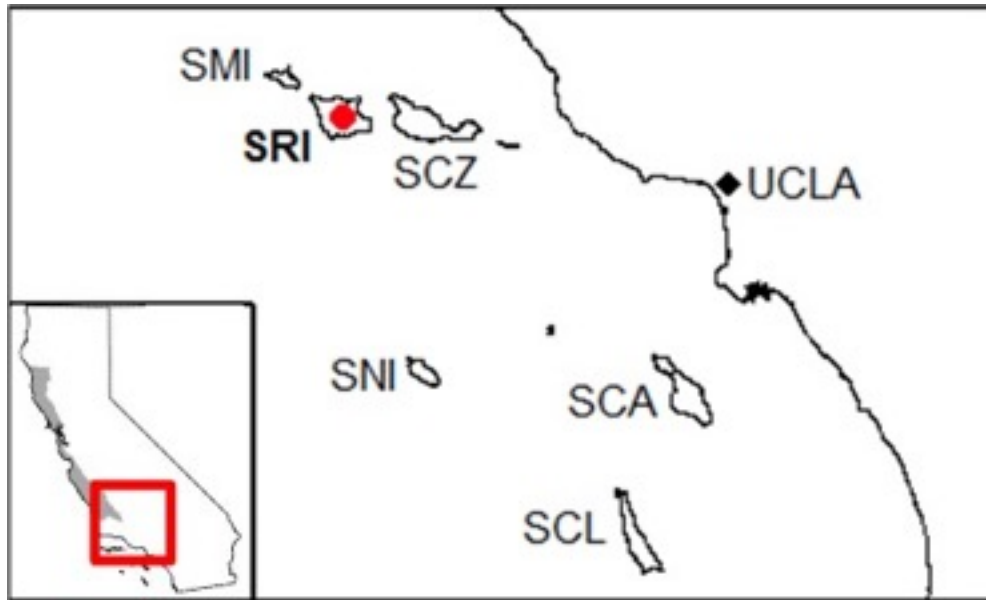


**Figure 4.2. The California Channel Islands and the stranding response range of The Marine Mammal Center (TMMC).** Showing the six islands with endemic island fox populations: San Miguel Island (SMI), Santa Rosa Island (SRI), Santa Cruz Island (SCZ), San Nicolas Island (SNI), Santa Catalina Island (SCA), and San Clemente Island (SCL). SMI, SNI and SCL are DoD lands. SRI (marked with red dot) is the site of the current leptospirosis outbreak among island foxes. The area of SRI is 215 km<sup>2</sup>. TMMC stranding range, i.e. the range within which it responds to and collects stranded marine mammals, is shaded in grey in the inset map of California.

#### *Ecology of island foxes*

The ecology and behavior of the island fox have been studied extensively (Collins, 1980; Coonan et al., 2010; Laughrin, 1977; Roemer, 1999); we summarize a few pertinent facts here. The island fox is the smallest canid in North America (mean adult weight 1.9 kg) and consumes a diverse diet of animal, insect, and plant matter (Crooks & Van Vuren, 1995; Cypher et al., 2011). Foxes have been observed scavenging on CSL carcasses, and pinniped content is sometimes found in their scat (Cypher et al., 2011, 2014; Laughrin, 1977; P. Collins,

unpublished). Foxes form mated pairs that maintain stable territories (Ralls et al., 2013; Roemer, 1999), and litters of 1-4 pups are born in April-May. By fall, juveniles either disperse away or (if population density is high) may remain in their parents' home range (Roemer et al., 2001). Adult survival is typically high because the species has no natural predators. Survival and fecundity exhibit negative density dependence (Bakker et al., 2009; Coonan et al., 2010).

Catastrophic declines on the three northern islands (SRI, SMI and SCZ) in the 1990s were driven by golden eagle predation, which arose from a cascade of human impacts including the role of introduced feral pigs and mule deer in attracting eagles (Roemer et al., 2001, 2002). These introduced species have been removed from SRI (in 1993 and 2012, respectively), and golden eagles have been relocated (Coonan et al., 2010; Knowlton et al., 2007). National Park Service (NPS)-led captive breeding programs were successful (Figure 4.3, Figure 4.4), and populations on all islands grew (Coonan et al., 2014). A population viability analysis based on 17 years of trapping data concluded that island fox populations are naturally small and fluctuate dramatically due to interactions between density dependence and environmental drivers (chiefly ENSO-driven rainfall), but are safe from extinction in the absence of eagle predation or equivalent additional mortality (Bakker et al., 2009). Crucially, this analysis did not account for disease risks. Notably, in 1999 the island fox population on Catalina Island suffered a 90% decline due to a catastrophic disease outbreak, probably caused by canine distemper virus (Timm et al., 2009).



**Figure 4.3. Captive breeding enclosures for island foxes on SRI.**



**Figure 4.4. NPS biologists released island foxes into the wild on SRI.**

### **California sea lions (CSL)**

CSL have a US stock of approximately 300,000 that migrates seasonally between rookery sites on DoD-owned islands – SMI, SNI, and SCL – in the California Channel Island archipelago (Figure 4.2) and coastal haulout sites from central California to Washington (Carretta et al., 2006). Since the passage of the Marine Mammal Protection Act in 1972, the US population of CSL has grown roughly six-fold, but is recently showing signs of density-dependent regulation and substantial drops in survival rates linked to oceanographic variability (DeLong et al., 2017; Laake et al., 2018).

#### *Ecology of CSL*

CSL are generalist predators whose diet and foraging behavior shift with ocean conditions; primary prey species include Pacific sardines, northern anchovies, Pacific hake, rockfish, and market squid (Melin et al., 2010; Stewart et al., 1991). Most foraging occurs in near-shore waters (<50 km from the coast), interspersed with time spent hauled out on coastal rocks and beaches, where they share space with other marine mammal species (Figure 4.5) (Lowry & Forney, 2005; Peterson & Bartholomew, 1967; Weise et al., 2006). Long-term demographic data for CSL are available from National Marine Fisheries Service (NMFS) population monitoring programs, which include over 40 years of population surveys. Furthermore, our team members at the NMFS Alaska Fisheries Science Center, Marine Mammal Laboratory (MML) have conducted the mark-resight study continuously since 1987, with several hundred CSL pups branded with unique numbers each year on SMI, and thousands of resights obtained in yearly surveys at SMI and Año Nuevo Island (ANI). Analyses of these data using

Cormack-Jolly-Seber models (Brownie & Robson, 1983) yield estimates of annual survivorship by sex and age class.



**Figure 4.5. CSL sharing a beach with northern elephant seal (*Mirounga angustirostris*) and Northern fur seals (*Callorhinus ursinus*).**

These analyses and on-going observations show that CSL demography is highly sensitive to non-stationary oceanographic conditions that have intensified in recent years (DeLong et al., 2017; Laake et al., 2018; Melin et al., 2010; Melin, Laake, et al., 2012; Melin, Orr, et al., 2012). While CSL pup counts at rookeries on SMI and SNI reflect marked population growth since 1970 (Figure 4.7), there were sharp drops in recruitment in 1984, 1993-1994, 1999, and 2004 linked to El Niño conditions that lower the primary and secondary productivity of the California Current ecosystem, leading to decreased prey availability (survival of older age classes may also be impacted) (Carretta et al., 2012; DeLong et al., 1991; Melin et al., 2010, 2012; Trillmich et al., 1991). Other oceanographic anomalies, such as the upwelling failures that occurred in 2009 and 2013, also impact CSL health and can cause dramatic reductions in pup survival (Melin et al., 2010). When our project was proposed, there was emerging recognition of on-going severe demographic impacts linked to abnormally warm sea surface temperatures (SST) in the Eastern Pacific Ocean beginning in late 2013. In fact, an Unusual Mortality Event (UME) was declared beginning in January 2013 (Fisheries, 2021), due to severe pup and yearling mortality linked to anomalous ocean conditions, and this UME was still on-going when our project commenced in 2016 (Figure 4.6).



**Figure 4.6. Malnourished CSL pups in rehabilitation at TMMC in 2014.**

### *Leptospirosis in CSL*

*L. interrogans* serovar Pomona was first detected in CSL in 1970 and has circulated persistently in CSL since at least 1984 (Buhnerkempe et al., 2013; Clark et al., 1983; Colagross-Schouten et al., 2002; Coonan et al., 2010, 2014; Garcelon et al., 1992; Meng et al., 2009). Through our collaboration with The Marine Mammal Center (TMMC), we have amassed remarkable long-term time series on leptospirosis in CSL, tracking disease incidence and seroprevalence from wild CSL that strand on the California coast (Figure 4.7). Outbreaks occur on the California coast each year, in the fall, and vary markedly in intensity with major outbreaks causing mass stranding and mortality every 3-5 years (Dierauf et al., 1985; Gerber et al., 1993; Greig et al., 2005; Gulland et al., 1996; Lloyd-Smith et al., 2007). When our project began, the factors causing these periodic major outbreaks were not understood, but proposed explanations ranged from environmental stress due to El Niño events to fluctuations in herd immunity (Gulland et al., 1996; Lloyd-Smith et al., 2007).

We had also studied *Leptospira* infection in free-ranging CSL, capturing and testing CSL every year since 2010 at haulouts on the central California coast (at ANI) and rookeries in the Channel Islands (at SMI). Our data showed that disease patterns in wild-caught CSL on the central California coast were reflected accurately by TMMC data from stranded animals, but patterns on the Channel Island rookeries were not (Figure 4.8). In particular, during the major outbreak observed in stranded CSL in 2011, seroprevalence and infection prevalence spiked in samples collected at ANI but remained at zero in samples collected at the SMI rookery. A year later, in fall 2012, a rise in infection prevalence and seroprevalence was detected at SMI, perhaps reflecting the migratory return of infected CSL that had been infected in the end of the 2011 outbreak on the coast, further north. Thus, while CSL could contact island foxes at rookeries and haulout sites on the Channel Islands, the time period of greatest risk was not yet understood.

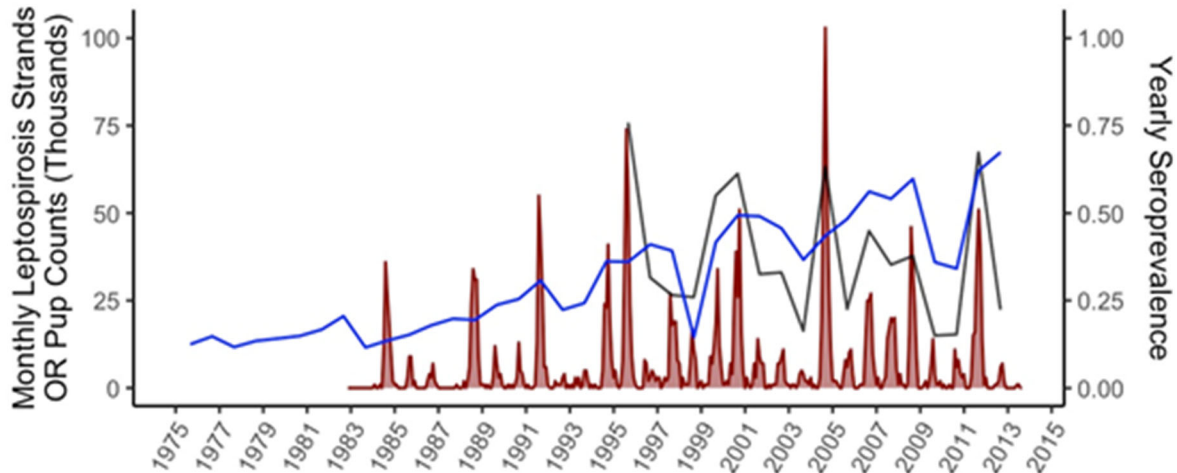


**Figure 4.7. California sea lion abundance and leptospirosis dynamics as of 2014.** This figure reflects our knowledge at the time our proposal was submitted. Number of CSL stranding at TMMC per month due to leptospirosis since 1984 (red filled curve). Outbreaks occur each fall but vary greatly in magnitude with major outbreaks every 3-5 years. Microscopic agglutination testing of serum for anti-*Leptospira* antibodies in CSL that have stranded since 1995 (red line) shows that annual seroprevalence tracks the patterns seen in the leptospirosis stranding record. The blue line is the estimated number of CSL pups born each year since 1970, showing that the population has been increasing steadily but there are major recruitment failures associated with El Niño events and other oceanographic anomalies.

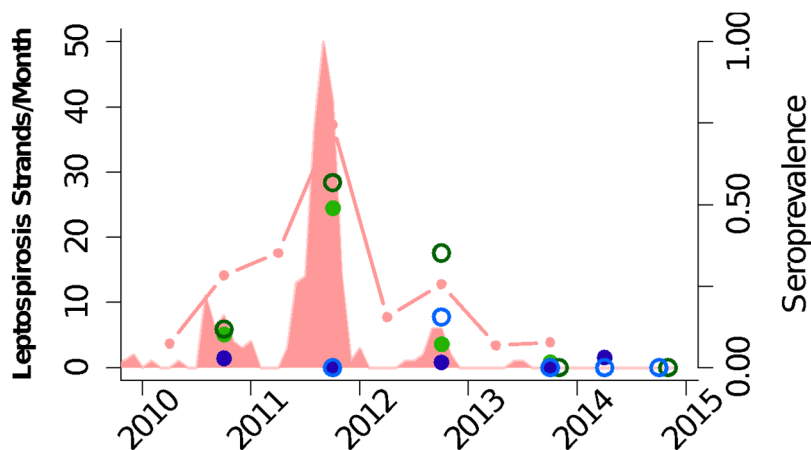


**Figure 4.8. Number of CSL stranding per month due to leptospirosis (pink shaded; 2010-14) and semi-annual seroprevalence in stranded CSL (pink line; 2010-13).** Seroprevalence (solid circles) and infection prevalence (hollow circles) of CSL captured on ANI (green) and SMI (blue) during 2-4 week periods in the fall (2010-2013) and spring (SMI 2014 only).

### ***Leptospira* in Santa Rosa Island foxes**

The SRI subspecies of fox declined to only 15 individuals in 2000 due to extensive predation by non-native golden eagles (*Aquila chrysaetos*). Between 2000-2001, all remaining individuals were brought into an on-island captive breeding program, making this subspecies of fox temporarily extinct from the wild for several years (Faine et al., 1999). Recolonization of

SRI by the foxes began in 2003 in a multi-year reintroduction program. Foxes were released back into the wild each year starting in 2003; after a few years of challenges, the wild population began to grow, and all captive foxes were released by 2009. The NPS closely monitored the reintroduced population by radiotelemetry and periodic biological sampling.

In fall 2010, evidence of *Leptospira* infection was identified in two juvenile foxes found dead on SRI. Our subsequent investigations revealed evidence of a large outbreak in the foxes (and to a lesser degree, in island spotted skunks (*Spilogale gracilis amphiala*)). Analysis of banked fox sera from 2009-2010 revealed high seroprevalences of anti-*Leptospira* antibodies among adult foxes across SRI, indicating a widespread outbreak (Figure 4.9). Sampling of fox and skunk urine in January 2011 identified active infections in both species, with the infecting strain indistinguishable by VNTR genetic typing from *Leptospira* isolates derived from CSL over the period 1970-2010 (Zuerner & Alt, 2009).

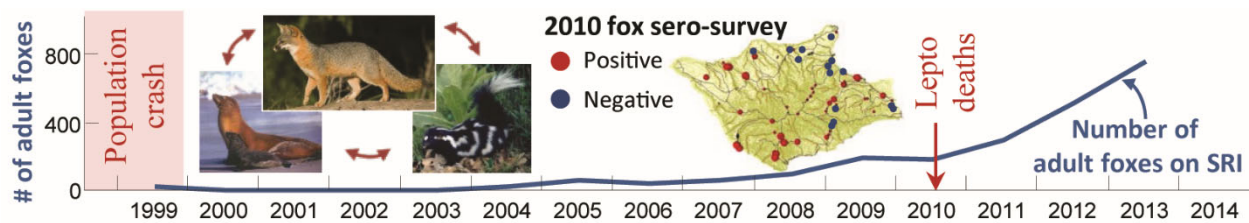


**Figure 4.9. Summary of island fox population growth and leptospirosis outbreak on Santa Rosa Island as of 2014.** This figure reflects our knowledge at the time our proposal was submitted. The growth of the SRI reintroduced wild fox population is shown in blue. The first detection of leptospirosis-affected animals in 2010 is shown by the red arrow, and the inset map shows results from an early survey for evidence of *Leptospira* exposure in foxes sampled in 2010. The inset photographs show the hypothesis, based on pathogen genetic data, that *Leptospira* was transmitting between island foxes, spotted skunks, and California sea lions.

### Possible origins of the SRI *Leptospira* outbreak

When we proposed this project, there was no evidence that the strain of *Leptospira* isolated from SRI foxes and skunks in 2011 was present on SRI before the fox population crashed, and foxes in the captive breeding program had appeared disease-free. Given the finding that the 2011 SRI fox and skunk isolates were genetically indistinguishable from CSL isolates by VNTR analysis, it seemed most plausible that the pathogen had been introduced to the island by infected CSL, possibly via foxes scavenging on CSL carcasses. Alternatively, the pathogen could have been present undetected in the captive foxes, or it might have come from other terrestrial species on SRI.

Animal diversity is low on the Channel Islands and varies slightly from island to island. SRI has three species of native terrestrial mammals: the island fox, the island spotted skunk, and the deer mouse (*Peromyscus maniculatus*). In the 1800s, the islands were used for ranching, and livestock were imported and raised on the islands. Livestock on SRI included sheep, pigs, cattle, deer, and elk. Sheep were eradicated in the early 1900s, pigs were removed in the early 1990s, and by 1998 all the cattle were removed (Knowlton et al., 2007). By the time of the fox decline in the late 1990s, deer and elk were the only remaining introduced mammals on SRI. The elk were eradicated by 2011 and the deer by 2013, leaving only the three native terrestrial mammals. None of these species were known to be infected by *Leptospira* on SRI prior to our work.

A major objective of our project was to determine the source of *Leptospira* on SRI, in order to better assess the risk to other island fox populations. We proposed to approach this question by three main avenues: analyzing banked samples and data to reconstruct the spatiotemporal origins of the outbreak; testing samples from other potential host species on SRI for exposure to *Leptospira*; and performing WGS of all available *Leptospira* isolates to gain a higher-resolution picture of their shared ancestry, with particular focus on the time to most recent common ancestor (TMRCA). In our proposal, we laid out the following guidelines for how different findings from this work would support different conclusions regarding the hypothesized source of the pathogen.

Hypothesized source	Reconstruction of fox outbreak	<i>Leptospira</i> in captive foxes	<i>Leptospira</i> in other SRI species	Genetic analysis
<i>Captive foxes</i>	<i>Leptospira</i> enters wild fox population with release of known-positive foxes.	<i>Leptospira</i> present in captive foxes	<i>Leptospira</i> present or not in other hosts.	TMRCA before 2000
<i>Terrestrial mammal community</i>	Early appearance of <i>Leptospira</i> , especially with inland or multiple origins.	Not present.	Present in other hosts.	TMRCA before 2004
<i>Introduced from outside (CSLs)</i>	Spatial origin on the coast (especially CSL haulout), any time from 2004-2008.	Not present.	Not present.	TMRCA in 2004 or later

**Table 4.1. Summary of results from each aim that would support different hypotheses about outbreak source.**

### Conservation concerns on SRI

Beyond the questions about where the outbreak came from, it was important to understand where it was going, and what the impacts on the recovering island fox population might be. At the time our project began, exposure to *Leptospira* was still widespread among SRI foxes, but it was unclear whether the pathogen could establish sustained endemic circulation in the small host population on the island. Similarly, the on-going importance of spotted skunks in the outbreak was unclear, and there was no information regarding the involvement of deer mice. The potential influence of climate on *Leptospira* on SRI was unknown, but the dynamics of this environmentally-transmitted pathogen were known to be influenced by precipitation in other settings.

When our project began, it was already clear that *Leptospira* was not having a severe impact on island fox population ecology – unlike the catastrophic epidemic of canine distemper virus in Catalina Island foxes in 1999 (Timm et al., 2009). Despite widespread exposure to *Leptospira* on SRI, as indicated by the 2009-2010 serosurvey results, the reintroduced fox population continued to grow (Figure 4.9). However, the pathogen had been associated with several known mortalities in young foxes, and given the rugged landscape and low proportion of the population covered by active telemetry-based surveillance, it was possible that many more

deaths had occurred undetected. It was also possible that the pathogen impacted recruitment, as *Leptospira* is associated with abortion in many host species (Adler, 2015). The growth of the SRI fox population had lagged that of neighboring islands (SMI and SCZ) during the post-reintroduction period – a pattern that had been attributed to residual golden eagle predation but could in fact be tied to leptospirosis. Our project aimed to determine whether more demographic impacts had occurred, including further deaths, reductions in fecundity, or robust signals of reduced population growth. Even a subtle demographic impact could destabilize this small population, putting it at greater risk the next time it was stressed by another factor such as a protracted drought.

### **Concerns on other islands**

The island fox subspecies on other Channel Islands, including those owned by DoD, appeared not to be impacted by *Leptospira*. In the aftermath of the discovery of the SRI outbreak, serum samples from the five other islands with foxes were analyzed by MAT and showed no patterns similar to those on SRI. (A low frequency of low-titer positive samples was detected on some islands, against a range of serovars; this is a common pattern in wildlife serosurveys for anti-*Leptospira* antibodies and may reflect exposure to non-pathogenic leptospires in the environment.) As our proposal underwent final review, concerns arose about the fox population on SNI, which underwent a sharp and mysterious decline from 2010-2015, due to increased juvenile and adult mortality of unknown cause (Coonan et al., 2015). At the request of the US Navy, which manages SNI, we added an investigation of a possible role for *Leptospira* in the SNI population decline to our project.

More broadly, the concern persisted that the strain of *Leptospira* causing an outbreak on SRI could be introduced to other island fox populations, particularly if it could be transmitted to foxes by CSL. This emphasized the importance of understanding the origins of the outbreak on SRI, characterizing possible routes of introduction to other islands, and quantifying the probability that it could successfully invade a naïve island fox population. From a management perspective, there were important questions about the speed with which such an invasion would be detected, under current surveillance protocols, particularly given the fact that the SRI outbreak was not detected until it had spread island-wide. Now that *Leptospira* was acknowledged as a pathogen impacting island foxes, could an invasion be detected sooner? If so, were active disease control measures such as vaccination warranted? And was it possible to anticipate high-risk periods for new introductions by better understanding the drivers of *Leptospira* dynamics in sea lions and how they respond to changing environmental conditions?

Our project set out to collect and analyze data to address these questions, with the proximate goal of informing management of the multi-host dynamics of *Leptospira* in the California coastal ecosystem, and the ultimate goal of supporting wildlife conservation, species management, and public health measures worldwide.

## 5. Materials and Methods

### 5.1. Origins of the Santa Rosa Island Outbreak

#### 5.1.1. Reconstruction of the fox outbreak up to 2010

##### *Laboratory analysis*

##### *Serology*

The Microscopic Agglutination Test (MAT) is the standard serologic test for anti-*Leptospira* antibodies. The test involves mixing serum with live antigens of a chosen set of leptospiral serovars. Since there are over 300 pathogenic serovars of *Leptospira*, MAT analyses are conventionally run against panels of locally relevant serovars. These tests are read microscopically for agglutination to a given serovar at a specific titration, and the titer level for a given sample is the highest titration at which 50% agglutination occurs.

The MAT is not an ideal test partially because it exhibits strong cross-reactivity among serovars, and thus does not definitively identify the infecting serovar (see section 5.3.2.4). Additionally, while this assay is inexpensive and demands little technology, it is time consuming and requires significant training as well as maintaining a collection of live antigens. A positive MAT test is also only a measure of past exposure and does not indicate a current infection because infected individuals can maintain positive antibody titers for long periods of time (Cumberland et al., 1999, 2001; Faine et al., 1999; Levett, 2001). Titer levels decline over time since exposure and can drop below the level defined as seropositive, so seronegativity does not necessarily imply that an animal has never been exposed to *Leptospira*. However, titer level may offer insights into the time of infection as the rate of titer decline, initial titer estimates, and potential antibody boosting by re-exposure become better understood.

In this study, serum samples were tested for presence of antibodies against *Leptospira* using MAT at the Centers for Disease Control in Atlanta, Georgia. Our genetic analyses have shown that the Santa Rosa Island outbreak strain is *Leptospira interrogans* serovar Pomona, but in order to characterize serovar cross-reactivity profiles, and to allow for the possibility of other strains circulating in the system, samples were tested against broader panels. In particular, all samples collected in 2012 and earlier were tested for antibodies against 10 or 20 serovars. The 10 serovar panel always included the following serovars: Autumnalis, Bratislava, Cynopteri, Djasiman, Icterohaemorrhagiae, Mankarso, Pomona, Pyrogenes and Wolffi. In most runs, the 10 serovar panel also included serovar Canicola; however, in one batch of samples, the panel included serovar Australis instead of Canicola. The 20 serovar panel always included the same serovars as the standard 10 panel (i.e. with Canicola instead of Australis) as well as the following serovars: Australis, Ballum, Bataviae, Celledoni, Grippotyphosa, Borincana, Javanica, Georgia, Alexi and Tarassovi. All samples were titrated to end-point titer to gain insight into the strength of the antibody response.

Island fox and skunk samples were considered seropositive against the outbreak strain if they had a titer of 1:100 or greater against either serovar Pomona or Autumnalis, because serovar Pomona has been identified as the strain that infects these two species, and the sera from island foxes exhibits strong cross-reactivity with serovar Autumnalis (see section 6.3.2.4). For analyses of quantitative titer levels, we used the titer for serovar Pomona unless specified otherwise. In the other host species studied here, test samples were considered positive if they had a titer of

1:100 or greater to any one of 5 serovars in a focal panel containing serovars Pomona, Autumnalis, Bratislava, Icterohaemorrhagiae or Djasiman, and interpreted in light of the reactivity profile.

#### *Polymerase chain reaction (PCR)*

Polymerase chain reaction (PCR) assays have been developed for leptospirosis testing, and PCR can be run on any tissue or fluid that may contain leptospire. It does not require successful culture of *Leptospira* isolates. With carefully chosen primers, PCR can accurately identify the pathogenic *Leptospira* species causing an infection, but cannot distinguish finer classifications such as serovars (Wu et al., 2014). Quantitative real time PCR (qPCR) can determine the amount of leptospiral genetic material present in the substance tested. Positive PCR and qPCR results indicate the presence of leptospire in the tissue or fluid analyzed and thus also indicate a current or recent infection. However, because PCR and qPCR cannot distinguish between living and dead leptospire, and nonviable DNA may remain present for some time in host tissues, some caution is required when interpreting these results as active infections (Wu et al., 2014).

In our studies, urine and frozen kidney samples were processed and tested for pathogenic *Leptospira* via qPCR. Whole frozen kidneys were sent directly to the diagnostic laboratory (see next paragraph). Urine was spun into a pellet and washed with phosphate buffered saline on the day of collection. The resulting pellet was stored frozen until it could be sent to the lab for the remainder of the analysis. Archived kidney samples that were stored in formalin fixed paraffin embedded blocks had 25 um scrolls of kidney tissue cut from the blocks and sent to the lab for extraction and testing.

Samples collected between 2010-2016 were tested at the Hollings Marine Laboratory and tested using methods from Wu et al., 2014. All other samples were tested at the Colorado State University Veterinary Diagnostic Laboratory (CSU). Samples tested at CSU were tested first using a slightly modified version of the methods developed by Wu. These modifications were to use QIAamp DNA Mini Kit Protocol instead of QIAamp Viral RNA Mini Kit Protocol for the extraction for both tissues and urine and to use VetMAX™-Plus Master Mix (4415327) as the Master Mix Kit instead of TaqMan Universal PCR Master Mix, no AmpErase UNG (4324018). The modifications were shown to be slightly more sensitive in a comparison of the methods conducted at CSU (unpublished). Samples that tested positive using the modified protocol were tested again using the Wu protocol so the results could be directly compared to results from previous testing done at the Hollings Marine Laboratory.

#### *Immunohistochemistry (IHC)*

Immunohistochemistry (IHC) is an assay that tests for antigens in infected tissues and is another available method to test for *Leptospira* infection (Szeredi & Haake, 2006). Two main benefits of IHC is the ability to visualize the distribution and location of leptospire in tissues and its ability to detect infections of *Leptospira* in formalin fixed tissues (thus enabling retrospective testing) (Szeredi & Haake, 2006).

Formalin fixed kidney tissue from mice, deer and skunks was sliced and placed into cassettes that were sent to Colorado State University Veterinary Diagnostic Labs, where they were placed on slides, stained, and tested via IHC. Formalin fixed paraffin embedded tissue from archived fox carcasses was cut and placed onto slides and sent to Colorado State University Veterinary Diagnostic Labs, where they were stained and tested via IHC.

### *Bacterial culture*

Culture is the most specific test available for leptospiral infection, but its sensitivity is very low (Faine et al., 1999; Levett, 2001). Cultures can be attempted from blood, urine, or kidney samples, though leptospire are only found in blood for a short period of time following initial infection. Cultures of *Leptospira* are difficult to grow because leptospire grow very slowly and have complex environmental and nutrient requirements. Consequently, it is common that an individual with an active infection will have a negative culture result (Adler, 2015). However, cultures are the only current method of definitively strain typing leptospire and one of a few assays that indicate a current infection. Traditionally, isolates have been strain-typed using molecular techniques such as pulsed-field gel electrophoresis (PFGE), restriction fragment length polymorphism (RFLP), or variable number of tandem repeat (VNTR) analysis. The techniques used have been advancing rapidly with several whole genome sequences of *Leptospira* species being completed since 2003 (Ahmed, et al., 2012; Ko et al., 2009; Zuerner & Bolin, 1997).

Sterile urine samples collected via cystocentesis were cultured by placing 1cc sterile urine into transport media then inoculating culture media with 0.1cc of the urine/transport media blend (Adler, 2015). Cultures were stored with lids lightly open in a dark room at room temperature until they were sent to the lab. Cultures from the 2010 season were sent to the USDA National Animal Disease Center in Ames, IA. Cultures from the 2012 season on were sent to the CDC in Atlanta, GA. Cultures from the 2011 season were sent to both USDA and CDC.

### *Bacterial strain typing and sequencing*

Isolates were obtained from positive cultures grown in the lab following the methods of Fouts (Fouts et al., 2016). When sufficient genetic material was available for an isolate, extractions were taken for PFGE and whole genome sequencing (WGS). For PFGE analysis, agarose plugs embedded with leptospiral DNA were prepared from each cell suspension. A slice was cut from each plug and the DNA was digested in 30 U NotI restriction enzyme at 37° for 2 hours. *Salmonella* serotype Braenderup H9812 was digested with 50 U XbaI for use as a DNA size standard. Plug slices containing the digested DNA were placed in the wells of a 1% agarose gel and electrophoresed in a Bio-Rad CHEF Mapper XA or CHEF-DRIII for 18 hours at 14°C with recirculating TBE buffer. The gel was stained with ethidium bromide following PFGE (Galloway & Levett, 2008).

### ***Sample collection and population monitoring: island foxes and spotted skunks***

#### *Timeline of island fox population on Santa Rosa Island*

The captive program began in 2000 and continued until 2009. Between 2001 and 2003, there were no wild foxes on the island, but, as the captive population bred successfully and external threats were reduced, foxes were reintroduced to the island in a series of releases beginning in 2003. After a rough start, the reintroduced population grew quickly, and the captive program was ended in 2009 (Figure 5.1.1.1). In fall 2010, evidence of *Leptospira* infection was identified in two juvenile foxes found dead on Santa Rosa Island, and, in January 2011, a field investigation led by our team confirmed the outbreak by obtaining isolates of *Leptospira interrogans* serovar Pomona from both island foxes and island spotted skunks. This section (5.1.1 and 6.1.1) focuses on the pre-decline wild foxes, the founding foxes, the captive foxes, and the post-reintroduction wild foxes through the 2010 season. For foxes, a season spans from

March of the given year through February of the subsequent year, which we refer to as the “fox year.”

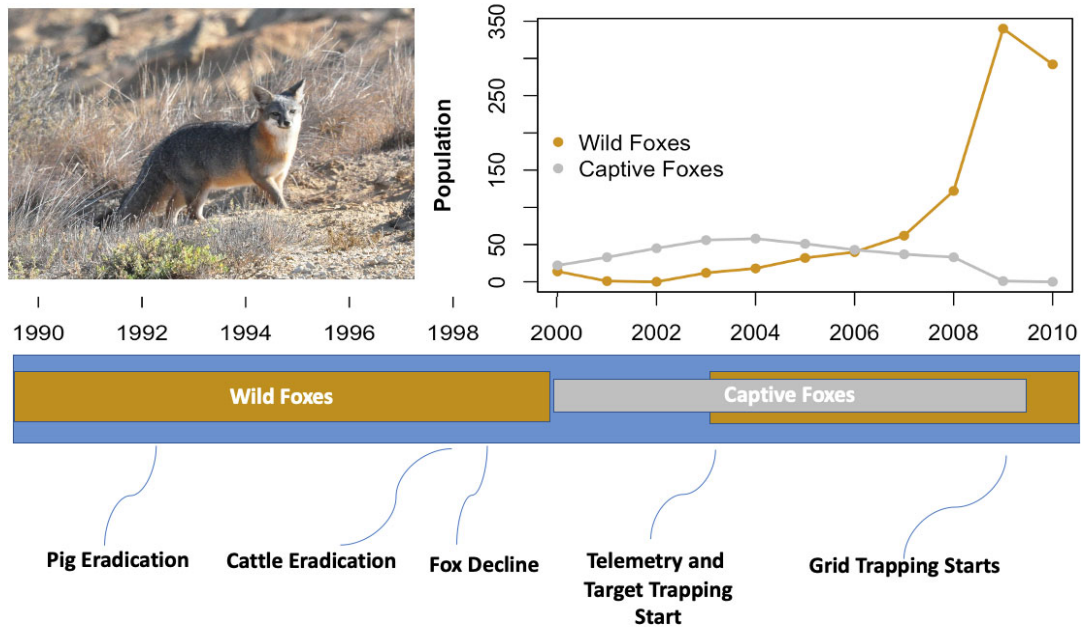


**Figure 5.1.1.1. Timeline of events on Santa Rosa Island, and population trajectories of captive and wild foxes until 2010.**

#### *Island foxes in captivity, 2000-2009*

A total of 102 foxes were part of the captive breeding program on Santa Rosa Island between 2000 and 2009, including a total of 17 brought in from the wild and 85 born in captivity. Fifteen foxes, the founding foxes, were brought into captivity between March 2000 and May 2001. These founding foxes consisted of 12 adults and 3 pups, including 10 females (8 adults, 2 pups) and 5 males (4 adults and 1 pup). Three of these adult females were pregnant and gave birth when they were brought into captivity, yielding 8 pups, 4 male and 4 female. An additional 2 wild born foxes, namely a female pup in 2004 and a male yearling in 2007, were brought into captivity after reintroduced foxes began breeding in the wild again. Foxes began being released back into the wild in late 2003, the final year of captive breeding was 2008, and the final captive fox was released in 2009. A total of 96 foxes were released because 5 foxes died while in captivity and 1 fox was permanently transferred to the Santa Barbara Zoo.

The captive facilities consisted of 26 wire mesh pens ranging from 45-60 m<sup>2</sup> in size located on Santa Rosa Island. Occasionally, foxes were housed individually; however, foxes were most often housed in mated pairs and with their current young pups if they had pups. Pairs were rearranged as needed depending on genetic recommendations and temperament. All pen moves, pairings, and reproduction were recorded in detail.

Captive foxes were given health exams at least twice a year during which body condition, weight, and reproductive status were recorded and blood samples were taken and archived. For this study, we tested 363 serum samples from 98 of the 102 captive foxes, including samples from 14 of the original 15 founding foxes (Table 5.1.1.1). We located 333 serum samples in the

National Park Service archives and tested these at CDC via MAT using the 10 serovar panel. We also had access to the samples tested in an earlier serological study (Clifford et al., 2006), which included 42 samples from foxes in captivity on Santa Rosa Island, of which 18 were collected in 2001 and 24 in 2002. 14 of these samples were from the founding foxes and 28 were from captive-born foxes. All of these samples were tested at Cornell Diagnostic Lab against 6 serovars, including Pomona and Autumnalis, and 12 were tested both at Cornell and CDC. These samples were used to compare the two labs, and we found Cornell to be less sensitive than CDC. Thus, when samples had been tested at both labs, we used the CDC results. The 10 serovar panel was used on all captive fox samples and all were titrated to end point titer. Formalin-fixed paraffin-embedded kidney samples from tissue blocks were obtained from the 5 foxes who died in captivity, and these samples were tested via IHC and PCR.

Season	N	Individuals w/ Serum	Total Serum
2000	22	0	0
2001	33	22	22
2002	45	34	36
2003	56	29	28
2004	58	39	40
2005	51	51	65
2006	43	42	64
2007	37	36	50
2008	33	33	57
2009	1	0	0

**Table 5.1.1.1. Captive fox population size (N), the number of individual foxes with test results, and the total number of serum samples analyzed in captivity.** Many individuals have multiple samples within a season.

*Wild island foxes: telemetry and mortality collection*

Foxes were fitted with VHF radio telemetry collars with mortality sensors and tracked regularly, beginning with the first releases in 2003 and continuing to the present. From 2003-2006, all reintroduced and wild born foxes were collared and tracked via radio telemetry, with the goal of obtaining a specific location with GPS coordinates on each fox once per week, and detecting the radio signal from each fox as often as possible. For clarity, all foxes, both reintroduced and wild-born, that were living in the wild post reintroduction in 2003 will be called “wild” foxes when referring to this group collectively. In cases that require a distinction between these groups, they will be called “reintroduced” and “wild born”. By 2007, the wild population had grown to over 60 animals, so a subset of the population was collared and tracked weekly via radio telemetry. In most years once the population was large enough, 40-50 individuals were collared at any given time; however, as animals died or collars failed, this number fluctuated. New collars were deployed on a rolling basis, with a peak of 92 individual foxes collared in a single year (Table 5.1.1.2). The carcass of any fox whose collar switched into mortality mode was collected as soon as possible and sent to UC Davis for a necropsy exam. Between 2005 and 2009, we recovered kidneys from 9 non-founder (captive-born reintroduced and post reintroduction wild-born) wild fox mortalities, which were preserved either in formalin-fixed

paraffin-embedded blocks or frozen. We tested these samples for evidence of *Leptospira* infection using PCR and or IHC.

Season	# Collared Foxes
2003	12
2004	23
2005	38
2006	55
2007	63
2008	92
2009	72
2010	63

**Table 5.1.1.2. Total number of actively-collared foxes during each season (fox-year).** Not all collars were active throughout the season, on average 40-50 collars were active at one time.

*Island foxes and spotted skunks: trapping and sampling*

The National Park Service has conducted annual trapping of foxes and skunks on Santa Rosa Island since 2004. From 2004-2008, when the wild populations were still very small, annual trapping was conducted on an as-needed basis in locations known to be occupied by target foxes. In 2009, the National Park Service began running 18 trapping grids spread across the island (Figure 5.1.1.2) each year to estimate densities and population sizes of the foxes and spotted skunks. Additional target trapping efforts were conducted to allow for the installation of radio collars, targeted sample collection, and administration of vaccines not completed on the grids. Each of the ladder grids was run for 6 consecutive nights in July or August each year, and target trapping occurred from July to January. Between 2003 and 2008, the wild fox population size was estimated by calculating the minimum number of foxes known to be alive through telemetry and trapping. Beginning in 2009, population sizes were estimated in the program DENSITY using the grid trapping data (Coonan et al., 2015).

Each captured fox was marked with a PIT tag and given a physical examination including sex, weight, body condition, age class, and reproductive status. Samples including blood, whiskers, parasites, and scat were collected from all foxes. Late in the 2010 season, when the *Leptospira* outbreak was detected, urine began being collected via cystocentesis.

In 2004 and 2005, captured spotted skunks were released without being tagged, examined, or sampled. In 2006-2008, spotted skunks were marked with PIT tags when captured and given a brief exam including weight, sex, and age class, but they did not have samples collected. In 2009 and most of 2010, only skunks caught on the grids were marked with PIT tags and examined. At the end of the 2010 season, after the *Leptospira* outbreak had been detected, serum and urine samples began being collected from skunks. From then on, any skunk captured that had samples collected was marked with a PIT tag and given a full examination.

Between 2003 and 2010, in 8830 trap nights, a total of 281 individual foxes were captured in 1384 total fox capture events. A total of 373 serum samples were collected, from 242 of the 281 individual foxes that were captured during this period (Table 5.1.1.3). Between 2004 and 2010, a minimum of 1085 individual skunks were captured in 2330 total skunk captures (Table 5.1.1.4). True numbers of individual skunks captured are unknown, since not all skunks were marked upon capture resulting in an unknown number of re-captures. We include

information on biological samples collected from 2010-2012 (i.e. beyond the focal period for this section), to support conclusions about the role of skunks as a competent host for *Leptospira* infection. From 2010-2012, 107 serum samples and 28 urine samples were collected from spotted skunks to test them for leptospirosis via MAT, PCR, and culture (Table 5.1.1.5).

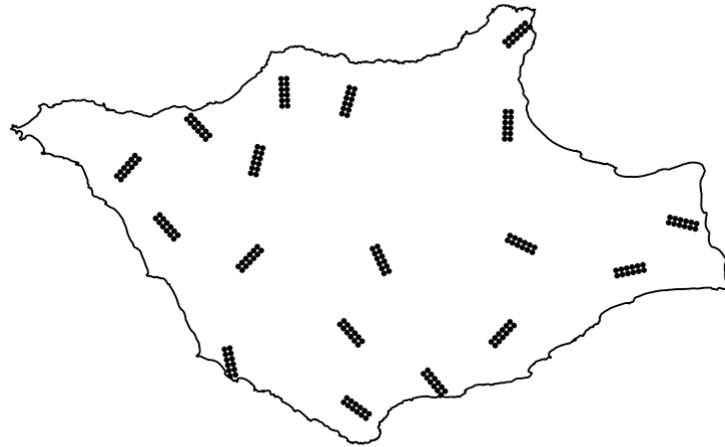


**Figure 5.1.1.2. Map of the 18 ladder grids on Santa Rosa Island.** These were run annually for 6 nights beginning in 2009 to mark and recapture Channel Island foxes and skunks.

Season	Population Estimate	Captures Total	Captures Individuals	Serum Total	Serum Individuals
2003	12	25	9	0	0
2004	24	64	18	2	2
2005	41	51	23	2	2
2006	58	111	39	33	31
2007	64	115	49	37	37
2008	122	262	96	46	46
2009	313-466	296	140	99	99
2010	233-351	460	164	154	144
Total		1384	281*	373	242*

**Table 5.1.1.3. Trapping data and sample collection for island foxes.** Data ranges from 2003 to 2010 and includes the wild fox population estimate, the number of total fox captures, the number of individual foxes captured, the total number of serum samples, and the number of individual foxes with serum samples. For 2003-2008, the population estimates are the minimum known number of foxes alive during that season from telemetry and trapping data. For 2009-2010, the population estimates are adult and pup combined 80% confidence interval population estimates from grid trapping. \*Total number of individuals captured and sampled is the number of unique individuals from 2003-2010 and is not the sum of the number of individuals within each season.

Season	Trap Nights	Captures Total	Captures With ID	Captures NoID	Unique IDs
2004	542	161	0	161	0
2005	368	68	1	67	1
2006	995	448	417	31	343
2007	682	293	293	0	255
2008	1612	629	614	15	443
2009	2089	445	282	163	179
2010	2542	286	122	164	91
Total	8830	2330	1729	601	1085*

**Table 5.1.1.4. Trapping data for island spotted skunks.** Data ranges from 2004-2010 and includes the number of trap nights, the total number of skunk captures, the number of captures with IDs, the number of captures without IDs, and the number of unique IDs captured. The number of unique individuals is unknown for years where there are captures that were not given an ID (i.e. for all years except 2007). \*The total number of unique IDs is the number of unique IDs between 2004-2010 and is not the sum of the number of unique IDs within each season.

Season	MAT	PCR	Culture
2010	9	0	8
2011	31	1	1
2012	67	19	15
Total	107	20	25

**Table 5.1.1.5. Samples collected from island spotted skunks.** Number of samples collected for MAT, PCR, and analysis from island spotted skunks in 2010-2012.

***Additional sample collection***

*Retrospective samples: feral pigs, 1987*

Nettles et. al. collected serum from 60 pigs on Santa Rosa Island in 1987 (Nettles et al., 1989). We located these samples and tested them for antibodies against *Leptospira* via MAT analysis. The 20 serovar panel was used for these samples and all were titrated to end point titers. No location data or individual metadata such as age or sex were available for these samples.

*Retrospective samples: island foxes, 1988*

Garcelon et. al. collected samples from all 6 island fox subspecies in 1988 (Garcelon et al., 1992). We located 48 of these samples collected from Santa Rosa Island in July 1988. Sex, age class, weight, and reproductive status were available for most of these samples. Exact location data was not available, though these samples were collected in two trapping sessions in the Northern and Eastern sections of the island. The 20 serovar MAT panel was used for these samples, and all were titrated to end point titers.

*Other terrestrial mammals: deer mice, 2012-2015*

Opportunistic collection of 72 adult and 20 juvenile Santa Rosa Island deer mice (*Peromyscus maniculatus*) occurred between 2012 and 2015. Island foxes tend to provision their mates and pups during fox trapping efforts. Especially in the summer months when the pups are

young, provisions of dead mice, birds, and occasionally skunks are left outside the trap. From 2012-2015, all mice provisioned to traps were collected. During the same period, all mice that were killed with snap traps during pest management efforts in National Park Service buildings on Santa Rosa Island were collected. Upon collection, the sex, age class, date, and location for each mouse was recorded and both kidneys were removed. One kidney per mouse was preserved in 10% buffered formalin to test for *Leptospira* via IHC. The second kidney from all but three of the mice was frozen and later tested for *Leptospira* via PCR. The mice consisted of 36 adult males, 35 adult females, 1 unknown sex adult, and 20 juvenile mice. Of these, 24 of the adults and 9 of the juvenile mice were collected during pest management, which was concentrated in a small section of the Eastern corner of the island where the few buildings are located. The remaining 48 adult and 11 juvenile samples were scattered across the northern half of the island.

#### *Other terrestrial mammals: mule deer, 2012-2013*

Urine, kidney, and serum samples were collected opportunistically from the last remaining deer on Santa Rosa Island by the National Park Service during the course of their deer removal efforts in 2012 and 2013. We were able to access these samples and test 27 individual deer (8 males, 19 females) for *Leptospira*. In particular, we tested urine from 21 of the deer via PCR and kidneys from 6 of the deer via IHC and PCR. Each deer had either urine or kidney tested (but not both), with the following two exceptions: one deer had both urine and kidney tested, while another deer had neither. We tested serum from 25 deer via MAT analysis using the 20 serovar panel, and all were titrated to endpoint titers. Ages were estimated for 5 of the deer sampled, and ranged from 1.5 – 6.5 years old. No location data were available for these samples; however, some of the last surviving deer were radio collared and tracked for over a year, and they were observed ranging over the entirety of the island.

#### **Data analysis**

##### *Pedigree analysis of captive foxes*

To assess opportunities for vertical or pseudo-vertical transmission of *Leptospira* between foxes in captivity, a pedigree of all captive island foxes was created using parentage data from the captive breeding records using the package kinship2 in R. Results from the serology MAT analyses were used to determine the pathogen exposure status of each of the individuals in the pedigree.

##### *Survival analysis*

Annual survival estimates for the fox year (March-February) were produced using radio-collar data described above. Estimates were made using the Kaplan-Meier estimator with staggered entry protocols described by Pollock (Pollock et al., 1989). Animals were added to the analysis when they were fitted with collars and censored when their collars were not functioning. All mortalities were confirmed upon carcass collection.

##### *Serological cross-reactivity profiles*

Given our focus on determining the origins of the current *Leptospira* outbreak on Santa Rosa Island, we were interested in identifying whether past serum samples from foxes and other host species reflect exposure to the same pathogen strain. The infecting strain cannot be determined directly from MAT results, due to the well-known issue of MAT cross-reactivity among *Leptospira* serovars. We sought to turn this problem into an opportunity (and a new tool),

by analyzing cross-reactivity profiles to assess whether different groups of samples could be attributed to the same infecting serovar.

To enable quantitative comparisons of cross-reactivity patterns, we first refined the MAT datasets to focus on a core set of 9 serovars (Autumnalis, Bratislava, Cynopteri, Djasiman, Icterohaemorrhagiae, Mankarso, Pomona, Pyrogenes and Wolffi). We retained only those samples for which all 9 serovars were tested, and we excluded samples for which all MAT results were negative since they gave no information on past exposure. MAT titers were log-transformed (via the transformation  $1+\log_2(\text{titer}/100)$  to convert the raw scale of 1:100, 1:200, 1:400... to 1,2,3...) prior to all analyses. Titers of <1:100 were recorded as 0.

For a given host population of interest, the cleaned and transformed MAT data from all sampled individuals were converted into a heat-map of MAT titers using the R package *ComplexHeatmaps* (Gu et al., 2016). These heatmaps depict the different serovars as columns, and different individual samples as rows, with colors indicating titer magnitude. The columns (i.e. serovars) were clustered using complete linkage hierarchical clustering, based on the Euclidean distance between the log-transformed titer values.

We sought to test whether samples derived from other host species (e.g. spotted skunks, feral pigs) or from foxes in other time periods (e.g. 1988 samples) reflected exposure to the same strain of *Leptospira* as the one causing the outbreak among Santa Rosa Channel Island foxes. To characterize the MAT cross-reactivity profile arising from the outbreak strain, we analyzed the hierarchical clustering patterns among serovars in the MAT results from wild island foxes from 2006-2013. The defining characteristic of these data was the presence of two distinct clades of serovars, based on titer levels: clade 1 included serovars Pomona, Djasiman and Autumnalis, while clade 2 included serovars Mankarso, Wolffi, Pyrogenes, Bratislava, Cynopteri and Icterohaemorrhagiae.

To assess whether MAT profiles from other sampled populations were consistent with the Santa Rosa Island outbreak strain, we tested whether those datasets exhibited a statistically significant separation into the same two serovar clades, using a permutation-based test of the null hypothesis that there was no significant difference between the two clades (Manly, 2017). To do this, we first calculated a statistic  $D$  which measures how strongly the two clades differ in a given dataset, while accounting for differences in overall MAT reactivity (which could arise from age of the sample or freeze-thaw cycles, or from differences among host species (see section 6.3.2.4)). From the MAT results from each individual serum sample, we calculated a net distance metric reflecting between-clade separation:

$$d = \sqrt{\left( \sum_{i \in C_1, j \in C_2} (S_{i,j}^2) - \left( \sum_{i \in C_1, j \in C_1} (S_{i,j})^2 + \sum_{i \in C_2, j \in C_2} (S_{i,j})^2 \right) \right)}$$

where  $C_1$  is clade 1,  $C_2$  is clade 2,  $S_{i,j}$  is the distance in  $\log_2$  units between the titers against serovars  $i$  and  $j$ , and the summations run over all serovars in the stated clades. The aggregate statistic  $D$  for a full sample set was the sum of all  $d$  scores from individual samples.

We then generated a null distribution of  $D$  values, by computing  $D$  for each of 1000 datasets where serovar labels were permuted (shuffled randomly) for each dataset. From this null distribution of  $D$  values, the P-value for the observed data was derived by computing the probability of observing a  $D$  value equal to or larger than the observed value under the null hypothesis. This P-value represents the probability of obtaining a  $D$  statistic of this magnitude or

greater under the null hypothesis where the sample pool does not exhibit the same two-clade structure as the fox outbreak strain.

### **5.1.2. Reconstructing the spatiotemporal origins of the SRI outbreak**

#### *Telemetry of reintroduced foxes*

From 2003-2006, all wild foxes were collared and tracked with very high frequency (VHF) radio telemetry collars. Precise GPS locations were collected weekly and supplemented with opportunistic detections (known throughout as survival checks). During and after 2007, only a subset of the wild population (40-50 individuals) was tracked due to growing population size. After the captive breeding program closed and the wild population was recovering, telemetry efforts shifted from weekly to biweekly.

Our location information consists of two data types: data with specific GPS locations (GPS data) and less precise location data without GPS coordinates (telemetry data). GPS data were collected for individual foxes at release, trap capture, carcass collection, or at a sighting and confirmation of a collared fox. GPS data were also generated via triangulation telemetry and estimated using the program Locate II (Nams, 1990). Our less precise telemetry data were generated via directional “Yagi” antennas or nondirectional “Omni” antennas, which were both used for routine telemetry life checks. During telemetry surveillance when a collar signal was heard but the fox was not seen or triangulated, the individual, date, and verbal description of the general area of the signal were recorded. If the received radio signal was very strong or came from a well-defined landscape feature such as a canyon, the location was recorded as that specific area. If the signal was heard with the directional antenna, the location at which the signal was detected and the direction from which it came were recorded. However, when the nondirectional antenna was used, only the location at which the signal was detected was recorded.

Given that the telemetry data was a written list of locations, landscape features, and directions rather than a set of GPS coordinates, the recorded descriptions were converted to a digital format for geospatial analysis. Each unique place description (n=10898) was converted to a spatial polygon, mapped using the ‘add polygon’ tool in Google Earth Pro, and saved as a .kml file (Figure 5.1.2.1).

#### *Trapping and sampling*

In addition to radio collars and telemetry survival checks, the National Park Service (NPS) has conducted annual trapping of foxes since 2004 to monitor the reintroduced fox population on SRI. From 2004-2008, target trapping was conducted on an as-needed basis in locations known to be occupied by foxes while the wild population was still small. In 2009, the NPS began a structured 18-grid trapping program on SRI to estimate densities and population sizes of the foxes. Additional target trapping efforts were conducted to install radio collars, for targeted sample collection, and to administer vaccines not completed on the grids. Each of the ladder grids was run for 6 consecutive nights in July or August each year, and target trapping occurred from July to January. The trapping dataset from 2004 to 2010 includes 8830 trap nights.



Black Mountain toward lower Dry and Soledad Canyons



Lower Main Road Paved with omni



**Figure 5.1.2.1. Spatial polygons converted from telemetry data.** Verbal descriptions of telemetry locations were mapped in Google Earth Pro and exported to R as a .kml file for analysis

#### *Estimating the spatiotemporal origin of the outbreak*

To identify the spatiotemporal origin of the outbreak, we focused on foxes with location data in the early reintroduction period between 2004 and 2006, that also had anti-*Leptospira* antibody titers from a positive MAT test in 2006 or 2007. These antibody titers were used to estimate posterior distributions for each fox's time of infection (TOI) using the titer kinetics model developed in our project (section 6.3.2.2). Twelve foxes have TOI estimates and location data available between 2004 and 2006 (Figure 5.1.2.2). Individuals who lack location data at the beginning of their TOI interval (e.g. Fox 26210; Figure 5.1.2.2) only provide partial information and do not inform where the beginning of the outbreak occurred. Additionally, many of these foxes have insufficient location data prior to 2006 to accurately interpolate their position during that time. Thus, our dataset only included the seven foxes with TOI intervals that were completely contained within the range of their available location data (e.g. Fox 14125; Figure 5.1.2.2) and had sufficient location data to estimate their movements through time.

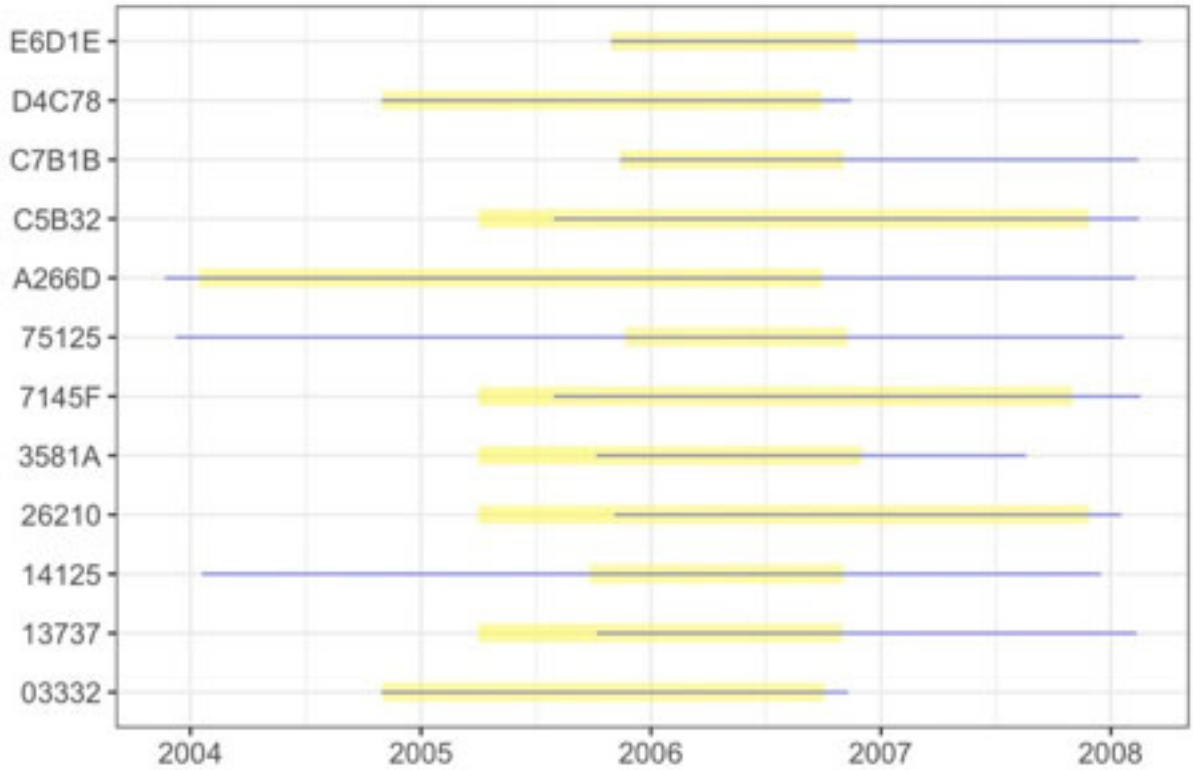


**Figure 5.1.2.2. Foxes with time of infection estimates and location data between 2004 and 2006.** Time of infection intervals were estimated using the titer kinetic model (section 6.3.2.3; yellow). Date ranges of location data for each fox are shown in blue.

#### *Interpolation of fox location data*

Fox location sequences contain both GPS and telemetry data. To represent the spatial error surrounding these measurements, we iteratively resampled the locations for each location date. If the location was GPS data, then a location was sampled from a 1km<sup>2</sup> buffer around the original GPS location, representing the spatial scale of fox movements for foraging and other purposes. If the data was telemetry, then a location was uniformly randomly sampled from within the telemetry polygon. To limit the variance in these samples, telemetry polygons were filtered to be less than 2 km<sup>2</sup> and have a length-to-width ratio less than 6.

Fox location data are sparse through time and consist of varying data types and levels of error. To address both of these challenges in tandem, we interpolated the fox locations through time using a generalized additive model (GAM) using a two-dimensional multivariate normal link (Wood et al., 2016; Wood, 2017). The GAM estimates a location for each date within the location interval using cubic regression splines, where the number of knots was chosen through a generalized cross-validation procedure (Wood, 2017). The fitting of the model was iteratively performed, resampling the locations of the foxes to account for the error surrounding the measurements. The R package *mgcv* was used for fitting (Wood, 2017).

### 5.1.3. Whole genome sequencing and phylogenetics

#### *Whole genome sequencing*

When sufficient genetic material was available for an isolate, DNA was extracted using Qiagen Blood Tissue Kit for whole genome sequencing (WGS). RNase was added before shipping the extractions to USDA National Animal Disease Center, where they were sequenced using Illumina MiSeq, targeting 80-fold coverage across the genome. Sequencing was conducted in three separate runs and produced 2x250 bp paired-end reads.

#### *Genome assembly*

Raw short reads were error-corrected and assembled using the shovill pipeline (<https://github.com/tseemann/shovill>). Briefly, the depth of the FASTQ files was reduced and adapters were trimmed using Trimmomatic version 0.39. Read sequencing errors were corrected and paired-end reads were pre-overlapped prior to assembly. Reads were assembled using SPAdes (Bankevich et al., 2012). Assembled contigs were error corrected by mapping the reads back to the contigs; low quality and short contigs were removed. The resulting contigs were annotated using PROKKA (<https://github.com/tseemann/prokka>), requiring a minimum contig length of 200 to ensure Genbank compliance. Core and accessory genes were identified using Roary (Page et al., 2015). In turn, Roary produced a core genome multi-FASTA alignment using MAFFT v7.475. All sites were required to have a base call in the final multi-sequence alignment, which ultimately contained 3,188,030 sites.

#### *Isolate selection*

In total, seventy-two isolates were sequenced from forty-nine unique hosts (Table A.1). We have duplicates in two ways: some hosts have two isolates from different tissues, and some isolates were resequenced in the last sequencing run. One isolate for each unique host was selected for analysis. When a host had two isolates from different tissues (7 CSL; 1 Northern elephant seal (NES)), the urine-cultured isolate was selected for the sea lions while the kidney isolate was selected for the elephant seal (since all other elephant seal isolates were from kidney tissue). Nearly all of these dual isolates were in the second sequencing run, and this selection resulted in a more even across-batch selection for the phylogenetic analyses. For resequenced isolates, the isolate sequenced in the third sequencing run was selected. This resulted in 13, 13, and 12 CSL isolates being selected from each sequencing run. We did not see substantial differences between any two isolates from the same individual host. Isolate selection is summarized in Table A.1.

#### *Multi-locus strain typing*

Multi-locus strain typing was performed by scanning the assembled contigs against three *Leptospira* PubMLST typing schemes using *mlst* (<https://github.com/tseemann/mlst>) (Ahmed et al., 2006; Boonsilp et al., 2013; Varni et al., 2014).

#### *Phylogenetic reconstruction of *L. interrogans* over time*

We reconstructed the evolutionary relationships among *L. interrogans* serovar Pomona isolates by incorporating molecular sequence and temporal data using a Bayesian Markov chain Monte Carlo (MCMC) analysis in BEAST v1.10.1 to estimate a time-calibrated phylogeny (Suchard et al., 2018). We applied a Hasegawa, Kishino, and Yano nucleotide substitution model with gamma-distributed rate heterogeneity and a proportion of invariant sites (HKY +  $\Gamma$  + I), and

we also selected an uncorrelated relaxed molecular clock model as the clock model prior in these phylogenetic analyses (Drummond et al., 2006; Hasegawa et al., 1985). Three independent MCMC chains were run for 100 million generations, and posterior distributions were sampled every 1,000 generations. Independent chains were combined using LogCombiner and the first 10% of each independent chain was discarded as burn-in. Model parameters were assessed for convergence and sufficient effective sample sizes (>200) in Tracer v1.7.1 (Rambaut et al., 2018). The maximum clade credibility tree was identified in TreeAnnotator (Suchard et al., 2018).

## 5.2. *Leptospira* in California Sea Lions

### 5.2.1. Extend long-term time series of leptospirosis in stranded CSL

The Marine Mammal Center collected data and samples from 3420 California sea lions that stranded along the central and northern coast of California (Figure 5.2.1.1) and were admitted for rehabilitation between January 1, 2015 and December 31, 2020. Of these, 391 were diagnosed with leptospirosis using characteristic serum chemistry results, clinical signs, and post-mortem findings when appropriate (Colagross-Schouten et al., 2002; Greig et al., 2005; Gulland et al., 1996). Clinical, morphometric, and demographic data as well as blood and urine were collected from all sea lions during the course of routine clinical care, and kidney samples were collected in those that died or were euthanized (as described in Prager et al. 2020). Samples were analyzed using MAT (N=1373) to assess prior exposure; PCR of urine or kidneys (N=304), or culture (N=634) and *Leptospira* isolation (N=65) from urine and kidney, to assess current infection; and serum chemistry analyses (N=2787) to assess clinical impact of leptospirosis (Table 6.2.1.1).

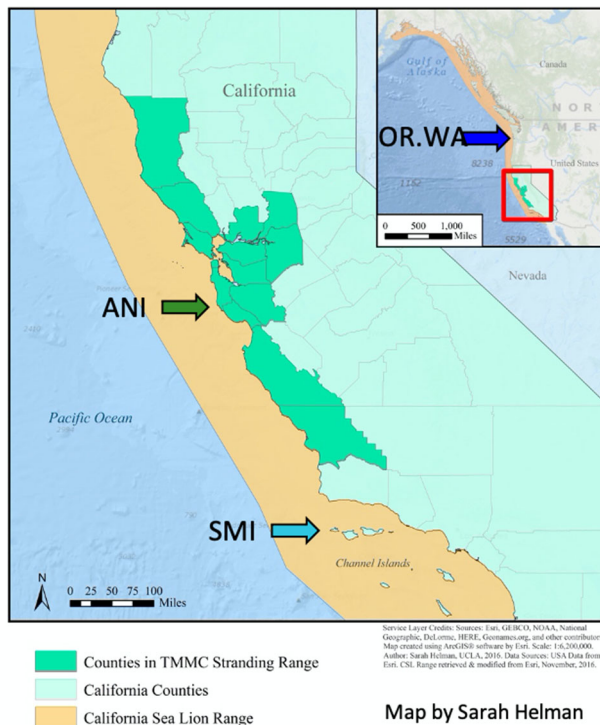


**Figure 5.2.1.1. Map of California sea lion sampling locations.** The map includes the Marine Mammal Center stranding range (in bright green), the California Channel Islands of the coast of southern California, and the three locations where wild, free-ranging sea lions were sampled – ANI (Año Nuevo Island), SMI (San Miguel Island), OR.WA (Oregon and Washington - shown in the inset). The area of the coast colored in orange indicates the California sea lion range.

Serum chemistry analyses were performed on an ACE Clinical Chemistry System (Alfa Wassermann Inc., West Caldwell, New Jersey, USA). Serum MAT was performed at the California Animal Health and Food Safety (CAHFS) laboratory, Davis, California, or at the CDC, Atlanta, Georgia, using live cultured *Leptospira* spp. (reference strains) to measure serum anti-*Leptospira* antibody titers. Samples run at CAHFS were run against a 1 or 6 serovar panel and samples run at the CDC were run against a 2 or 19 serovar panel (as described in (Prager et al., 2015, 2020)). We only report MAT titer results against *L. interrogans* serovar Pomona as historically this is the strain that elicits the highest MAT titer in the majority of California sea lions tested (Lloyd-Smith et al., 2007), and it is the only serovar ever isolated from this host species over five decades of study (Prager et al., 2013; Zuerner & Alt, 2009). Serum samples were tested at doubling dilutions starting from 1:100, and agglutination was read using dark field microscopy. Endpoint titers were reported as the highest dilution that agglutinated at least 50% of the cells for the strain tested (Dikken & Kmety, 1978). Titer results were log transformed for ease of interpretation using the following formula:  $\log_2(\text{titer}/100) + 1$ , thus a titer of 1:100 = 1, 1:200 = 2, etc. Titers reported as <1:100 were set equal to 0 on both the log and regular scale. Throughout this section, “antibody titer” refers to this log transformed titer value. All animals with a detectable titer (i.e.  $\geq 1:100$ ) were considered seropositive and assumed to have been infected with *Leptospira* at some point.

We assessed leptospiral DNA shedding in urine using real-time PCR (Wu et al., 2014). Because urine was collected under anesthesia, and anesthesia can pose a health risk to compromised animals, urine was collected only from sea lions undergoing anesthesia for other clinical purposes or during necropsy; anesthesia was never performed for the sole purpose of collecting a study sample. Individuals shedding leptospiral DNA were considered infected and infectious because the primary mode of transmission of *Leptospira* is by either direct or indirect contact with leptospire shed in the urine of infected individuals (Ellis, 2015).

All California sea lion samples were collected under authority of Marine Mammal Protection Act Permits No. 932-1905-00/MA-009526 and No. 932-1489-10 issued by the National Marine Fisheries Service (NMFS), NMFS Permit Numbers 17115-03, 16087-03, and 13430. The sample collection protocol was approved by the Institutional Animal Care and Use Committees (IACUC) of The Marine Mammal Center (Sausalito, CA; protocol # 2008-3), the University of California Los Angeles (ARC # 2012-035-12), and the Marine Mammal Laboratory (Alaska Northwest 2013-1 and 2013-5). The Marine Mammal Center and the Marine Mammal Laboratory adhere to the national standards of the US Public Health Service Policy on the Humane Care and Use of Laboratory Animals and the USDA Animal Welfare Act. UCLA is accredited by AAALAC International and adheres to the national standards of the US Public Health Service Policy on the Humane Care and Use of Laboratory Animals and the USDA Animal Welfare Act. Isoflurane gas was used to anesthetize all wild-caught, free-ranging sea lions for sampling, and from all stranded sea lions from which urine was collected.

### **5.2.2. Extend long-term time series of CSL demography**

California sea lion mark-resight-recovery efforts were conducted from 2015 through 2018 (as described in (DeLong et al., 2017)), extending this long-term time-series to 33 years (1987-2019; Table 6.2.2.1). Briefly, approximately 300 California sea lion pups were weighed and branded on San Miguel Island each year in late September or early October (i.e. at roughly 4 months old). A subset of branded pups were reweighed in February of the following year (i.e. at roughly 8 months old), and mean weights were calculated by age and sex. Brand-resights of all

age and sex classes were conducted on San Miguel Island and Año Nuevo Island at key timepoints throughout the year. These data were then analyzed using a Cormack-Jolly-Seber model to estimate age-specific survival. The modeling approach is as described in DeLong et al. (DeLong et al., 2017), however the R (R Core Team, 2019) package `markedTMB` (Laake, 2020), a derivative of `marked` (Laake, 2013), was used rather than `RMark` (Laake, 2013), and a multi-state model was used to estimate movement between locations. Survival estimates and pup counts were then used to numerically reconstruct the population by age and sex class as described previously (Laake et al., 2018), with the exception that density-dependent effects were not included.

### **5.2.3. Understand how intrinsic and extrinsic non-stationarities drive leptospirosis outbreaks in CSL**

#### ***5.2.3.1. The endemic period***

##### *Leptospirosis data*

Since 1983, California sea lions (*Zalophus californianus*) stranding along the central California coast (37°42'N, 123°05'W to 35°59'N, 121°30'W) have been rescued and treated by TMMC. Weight, sex, and estimated age class of all sea lions are recorded. Leptospirosis diagnosis was based on a combination of clinical symptoms and serum chemistry analysis, as described in (Gulland et al., 1996; Lloyd-Smith et al., 2007). Annual case numbers were calculated as the total number of cases that strand between July 1st of the current observation year and June 30th of the following year. Such July-June years are typically used as sea lions observation years because they correspond more closely to their biological breeding cycle (DeLong et al., 2017).

To derive a normalized, continuous measure of leptospirosis outbreak intensity, we divided the total number of leptospirosis cases by the total size of the sea lion population that year (excluding pups), taken from the demographic reconstruction conducted by (Laake et al., 2018). To obtain a categorical classification of outbreak intensity, years were divided into "weak outbreak", "medium outbreak", or "strong outbreak" years using threshold values 0.00045 and 0.0011 cases/population size, determined using k-means clustering (using core R (R Core Team, 2018) function `kmeans`).

##### *Susceptible reconstruction*

The supply of susceptible hosts is a crucial driver of the dynamics of immunizing infections. It is often called an 'intrinsic driver' since it arises from factors intrinsic to the host-pathogen system. We estimated temporal changes in relative susceptibility of the sea lion population by combining long-term datasets on sea lion recruitment, survival, and leptospirosis cases, building on a method developed for human childhood infections (Finkenstädt & Grenfell, 2000). The existing method does not account for survival as this effect is generally negligible for humans. For most animals, however, variation in survival is likely to impact demography. DeLong and colleagues found strong interannual variation in survival of young sea lions, which likely have a significant effect on how many susceptible sea lions are present in the population each year (DeLong et al., 2017). We therefore extended the existing method (Finkenstädt & Grenfell, 2000) so that it could take into account age- and sex-specific survival. We combined the annual cases time series (see section 6.2.1.1, Figure 6.2.1.1) data with a recent time series of

estimates of sea lion population size (see section 6.2.2, Figure 6.2.2.2) for all age and sex classes (Laake et al., 2018), and computed the quantity:

$$S_{a,t} = S_{a-1,t-1} \sigma_{a-1,t-1} \left(1 - \frac{1}{P_{obs}} \frac{C_{a-1,t-1}}{S_{a-1,t-1}}\right),$$

where  $S$  is the number of susceptibles,  $a$  is the age of the animals in the  $S$  cohort being calculated,  $t$  is the year for which  $S$  is being estimated,  $\sigma_{a-1,t-1}$  is the proportion of animals aged  $a-1$  in year  $t-1$  that survives to year  $t$  (and thus become age  $a$ ),  $P_{obs}$  is the probability of observing a leptospirosis case,  $C_{a-1,t-1}$  is the number of stranded leptospirosis cases of age  $a-1$  in year  $t-1$ , and  $S_{a-1,t-1}$  is the number of susceptibles of age  $a-1$  in year  $t-1$ .

For any given year  $t$ , this method estimates the number of susceptible individuals of age  $a$  that remain in the population after accounting for loss due to infection and mortality (using survival estimated in (DeLong et al., 2017)). All individuals were assumed to be susceptible in 1983, based on the fact that no confirmed cases of leptospirosis in CSL were observed from the start of observations at TMMC in 1975 until mid-1984.

We do not know the value of parameter  $P_{obs}$ , which is the proportion of infected individuals that end up stranding and being detected within the operating range of TMMC. Because  $P_{obs}$  affects estimation of the absolute number of susceptibles, we tested a range of values for  $P_{obs}$ , and found that for all values that do not result in over-estimates of the number of susceptibles (i.e. returning values larger than the population size), the patterns of the susceptibility index were highly similar after scaling to mean 0 and standard deviation 1, and normalizing susceptibles by dividing by population size. We therefore arbitrarily chose a mid-range value of  $P_{obs} = 0.01$  and used the normalized and scaled (mean = 0, SD = 1) proportion of susceptibles, as this represents the relative changes in susceptibility over time that we are interested in.

#### *Analysis of sex and age classes associated with Leptospira transmission*

A key question is which sex and age classes are most important for driving *Leptospira* transmission. We tested this by calculating several versions of the proportion of susceptibles, each of which includes a different combination of sex and age classes (Figure 6.2.3.2). For each of these reconstructions, a univariate regression model (generalized linear model with log link function and Gamma error distribution) was fit with the number of cases divided by population size as outcome variable. Model fits were compared using cross-validation statistics (as described below in the section on model selection), and these fits were used as a basis for assessing which sex and age classes might be the most important determinants of susceptibility in the population. The tested combinations are shown in Table 6.2.3.1.

#### *Testing for indirect influence of the environment via demographic processes*

The main goal of this study is to disentangle the relative contributions of susceptibles and environment to outbreak size. There are two pathways through which environment could affect transmission: (1) directly through effects on body condition or behavior that alter an individual's immune function or the contacts between individuals, and (2) indirectly by affecting the proportion of susceptibles through effects on sea lion survival and birth rate. Here, we assessed evidence for the latter by creating a new estimate of susceptibles that removes observed interannual variation in survival and birth rate caused by environmental and other factors. This variable was then compared with the original susceptible reconstruction in order to estimate

whether demographic variation is an important contributor to variation in outbreaks of leptospirosis.

The new estimate of susceptibles was calculated using the same method used for the original susceptible reconstruction, but instead using new estimates of population size that were based on smoothed birth rates and survival. Smoothed annual birth rates are the values predicted by a linear regression fitted to the full birth rate time series, which effectively smooths out annual variation while retaining the observed overall increase in birth rates. Smoothed survival was calculated by taking the overall mean for each age class, which removes annual variation but retains age-specific differences in survival. Finally, this estimate of susceptibles was divided by the smoothed population size (calculated using the smoothed birth rate and survival estimates).

The contributions of the two estimates to outbreak size were then compared by fitting a model for each estimate, using the approach described above.

### *Environmental covariates*

Out of many potential environmental variables, we selected a small number that may be important for different aspects of sea lion biology. This selection was based on existing knowledge on sea lions and hypothesized influences on *Leptospira* transmission dynamics.

Coastal upwelling is crucial for ecosystem productivity, as upwelling currents transport nutrients to the coastal ecosystem (Bograd et al., 2009). Optimal nutrient availability occurs when downwelling and upwelling are intermittent, due to a trade-off between nutrient transport from deep currents to the surface and oceanward removal of nutrients already at the surface, analogous to a conveyor belt (Menge & Menge, 2013). Upwelling conditions have rapid effects on the abundance and location of fish, including prey species such as anchovy and sardine important to sea lions (Chavez et al., 2003). In the short term, the location of prey species is strongly linked to local upwelling conditions, while conditions over longer periods will affect both the location and abundance of fish (Chavez et al., 2003). Down- and upwelling are seasonal, and the earlier in the year the period dominated by upwelling starts, the higher that year's ecosystem productivity tends to be (Bograd et al., 2009). This annual start of the upwelling season is called spring transition. Both coastal upwelling and timing of spring transition are therefore likely to be important for sea lion survival (prey abundance) and movement/mixing (prey location). Like upwelling, sea surface temperature (SST) is known to affect fish abundance and location, and significant correlations between SST and sea lion foraging behavior, as well as survival, have been observed (Melin et al., 2008). Upwelling, spring transition, and SST are three potentially important abiotic variables affecting sea lion condition and movement. We further include two biotic variables as proxies for cumulative environmental conditions experienced by sea lions over the course of the year preceding an outbreak. Pup survival is a proxy for conditions affecting lactating females, and yearling survival is a proxy for conditions affecting young sea lions that forage independently.

Sea surface temperature (SST) data are freely available from the National Data Buoy Center (NOAA) at [www.ndbc.noaa.gov](http://www.ndbc.noaa.gov). To represent the southern sea lion range, we used data from buoy 46025 (33.749N, 119.053W). For the center of the range, there is no single buoy for which data are available for the entire study period, so instead we had to use a combination of buoys 46026 (37.755N, 122.839W), 46028 (35.712N, 121.858W), and 46042 (36.785N, 122.398W). For the north of the range, we used a combination of buoys 46010 (46.200N, 124.200W), 46029 (46.143N, 124.485W), and 46089 (45.925N, 125.771W) (Figure 5.2.3.1). Upwelling index data are freely available from the Pacific Fisheries Environmental Laboratory (NOAA) at [www.pfeg.noaa.gov](http://www.pfeg.noaa.gov). These were used as a measure of upwelling conditions and to

calculate the timing of spring transition, calculated as the day of the first half of the calendar year on which the cumulative upwelling index reaches a minimum, following (Bograd et al., 2009). Upwelling data measured at latitudes 36N and 39N were used to represent conditions in the south and center of the sea lion range. Figure 5.2.3.1 shows the location of each buoy and each oceanographic variable that is under consideration for model selection. In order to allow direct comparison of fitted effect sizes of each variable in a model, anomaly data were used. Monthly SST and upwelling anomalies were calculated by subtracting the overall mean value of a month from the observed value for that month, so that only the relative variation over time was used for each variable. For each of the two periods considered for these two variables (Jun-Jul and Aug-Sep-Oct), the mean for those two or three months was used. Annual anomaly data were used for the timing of spring transition and for pup and yearling survival.

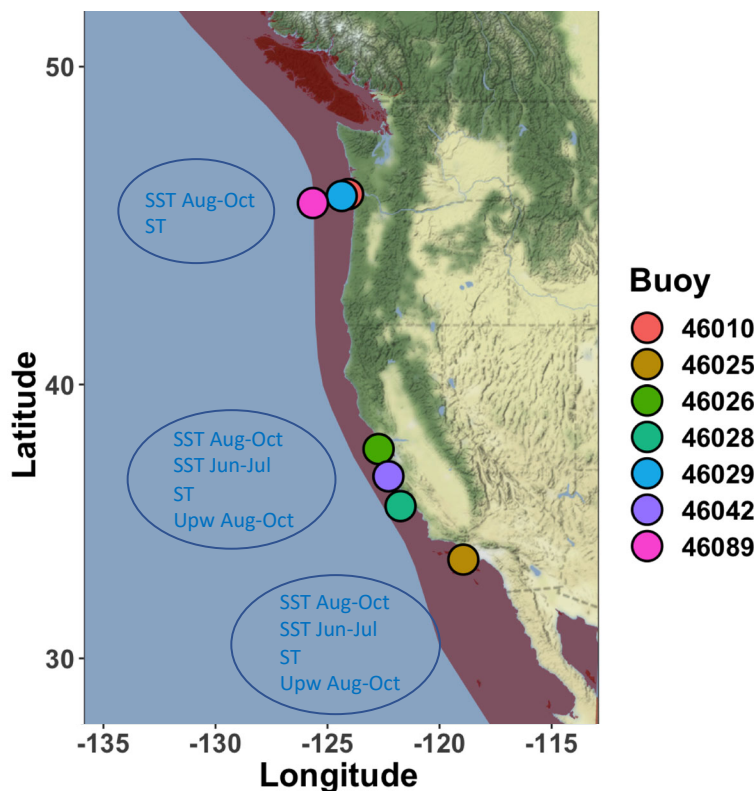


**Figure 5.2.3.1. Map of the US West Coast, the occurrence range of CSL, and buoy locations.**

Shows most of the occurrence range of California sea lions (source: IUCN Red List), buoy locations of all buoys used for environmental data (source: National Data Buoy Center, NOAA), and the location of environmental variables used for model selection (SST = sea surface temperature, ST = timing of spring transition, Upw = Upwelling index). Map created using packages `rgdal` (Bivand et al., 2018), `ggmap` (Kahle & Wickham, 2013), `ggplot2` (Wickham, 2016) in R (R Core Team, 2018).

### *Model fitting and model selection*

The main goal of this study is to identify important demographic and environmental drivers of *Leptospira* transmission, as represented by interannual variation in outbreak size. To determine which combination of variables is best able to explain annual outbreak size, we used generalized additive models that allow for nonlinear effects of variables. Natural splines were used as nonlinear functions, limiting the number of knots to 1 in order to ensure that variable effects can be interpreted in a meaningful way. A Gamma error distribution and log link function were used to account for over-dispersed proportional data (number of cases divided by population size) constrained to be larger than 0 (Hardin & Hilbe, 2002). In order to limit model complexity and retain biological interpretability, the number of variables in a model was restricted to be between one and four.

Selection of top models was done using cross-validation to assess out-of-sample predictive accuracy. Owing to the autocorrelated nature of time series data, regular leave-one-out cross-validation would not be appropriate, so instead we used  $h\nu$ -block cross-validation, where one focus ( $h$ ) datapoint as well as two ( $\nu$ ) prior and two following datapoints were removed from the training set, and the focus point was predicted with the model trained on the remaining datapoints (Racine, 2000). This was repeated for each datapoint in the time series. The out-of-sample predictions for all datapoints were stored, and this full set of predictions was compared statistically with the observed data.

We used a combination of two statistics to assess model fit and to rank models. Adjusted  $R^2$  (adjusted to penalize for larger numbers of variables (Mittlböck & Heinzl, 2002), using  $1 - \frac{\text{Deviance}_i}{\frac{n-p-1}{\text{Deviance}_{null}}}$ , where  $\text{Deviance}_i$  = the deviance of model  $i$ ,  $\text{Deviance}_0$  = deviance of the null model,  $n$  = sample size and  $p$  = number of parameters) captures the overall fit of the model to observations, but  $R^2$  is sensitive to large differences between observed and predicted values. This means that even if the model would, for example, predict all outbreak years accurately except for one year with a large outbreak, the  $R^2$  value might be much lower than that of a model that results in worse predictions for most years but predicts one very large outbreak year well. It is therefore not optimal for situations with over-dispersed data. In order to balance this effect and introduce more biological relevance into the model selection procedure, we implemented an additional “Feature Mismatch” (FM) statistic. To calculate the FM value, outbreak years were first categorized into "weak", "medium" and "strong" outbreaks as described above. Each predicted datapoint was then given a mismatch score to indicate how strongly its outbreak category differs from the observed category for that year, receiving 0 when the outbreak was in the same category, 1 when they differ by one degree (weak vs. medium or medium vs. strong), and 2 when strong was predicted for a weak-outbreak year or vice versa. The FM value for a model is the sum of mismatch scores for all predicted datapoints (i.e. the lower the FM value, the better the correspondence between predicted and observed time series of outbreak categories). Finally, the models were ranked taking into account both Adjusted  $R^2$  and FM by summing the relative ranks within each statistic.

After this initial model selection step using cross-validation, the 20 top-ranked models were fit to the full dataset, and Akaike weights (Burnham & Anderson, 2002) were computed for all models. Akaike weights use AIC values to calculate a relative measure of importance of each model in a selection of models

### *Environment and body condition*

Spring transition is suspected to influence transmission through effects on sea lion body condition and immunity. As a preliminary look at the biological mechanisms that link environment and transmission, we tested the correlation between body condition and spring transition south. As a proxy for body condition, we used body mass index (BMI; body weight (kg) / body length (m)<sup>2</sup>). Gaussian linear regression and ANOVA were used to test the correlation between the dependent variable, BMI, and spring transition. Because BMI is dependent on age, the interaction between age class and spring transition was tested and, if significant, a regression model was fit for each age class. Sea lions can experience significant morbidity from causes other than leptospirosis (Greig et al., 2005), which can affect body condition and possibly the correlation between environment and body condition. We therefore tested the interactive effect of the most important co-morbidities (pneumonia, domoic acid

toxicity, malnutrition) on the relationship between environment and body condition by including each of these comorbidities separately in the regression models.

There was a significant negative correlation between BMI and spring transition south for all age classes except adults (test statistics for regression incl. all ages: effect est. =  $-0.5 \pm 0.2$ , F-value = 49.1, df = 8759, P-value < 0.0001; also reported in section 6.2.3.1). Analyses and results on the effects of comorbidities (i.e. having been diagnosed with pneumonia, domoic acid toxicity, or malnutrition) on the correlation between BMI and spring transition can be found in the appendix for 6.2.3.1. These results are provided for completeness, but together indicate that the effects of comorbidities are inconsistent and only seen for some age classes.

### *Real-time prediction*

A model that can adequately predict outbreak size ahead of time would not only increase confidence in the selected variables, but would also help the preparedness of rescue centers along the US Pacific Coast and the pathogen control and risk communication strategies of agencies working to mitigate risk to humans, their pets, and species of conservation concern that share the coastal environment where sick sea lions strand. We therefore tested how well different models were able to predict outbreak size ahead of the outbreak season. We aimed to predict outbreak size of year  $t$  using models fitted to all data up to year  $t - 1$ , which would resemble a realistic situation where all past data are available. The starting dataset for this one-step ahead prediction consisted of the first 14 years (1984-1997) and was used to predict year 15 (1998). The second dataset then included the first 15 years (1984-1998) and was used to predict year 16 (1999), and so on until 2012. This resulted in a dataset of 15 predicted years (1998-2012).

Candidate variables for the prediction models included all variables available before or at the start of the outbreak season (August): susceptibles, spring transition (south, central, north), SST (south, central), yearling and pup survival, and the number of cases in the preceding year. We fit generalized linear models with Gamma error distribution and log-link function (as opposed to a generalized additive model, which was no longer required because the only nonlinear function that had been estimated was for upwelling and this variable was not a candidate variable here). A maximum of three variables in one model was allowed. Adjusted  $R^2$  and FM scores of the combined dataset of all predicted years were used as model selection statistics. The five top scoring models were then used to calculate a model-averaged prediction for each year. This was done for each year by first calculating the AIC values for the fit of each of the five models to the years preceding the predicted year and then using these AIC values to calculate Akaike weights, which then allowed the calculation of a weighted average prediction.

### *Long-term prediction of climate change impacts*

The finding that leptospirosis outbreaks in sea lions are driven by environmental conditions provides an opportunity for assessing potential effects of climate change on future outbreak size. Existing research on climate change effects on the California Current system provides a solid basis for simulating the effects of different climate change scenarios on leptospirosis outbreak size.

The top model resulting from the main model selection procedure was used to predict outbreak size under various simulated environmental conditions based on published literature. We considered two types of scenarios – altered mean conditions and increased variation – separately as well as in combination. First, simulated values were generated for each of the three environmental variables in the top model. For each year of the existing dataset, outbreak size was then predicted using the fitted functions of the top model, but in a stepwise manner in order to

realistically reconstruct susceptibles. For the first year, the original proportion of susceptibles was used as input for the model, combined with that year's simulated values for the three environmental variables. This resulted in a predicted outbreak size for the first year. In order to predict the next year, we first performed susceptible reconstruction taking into account the observed survival and population size data, but, instead of using the observed number of cases for the preceding year, we used the predicted number of cases instead. This new value for susceptibles was then used as input for the model in order to predict outbreak size in the second year. This procedure was applied to all remaining years. Note that the environment is also known to directly affect sea lion survival, which may in turn affect transmission rates and outbreak size. This effect was not included in these models because the correlation between the different environmental variables and sea lion survival is unknown.

Simulations of the environmental variables were based on published predictions. Upwelling in the south of the sea lion range was predicted to become weaker during summer (Brady et al., 2017), and spring transition was predicted to start later in the year (Bakun et al., 2015; Barth et al., 2007; Schwing et al., 2006). As SST correlates inversely with upwelling (upwelling water lowers SST), SST was expected to increase (Brady et al., 2017).

#### *Software*

All data manipulation, statistics and plotting were done using R software (R Core Team, 2018), and R packages ggplot2 (Wickham, 2016), ggmap (Kahle & Wickham, 2013), mgcv (S. Wood, 2011), gganimate (Pedersen & Robinson, 2019), dplyr (Wickham et al., 2019).

#### **5.2.3.2. Fadeout and re-emergence**

Datasets compiled in other sections of this report were used to characterize the observed fadeout and reemergence of *Leptospira* in the California sea lion population (first described in 6.2.1) and to identify the underlying mechanisms driving these events. These datasets include the long-term time-series of *Leptospira* in stranded California sea lions (6.2.1), of sea lion demography, movement, and pup weight (6.2.2), and of *Leptospira* in wild-caught, free-ranging California sea lions (6.3.6).

### **5.3. Understanding the Santa Rosa Island outbreak**

#### **5.3.1. Long-term surveillance of the leptospirosis outbreak on Santa Rosa Island**

##### ***Sample collection and population monitoring: island foxes and spotted skunks***

##### *Trap set-up*

Foxes and skunks were trapped on grids annually from 2009 through 2020 on 18 twelve-trap grids, each run for 6 consecutive nights (Figure 5.1.1.2). Grids were run in July and August most years, with two years extending slightly later into the fall. Tomahawk live traps (Tomahawk Live Trap, Tomahawk, WI, USA; 0.66m X 0.23 m X 0.23m) were baited with dog kibble and had loganberry lure placed on and around each trap each day. Traps were checked once a day every morning and left open for 24 hours (Figure 5.3.1.1). In addition to the annual grid trapping, supplemental target trapping to administer vaccinations, fit radio collars, and collect additional samples was conducted between July and February of each fox year from

2003-2020. As in section 5.1, a fox year is defined as March through February, and corresponds with the beginning of the fox breeding season (since pupping begins each year in March).



**Figure 5.3.1.1. Island fox in a Tomahawk trap.**

#### *Fox sample and data collection*

Upon capture all foxes were scanned for a passive integrated transponder (PIT tag) to uniquely identify each individual. If it was the first time a fox was captured, the fox was injected with a PIT tag. During handling, foxes were weighed, sexed, assessed for overall condition, parasite load, reproductive status, body condition, and age class. Body condition was assessed on a scale of 1-5, where 5 is obese, 1 is emaciated, and 3 is optimal. Age class was determined by tooth wear on a scale of 0 to 4 with 0s being pups and age classes 1-4 being adults (Wood, 1958). Female reproductive status was classified into three categories: not active, lactating, and signs of lactation. Blood was collected from as many foxes as possible during trapping with 1-3 samples collected per fox throughout the trapping season. Up to 10 ml of blood per adult fox and 4 ml of blood per pup was collected by venipuncture with a 22 gauge, 1 inch needle (Figure 5.3.1.2). Urine was collected from foxes when possible beginning in 2011. Urine was collected via cystocentesis using a 22 gauge, 1 inch needle (Figure 5.3.1.2), or on occasion via “free catch” opportunistically during the examination

Foxes began being released back into the wild in 2003 and were closely monitored from the beginning. Therefore, during the course of this long-term study, an impressively large and comprehensive database was assembled, which provides the foundation for our investigations into *Leptospira* dynamics in foxes on SRI. This database consists of 18 years of trapping data, 12 years of grid trapping data, 18 years of sample collection, and 16 years of test results from samples collected from wild (vs. captive foxes during the breeding program, which ended in 2009) Channel Island foxes (Table 5.3.1.1, Table 5.3.1.2). These data represent 7854 captures of 1653 individual wild foxes. Serological analysis by MAT has been conducted on 2898 serum samples, from 1385 unique individuals; PCR results have been obtained from 993 urine samples,

from 598 unique individuals; culture results have been obtained from 834 urine samples, from 518 unique individuals (Table 5.3.1.2).



**Figure 5.3.1.2. Collecting blood and urine samples from island foxes.** (Left) Blood collection by venipuncture. (Right) Urine collection by cystocentesis.

The long-term nature of the study, combined with the fact that the SRI island foxes are a relatively small population on an isolated island, means that many individual animals have been repeatedly trapped and sampled over multiple years (Table 5.3.2.1). 1385 individual foxes were tested for evidence of antibodies against *Leptospira* via MAT; of those, 221 were tested at least four times, and 1 was tested 11 times. 598 individual foxes were tested for evidence of infection and shedding via urine PCR; of those, 243 were tested more than once, and 1 was tested 8 times. Thus, the data set provides the rare opportunity to explore longitudinal patterns within individual foxes, as well as the cross-sectional patterns traditionally used to investigate most wildlife disease systems.

<b>Fox Year</b>	<b>Captures Total</b>	<b>Individuals Total</b>	<b>Captures Grids</b>	<b>Individuals Grids</b>
<b>2003</b>	25	9	NA	NA
<b>2004</b>	64	18	NA	NA
<b>2005</b>	51	24	NA	NA
<b>2006</b>	111	39	NA	NA
<b>2007</b>	115	49	NA	NA
<b>2008</b>	262	96	NA	NA
<b>2009</b>	296	140	126	67
<b>2010</b>	472	166	132	63
<b>2011</b>	282	164	171	86
<b>2012</b>	370	191	317	152
<b>2013</b>	668	307	371	152
<b>2014</b>	688	304	418	148
<b>2015</b>	727	292	589	219
<b>2016</b>	731	285	671	239
<b>2017</b>	742	363	561	235
<b>2018</b>	862	377	694	274
<b>2019</b>	750	316	642	245
<b>2020</b>	638	308	570	267
<b>Total</b>	7854	1653*	5262	1047*

**Table 5.3.1.1. Trapping data for Channel Island foxes, including the number of total captures and unique individual wild foxes captured from 2003 to 2020.** The first two columns show the total numbers combining target trapping and grids, while the last two columns show the numbers for grid trapping only. \*Total number of individuals captured is the number of unique individuals from 2003-2020 not the sum of number of individuals within each season.

<b>Fox Year</b>	<b>MAT Total</b>	<b>MAT Individuals</b>	<b>PCR Total</b>	<b>PCR Individuals</b>	<b>Culture Total</b>	<b>Culture Individuals</b>	<b>IHC Total</b>	<b>IHC Individuals</b>	<b>SerumChem Total</b>	<b>SerumChem Individuals</b>
<b>2004</b>	2	2	1	1	0	0	1	1	6	6
<b>2005</b>	2	2	0	0	0	0	0	0	17	16
<b>2006</b>	33	31	4	4	0	0	3	3	40	33
<b>2007</b>	37	37	3	3	0	0	0	0	32	32
<b>2008</b>	46	46	2	2	0	0	2	2	5	5
<b>2009</b>	99	99	1	0	0	0	1	1	22	22
<b>2010</b>	154	144	1	1	11	11	1	1	34	29
<b>2011</b>	161	153	33	33	36	36	0	0	53	51
<b>2012</b>	184	181	45	44	39	38	0	0	53	51
<b>2013</b>	341	292	186	166	158	122	0	0	102	88
<b>2014</b>	336	303	217	198	198	182	0	0	80	73
<b>2015</b>	309	283	191	175	178	160	0	0	73	64
<b>2016</b>	266	265	56	56	56	56	0	0	0	0
<b>2017</b>	299	296	75	75	67	67	0	0	0	0
<b>2018</b>	341	328	55	53	50	48	0	0	0	0
<b>2019</b>	288	284	123	120	41	41	0	0	0	0
<b>Total</b>	2898	1385*	993	598*	834	518*	8	7*	517	207*

**Table 5.3.1.2. Samples from wild Channel Island foxes.** Data includes the number of samples collected for MAT, PCR, Culture, and IHC analysis by total samples collected (Total) and by unique individual island fox (Individuals) in 2004-2019. \*Total number of individuals sampled is the number of unique individuals sampled per test type from 2004-2019 not the sum of number of individuals within each season.

### *Skunk sample and data collection*

Upon capture during grid trapping, all skunks were scanned for PIT tags and newly captured skunks were injected with PIT tags. During target trapping, however, not all skunks were individually marked in all years. Skunks were not tagged in 2004-2005. Most skunks were individually tagged in 2006-2008 and again in 2011-2020. However, during target trapping in 2009-2010, many skunks were not individually tagged. PIT tagged skunks were weighed, assessed for overall condition, parasite load, tooth wear, and age class. Skunks were classified as either adults or juveniles as determined by weight and tooth wear. When possible, blood was collected via jugular venipuncture using a 23 gauge 1 inch needle, and urine was collected via free catch, expression (via palpation of the bladder and exertion of gentle pressure), or cystocentesis. These procedures are very challenging in the field due to the skunks' small size, therefore sample sizes are lower than trapping events.

Between 2003 and 2020, during the course of 25743 trap nights, there were 3392 skunks captured (Table 5.3.1.3), of which at least 1638 were unique individuals. However, the true number of unique individuals is unknown since some skunks were not PIT tagged. Of samples collected between 2011 and 2019, 336 skunk sera have been analyzed for anti-*Leptospira* antibodies by MAT (excluding duplicates of samples that were retested), 75 urine or kidney samples have been analyzed for *Leptospira* DNA via PCR, and culture and *Leptospira isolation* has been attempted on 32 urine samples (Table 5.3.1.4).

### *Sample processing in the field*

After collection in the field, blood was placed into a red-top tube and then into a cooler with ice. Usually between 3-5 hours after collection, blood samples were centrifuged to separate the serum and red blood cells. Serum was aliquoted into 2 ml cryovials, and samples were then placed immediately into a -20°C freezer. Beginning in 2010, all stored samples were transferred to a -80°C freezer, and new samples were placed into the ultra-cold freezer within 1-6 months of collection.

Upon collection, 1cc of sterile urine was placed into transport media, and then 0.1cc of the urine/transport media mixture was inoculated into culture media (Adler & de la Peña Moctezuma, 2010). The remaining urine was placed into a red top tube and immediately placed into a cooler of ice. Within 3-5 hours of collection, the whole urine was centrifuged for 20 minutes until a pellet formed. The supernatant was discarded, and the pellet retained. The pellet was then resuspended in 1cc of phosphate buffered saline and centrifuged for an additional 20 min. The rinsed pellet was then immediately stored in a -20°C freezer (Wu et al., 2014).

<b>Fox Year</b>	<b>Trap Nights</b>	<b>Captures Total</b>	<b>Captures With ID</b>	<b>Captures No ID</b>	<b>Unique IDs</b>
<b>2004</b>	542	161	0	161	0
<b>2005</b>	368	68	1	67	1
<b>2006</b>	995	448	417	31	343
<b>2007</b>	682	293	293	0	255
<b>2008</b>	1612	629	614	15	443
<b>2009</b>	2089	445	282	163	179
<b>2010</b>	2573	291	122	169	91
<b>2011</b>	1689	199	167	32	129
<b>2012</b>	1592	221	204	17	168
<b>2013</b>	2045	257	239	18	177
<b>2014</b>	2005	201	192	9	146
<b>2015</b>	1710	51	51	0	41
<b>2016</b>	1477	32	30	2	26
<b>2017</b>	1656	20	19	1	19
<b>2018</b>	1678	16	16	0	15
<b>2019</b>	1538	17	17	0	16
<b>2020</b>	1492	43	43	0	37
<b>Total</b>	<b>25743</b>	<b>3392</b>	<b>2707</b>	<b>685</b>	<b>1638*</b>

**Table 5.3.1.3. Trapping data for island spotted skunks, 2004-2020.** Data includes the number of trap nights, the total number of skunk captures, the number of captures with IDs, the number of captures without IDs, and the number of unique IDs captured. Number of individuals is unknown in years where there are captures that were not given an ID. \*The total number of unique IDs is the number of unique IDs between 2004 – 2020 not the sum of the number of unique IDs captured each season.

<b>Fox Year</b>	<b>MAT</b>	<b>PCR</b>	<b>Culture</b>
<b>2010</b>	9	0	8
<b>2011</b>	31	1	1
<b>2012</b>	70	19	15
<b>2013</b>	89	31	6
<b>2014</b>	94	18	2
<b>2015</b>	25	2	0
<b>2016</b>	7	2	0
<b>2017</b>	0	0	0
<b>2018</b>	4	0	0
<b>2019</b>	7	2	0
<b>Total</b>	<b>336</b>	<b>75</b>	<b>32</b>

**Table 5.3.1.4. Samples from island spotted skunks, 2010-2019.** Data includes the number of samples collected for MAT, PCR, and Culture analysis from island spotted skunks in 2010-2019.

## ***Sample analysis***

### ***Microscopic agglutination test (MAT)***

Serum samples were tested for the presence of antibodies against *Leptospira* using MAT as described in section 5.1. Fox serum samples collected prior to 2016 were tested at the CDC. However, the CDC lab became overwhelmed with public health emergencies, and so fox samples from 2016-2019 were tested at the Animal Health Diagnostic Center (ADHC) in Ithaca, New York. To calibrate between the labs, 90 samples were tested at both CDC and ADHC. All samples analyzed at CDC were titrated to endpoint against serovars Pomona and Autumnalis, while samples analyzed at ADHC were only taken to endpoint against serovar Pomona (see sections 5.3.2.5 and 6.3.2.5 for more detail). Due to variation in MAT results between the two labs (analyzed in section 6.3.2.4), fox samples were considered to have a positive MAT test if they had a titer equal to or greater than 1:100 against either serovar Pomona or Autumnalis at CDC, or a titer greater than 1:100 against serovar Pomona at ADHC. For quantitative analyses of MAT titer levels, the samples tested at ADHC were corrected to match the sensitivity of CDC data by subtracting one two-fold dilution.

All skunk serum samples were tested at CDC and were considered positive if they had a titer of 1:100 or greater against either serovar Pomona or Autumnalis. Skunk samples collected in 2016 and later were also tested at ADHC, however the two labs returned vastly different results for skunk samples. For all longitudinal analyses of skunk samples, the results from CDC were used to maintain consistency. Results from ADHC, which had a much higher sensitivity in the skunk samples, are presented in Table A.5.

### ***Polymerase chain reaction (PCR)***

Urine and frozen kidney samples were processed and tested for pathogenic *Leptospira* via real-time PCR as described in section 5.1.1.

### ***Bacterial culture***

Sterile urine samples collected via cystocentesis were cultured by placing 1cc sterile urine into transport media then inoculating culture media with 0.1cc of the urine/transport media blend (Adler, 2015). Cultures were stored with lids partially unscrewed to allow in a small amount of air, and they were kept in a dark room at room temperature until they were sent to the lab. Cultures from the 2010 season were sent to the USDA National Animal Disease Center in Ames, IA. Cultures from the 2012 season on were sent to the CDC in Atlanta, GA. Cultures from the 2011 season were sent to both USDA and CDC.

### ***Immunohistochemistry (IHC)***

As described in 5.1.1, IHC analysis was conducted on tissue from a small number of fox carcasses that were recovered in suitable condition. Formalin fixed paraffin embedded tissue from archived fox carcasses was cut and placed onto slides and sent to Colorado State University Veterinary Diagnostic Labs to be stained and tested via IHC.

### ***Calculation of seroprevalence and prevalence***

Seroprevalence and infection prevalence were calculated for each fox year (March – February). Seroprevalence was calculated from MAT data using the thresholds defined above, and infection prevalence was calculated from PCR and IHC data for foxes and PCR and culture data for skunks. Skunk tissue was not examined via IHC, and there was never a fox that had a

positive culture that did not also have a positive PCR, so those tests were not used for those species in calculating prevalence. For each individual and each diagnostic test type, one test result was used per fox year to compute seroprevalence (MAT) or infection prevalence (PCR or IHC). If an individual had mixed test results within a year, the positive test result was used. Uncertainties were calculated as 95% binomial confidence intervals.

### 5.3.2. Analyze data to understand the ecology of leptospirosis in island foxes

#### 5.3.2.1. Longitudinal data

##### *Fox sample and data collection*

The long-term nature of this study, combined with the fact that the SRI island foxes are a relatively small population on an isolated island, means that many individual animals have been repeatedly trapped and sampled over multiple years (Table 5.3.2.1). 1385 individual foxes were tested for evidence of antibodies against *Leptospira* via MAT; of those, 221 were tested at least four times, and 1 was tested 11 times. 598 individual foxes were tested for evidence of infection and shedding via urine PCR; of those, 243 were tested more than once, and 1 was tested 8 times. Thus, the data set provides the rare opportunity to explore longitudinal patterns within individual foxes, as well as the cross-sectional patterns traditionally used to investigate most wildlife disease systems.

N Tests	1	2	3	4	5	6	7	8	9	10	11
N Foxes MAT	1385	638	378	221	127	70	37	22	10	5	1
N Foxes PCR	598	243	93	36	14	5	1	1	0	0	0

**Table 5.3.2.1. Number of individual foxes with longitudinal data on exposure (MAT) and infection (PCR) status.** The numbers shown indicate how many foxes were tested at least N times by a given assay. For example, 127 individual foxes have been tested at least 5 times by MAT and, of these, 70 have been tested at least 6 times, and so on. This table only includes samples collected while each fox was in the wild. Captive-born foxes that were released to the wild were tested many more times while in captivity.

#### 5.3.2.2. Modeling antibody kinetics to estimate time of infection

Knowing when individuals got infected with a pathogen can dramatically boost insights into infectious disease dynamics, both within and between hosts (Handel & Rohani, 2015; Pepin et al., 2017). This knowledge allows estimation of incidence (the number of new infections over time) and force of infection (the rate at which susceptible individuals become infected), which are quantities that are fundamental to modeling and predicting transmission dynamics (Heisey et al., 2006; Weitz et al., 2020) as well as developing mitigation strategies (Caley & Hone, 2004; Weitz et al., 2020).

Knowledge of individual infection times is also relevant to a wide range of pathogen-related factors, including interpretation of the time course of clinical signs of disease (Hawley et al., 2011), vaccine efficacy (Antia et al., 2018), risk factors for infection (Borremans et al., 2011; Pepin et al., 2019), pathogen spillover (Smith et al., 2014), effects of disease on wildlife health and survival (Tersago et al., 2012), pathogen immunity (Epstein et al., 2013), and tracing infection sources (Craft, 2015). However, even though a variety of data sources can theoretically

be used to estimate infection time (e.g. clinical signs of disease, antibody concentration, outbreak seasonality, contact tracing), there are a number of significant challenges that limit the widespread adoption of time-of-infection approaches, particularly in wildlife. Key challenges include determining methods to incorporate individual variation in response to infection (Simonsen et al., 2009; Teunis et al., 2002), integrate different data sources (Borremans et al., 2016), address interval-censored data (Wilber et al., 2020), model the anamnestic response to reinfection (Pothin et al., 2016), and deal with antibody cross-reactivity. A currently unresolved major challenge is how to model biomarker dynamics when there is no population of individuals with a known infection time, which is particularly common in wildlife studies.

Models of the dynamics of serological biomarkers, such as antibodies or pathogen DNA/RNA, constitute the foundation of most time-of-infection estimation methods (Brookmeyer & Gail, 1988; Gilbert et al., 2013; Teunis et al., 2016) in the rapidly expanding field of quantitative serology (Boni et al., 2019; Pepin et al., 2017; Teunis et al., 2012). The presence and concentration of such biomarkers can contain information about whether and when an individual has been infected (Borremans et al., 2016), the degree of immunity (Röltgen et al., 2020), infection severity (Vaughn et al., 2000), and whether and for how long they are infectious (Hardestam et al., 2008; Prager et al., 2020). Crucially, a biomarker can be used for such purposes only after its relevant properties have been quantified and when a model exists for how its presence or concentration correlates with the information of interest (e.g. time since infection). For example, a model of immunity to reinfection with rabies virus in vaccinated wildlife suggests that protective immunity should occur when the level of specific neutralizing antibodies is above a certain threshold (Moore et al., 2017). While biomarker models can range from purely conceptual to mathematical, they must exist before interpretation of new data is possible.

Antibody dynamics can be a particularly rich source of information about time of infection. Following infection, the humoral immune response results in the production of different types of antibodies that are produced at different rates and in different quantities. Antibody levels decline after reaching a peak level shortly after infection, and this decay happens at a certain rate. When this rate is known, antibody levels measured at some later point can potentially be used to determine how long ago an individual was infected (Boni et al., 2019; Teunis et al., 2012). This in turn opens up the possibility to improve difficult-to-collect data on incidence in the population (Pepin et al., 2017; Wilber et al., 2020) and to estimate whether and for how much longer an individual is immune to reinfection (Borremans et al., 2015).

Antibody dynamic models typically consist of three parts: (1) increasing phase (often ignored because it is typically short), (2) peak level, (3) decay phase (Teunis et al., 2016). Each of these parts needs at least one parameter to describe the functional shape of the antibody dynamics, and there are specific data requirements for estimating these parameters. The optimal situation for parameter estimation is the availability of experimental data where the time of infection is known for multiple individuals, combined with frequent longitudinal sampling of each individual until antibodies are no longer detectable. For example, experimental infection of the African rodent *Mastomys natalensis* with an arenavirus, followed by frequent sampling for the entire lifetime, enabled the development of an antibody dynamic model that could then be used to estimate time of infection of wild rodents based on a limited number of samples (Borremans et al., 2015, 2016). Similarly, experimental data on influenza A in snow geese and mallards have been used to model the antibody response following infection, and subsequently estimate infection times and population-level force of infection (Pepin et al., 2017).

Unknown infection times are particularly problematic for studies on wildlife infectious disease dynamics, where the periods between sampling can be long, sampling sizes are typically low, and experimental infections followed by longitudinal sampling are not feasible (Gilbert et al., 2013). This has likely been a major reason that quantitative serology methods have not yet been widely adopted in wildlife disease ecology (Gilbert et al., 2013). A standard approach to determining an animal's time of infection is to take the midpoint between the interval bounded by the most recent time at which an individual is known to be antibody-negative and the first positive sample, or to consider this interval as a uniform distribution for infection. For example, a study on cowpox virus in field voles (*Microtus agrestis*) assumed a uniform infection probability of 2 weeks prior to the last negative result and 2 weeks prior to the first positive result, based on the assumption (i.e. a model) that antibodies are detectable 2 weeks after infection (Begon et al., 2009). Similarly, the time of seroconversion to Rift Valley fever virus in livestock used the midpoint between negative and positive samples taken at 1- to 2-month intervals (van den Bergh et al., 2019), which were subsequently used to estimate incidence over time. As the potential error on this estimate can be large (up to two months), improved estimates of infection or seroconversion time obtained through quantitative serology could result in dramatic reductions in incidence estimation error.

Here, we present a general approach for modeling antibody dynamics when sampling is sparse and infection times are unknown (Figure 5.3.2.1). The approach uses Bayesian MCMC inference to integrate different sources of information about model parameters, with full consideration and propagation of uncertainty. Additionally, we show how the simultaneous integration of the dynamics of other biomarkers can lead to synergistic improvements in parameter fitting and infection time estimation. We apply this approach to Channel Island foxes (*Urocyon littoralis*) infected with *Leptospira interrogans* serovar Pomona. The framework presented here provides a way to deal with unknown infection times when modeling biomarker dynamics, which we hope will stimulate the more widespread use of quantitative serology in disease ecology.

#### *Antibody titer data*

This analysis used quantitative antibody titer data derived from MAT assays performed on serum samples from island foxes on SRI, as described in section 5.3.1. Antibody levels were log-transformed so that each unit change corresponds with a two-fold dilution step

$$(\log_2 \left( \frac{\text{dilution}}{100} \right) + 1).$$

Here, we used *Leptospira interrogans* serovar Pomona and serovar Autumnalis for antibody decay modelling and peak antibody time estimation. While the study population is known to be infected with serovar Pomona, MAT assays can cross-react strongly (sections 5.3.2.4 and 6.3.2.4), which means that MAT tests can also test positive for other serovars (Levett, 2003). As antibodies of foxes infected with serovar Pomona show a strong MAT signal for both serovar Pomona and serovar Autumnalis, we leveraged both data sources to improve model parameter fitting and infection time estimation.

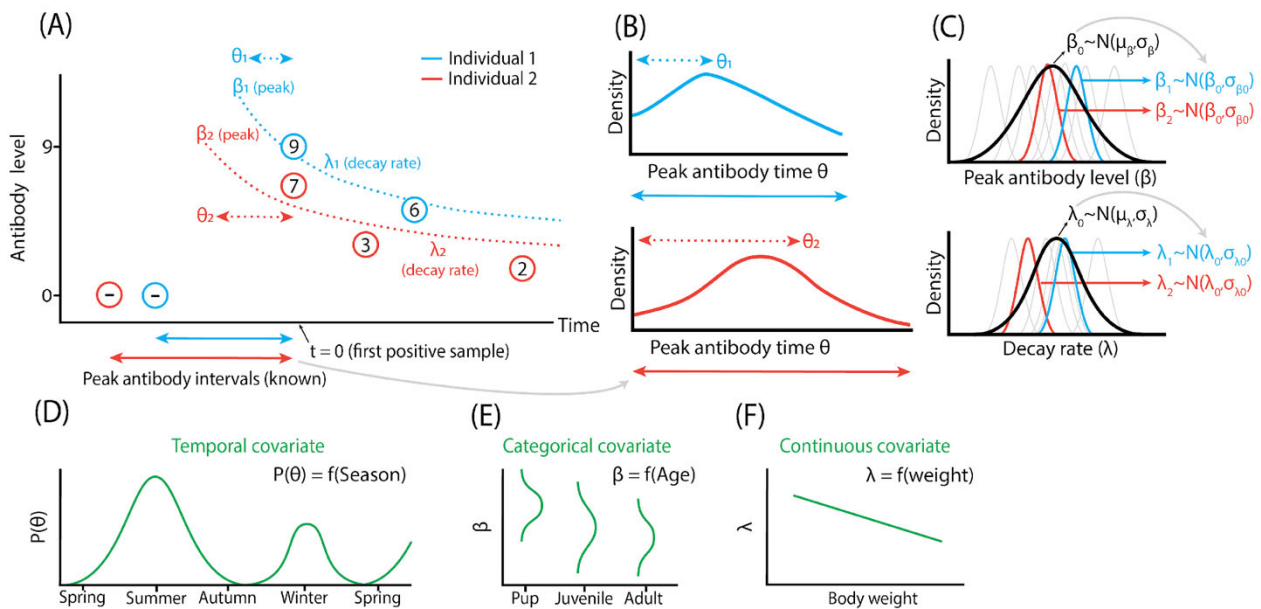


**Figure 5.3.2.1. Schematic of antibody kinetic model and the use of informative data.** Bayesian inference offers a framework to use multiple sources of information to construct biomarker models and estimate individual peak antibody time. Panel (A) illustrates observed antibody level data (circled levels) for two individuals that are used to estimate model parameters  $\beta$  (peak level) and  $\lambda$  (decay rate), with the ultimate goal of estimating peak antibody time  $\theta_i$  for each individual  $i$ . Dotted lines show possible unobserved models. Intervals between the last negative and first positive samples can be used as prior information to bound possible peak antibody times  $\theta_i$  (Panel B: posterior probabilities indicating the most likely peak antibody times). Model parameters can be estimated at the individual level ( $\beta_i$  and  $\lambda_i$ ), while simultaneously estimating the mean and variation of these parameters at the population level ( $\beta_0, \sigma_{\beta_0}, \lambda_0, \sigma_{\lambda_0}$ ) in a hierarchical way (C). When available (not in our study), other types of information can be used to improve estimates of the different model parameters, e.g. seasonal fluctuations in infection risk provide information about  $\theta_i$  (D), while age-dependent infection risk (E) or a continuous covariate such as body weight (F) can provide information about  $\beta_i$  or  $\lambda_i$ .

### Candidate models

Prior to model fitting, candidate models of antibody decay had to be chosen based on preliminary exploration of the data. Generally, aspects to keep in mind when selecting candidate models are the possible shapes a function can have and the number of unknown function parameters. A model with more parameters results in higher flexibility, but this can increase the risk of overfitting and lower the predictability of new data (Bolker, 2008). There are several functions that have been used to model antibody decay, with the single (i.e. constant decay rate) and double (i.e. gradually decreasing decay rate) exponential functions being the most common (Boni et al., 2019; Teunis et al., 2016). When initial decay is significantly faster than later decay, alternative functions such as a power function can be used (Teunis et al., 2016). As shown in (Teunis et al., 2016), the power function may be particularly useful as it can accommodate a wide range of decay shapes with only two decay parameters. Additionally, the specifics of a power function support hypothesized underlying biological processes such as variation in the rate at which different sites in the body produce antibodies (Teunis et al., 2016). When empirical

antibody kinetics do not resemble any existing functions, a flexible function such as a smoothed spline may need to be used (Borremans et al., 2016).

Based on initial data exploration and visualization we selected three candidate functions. Single exponential:  $\mu_{i,t} = \beta_i e^{-\lambda_i(t+\theta_i)}$ ; double exponential:  $\log(\mu_{i,t}) = \log(\beta_i) e^{\lambda_i(t+\theta_i)}$ ; power:  $\log(\mu_{i,t}) = \frac{1}{1-r_i} \log \log \left( \beta_i^{(1-r_i)} - (1-r_i)v_i(t+\theta_i) \right)$ ; where  $\mu_{i,t}$  is the observed antibody level of individual  $i$  sampled at time  $t$ . Here,  $t$  is defined as the time since an individual's first positive sample, but this can be any time unit, including calendar time, as long as it is consistent across individuals.  $\beta_i$  and  $\lambda_i$  are the peak antibody level and antibody decay rate of individual  $i$ .  $r_i$  and  $v_i$  are the shape and scale parameters of the power function.  $\theta_i$  is the time of peak antibody level relative to the first observed positive sample of individual  $i$  (i.e. the number of days between an individual's estimated time of peak antibody level and its first observed positive sample), resulting in negative  $\theta_i$  values up to 0 (which would mean that the peak antibody level coincides with the first positive sample). Note that we estimated the peak antibody level time and did not attempt to model the preceding period during which antibody levels increase, which is a limitation imposed by the low temporal resolution of our data relative to the increase period. In situations where data do allow quantification of the increase period, the increase and decrease phases are typically modeled as two different functions connected at the peak antibody level time (de Graaf et al., 2014; Teunis et al., 2016).

### *Bayesian MCMC model fitting*

Model fitting was done using a Bayesian Markov Chain Monte Carlo (MCMC) approach, as implemented in the software rJAGS (Plummer, 2019). A log-normal error distribution was assumed for antibody levels. Six parallel chains were run for 60,000 iterations, assessing chain convergence visually and with the Gelman-Rubin diagnostic (Brooks & Gelman, 1998). Following a burn-in period of 10,000 iterations, posterior estimates were calculated for the last 50,000 iterations.

The key advantage of using a Bayesian approach for modelling antibody decay with unknown times of infection is the explicit incorporation of prior information as informative prior distributions for parameters. Here, we used informative priors for peak antibody level time  $\theta_i$  and peak antibody level  $\beta_i$ , as described below. We further aimed to capture the biological variation in the model parameters across the population, so that we would have individual estimates as well as estimates of the mean and variation at the population level. This was possible by extending the Bayesian framework to a hierarchical structure, where the population-level parameters (now called hyperparameters) were estimated explicitly, and the individual-level parameters were drawn from these population-level distributions (Gelman & Hill, 2007). This meant that individual-level parameters were modeled using prior distributions  $p(\log(\beta_i)) \sim N(\beta_0, \sigma_{\beta_0})$ ,  $p(\lambda_i) \sim N(\lambda_0, \sigma_{\lambda_0})$ ,  $p(\log(r_i)) \sim N(r_0, \sigma_{r_0})$  and  $p(\log(v_i)) \sim N(v_0, \sigma_{v_0})$ , where  $\beta_0$ ,  $\sigma_{\beta_0}$ ,  $\lambda_0$ ,  $\sigma_{\lambda_0}$ ,  $r_0$  and  $\sigma_{r_0}$  are the hyperparameters of the hierarchical model: population-level means and standard deviations (sd) of peak antibody level (mean  $\beta_0$ , sd  $\sigma_{\beta_0}$ ), exponential decay rate (mean  $\lambda_0$ , sd  $\sigma_{\lambda_0}$ ) and power function shape (mean  $r_0$ , sd  $\sigma_{r_0}$ ) and scale (mean  $v_0$ , sd  $\sigma_{v_0}$ ). Each of these hyperparameters had their own (hyper-)prior distribution (listed in Supplementary Information).

Parameter estimation and overall model performance can be greatly improved by combining data from multiple biomarkers or other covariates such as age, incidence seasonality, and other infection risk factors (Borremans et al., 2016). As an example, we therefore

implemented an additional biomarker: antibody levels against *L. interrogans* serovar Autumnalis. This was possible using a joint-likelihood approach within the hierarchical Bayesian framework (Isaac et al., 2020). This is a simple extension of single-biomarker fitting, where two separate models (in this case, one for serovar Pomona and one for serovar Autumnalis) are fitted simultaneously while sharing the same individual peak antibody time parameter  $\theta_i$ . This increases the likelihood of accepting parameter values that are supported by the different biomarker datasets, and can result in more precise posterior estimates. Last, because Pomona and Autumnalis antibody levels are correlated, this potential correlation was implemented in the model by using a multivariate normal distribution for both Peak antibody parameters.

Because samples were processed at two different labs over the course of the study, an additive lab effect parameter was added to the model. This allows for antibody levels of the labs to be higher or lower.

The JAGS code used for model fitting has been provided as supplemental information for 5.3.2.2 in Appendix C. Posterior 95% credible intervals (CrI) were calculated as highest density intervals using the function ‘dens’ of R package HDInterval (Meredith & Krushke, 2018).

#### *Prior distribution of peak antibody time*

Peak antibody time  $\theta_i$  was bound by the interval between the most recent negative sample (a negative test result or birth date) and the first positive sample (“peak antibody interval”). When available for an individual, this information was incorporated as a uniform prior distribution for  $\theta_i$  with minimum  $\theta_{min}$  and maximum 0:  $p(\theta_i) \sim U(\theta_{min}, 0)$ . Alternative data to inform  $\theta_i$  include age (birth date), average lifespan when age data are not available, known seasonality in infection risk, onset of clinical signs of disease, and any other variable that provides information about when infection was more or less likely. The probability distribution translating this information to a prior distribution can assume any shape and is not restricted to a uniform distribution as used here for the bounded peak antibody interval.

#### *Prior distribution of peak antibody level*

Another source of information that was used to improve model fitting is the distribution of peak antibody levels of recently infected foxes, which informs population-level mean and sd  $\beta_0$  and  $\sigma_{\beta_0}$ . This was done by selecting a subset of foxes that were infected as recently as possible (prior to their first positive sample), balancing the trade-off between sample size, which must be sufficiently large to provide a useful distribution, and recent infection time. We chose a maximum time of 250 days between the first positive and last negative sample as “recently infected”. Although this was still a large window, this was a limitation resulting from the field sampling frequency. While far from ideal, it does provide a good opportunity to illustrate the strength of the approach in improving peak antibody time estimation. The limit of 250 days resulted in 54 foxes that were used to get an informed sense of the distribution of peak antibody levels at the population level. Normal distributions were fitted to the frequency distribution of the antibody levels of the first positive samples. Fitted parameters were mean 7 and sd 3  $\log_2$  dilutions for serovar Pomona and mean 6.8 and sd 2.7  $\log_2$  dilutions for serovar Autumnalis. Normal distributions were fitted using the fitdistr function in R package MASS (Venables & Ripley, 2002). More details are provided in Appendix C for this section.

#### *Model fitting*

Model fitting was done using data from foxes that had at least 2 positive samples preceded by a negative one that determines the peak antibody interval. There were 34 foxes that

exhibited signs of antibody boosting (possibly due to re-exposure to the pathogen), defined here as an antibody level increase  $> 2 \log_2$  units between samples. Because the antibody model does not accommodate secondary increases in antibody level, these samples were removed from the dataset, starting from the sample preceding the increase. These filtering rules were applied to both serovars, with boosting samples only removed when the signal was present for serovar Pomona.

Model fits were compared using the leave-one-out cross-validation information criterion LOOIC (Vehtari et al., 2017) using R package loo (Vehtari et al., 2020). Additionally, we used two measures that show the degree to which a model improves estimation of peak antibody time  $\theta_i$  relative to the uniformly distributed peak antibody interval bound by the last negative and first positive sample. The first is “% peak antibody interval reduction,” which is the percentage by which the peak antibody interval size was reduced when taking the 95% CrI of the posterior distribution as the new interval. For example, if the original interval size is 250 days (i.e. number of days between the most recent negative and first positive samples), and the model results in a posterior distribution of  $\theta_i$  for which the 95% CrI ranges from 200 to 20 days prior, the % reduction would be  $100 - \left(\frac{200-20}{250}\right) * 100 = 28\%$ . While this measure is useful because it is easy to interpret, it does not consider the fact that probabilities within the 95% CrI are not equal, and some  $\theta_i$  will have a higher probability than others. We therefore used a second measure that does, which is relative entropy (or Kullback-Leibler divergence) (Kullback & Leibler, 1951). Relative entropy (units = “bits”) quantifies the difference in information content between two distributions, which in this case are the uniform prior distribution (peak antibody interval) and the posterior distribution of  $\theta_i$ . Relative entropy  $D_{KL}(P||Q) = \sum_x P(x) \log_2 \frac{P(x)}{Q(x)}$ , where  $P(x)$  and  $Q(x)$  are the posterior and prior distributions defined over the same range of values  $x$  (Burnham and Anderson, 2002). The values of  $x$  are individual-specific and adopt every possible value of  $\theta_i$  as determined by the uniform prior peak antibody interval. The higher the relative entropy value, the more information was present in the posterior distribution relative to the uniform prior.

### *Sensitivity analysis using simulated data*

To assess model performance given the limitations of our dataset, we simulated data resembling what was observed. Antibody levels were simulated for 75 individuals, where peak antibody level and decay rate were randomly sampled from a normal distribution and 2 to 5 samples (random sample size) were generated for sampling times up to 2,000 days after peak antibody level. Random noise was added to antibody levels to simulate real variation (see Appendix C for details). For model fitting using simulated data, the peak antibody sample was excluded from the simulated dataset, again to simulate what was observed. To test model sensitivity to different assumptions, parameter estimation was done for multiple simulated datasets that were generated using a range of standard deviations for peak antibody level and decay rate simulation. Details are provided in Appendix C. We then tested how different combinations of peak antibody level variation and decay rate affect model performance, as it may be expected that faster decay and/or smaller peak antibody level variation will constrain the possible peak antibody time window, which in turn would affect how well peak antibody time  $\theta_i$  can be estimated.

## Software

All data preparation, analysis, and plotting was done in R (R Core Team, 2019) using packages ggplot2 (Wickham, 2016), rjags (Plummer, 2019), ggridges (Wilke, 2020), dplyr (Wickham et al., 2019), patchwork (T. L. Pedersen, 2019), loo (Vehtari et al., 2020), R2OpenBUGS (Sturtz et al., 2005) and HDInterval (Meredith & Krushke, 2018).

### 5.3.2.3. Risk factors for infection

#### Study period and study cohort

The National Park Service monitored the island foxes throughout captivity, reintroduction, and recolonization of the island. From 2001 to 2008, serum samples were taken from the foxes taken into a captive breeding program and their captive-born offspring. All captive individuals were sampled 1-4 months prior to reintroduction into the wild. During reintroduction (2004 - 2008), foxes were captured using target trapping at least annually for health evaluations. After the reintroduction period (2009 - 2019), the fox population was monitored through grid trapping and target trapping; serum and urine were collected when possible.

The cohort analyzed in this study consisted of 1226 foxes. To be included in this dataset, individuals were required to have a known release date from captivity (with a negative MAT result in their last captive test) or a known year of birth in the wild. All individuals that ever tested seronegative during the study period were included in the dataset. Foxes that seroconverted were only included in the dataset if they ever had a positive MAT against *L. interrogans* serovar Pomona.

#### Overview of survival analysis

Survival analysis evaluates the dependency of time-to-event data (e.g. time to death or time to infection) on explanatory variables and involves two primary quantities: the survival function and the hazard function. The survival function,  $S(t)$ , gives the probability of surviving up to time  $t$ , where the event of interest occurs at time  $T$ , and takes the following form:

$$S(t) = P(T \geq t), 0 < t < \infty$$

The hazard function,  $h(t)$ , is the instantaneous rate of the event occurrence and is composed of the conditional probability that the event will occur in the time interval  $[t, t + \Delta t)$ , given that the event has not occurred, relative to the interval width. In the context of infectious diseases, when the event of interest is the infection of a susceptible host individual, the hazard function is also known as the *force of infection*.

$$h(t) = \lim_{\Delta t \rightarrow 0} P(t \leq T < t + \Delta t | T \geq t) / \Delta t$$

A key attribute of survival analysis is its ability to deal with censored data. Event data can be censored in four ways (uncensored, right-, left-, and interval-censored), and multiple types of censoring can occur within a single dataset. When the time of the event (e.g. death or disease onset) is known exactly, the data is uncensored. However, this type of data only occurs with continuous monitoring and is very rare in wildlife studies. Right-censoring occurs when the time of the event is greater than the observed time (Figure 5.3.2.2; top). In other words, if the

event has not occurred by the end of the study but may occur at a later date, the individual is right-censored. Left-censoring is much less common than right-censoring and is defined by the occurrence of the event prior to the start of the study (Sun, 2006). No individuals in this study are classified as left-censored. Finally, interval censoring describes the situation when subjects are not continuously observed, as in most wildlife trapping and sampling schemes, so the time of the event falls within an interval of time, rather than being exactly measured. In our study, the bounds of the seroconversion intervals are defined by an individual’s last negative test and first positive test (Figure 5.3.2.2; middle/bottom).

For survival analysis, it is also crucial to choose an appropriate time scale and origin. This choice governs the interpretation of survival times and allows a clear understanding of how age and temporal factors are accounted for within the models. In our study, we use days-since-birth/release as our time origin and scale. The time-at-risk for foxes which were kept in captivity begins when they were released as seronegatives (Figure 5.3.2.2; bottom). However, the majority of the foxes in our dataset were wild-born, and, therefore, their time-at-risk begins at birth (assumed to be 1 April).

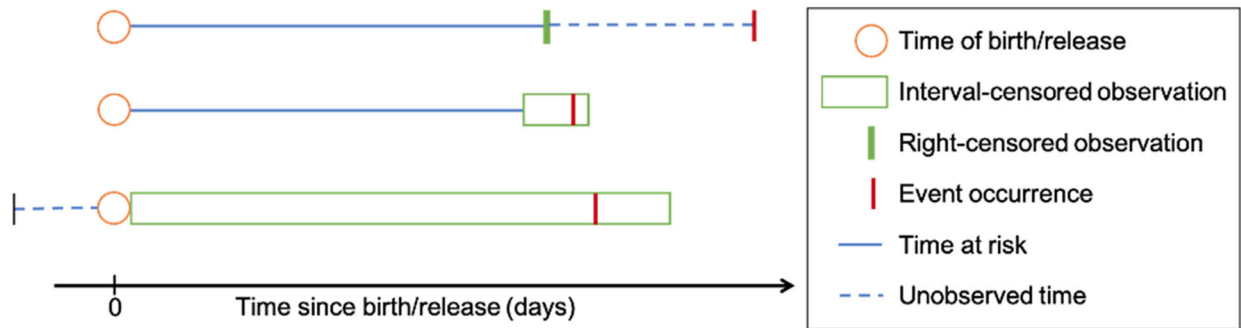


**Figure 5.3.2.2. Schematic of censored data types in the context of the fox system.** Solid blue lines denote survival time within the observation period, whereas dotted blue lines indicate unobserved time. Each individual enters the study (orange circles) when they are born in the wild (top/middle) or are released from captivity as seronegatives (bottom) and begin their period at risk of infection on the island. Some individuals (middle/bottom) experience the event (red line) during the study time but are interval censored (where the green box represents the time from the last negative test to the first positive test). Other individuals are right censored (top) and do not experience the event during the time of the study, but they may or may not experience the event thereafter. The bottom panel also illustrates a long seroconversion interval, where an individual was negative when released from captivity but was positive upon its first capture.

### *Data Imputation*

Modeling interval-censored time-to-event data with time-varying covariates such as precipitation or temperature is challenging in survival analysis, as these two characteristics are rarely addressed together (Fieberg & DelGiudice, 2009; Zhang et al., 2018). Some approaches have been proposed to address both issues such as Bayesian joint modeling and data imputation (Campbell et al., 2019; Vandormael et al., 2020). Joint modeling is most appropriate when the time-varying covariates exist at the individual level, such as time-varying biomarkers. Data imputation is a more flexible approach, which addresses the uncertainties of interval-censoring by imputing a time of infection in a systematic way, giving rise to augmented datasets with precise event times, which enable the use of standard techniques for time-varying covariates.

However, when censoring intervals are large (on the scale of years, as they can be in our study), imputing the time of infection with standard imputation techniques (e.g. using the midpoint of the interval, or a uniformly random point in the interval) can cause significant bias (Vandormael et al., 2020).

Rather than using a standard technique to impute the time of infection for each individual in an uninformed manner, we generate biologically-informed time of infection estimates using the titer kinetics model described in section 5.3.2.3. This model uses longitudinal and quantitative serology data to estimate the posterior probability that infection occurred on each day in an individual fox’s seroconversion interval (Figure 5.3.2.2; green boxes). Using these probabilities as weights, we can sample the time of infection in an informed way and assume that the event date is known exactly, which enables the incorporation of time-varying covariates more easily.

*Counting process formulation*

To incorporate time-varying covariates into a proportional hazards model, the data must be transformed into a counting process formulation (Fieberg & DelGiudice, 2009). Each risk interval is subdivided into smaller intervals over which the time-varying covariates can be assigned. This formulation assures that survival time is accurately accrued and that the covariates can be updated through time, with appropriate temporal resolution (e.g. monthly or annually). In this study, we divided every individual’s risk time into monthly intervals (Table 5.3.2.2).

Full risk interval (days)	Full risk interval (by date)	Subdivided risk interval (days)	Subdivided risk interval (by date)
[0, 100)	[04-01-2005, 7-10-2005)	[0, 30)	[04-01-2005, 05-01-2005)
[0, 100)	[04-01-2005, 7-10-2005)	[30, 61)	[05-01-2005, 06-01-2005)
[0, 100)	[04-01-2005, 7-10-2005)	[61, 91)	[06-01-2005, 07-01-2005)
[0, 100)	[04-01-2005, 7-10-2005)	[91, 100)	[07-01-2005, 07-10-2005)

**Table 5.3.2.2. Example of a counting process formulation for a single individual's risk time.**

*Candidate risk factors for infection with Leptospira*

Based on our knowledge of the host-pathogen system and the ecology of SRI, we investigated three groups of covariates as potential risk factors for foxes to become infected with *Leptospira*: individual-level, abiotic environmental, and biotic environmental (Table 6.3.2.4). Sex is the only individual-level variation we accounted for, and it was recorded upon birth within captivity or first capture of the fox on the island.

Abiotic environmental covariates included precipitation, temperature, and relative humidity. Daily measurements for these variables were obtained for Santa Rosa Island from 2003-2020 from the Western Regional Climate Center (WRCC) in Reno, Nevada. Monthly averages were calculated for temperature and relative humidity. For precipitation, we created three covariates that captured cumulative total precipitation over the past 1, 12, and 24 months. The *precip1* variable was intended to capture the immediate effect of rainfall, which could affect *Leptospira* transmission via puddles, wet vegetation, or changes in animal behavior. The

*precip12* and *precip24* capture the past one and two rainy seasons (i.e. winters) in the highly seasonal Mediterranean climate on SRI, which affect the hydrology of the island and have bottom-up effects across the island ecosystem. These longer-term variables would also capture the impact of extended drought periods.

Within the biotic environmental category, fox abundance was estimated annually by the National Park Service using trapping and radiocollar telemetry data. Between 2004 and 2009, fox captures were primarily obtained through target trapping. In 2009, NPS biologists switched to a grid trapping scheme. Throughout the same period of time, the skunk population was loosely monitored via by-catch in fox traps. Skunk abundance was estimated as the number of skunk captures per trap-night. Estimation of skunk abundance is fundamentally uncertain because the trapping strategy and effort varied across the study time and traps were frequently saturated by foxes, particularly in the later years of our study.

Because we know that the primary driver of infection risk during an outbreak is the prevalence of infectious individuals, we also included yearly pup seroprevalence as an index of the island-wide force of infection each year. Although PCR positivity in urine samples would be a more direct measure of active shedding island-wide, we lack PCR data in the early phase of the outbreak and reintroduction (2004-2010). However, between 2011 and 2019, pup seroprevalence and PCR positivity are strongly correlated (Figure 6.3.1.2), so we used pup seroprevalence as a proxy for active infections on the island. Our primary aim in this analysis is to determine extrinsic factors that affect *Leptospira* risk, but we wanted to control for this dominant factor to ensure that our findings were robust. In our final analyses, we determined the best model that excludes pup seroprevalence, then tested whether its conclusions were robust to the addition of pup seroprevalence as a proxy for outbreak context.

#### *Imputation and Hazard modeling*

We performed 100 bootstrap runs in which time of infection was imputed with the weighted probabilities generated from the titer kinetic model. The full dataset was subdivided into a counting process formulation by month, and standardized, time-varying covariates were assigned to each interval. All covariates were standardized to have a mean of 0 and a standard deviation of 1. Then, we fit a series of univariable Cox proportional hazards models to assess the effect of individual covariates on the hazard rate using the *survival* package in R version 4.0.5 (R Core Team, 2021; Therneau, 2021).

#### *Variable selection*

Broadly, we were interested in which biotic and abiotic factors affect infection risk of *Leptospira*. After controlling for individual-level variation (sex), we included the best-performing covariate from each environmental category to form a multivariate model. We compared different multivariate models using AIC scores to balance parsimony with goodness of fit (Burnham & Anderson, 2002). We evaluated our final multivariate model with and without pup seroprevalence included, to evaluate the robustness of the core findings, and the potential benefit of including disease data in such a model when available.

#### **5.3.2.4. Analysis of host species effects and laboratory effects on serological reactivity profiles**

Serology is a vital tool in wildlife disease surveillance, due to the relative ease of collecting and storing serum samples, and the fact that detecting animals with past exposure (hence with antibodies detectable by serology) is generally easier than finding animals with

current infection (with pathogens detectable by PCR or culture). Yet serology is well recognized to present many challenges, including the potential for cross-reactivity and the difficulties in interpreting quantitative titer levels or even setting thresholds for positivity (Gilbert et al., 2013). These challenges are exacerbated for multi-strain pathogens such as *Leptospira*, and for multi-host systems where different host species could exhibit systematically different serologic responses.

However, given the extraordinary wealth of serum samples available for our system, and the difficulty in obtaining culture isolates of *Leptospira* for definitive strain typing, we had high incentive to strengthen our ability to interpret serological data in our system. In this study, we leveraged the depth and duration of our dataset, and our unique system with one circulating serovar of *Leptospira interrogans* in three sympatric wildlife host species, to undertake an investigation of the reliability of MAT as a tool to infer epidemiological processes. We emphasize the interpretation of maximum titers as markers of infecting serovar and the interpretation of quantitative titer levels as markers of time since exposure. We also explored the potential confounding effects of different host species and different laboratories. Our results suggest that while MAT reactivity profiles can provide powerful insight into *Leptospira* epidemiology (see section 6.1.1), all MAT results from multi-host systems must be interpreted with appropriate consideration of host species effects.

#### *Study Animals and Sample Collection*

Our dataset comprises samples from California sea lions (*Zalophus californianus*), Channel Island foxes (*Urocyon littoralis*), and island spotted skunks (*Spilogale gracilis*) with confirmed infections of *L. interrogans* serovar Pomona. The majority of sea lion samples (n=108) were collected from sea lions that had stranded along the central California coast between 2005-2016, were in rehabilitation at The Marine Mammal Center (TMMC; Sausalito, California), and had been diagnosed with acute leptospirosis (97/108) based on clinical signs, serum chemistry results, and necropsy data (Greig et al., 2005). An additional thirty sea lion samples were collected between 2010 and 2016 from free-ranging wild sea lions from the central California coast and northern Oregon, as described in Prager et al., 2020. Samples from island foxes (n=4) and island spotted skunks (n=60) were collected between 2011 and 2016 during the course of annual grid and target trapping on SRI. Fox and sea lion data include both sexes and all age classes, while all four skunks were male.

#### *Sample Analysis*

All animals included in this study had PCR-confirmed infection, and the infecting *Leptospira* serovar was confirmed as *L. interrogans* serovar Pomona using PFGE as described previously on all cultured isolates ( $N_{\text{CSL}} = 19$ ,  $N_{\text{fox}} = 11$ ,  $N_{\text{skunk}} = 1$ ) (Chirathaworn et al., 2014; Dikken & Kmety, 1978).

Serum samples were tested by MAT against a panel of five *Leptospira* serovars comprising serovars Pomona, Autumnalis, Djasiman, Bratislava, and Icterohaemorrhagiae, which respectively belong in serogroups Pomona, Autumnalis, Djasiman, Australis, and Icterohaemorrhagiae (Levett, 2001). While many samples were tested against more than these five serovars, for this analysis we excluded serovars that were not tested for all host species, or that yielded almost entirely negative results for all species.

All serum samples included in this study were MAT analyzed at the CDC in Atlanta, Georgia and were run to endpoint dilution. Titer results were log-transformed for ease of

interpretation using the following formula:  $\log_2(\text{titer}/100) + 1$ , thus a titer of 1:100 = 1, 1:200=2, etc. Titers reported as <1:100 were set equal to 0.

In a separate analysis focusing on variability among laboratories, a subset of 46 fox sera were MAT analyzed at three reference laboratories using a 2-serovar panel (Pomona and Autumnalis). In the results, the labs are referred to as Labs A, B, and C. At all three labs, antibody titers against serovar Pomona were evaluated to endpoint. For serovar Autumnalis, at Lab A, 43/46 samples were titrated to endpoint and 3/46 were only tested at a dilution of 1:100 (all were positive); at Lab B, all 46 samples were titrated to endpoint; at Lab C, all 46 serum samples were titrated to a 1:6400 dilution ( $\log_2$  titer = 7), but not beyond. Thirty-two of the samples tested at Lab C were positive at dilutions less than 1:6400, but endpoint titers for the 14 samples that were still positive at the 1:6400 dilution are unknown.

### *Data Selection*

For our analyses of within and between host antibody cross-reactivity patterns, we selected MAT results from animals for which there was at least one positive urine PCR or culture result, indicating current *Leptospira* infection. Whenever possible, we selected serum samples that had corresponding isolates enabling PFGE confirmation that the host was infected with *L. interrogans* serovar Pomona. To achieve a sufficient sample size for our analyses, we also included serum samples from individuals where PFGE confirmation was not possible; given our extensive study of the ecology of *Leptospira* in these systems, in which *L. interrogans* serovar Pomona is the only serovar detected in the post-captivity SRI outbreak or in CSL samples spanning decades, we assume that all seropositive individuals were initially infected with serovar Pomona. In supplementary analyses using only PFGE-confirmed individuals, our findings were consistent with those seen in our full dataset.

For individuals that had been sampled longitudinally, we selected the MAT result from the serum sample with a collection date closest to that of the positive urine sample. The majority (55/60) of fox and all (4/4) skunk MAT results were from sera collected on the same day as the *Leptospira* PCR or culture positive urine. Sea lion serum samples used for MAT were collected within 14 days of the date that the PCR or culture positive urine or kidney sample was collected. For our analyses of relative titer magnitudes, we standardized antibody titer levels by dividing a given antibody titer by the highest antibody titer detected against any serovar in the 5-serovar MAT panel run for that serum sample.

To compare MAT results across laboratories, a subset of forty-six fox serum samples were evaluated at three certified testing laboratories as described above (see section on Sample Analysis). Fox serum samples were chosen for this lab comparison based on MAT titer results from Lab A. For each MAT antibody titer level ranging from 1:100-1:51200, three serum samples with that MAT antibody titer against serovar Pomona, as reported by Lab A, were selected where possible (Table A.10). In addition to these 30 samples, we included a further 10 samples that had no detectable antibodies against serovars Pomona and Autumnalis at Lab A, and six samples that had no detectable antibodies against serovar Pomona but were MAT positive against serovar Autumnalis at Lab A.

### **5.3.3. Impacts of *Leptospira* on the demography of island foxes**

#### *Tracking mortality in radio-collared foxes*

From 2003-2006, all reintroduced and wild born foxes were equipped with radio collars and tracked via radio telemetry, with the goal of detecting the radio signal from each fox at least

once per week. From 2007 onward, the wild population exceeded 60 animals, so a subset of the population (typically 40-50 individuals) was collared and tracked weekly. NPS biologists made a concerted effort to learn the cause of death of any collared fox that died. When a radio collar switched into mortality mode, efforts were made to collect the carcass as rapidly as possible so that a necropsy could be conducted at UC Davis. Between 2004 and 2010, kidneys from 12 wild fox mortalities were recovered and preserved either in formalin-fixed paraffin-embedded blocks or frozen. We tested these kidney samples for evidence of *Leptospira* infection using PCR and IHC. This high-frequency tracking of a substantial proportion of the wild fox population enabled a high-resolution view of mortality associated with *Leptospira* infection during these early years.

#### *Demographic impacts: early phase (2004-2010)*

We gathered detailed records of individual fox histories from field notes and records, as described in section 5.1.1. Necropsy reports were obtained from the pathology lab at UC Davis, and all information on cause of death was collected for wild foxes that died between 2004 and 2010. This analysis is restricted to captive-born animals that were reintroduced and wild-born animals born into the reintroduced population, since some founder animals showed signs of exposure from before the period of captivity.

Annual survival probabilities were estimated for all reintroduced and wild-born foxes, with years defined as fox years, i.e. from March to February. Survival probability estimates and 95% confidence intervals were obtained by Kaplan-Meier analysis, implemented in R (R Core Team, 2019).

#### *Demographic impacts: later phase (2009-2020)*

Analyses of further demographic impacts based on data collected from 2009-2020 are still underway. To support these analyses, we developed an algorithm to classify foxes with respect to their *Leptospira* infection status (Figure 5.3.3.1). This decision tree algorithm uses the capture and testing history of each fox, including PCR/culture, MAT titer, and serum chemistry data, to classify each fox at each capture event as Susceptible, Unknown infection status, Recent Infection (i.e. infected in the same year as it was trapped), or Prior Infection (infected in a past fox year). Based on these classifications, we are investigating the potential impact of *Leptospira* on island fox survival and reproductive success on SRI.

In particular, to assess impacts on fox survival, we are using capture-mark-recapture analysis, with two distinct approaches based on the data type. The first uses a closed multi-state robust design model, where the state is the *Leptospira* infection status of the subject fox, to analyze data collected on the trapping grids (Figure 5.1.1.2). The second uses a known fates analysis to analyze data collected from radio-collared animals. Both approaches will account for other factors suspected to impact fox survival, including the covariates analyzed in section 5.3.2.3. To assess impacts of *Leptospira* infection on fox reproduction, we are using two approaches, which include: (1) analyzing whether the reproductive state of adult female foxes (as determined during trapping and sampling activities described in section 5.3.1) is correlated with their *Leptospira* infection status, and (2) analyzing whether the pup:female ratio each year is correlated with the prevalence of *Leptospira* infection, both on individual trapping grids as well as island-wide.

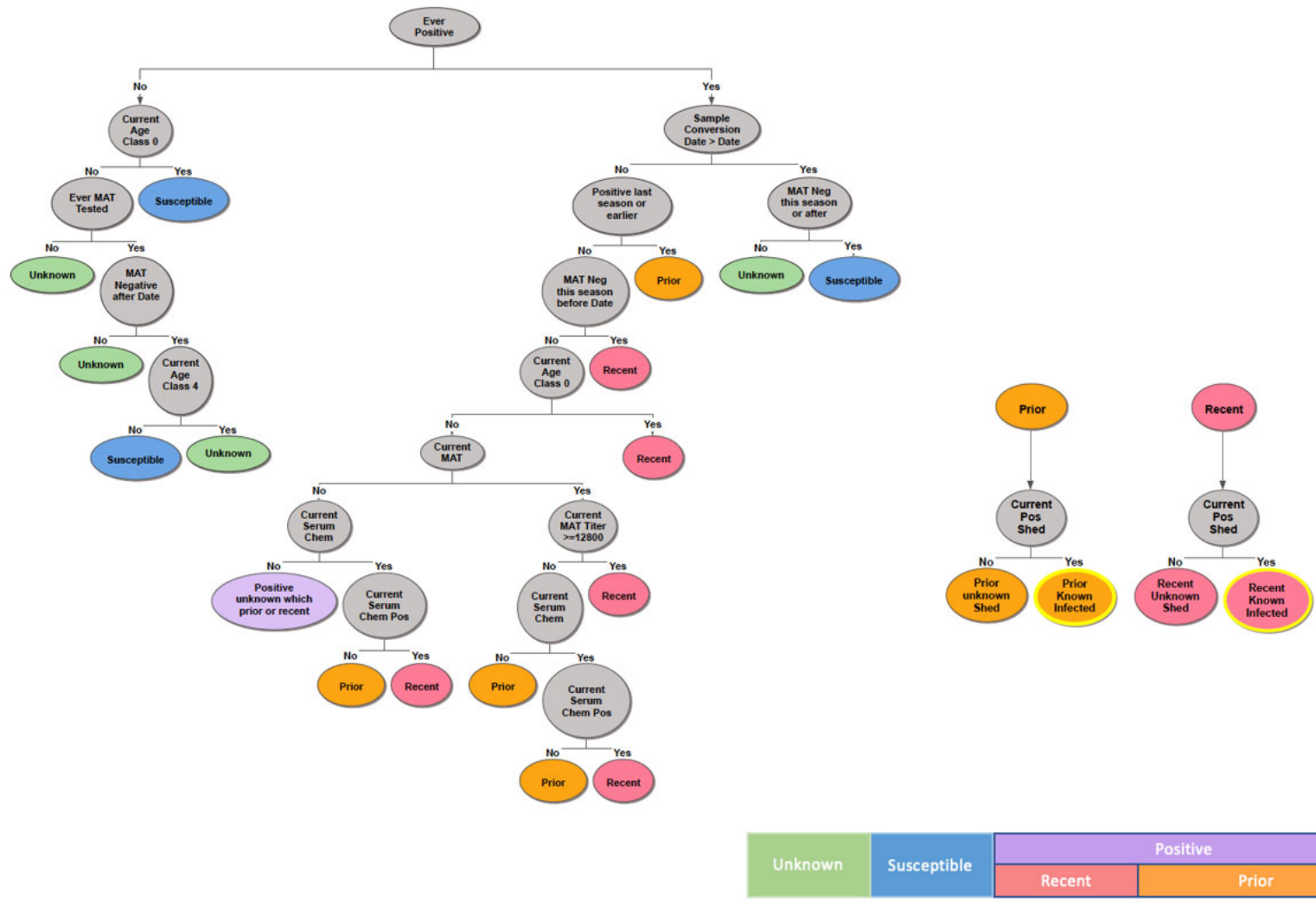


**Figure 5.3.3.1. Decision tree to establish island fox infection status from capture and testing data.** This decision tree uses the capture and testing history of individual foxes to classify their infection state at a given capture event. ‘Ever Positive’ = Yes if the fox has any positive test for *Leptospira* infection or exposure in its record, before or after the capture event in question. ‘Sample Conversion Date’ is the date of the first positive result, and ‘Date’ is the date of the capture event in question.

### 5.3.4. Transmission dynamics model for *Leptospira* in island foxes on SRI

#### *Stochastic simulation model for Leptospira transmission*

We developed a mechanistic model to simulate the demography and movement of island foxes on SRI, and the transmission dynamics of *Leptospira* in the fox population. It is a compartmental model where foxes are assigned to states indicating their age, location, and infection status (see Figure 5.3.4.1). Age states are pup (age [0-1) years) and adult (age [1-maximum) years). The location states correspond with 15 functional patches on Santa Rosa Island, described below. Infection states are susceptible (S), infected/infectious (I) and recovered/immune (R).

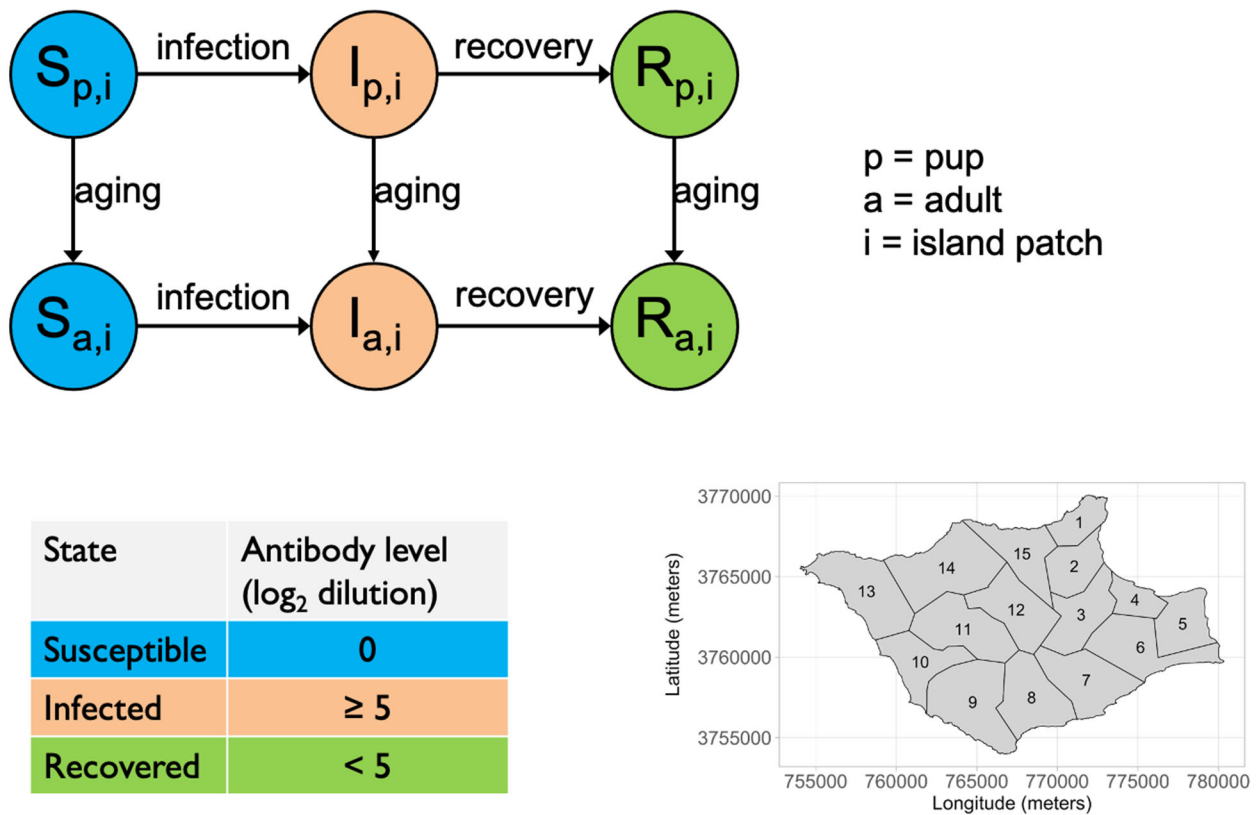


**Figure 5.3.4.1. Schematic of *Leptospira* transmission model for SRI.** The flow diagram summarizes the disease states (Susceptible, Infected, Recovered) with subscripts indicating the age class and island patch location of the fox. The table shows the connection between infection states and anti-*Leptospira* antibody titers, and the map shows SRI divided into 15 functional patches.

The model is a continuous-time stochastic simulation, implemented with an adaptive tau-leaping algorithm using the R package *adaptivetau*. Individuals in the model undergo stochastic

transitions between states, as represented by the corresponding system of coupled differential equations:

$$\begin{aligned}
\frac{dS_{p,i}}{dt} &= F_{y,t} \frac{N_i}{2} - \lambda_i S_{p,i} - \mu_{p,y} S_{p,i} - \alpha_t S_{p,i} \\
\frac{dS_{a,i}}{dt} &= \alpha_t S_{p,i} - \lambda_i S_{a,i} - \mu_{a,y} S_{a,i} \\
\frac{dI_{p,i}}{dt} &= \lambda_i S_{p,i} - \mu_{p,y} I_{p,i} - \alpha_t I_{p,i} - \gamma I_{p,i} \\
\frac{dI_{a,i}}{dt} &= \alpha_t I_{p,i} + \lambda_i S_{a,i} - \mu_{a,y} I_{a,i} - \gamma I_{a,i} \\
\frac{dR_{p,i}}{dt} &= \gamma I_{p,i} - \mu_{p,y} R_{p,i} - \alpha_t R_{p,i} \\
\frac{dR_{a,i}}{dt} &= \alpha_t R_{p,i} + \gamma I_{a,i} - \mu_{a,y} R_{a,i}, \\
\lambda_i &= 1.15\rho_m \left( \beta_i (I_{p,i} + I_{a,i}) \frac{1}{N^q} + c\beta_i \sum_{ij=1}^n (I_{p,ij} + I_{a,ij}) \frac{1}{N^q} + \beta_{skunk,t} \right)
\end{aligned}$$

where  $p$  are pups,  $a$  are adults,  $i$  indicates a fox's patch and  $ij$  each patch  $j$  adjacent to patch  $i$ .  $F_t$  is year-specific fertility (number of pups per female, approximated as  $\frac{N_i}{2}$ ), with births occurring March through May with a peak in April, implemented as a normal distribution so most births happen April 15th. Pups born in a given year enter the population as susceptibles 2.5 months later.  $\mu_{p/a,t}$  is year-specific and age-specific mortality ( $\mu_{p/a,t}$  is 1-survival  $\phi_{p/a,t}$ , see below),  $\alpha_t$  is the aging rate that ensures that each year all of last-year's pups become adults (June 1 to 10),  $\gamma$  is the rate at which infectious foxes become immune (i.e. 1/infectious period).  $\lambda_i$  is the force of infection at patch  $i$ , consisting of density-dependent transmission from foxes in the same patch ( $\beta_i (I_{p,i} + I_{a,i}) \frac{1}{N^q}$ ), transmission from foxes in directly adjacent patches  $ij$  ( $c\beta_i \sum_{ij=1}^n (I_{p,ij} + I_{a,ij}) \frac{1}{N^q}$ ), and transmission from skunks ( $\beta_{skunk,t}$ ) which is assumed to contribute to transmission in the fox population only until 2006, to test whether fox-to-fox transmission can sustain the outbreak after the initial spillover.

Because fox behavior and contact with environmental leptospire may depend on fox population density,  $\beta_i$  was implemented as a density-dependent function. Because the shape of the transmission-density function can have strong effects on pathogen invasion and persistence, we used a power function to model density-dependence, following Smith et al., 2009, where  $q$  can range from 0 (linear density-dependence) to 1 (density-independent). Last, as force of infection has been found to be affected by preceding rainfall,  $\beta_i$  was made time-dependent by multiplying by a factor  $1.15\rho_t$ , where  $\rho_t$  is the month-specific cumulative rainfall over the preceding 24 months times the estimated hazard ratio.

Movement between patches was implemented seasonally (Mar-May, Jun-Aug, Sep-Nov, Dec-Feb), where the probability of moving is season- and year-specific as estimated from fox movement data (see below). When a fox moves, the probability of moving to a certain patch is

specific for each patch-pair combination, again as estimated directly from movement data. This implementation ensures that the observed changes in movements throughout the different stages of the fox reintroduction process are incorporated, as they are likely to affect mixing and transmission. Each of the 6 infection- and age-specific states shown above was implemented for each of the 15 functional patches on SRI, resulting in 90 states between which transitions are possible. All states and transitions can be seen in the accompanying R code.

### ***Dividing SRI into functional patches***

We divided SRI into 15 patches to represent functional areas of use by island foxes (Figure 5.3.4.2). These functional patches were designed based on extensive knowledge of island fox movement patterns and behavior, derived from team member Angela Guglielmino’s 11 years of tracking island foxes on SRI via radio telemetry. Patches were created in ARCGIS10.3.1, using the ‘cut polygons’ tool to divide an existing polygon shapefile of the boundary of SRI into 15 functional patches. Contour, road, and stream layers were added to the layout to guide in patch creation, with particular consideration given to topography (especially ridge lines and canyons), stream beds, and roadways. Foxes are known to travel the road systems and stream beds, are more likely to use one canyon rather than multiple canyons, and are less likely to cross over the tallest ridges of the island. Patches were created by snapping straight lines onto the original shapefile of the SRI boundary until 15 smaller polygons fit completely within the larger original boundary polygon. These smaller polygons were saved as individual polygon shapefiles and imported into R where they were merged together into a spatial polygons data frame with each patch treated as a separate object within the data frame.

The patches were chosen to balance accurate representation of fox behavior with the need for a parsimonious data structure to support statistical analyses. Some individual foxes are known to have had territories that encompass space in more than one of the functional patches, but the patches are an approximate mapping of patterns of fox utilization of the island.

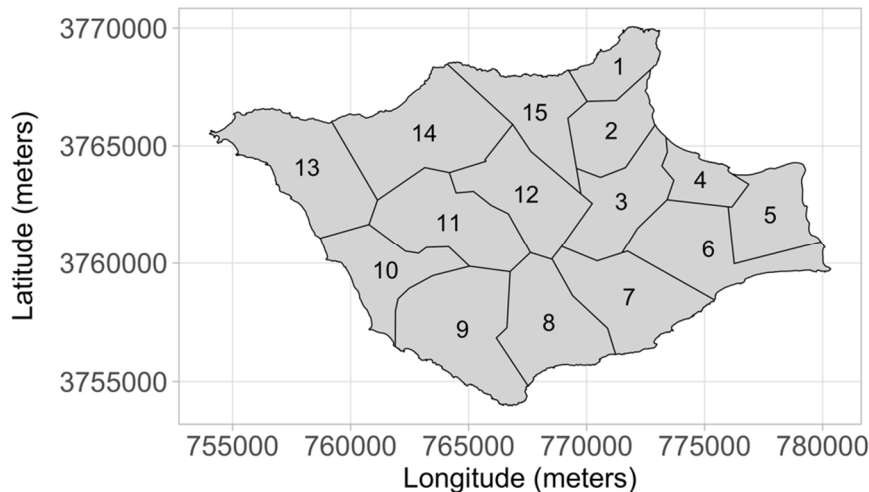


**Figure 5.3.4.2. Santa Rosa Island divided into 15 functional patches.**

### ***Parameter estimation***

Movement and demographic parameters were estimated using analyses of location and abundance data (see below). An analysis of the correlation between PCR status and antibody level was used to assign observed data to the states (S, I, R) used in the model, which was crucial for fitting infection parameters to observed data. Infection parameters  $\beta_i$ ,  $\beta_{iv}$ ,  $\beta_{skunk,t}$ , and  $q$  were fitted to data using Approximate Bayesian Computation (ABC). This method allows the use of one or multiple custom metrics instead of likelihoods for fitting and thereby provides a solution when observed data have significant gaps (in this case due to seasonal sampling) and hidden states (i.e. because the S, I, and R disease states in the model cannot be directly observed). ABC model fitting was done using an emulator, where locally weighted regression was used to design a statistical model of the data by regressing the parameters used for a limited number of simulations against the fitting metrics generated by the simulation, after which this statistical model is used for ABC rejection fitting. This dramatically speeds up processing times, which was necessary because of the long run-times of the simulation model. ABC fitting was done using R package EasyABC. Prior distributions for parameter values were informed by separate analyses of infection parameters (described below). Prior distributions used were:

$$\beta_i \sim \text{Uniform}(0.01, 0.13)$$

$$\beta_{skunk} \sim \text{Uniform}(0.008, 0.1)$$

$$q \sim \text{Uniform}(0.8, 1)$$

$$1/\gamma \sim \text{Uniform}(150, 550)$$

Four metrics were used simultaneously for model fitting: the annual proportion of pups in the I and R states (I+R/N), a binary indicator of whether pup seroprevalence was larger than 0.5 in 2006, the annual proportion of adults in the I state, and the annual proportion of adults in the R state. The observation process was matched by randomly sampling equal annual sampling sizes in the same months as the observed data. 1,000 simulation iterations were used to fit the regression model, followed by 400,000 ABC rejection iterations of which the 10% best-fitting parameter combinations were retained. In order to limit the number of parameters to be estimated and thereby improve inference,  $c$  (transmission from adjacent patches as a proportion of  $\beta_i$ ) was assumed to be 0.1.

### ***Demographic parameters***

Foxes are classified as pups or adults, for ages [0-1) years or [1-lifespan] respectively. Demography in the model is determined by three parameters: fertility ( $F$ ; the number of pups per female), pup survival ( $\phi_p$ ; proportion of pups surviving to adulthood) and adult survival ( $\phi_A$ ; proportion of adult foxes surviving from year  $t - 1$  to  $t$ ). Parameter values were approximated using a Bayesian state-space model fitted to annual estimates of pup and adult abundance. The model consisted of the following equations:

$$N_{p,t} \sim \text{Normal}(v_{p,t}, e_{p,t})$$

$$N_{a,t} \sim \text{Normal}(v_{a,t}, e_{a,t})$$

$$\begin{aligned}
v_{p,t} &\sim \text{Poisson}(\Omega_{p,t}) \\
\Omega_{p,t} &= F_t \frac{v_{a,t-1}}{2} \\
v_{a,t} &= \Omega_{ap,t} + \Omega_{aa,t} + R_t \\
\Omega_{ap,t} &\sim \text{Binomial}(\phi_{p,t}, v_{p,t-1}) \\
\Omega_{aa,t} &\sim \text{Binomial}(\phi_{a,t}, v_{a,t-1}) \\
F_t &\sim \text{Gamma}(25, 0.03) \\
\phi_{p,t} &\sim \text{Beta}(5, 1.5) \\
\phi_{a,t} &\sim \text{Beta}(5, 1.5)
\end{aligned}$$

where  $N_{p,t}$  and  $N_{a,t}$  are the estimates ('observed data', estimated by NPS from trapping data) of population size for pups ( $p$ ) and adults ( $a$ ) in year  $t$ ,  $v_{p,t}$  and  $v_{a,t}$  are the unobserved 'true' annual population sizes,  $\Omega_{ap,t}$  is the number of adults in year  $t$  following the survival of pups from the preceding year  $t - 1$ ,  $\Omega_{aa,t}$  is the annual number of adults following the survival of adults from the preceding year  $t - 1$ ,  $\phi_{p,t}$  is the proportion of pups surviving from year  $t - 1$  to  $t$ ,  $\phi_{a,t}$  is the proportion of adults surviving from year  $t - 1$  to  $t$ ,  $R_t$  is the number of adult foxes released in year  $t$  (13,17,13,12,31,0,0,0,0,0,0,0,0,0,0 for 2004-2019),  $e_{p,t}$  and  $e_{a,t}$  are the standard deviations for the observation errors of pup and adult population sizes in year  $t$ , calculated from the 80% confidence intervals of the NPS mark recapture estimates.

Prior distributions are informative, with parameter values based on general knowledge of island fox biology (Coonan et al., 2010).

We fitted and compared four models, all of which included year-specific fertility and either year-specific (models 1 and 3) or constant (models 2 and 4) pup survival, and either year-specific (models 1 and 4) or constant (models 2 and 3) adult survival. Model fits were compared using DIC values.

JAGS was used in R using the jagsUI package for MCMC sampling of model parameters, using 6 chains, 10,000 burn-in iterations, 50,000 sampling iterations (thinning = 2). Chain convergence was assessed visually and using the Gelman-Rubin diagnostic.

### ***Movement parameters***

Because fox movement is likely to be a determining factor for *Leptospira* transmission, it was incorporated in the transmission model. Available movement data on individually marked foxes consists of a combination of trapping, VHF-telemetry, and GPS collar data, from 2004 through 2016. Fox location data were assigned to one of 15 patches on the island (Figure 5.3.4.2).

Movement between patches was analyzed for different years and seasons (1 = March-May, 2 = June-August, 3 = September-November, 4 = December-February). We estimated (1) the probability of moving to a different patch in a given season, (2) the frequency distribution of the patch distance when moving, and (3) the probability of moving between all pairs of patches. The probability of moving in a given season was calculated as the proportion of foxes observed in more than one patch, out of all foxes that were observed at least twice within the same season. Movement distance was calculated as the largest distance between patches visited within a season, for those foxes that visited at least 2 patches. These statistics were calculated for different time periods between 2004 and 2016 because population densities differed strongly between these periods, as the fox population recolonized the island, and movement behavior is likely density-dependent. The probability of moving between specific patch pairs was estimated by calculating the proportion of foxes that moved to each destination patch from a certain origin patch.

### ***Infection parameters***

In order to link infection state (susceptible, infectious, recovered) to observed data, as well as to estimate infectious period, we analyzed patterns in PCR and MAT data collected from wild foxes. Correlations between PCR results (positive or negative) and antibody levels against *Leptospira interrogans* serovar Pomona were analyzed using frequency distributions of antibody level for PCR-negative and PCR-positive samples, the proportions of PCR-negative and PCR-positive samples for each possible antibody level, and frequency distributions of the estimated time of infection for PCR-negative and PCR-positive samples. A distribution of possible times of infection was estimated for each sample in three steps.

First, a random sample of possible infection times was generated based on the estimated distribution of possible peak antibody levels in the fox population. Next, for each possible antibody level (1 through 12 log<sub>2</sub> dilution units) the time since infection (approximated as time since peak antibody level) was calculated, using each of the possible peak antibody levels generated in the previous step. When the antibody level was higher than a peak antibody level, the infection time was assumed to be 0 (these times are removed afterwards in order to obtain a clean distribution of infection times). This was done separately for PCR-negative and PCR-positive samples, resulting in a distribution of possible infection times for each group.

### ***Invasion, persistence, and monitoring***

Using the estimated parameter values, different scenarios were simulated. First, we simulated the probability of successful invasion of *Leptospira* in a stable population of susceptible foxes near carrying capacity. Every iteration, one infected fox was introduced in one of the four seasons of the first simulation year. Invasion was considered to be successful if at least one infected fox was still present at the start of the tenth simulation year. This was repeated 500 times, with the invasion probability defined as the proportion of successful invasions. Similarly, we estimated probability that the pathogen could maintain persistent circulation once it establishes endemic circulation on the island. The system was initiated with 20% of foxes in the infected state, an 55% of foxes in the recovered state. Successful persistence was defined as the presence of at least one infected fox at the start of the tenth simulation year.

We then tested the effect of abnormal demographic and environmental periods on persistence probabilities by randomly including a period of three consecutive years during which

birth rate and adult survival rate were reduced by 30%, or cumulative rainfall was reduced or increased by 30%. We estimated invasion probabilities under the same scenarios, assuming the initial introduction occurred at the start of the three-year anomalous period. In order to simulate normal conditions, each simulation randomly generates birth rates, adult mortality rates, and rainfall values. Adult mortality values were simulated from a gamma distribution with shape and rate parameters chosen so that the mean value was the mean of the last 10 observed mortality values, and standard deviation of these values divided by two to avoid excessive variability. Annual birth rate was chosen so that annual mortality was balanced out, on average, ensuring a stable population. This resulted in a mean birth rate of 0.45, and using the standard deviation of last five observed years divided by two, again to avoid excessive variability. A gamma distribution was used to randomly generate annual birth rates, with shape and rate parameters calculated based on the mean and standard deviation. Monthly rainfall values were generated using a normal distribution with mean and standard deviation equal to the mean and standard deviation of the values observed for a given month.

Last, we tested the effect of different monitoring strategies on the time delay before detecting *Leptospira* infection in the population. We tested monitoring strategies for two scenarios of endemic transmission (with the fox population near carrying capacity, or at half of carrying capacity) and two scenarios of *Leptospira* invasion (following introduction of one infected fox in a population near carrying capacity, or at half of carrying capacity). For each of these scenarios, the different monitoring strategies were applied to 20 simulation runs. Monitoring strategies consisted of sampling a certain number of foxes (ranging from 1 to 100) within a given month, where months were spaced at quarterly, semi-annual, and annual intervals. This resembles realistic sampling designs where the number of foxes, the duration of a sampling session, and the frequency of sampling sessions, are relatively limited.

### **5.3.5. Transmission dynamics model for *Leptospira* in island foxes on San Clemente Island**

To assess the probability of successful invasion of *Leptospira* in the San Clemente Island (SCL) fox population, we adapted an existing model of rabies and canine distemper virus transmission on SCL (Sanchez & Hudgens, 2020). We implemented the model in C++ to reduce processing time, and we used transmission parameters (infectious period and force of infection) specific to *Leptospira* based on those estimated with the Santa Rosa Island transmission model. Briefly, the model implemented observed variation in fox population density across the island, and transmission correlated linearly with home range overlap, which has been shown to be a good proxy for contacts between foxes. This allowed us to estimate the probability of successful *Leptospira* invasion in a fully susceptible population, by simulating two years following the introduction of an infected fox and counting the proportion of simulations in which an infected fox was still present by the end of the two years. This was done 1000 times for a population at normal population size (carrying capacity), and 1000 times for a population at half the carrying capacity. For each of these two scenarios, we further implemented different sampling strategies for detecting the pathogen, using the same scenarios we applied to the Santa Rosa Island model.

### **5.3.6. Determine when infected CSL are found on the islands, during and after a major outbreak**

*Leptospira* has circulated in California sea lions for decades, and CSL have haulouts and rookeries on the Channel Islands where they could potentially transmit the pathogen to island foxes. Indeed, at the outset of our study, we hypothesized that California sea lions were the

source of *Leptospira* that initiated the outbreak in SRI foxes. While this hypothesis was rejected, it remains plausible that future risk to other island fox populations (including those on DoD-owned rookery islands SMI, SNI, and SCL) will be driven by the presence of infected sea lions. Our sampling of the wild, free-ranging sea lion population on San Miguel Island during the last outbreak cycle prior to fadeout (i.e. 2010-2012) detected no evidence of *Leptospira* shedding by CSL during the large 2011 outbreak, but *Leptospira* shedding by CSL was detected the following year in 2012. To determine how exposure risk on the islands relates to major leptospirosis outbreaks observed in CSL on the coast, we sampled wild-caught, free-ranging California sea lions throughout their range (Figure 5.2.1.1). This work aimed to test whether *Leptospira*-infected CSL reach the rookeries only the year following a major outbreak on the coast, as suggested by our prior observations in 2010-12.

This work extended a long-term program to sample free-ranging CSL on rookery islands and coastal sites to assess their exposure to *Leptospira*, and to understand these patterns relative to those seen in the CSL stranding data from the Marine Mammal Center. Urine (n=1304) and serum (n=1492) samples were collected from anesthetized, physically restrained, or euthanized sea lions (n=1526) handled between January 2008 and November 2019 from three regions – the Channel Islands (San Miguel and San Nicolas Islands), central California (Año Nuevo Island, Monterey, and San Francisco’s Pier 39), and northern Oregon (Astoria and Willamette Dam) and southern Washington (Bonneville Dam; Table 6.3.6.1). The unexpected fadeout of *Leptospira* from the sea lion population (described in 6.2.1 and 6.2.3.2) led to the need to further extend our sampling beyond the original sampling plan, which we accomplished via approved reprogramming of DoD funds and leveraging of non-DoD funds. Ultimately, DoD SERDP funded work conducted on San Miguel Island between September 2016 through the end of 2017, as originally planned, in addition to one more expedition in the fall of 2019 to sample the vital post-outbreak year. All other fieldwork on San Miguel Island, including that done in 2018, and at sites other than San Miguel Island, was conducted under other funding sources. Samples from Willamette and Bonneville Dams were contributed to our project by collaborators with Oregon and Washington Departments of Fish and Wildlife from sea lions euthanized under NMFS Authorization to eligible states and tribes under MMPA Section 120(h), (14 Aug. 2020).

All urine collection from live animals occurred under anesthesia, and to minimize anesthetic risk, only apparently healthy animals were captured and sampled (Figure 5.3.6.1). Urine was collected by sterile catheterization (Figure 5.3.6.2). Estimated ages of sea lions captured in California ranged from 1 to 5 years, and those from Oregon and Washington were 6 years or older. Oregon and Washington animals were all males as females do not range that far north, and both sexes were sampled from all other locations. These animals represent a cross-sectional sampling of the apparently healthy, wild, free-ranging population. Serum chemistry analyses, MAT, PCR, and culture as well as NOAA permits and IACUC permissions are as described in 5.2.1.



**Figure 5.3.6.1. Anesthetizing CSL in the field.** (Top) CSL were anesthetized with Focal species in the project: Island fox (*Urocyon littoralis*), *Leptospira interrogans*, and California sea lions (*Zalophus californianus*).



**Figure 5.3.6.2. Collecting urine from an anesthetized CSL by catheterization.**

### **5.3.7. Investigation of the declining fox population on San Nicolas Island**

#### ***Serology***

MAT analysis was conducted on 246 serum samples from San Nicolas Island (SNI) between 2010 – 2015, which included samples from 222 adults and 24 pups. MAT was performed at the CDC in Atlanta, Georgia. All samples were tested against 20 serovars of *Leptospira*, and this 20 serovar panel included the following serovars: Alexi, Australis, Autumnalis, Ballum, Bataviae, Borincana, Bratislava, Canicola, Celledoni, Cynopteri, Djasiman, Georgia, Grippytyphosa, Icterohaemorrhagiae, Javanica, Mankarso, Pomona, Pyrogenes, Tarassovi, and Wolffi. Unless stated otherwise, foxes were categorized as positive if they had an antibody titer greater than or equal to 1:100 for any serovar. Pairwise chi square testing was used to compare seroprevalances between pairs of seasons, 2010-2011, 2012-2013, and 2014-2015.

#### ***Cross-reactivity analysis***

We compared the serologic cross-reactivity profiles of SNI and SRI wild foxes using the analytic approach developed and described in sections 5.1.1. and 6.1.1. As the approach focuses on a core set of 9 serovars (Autumnalis, Bratislava, Cynopteri, Djasiman, Icterohaemorrhagiae, Mankarso, Pomona, Pyrogenes, and Wolffi), SNI foxes that were positive only against other serovars were not included in this analysis.

#### ***Mortality data***

We received the SNI fox mortality database from the US Navy. We filtered the database to focus on mortalities from natural or unknown causes, which may have been associated with *Leptospira* infection. To do so, we removed all anthropogenic mortalities, including those categorized as death due to entrapment, vehicle strike, drowning, electrocution, euthanasia, and trauma. We also excluded 24 mortalities estimated to be from 2010 or 2011, for which carcasses were found unlabeled in a freezer but have no information on location, date, or cause of death.

All other categories were kept including unknown, unknown trauma, possible vehicle strikes, and those with unspecified causes. In periods from 2006-2009 and 2014-2017, a subset of island foxes on SNI were fitted with VHF collars with mortality sensors and tracked on a weekly basis via radio telemetry. Detection of island fox carcasses is expected to be higher in years when foxes were tracked via radio telemetry, however this should not bias the spatial distribution of mortalities that we analyze here.

### ***Comparison of seroprevalance data with mortality data***

Seroprevalance data and mortality data were analyzed to test for a relationship between SNI fox mortalities and evidence of exposure to *Leptospira*. To aggregate the data spatially, the island was divided into 4 segments using quartiles of the longitude range of SNI (Figure 5.3.7.1). Seroprevalance and number of non-anthropogenic mortalities was calculated for each quarter of SNI during each year from 2010 to 2015, yielding 24 year\*quarter data points. For 5 of these points, seroprevalance could not be calculated as no samples were collected from that quarter in that year so those points were excluded from the analysis. The number of mortalities in each year\*quarter was plotted against the corresponding seroprevalance estimate, and a negative binomial regression was run to test for a relationship. To test robustness of our findings to the arbitrary spatial subdivision of the island, the analysis was repeated by dividing the island into 3 segments instead of 4 (Figure 5.3.7.1). In this analysis, only one point was dropped due to a lack of seroprevalance data for that segment in a given year.

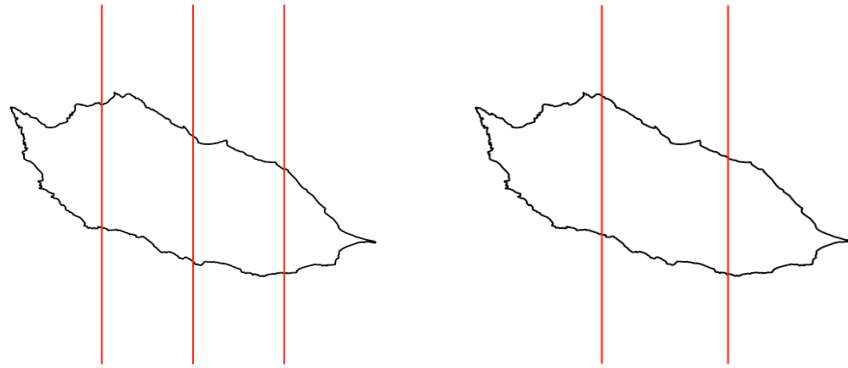


**Figure 5.3.7.1. Spatial subdivision of San Nicolas Island.** Maps showing the lines dividing the island into 4 and 3 segments for statistical analysis.

### ***Necropsy report analysis***

Necropsy reports of all SNI mortalities from 1980-2017 and resulting from both anthropogenic and natural causes were reviewed to look for clinical signs of leptospirosis. For this broad review, any kidney abnormalities other than those caused by trauma were considered possible signs of leptospirosis. These abnormalities included necropsy comments of interstitial nephritis, karyomegaly, amyloidosis, renal cortical fibrosis, glomerulonephritis, fibrosis, and renal disease.

Kidneys were not always present to be evaluated due to severe trauma or necrosis. When kidneys were known to be missing from carcasses, those carcasses were not included in the tally of animals analyzed. However, in some reports, it was not noted whether the kidney was missing or if it was in normal condition, so there was nothing to report.

## 6. Results and Discussion

### 6.1. Origins of the Santa Rosa Island Outbreak

#### 6.1.1. Reconstruction of the fox outbreak up to 2010

##### *Exposure to *Leptospira* was widespread on Santa Rosa Island in the 1980s*

Previous serological studies of mammals on Santa Rosa Island had indicated no persuasive evidence of exposure to *Leptospira* at the levels seen in the reintroduced foxes. A study analyzing island fox sera collected in 1988 reported no seropositives but only tested against serovars Canicola and Icterohaemorrhagiae (Garcelon et al., 1992). A study of 14 of the 15 Channel Island foxes taken into captivity in 2000-2001 showed 2/14 individuals with low-titer positive results against serovar Pomona (Clifford et al., 2006). These profiles differed markedly from the MAT profile seen in foxes sampled during the Santa Rosa Island outbreak, so we previously hypothesized that the current outbreak strain of *Leptospira* was absent from Santa Rosa Island prior to the captive program.

To investigate the history of *Leptospira* exposure on Santa Rosa Island, we accessed and analyzed banked serum samples from feral pigs and island foxes. We analyzed 60 samples collected from pigs in 1987 and 43 samples collected from island foxes in 1988. We also analyzed all serum samples available from captive foxes from 2000-2008, which included reanalyzing samples from the wild foxes brought into captivity (the “founding foxes”). These samples were analyzed against a broader set of 20 *Leptospira* serovars at the CDC laboratory in 2015 and 2016, which yielded results with higher sensitivity than in past studies.

We detected a 62% (95%CI, 48%-74%) seroprevalence (37/60) in the 1987 pig samples. The pig sera reacted to 11 different serovars in total including serovar Pomona; 49% of individual pigs reacted to just one serovar, while the others reacted to between 2 and 11 serovars. 46% (17/37) of MAT positive pigs had serovar Pomona as their highest titer (or tied for the highest titer), while 51% (19/37) were negative for serovar Pomona but reacted to other serovars. Pomona titers ranged from 0 to 1:6400 with 70% of the individuals having low titers at or below 1:200 (Table 6.1.1.1, Figure 6.1.1.1).

	0	100	200	400	800	1600	3200	6400
Pomona Titer	19	4	8	4	1	0	0	1
Highest Titer	0	14	12	7	3	0	0	1

**Table 6.1.1.1. MAT titer values from 1987 Santa Rosa Island pig samples.** Frequency table of the MAT titer against serovar Pomona and the highest MAT titer against any serovar for the seropositive pig samples.

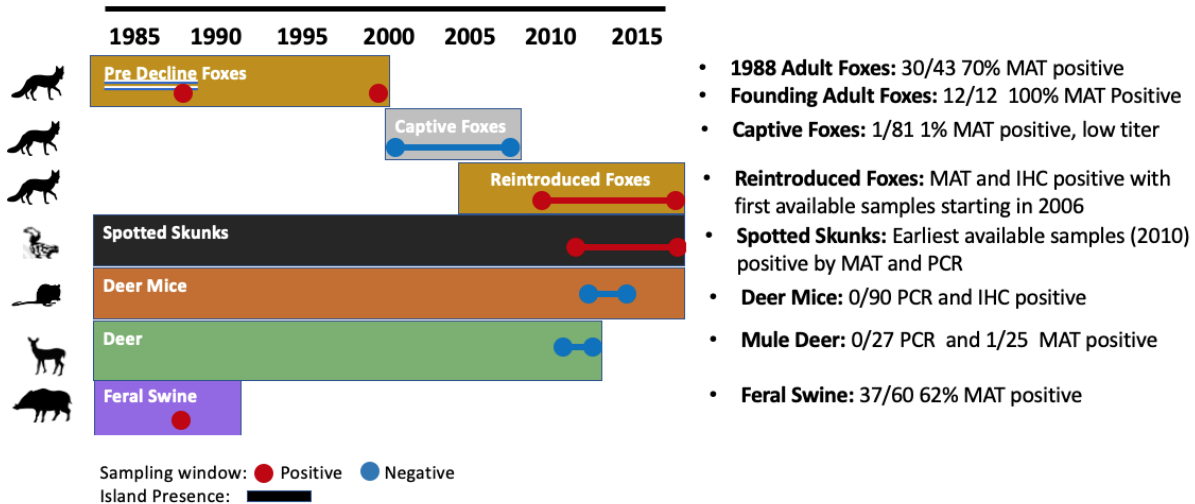


**Figure 6.1.1.1. Santa Rosa Island species and testing timeline.** Timeline of the presence of species on Santa Rosa Island in colored rectangles, with the sampling window for each species indicated by a dot for a single sampling period or a line for a sampling window. Blue sampling windows indicate negative test results and red indicates positive test results.

We detected a 70% (95%CI, 54%-83%) seroprevalence (30/43) in the samples collected from adult island foxes on Santa Rosa Island in 1988. We found a 0% seroprevalence (0/4) in samples collected from fox pups in 1988, and one sample of unknown sex and age class was positive (Figure 6.1.1.1, Table 6.1.1.2). Foxes reacted to 11 different serovars in total, with individual foxes reacting to between 1 and 9 serovars (Table 6.1.1.3). 23% (7/31) of seropositive foxes had serovar Pomona as their highest titer (or tied for their highest titer), and titers against serovar Pomona ranged from 0 to 1:3200. 35% (11/31) were negative to Pomona but reacted against serovar Autumnalis. This serological profile (i.e. Autumnalis being higher than Pomona, or Autumnalis being positive while Pomona is negative) is a common pattern with our outbreak strain in the foxes in samples collected after 2010 (see section 6.3.2.4).

These positive results from pigs in 1987 and foxes in 1988 indicate that some strain of *Leptospira*, with high MAT reactivity against serovar Pomona, was widespread on Santa Rosa Island since at least the late 1980s. Further analysis into the cross-reactivity patterns, which compares these results with those from captive foxes and post-reintroduction wild foxes, are presented later in the results (see section 6.3.2.4).

	Adult		Pup		Unknown		Total	
	% positive	N	% positive	N	% positive	N	% positive	N
<b>Male</b>	75%	16	0	1	--	0	71%	17
<b>Female</b>	67%	27	0	3	--	0	60%	30
<b>Unknown</b>	--	0	--	0	100%	1	100%	1
<b>Total</b>	70%	43	0	4	100%	1	65%	48

**Table 6.1.1.2. Serology results from 1988 island foxes.** Data includes the MAT seroprevalence of the 1988 island fox serum samples against any serovar in the panel by sex and age class.

	0	100	200	400	800	1600	3200	6400
<b>Pomona Titer</b>	13	3	9	3	3	1	1	0
<b>Highest Titer</b>	0	6	9	12	1	1	2	2

**Table 6.1.1.3. MAT titer values from 1988 Santa Rosa Island fox samples.** Data presented is a frequency table of the MAT titer against serovar Pomona and the highest MAT titer against any serovar for the 1988 fox serum samples.

***The founders of the captive fox population were positive for Leptospira exposure***

After learning that *Leptospira* was present in pigs and foxes on Santa Rosa Island in the late 1980s, we re-analyzed samples from the 15 founding foxes that were taken into captivity between March 2000 and May 2001. Contrary to previous results (Clifford et al., 2006), our analyses (which included more samples and tested against more serovars, in a lab and time period with higher-sensitivity MAT techniques) found that all adult founding foxes showed evidence of exposure to *Leptospira*. 14 of the 15 founding foxes had serum tested via MAT analysis, including all 12 adults and 2 of 3 pups. All 12 adults had positive titers, but both pups were negative (Figure 6.1.1.2). Of the seropositive founding foxes, the titers against serovar Pomona tested at CDC ranged from 0 to 1:400, while the highest titers against any serovar ranged from 1:100 – 1:6400. The 12 adult founders with MAT tests had multiple MAT tests per individual with 53 total positive MAT tests (from samples tested at CDC) for these individuals when they were in captivity. 58% (7/12) of the founding adults had at least one test with positive results against serovar Pomona. 42% (5/12) of the founding adults never had a positive test against serovar Pomona, however each of these foxes had positive tests against serovar Autumnalis. Overall, 11% (6/53) of the samples had serovar Pomona as the highest (or tied for highest) titer, while 51% (27/53) of the samples were negative to serovar Pomona but positive to serovar Autumnalis as well as other serovars. Again, our studies show this serologic profile is typical for the outbreak strain in island foxes (section 6.3.2.4).

These results were all from samples taken 1 to 4 years after the founders were brought into captivity. For all but one of the adults, the first sample tested at CDC was positive, though most of these individuals had an earlier negative test at Cornell. The adult whose first CDC test was negative was positive in some future tests. This pattern could be explained by transmission during the early phase of captivity or false-negative results (potentially because of low test sensitivity or sample degradation due to long-term storage and freeze-thaw cycles). Of these, we believe false-negative results are the most plausible because all of these initial negative samples were tested at Cornell in the early 2000's, and more recent testing has revealed that these early

tests had low sensitivity. The samples were also not tested against serovar Autumnalis, which is a serovar that dominates the foxes' MAT reactivity against the outbreak strain. The first sample tested at CDC for each of these individuals was positive.

Four of the adult founding foxes, including the one fox that did not have a serum sample available, died in captivity and had kidney tissue archived (formalin-fixed and paraffin-embedded). One captive-born fox also had kidney tissue available. We tested these kidney tissues for the presence of *Leptospira* via IHC and PCR. Four of the samples were negative via IHC. The fifth, which was from the founding fox that did not have a serum sample, showed possible presence of the bacteria, but the pathologist could not state definitively whether the test was positive or negative (Figure 6.1.1.2). The PCR results from all formalin-fixed and paraffin-embedded kidney samples were negative, though sensitivity of the assay on samples preserved in this manner is unknown and expected to be low. The founding foxes with kidney samples had been in captivity for 1, 4, 6, and 9 years when they died, and it was the fox that died one year after being brought into captivity that showed a suspect positive result via IHC. This contributes to the evidence that the founding foxes had been exposed in the wild but were probably not shedding the bacteria beyond the initial period of captivity.



### ***Leptospira did not persist in the captive population***

After confirming widespread exposure to *Leptospira* in the foxes that founded the captive population, we tested serum samples from the remainder of the captive population (i.e. those born in captivity). We were able to test samples from 81 of the 85 captive-born foxes, collected while in captivity, and only 1 of those (1%) had any positive MAT titers. The one fox with a positive MAT result was among the 8 pups born in captivity months after their mothers were brought in from the wild. This individual was never positive to serovar Pomona. He was positive to serovar Bratislava with an unknown titer at Cornell in 2001 when he was 1 year old, and he was positive to serovars Autumnalis and Djasiman, both at titers 1:200 at CDC, both times he was tested when he was 4 and 5 years old in 2004 and 2005.

It is unclear why this captive-born fox tested positive in captivity. The tests could be false positives since they are very low titers to very few serovars. This fox was not tested until he was an adult, so we do not know his exposure status as a pup, but the positive results do not look like maternal antibodies, which typically last only a few months after birth. He could have been infected by vertical or pseudo-vertical transmission from his mother who had been captured with positive MAT results reflecting exposure to *Leptospira* while in the wild just prior to his birth. However, both of his litter mates always tested negative throughout captivity. 39 pups overall were born to mothers who ever tested positive in captivity. 37 of these had MAT tests during their time in captivity and only 1/37 ever had a positive test, showing that vertical transmission from the founders was very inefficient.

A pedigree of the founding and captive born foxes was created to help visualize the lineages and disease states of the foxes in captivity and to look for any evidence of vertical transmission (Figure 6.1.1.3). The lack of any more positive captive-born foxes, other than the one individual with possible vertical transmission, is evidence that transmission between captive foxes was virtually non-existent. We conclude that *Leptospira* did not persist in the captive fox population, either because the precautions taken to limit disease transmission were effective or possibly because the exposed founding foxes were no longer transmitting leptospires at infectious levels when they were brought into captivity.

# Santa Rosa Island Fox Pedigree

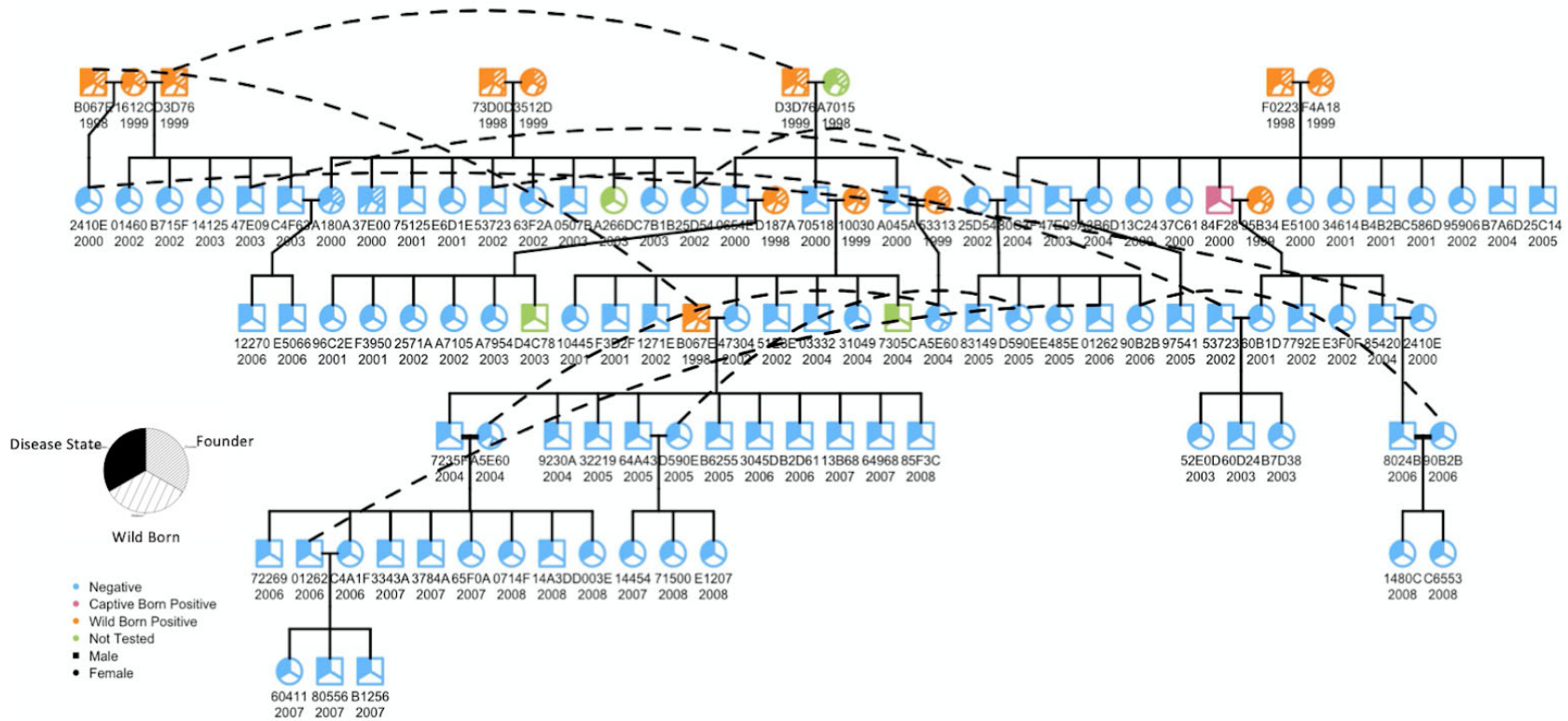


**Figure 6.1.1.3. Pedigree of captive fox population with disease state, birth status, and sex for each individual.** Males are circles, females are squares. Individuals that appear in the chart more than once are connected by a dotted line. If the individual was wild-born, the bottom third of the tile is hatched. If the individual is a founder, the right third of the tile is hatched. The solid left third of the tile is colored to indicate the disease state of the individual: green if unknown, blue if negative, orange if a wild-born positive fox, salmon if a captive-born positive fox. Wild born positive female, 07061, did not produce offspring so is omitted from the pedigree.

### *The Leptospira outbreak expanded rapidly in the reintroduced fox population*

Release of foxes from captivity began in late 2003 and continued with pulses of releases each fall from 2004-2009 (Figure 6.1.1.1). Early results were mixed, with many rapid mortalities and foxes taken back into captivity, but over this period the wild fox population grew steadily (Figure 5.1.1.1). Because the pathogen did not spread among the captive foxes, most individuals were not exposed prior to release (Figure 6.1.1.1). However, our retrospective analysis of serum and kidney samples shows that by 2006 exposure to *Leptospira* was spreading with alarming speed in the reintroduced population.

In 2006, the first year a large sample (i.e. more than 2) of the wild fox population was tested via MAT, exposure to *Leptospira* was widespread with a 63% (95%CI, 35%-85%) seroprevalence in adult foxes and 67% (95%CI, 38%-88%) seroprevalence in pups (Figure 6.1.1.4, Table 6.1.1.4). Seropositive foxes were found over much of the island's area, with the exception of the eastern tip (Figure 6.1.1.5). The high seroprevalence detected in pups in 2006 indicates a very high force of infection in 2006, with two thirds of pups converting from susceptible to infected within months of their birth. We interpret these MAT results as true exposures and not maternal antibodies because all the sampling occurred between September 2006 and January 2007, which is well beyond the window when we would expect to see maternal antibodies in foxes that are born between March and May (Adler & de la Peña Moctezuma, 2010).

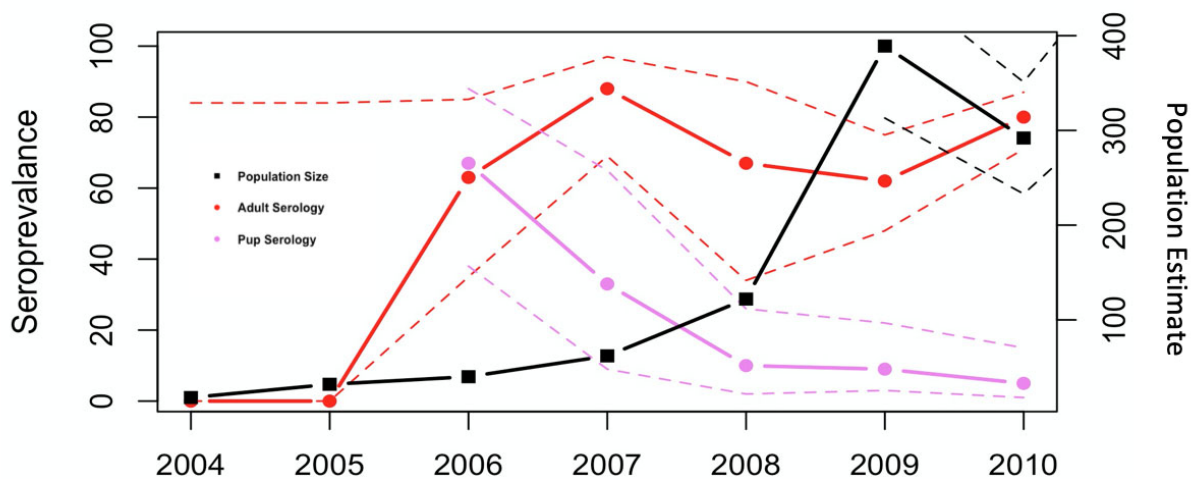


**Figure 6.1.1.4. Seroprevalence of reintroduced Channel Island foxes by age group, 2004-2010.** The island fox population estimate is in black. The adult fox seroprevalence is in red and the fox pup seroprevalence is in pink. Dashed lines are 95% confidence intervals for seroprevalence and 80% confidence intervals for population estimate.

		2004	2005	2006	2007	2008	2009	2010
All	Positive	0	0	20	26	12	38	82
	N	2	2	31	37	46	99	144
	SP	0%	0%	65%	70%	26%	38%	57%
	95%CI	0%-84%	0%-84%	45%-81%	53%-84%	14%-41%	29%-48%	48%-65%
Adult	Positive	0	0	10	22	8	34	80
	N	2	2	16	25	12	55	100
	SP	0%	0%	63%	88%	67%	62%	80%
	95%CI	0%-84%	0%-84%	35%-85%	69%-97%	16%-43%	48%-75%	48%-65%
Pups	Positive	0	0	10	4	3	4	2
	N	0	0	15	12	31	44	44
	SP	NA	NA	67%	33%	10%	9%	5%
	95%CI	NA	NA	38%-88%	9%-65%	2%-26%	3%-22%	1%-15%

**Table 6.1.1.4. Seroprevalence of reintroduced Channel Island foxes by age class, 2004-2010.** Results are shown for all foxes, adults only, and pups only. N indicates the number of samples analyzed for each age group in each year. SP indicates the seroprevalence estimate, and 95% CI shows the 95% confidence interval around the seroprevalence estimate.

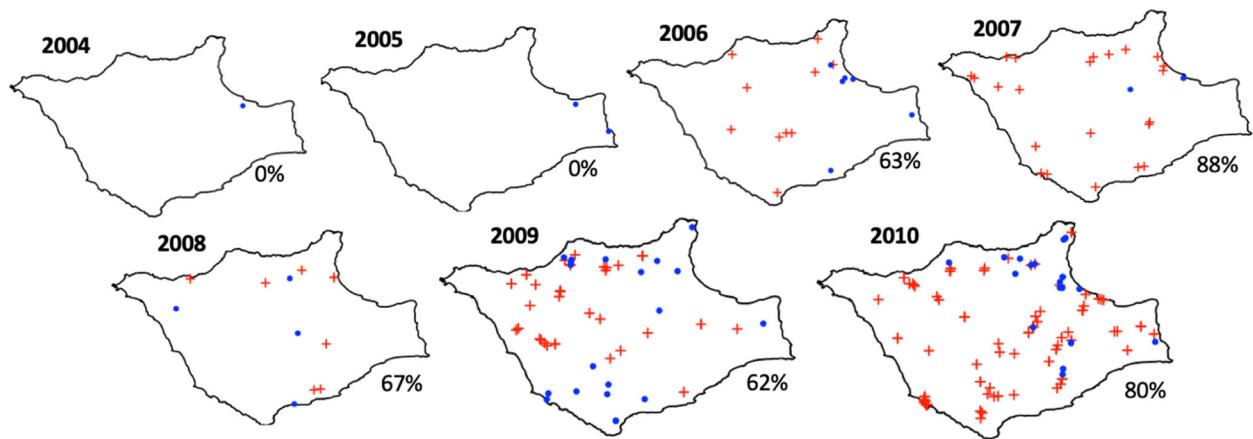


**Figure 6.1.1.5. Maps of MAT serology results for adult island foxes on Santa Rosa Island, 2004-2010.** Blue circles indicate negative MAT results. Red crosses indicate positive MAT results. Numbers indicate seroprevalence among adult foxes alive during that year.

Serum samples for the small populations of wild foxes in 2004 and 2005 are very limited, posing serious challenges to direct assessment of *Leptospira* exposure in the earliest phase of the reintroduction program. Due to the very small population size and rapid mortalities or recaptures of released foxes, only 2 foxes were tested via MAT in each of 2004 and 2005 and they were all negative against the outbreak strain. The 2 samples from 2004 were from adult foxes taken 5 and 10 months after being released and the 2 samples from 2005 were from adult foxes taken 11 and 20 months after being released (Figure 6.1.1.5, Table 6.1.1.4).

The earliest concrete evidence of *Leptospira* infection in the wild fox population comes from a kidney sample collected at necropsy from an individual found dead in March 2006, which was positive by PCR. This animal was seronegative in captivity in August 2005, then was released to the wild in October 2005. Thus, it became infected in the wild during the brief window from October 2005 to March 2006. Details on this and other early mortalities associated with *Leptospira* are reported in section 6.3.3.

The exposure pattern seen in the reintroduced foxes is also evident in wild-born foxes in the reintroduced population during this period. We compiled an extraordinarily high-resolution picture of these dynamics by reviewing the full records associated with each individual fox that was released from captivity or born in the wild from 2003-2007 (Figure 6.1.1.6). This figure shows when each individual was born, periods when they were captive or wild, when they were tested for *Leptospira*, and when they died or went missing. The figure shows the high proportion of foxes testing MAT positive shortly after birth or release once widespread sampling via MAT was initiated in 2006, with many foxes testing positive within months of their birth or release. It also shows a large number of rapid mortalities during this time, as analyzed in section 6.3.3.

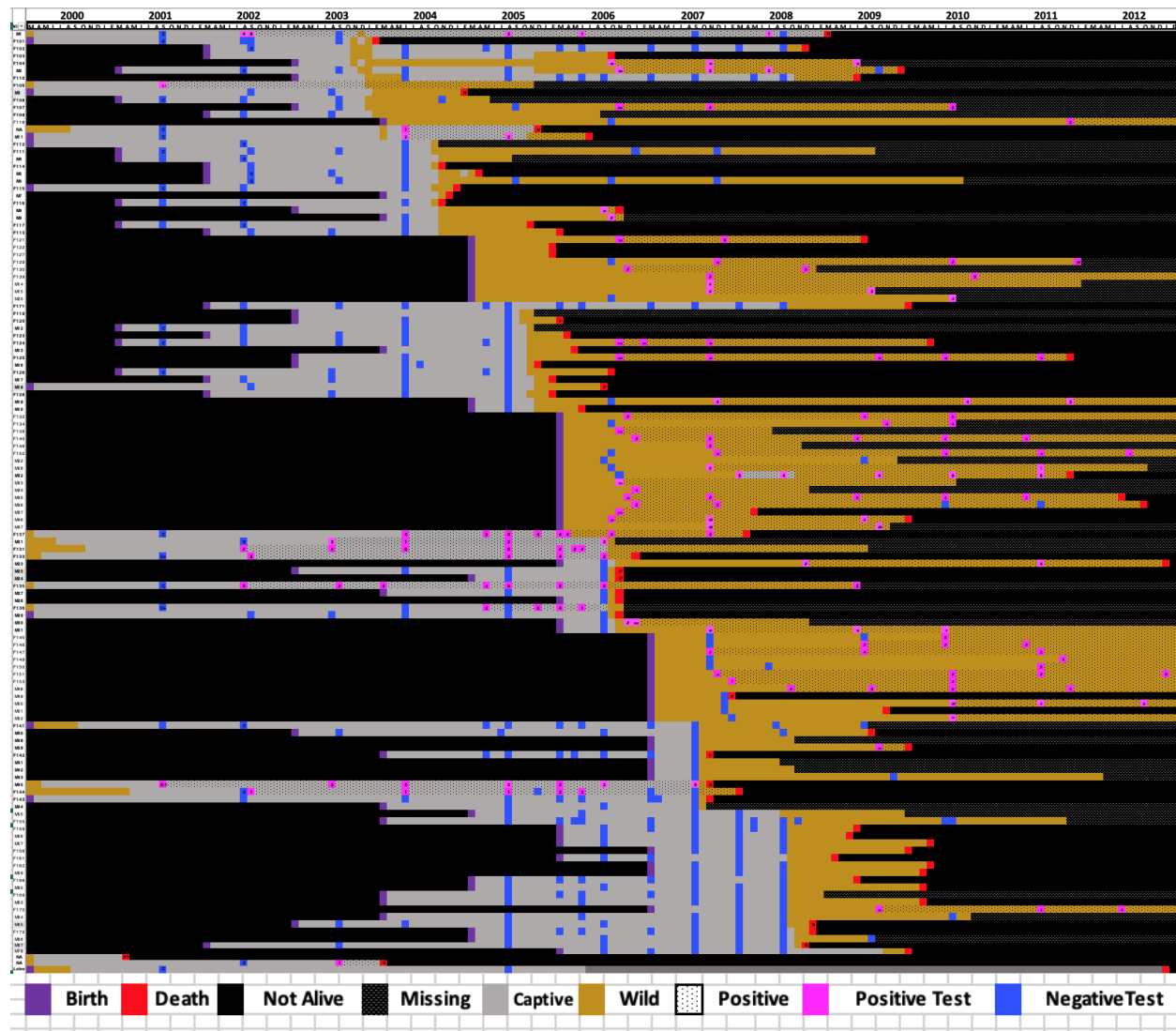


**Figure 6.1.1.6. Individual timelines of locations, sample collections, and test results for all foxes released from captivity or born into the wild between 2003-2007.** Foxes are shown in order of release/birth date. Brown squares indicate months when the fox was in the wild; grey squares indicate captivity. A blue square is a negative MAT result and a pink square is a positive MAT result. A ‘C’ in the box indicates the result is from Clifford et al. 2006. Purple squares indicate the month the fox was born; red squares show the month the fox died. In red squares, a ‘P’ indicates a positive and ‘N’ a negative IHC or PCR result on the kidney. Stippled areas show the period following first positive test result for each individual.

Further insight can be gained from the 2006 data by evaluating MAT titer levels, given that antibody titers peak shortly after initial exposure and then decay over time (Borremans et al., 2016; Pepin et al., 2017). 20 out of 31 individuals tested in the wild in the 2006 season were seropositive. Within this group, 11 foxes (5 adults and 6 pups) showed signs of recent infection with very high titers against serovar Pomona of 1:12,800 (4 animals), 1:25,600 (3 animals) and 1:51,200 (4 animals). These animals likely were infected in 2006. The 9 other positive foxes (5

adults and 4 pups) showed lower titers against serovar Pomona, indicating possible earlier dates of infection.

We analyzed these MAT data by applying the antibody titer kinetic model developed from SRI fox data (presented in section 6.3.2.2). This Bayesian model yields a posterior distribution for the time of infection of each seropositive animal, based on their MAT titer and window of possible exposure. We combined these findings with data on the windows of exposure for foxes that tested positive for *Leptospira* at necropsy (presented in section 6.3.3), to arrive at our best synthesis of evidence for the temporal origin of the outbreak. While there is inevitable uncertainty for each individual, in aggregate the data point to an origin in the second half of 2005 (Figure 6.1.1.7). Two foxes have their median posterior date of infection in November-December 2005, and there are 7 foxes with >30% probability of having been infected by the end of that year. It is possible that one or two infections occurred before mid-2005, but the data and samples do not exist to pin this down. The latest possible date for the first infection is March 2006, and it is clear that the outbreak had considerable momentum by mid-2006.

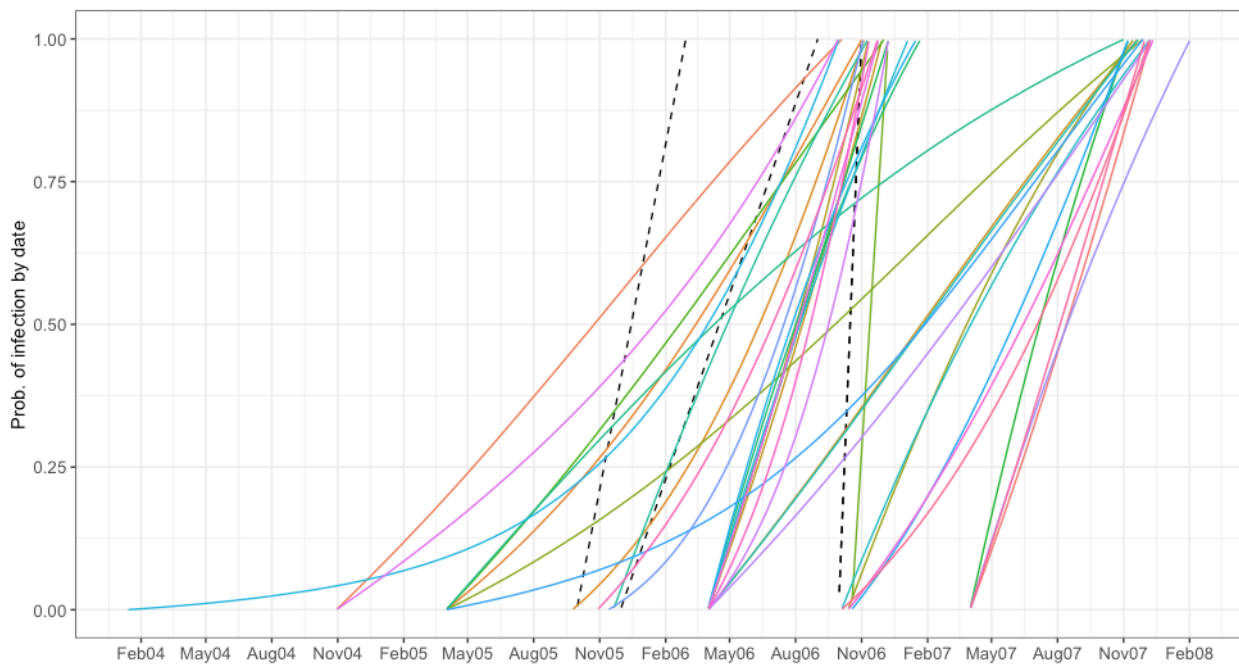


**Figure 6.1.1.7. Estimated times of infection for the first infected foxes in the outbreak.** Each line corresponds to an individual fox that tested positive for *Leptospira* by MAT or PCR by 2007. The lines show the cumulative probability that the individual was infected by a given date; each line starts at 0 when a fox is released or born and ends at 1 when that fox tests positive. Solid lines are cumulative distribution functions for the posterior probability estimated from the first positive MAT titer level. Dashed lines show individuals who were PCR-positive for *Leptospira* at necropsy, whose posterior date of infection was assumed to be uniformly distributed over the window of possible exposure.

### ***Leptospira strains from before and after the captive period appear the same***

We have established that *Leptospira* was widespread on Santa Rosa Island before the foxes were taken into captivity, and that the reintroduced fox population showed signs of high

exposure within a few years (or less) of being released from captivity. We do not have bacterial isolates from before captivity, so we cannot use genetic methods to test whether the *Leptospira* strains from before and after the captive period were the same. MAT analyses show strong cross-reactivity, so cannot be interpreted simply to determine the infecting serovar. Instead, we developed a novel statistical approach to analyze the cross-reactivity profiles, to assess evidence that the same strain was responsible for the seropositivity observed in different time periods and host species.

We used the cross-reactivity profile from the island foxes sampled during the outbreak as our point of reference, since these data are most abundant and are linked to pathogen isolates that we have characterized genetically. These MAT data exhibit a strong two-clade pattern, with highest titers against serovar Pomona (the true infecting serovar), Djasiman, and Autumnalis (Figure 24). Using our permutation test, we determined that the MAT data from island foxes sampled before the captive period exhibit the same cross-reactivity profiles and hence appear to represent exposure to the same strain of *Leptospira*. The characteristic clade structure is significantly present in the MAT profile from wild foxes sampled in 1988 (Figure 6.1.1.9,  $p=0.012$ ) and the profile from wild foxes taken into captivity in 2000-2001 (Figure 6.1.1.10,  $p=0.011$ ). We also analyzed the profile from feral pigs sampled in 1987, which showed similar structure but was not quite significant at the  $\alpha=0.05$  level (Figure 6.1.1.11,  $p=0.083$ ). In our work on cross-reactivity in *Leptospira* serology, we show that quantitative titers and cross-reactivity patterns vary across host species (section 6.3.2.4), so we speculate that the pigs and foxes may still reflect exposure to the same strain, since it was circulating in island foxes at that time.

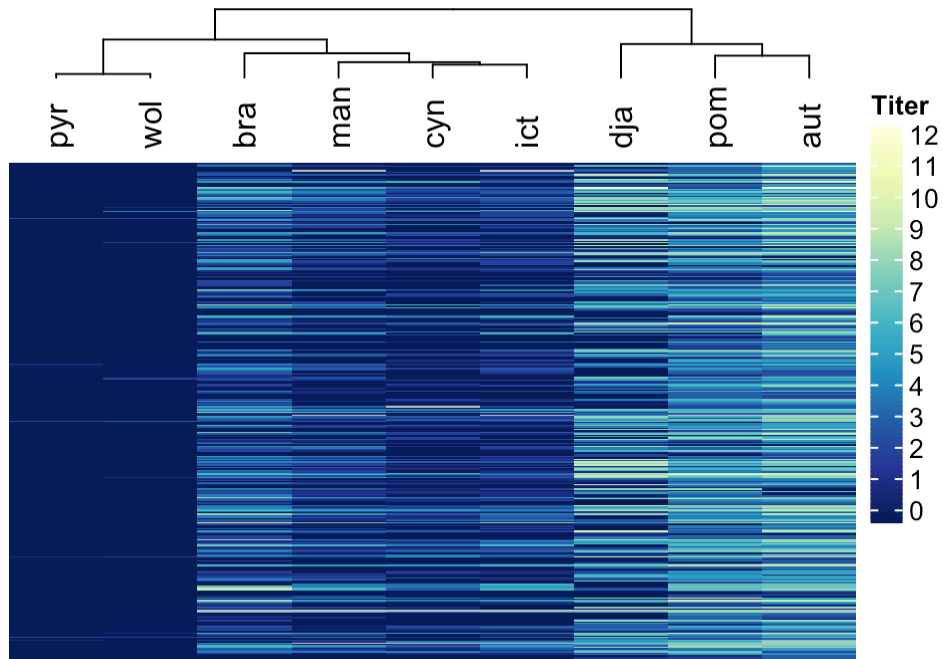


**Figure 24. MAT cross-reactivity profile for island foxes sampled during the outbreak, between 2006 and 2013 Island foxes.** Each row represents an individual fox, and the colors show the magnitude of the MAT titer against the serovar shown in the column header. The dendrogram shows the serovar clustering pattern of the cross-reactivity profile. Serovars are abbreviated as follows: aut=Autumnalis, bra=Bratislava, cyn=Cynopteri, dja=Djasiman, ict=Icterohaemorrhagiae, man=Mankarso, pom=Pomona, pyr= Pyrogenes and wol=Wolffi.

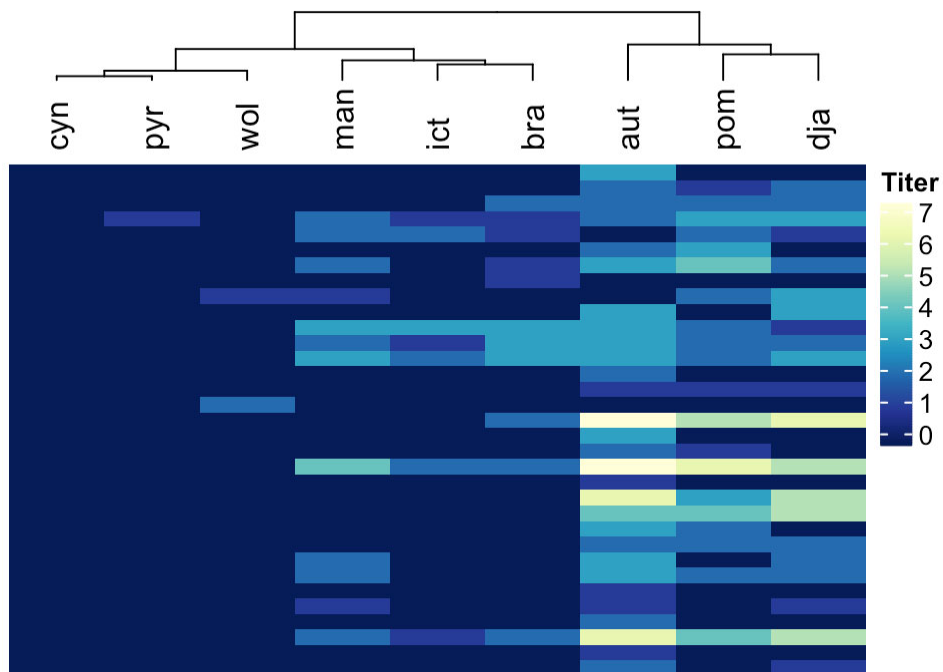


**Figure 6.1.1.9. MAT cross-reactivity profile for 1988 Channel Island foxes.** P-value = 0.01196, N=31.

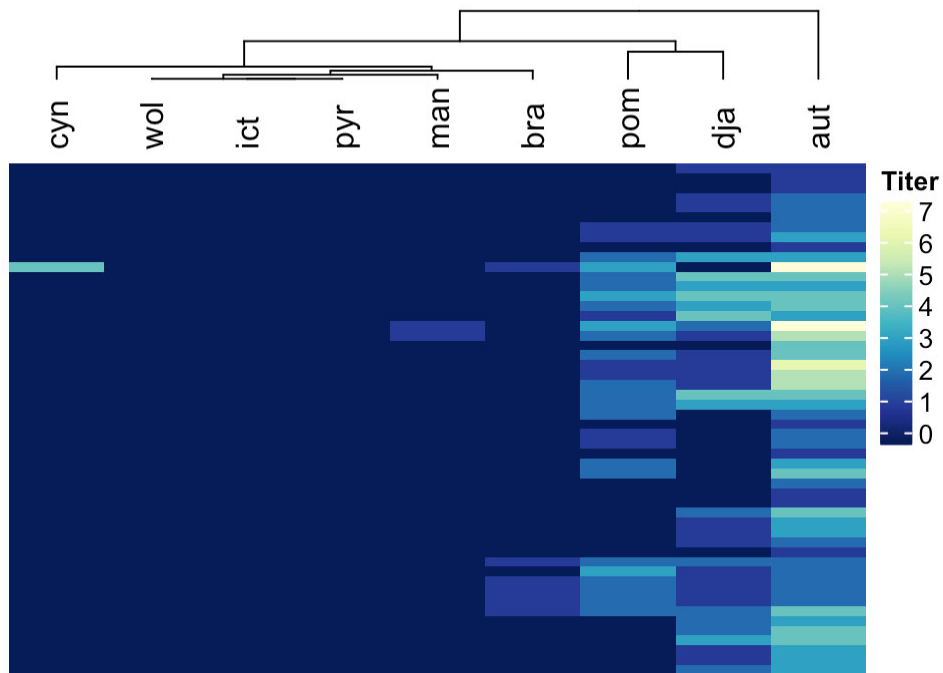


**Figure 6.1.1.10. MAT cross-reactivity profile for Channel Island foxes taken into captivity in 2000 and 2001. P-value = 0.0115, N=52.**

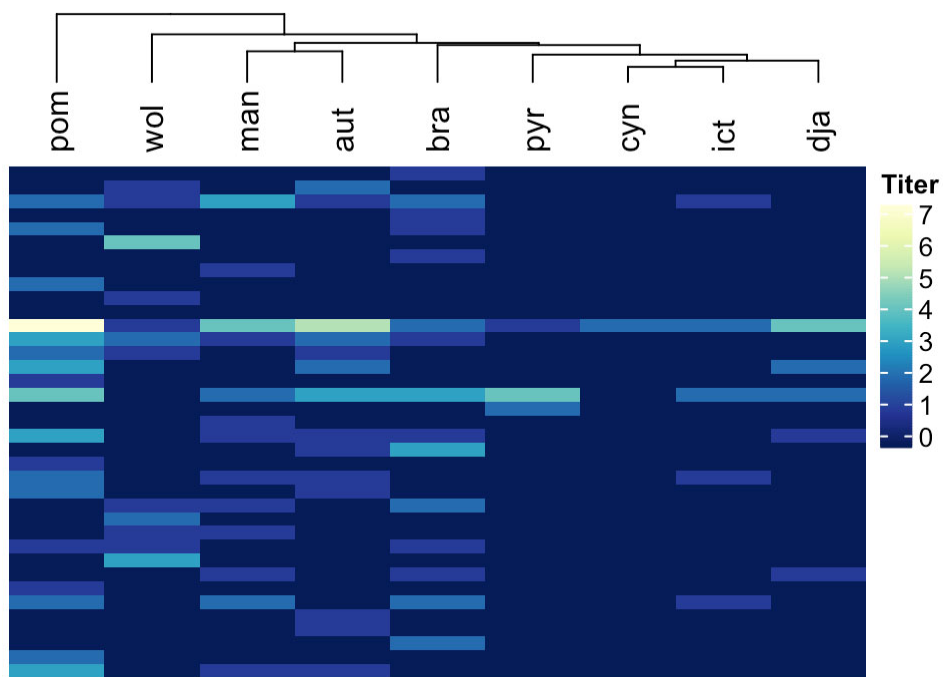


**Figure 6.1.1.11. MAT cross-reactivity profile for 1987 feral pigs on Santa Rosa Island. P-value = 0.08334, N= 37.**

The main difference between MAT data collected from Channel Island foxes before and after the captive period is the magnitude of titer values. Post-reintroduction foxes exhibit peak titers ranging from 1:100 to 1:204800, while the 1988 and 2000-2001 foxes exhibit peak titers from 1:100 to 1:6400. The lower titers seen in older samples could be due to long-term storage of the archived samples, more freeze-thaw cycles, or the possibility that individuals were sampled further from the time of their initial infections so their titers had decayed.

***The pathogen may have persisted on Santa Rosa Island in island spotted skunks while foxes were absent***

After learning that the bacteria did not persist in the captive foxes and that the reintroduced foxes were quickly acquiring the bacteria upon release back into the wild, we investigated possible reservoirs of infection that would explain persistence on Santa Rosa Island while all island foxes were in captivity and that could act as a source for exposure of the reintroduced foxes. We investigated whether the other terrestrial species present on the island could have acted as maintenance hosts for *Leptospira* while the foxes were in captivity. We tested three of the four terrestrial mammal species present on Santa Rosa Island when the foxes were released: the mice, deer, and skunks. We were unable to test the elk as they were eradicated by the time we were collecting samples, and no samples from elk were archived.

We tested 72 mouse kidney samples, collected between 2012 and 2015, and all came back negative via IHC (0/72) and PCR (0/69) (Table 6.1.1.5). This is strong evidence that the mice on Santa Rosa Island are not a host to the *Leptospira* bacteria, which is consistent with the broader literature that mice are not known hosts for *Leptospira* serovar Pomona (Bolin & Zuerner, 1996; Zuerner & Alt, 2009). While the samples are only from the northern half of the island (Figure 6.1.1.12), this is the region associated with highest infection risk in the reintroduced foxes during the early phase of the outbreak. Therefore, if the mice were a reservoir host and the source of infection to the reintroduced foxes, we would expect to have had some positive results in the samples we tested.

Sample year	Individuals sampled	PCR	IHC
2012	16	0/13	0/16
2013	8	0/8	0/8
2014	38	0/38	0/38
2015	10	0/10	0/10
<b>Total</b>	72	0/69	0/72

**Table 6.1.1.5. PCR and IHC results for deer mouse kidney samples.** PCR and IHC values are reported as the number of positive samples / number samples tested.

We tested samples from 27 mule deer that were collected in the course of their eradication from Santa Rosa Island in 2012 and 2013 using a combination of IHC, PCR and MAT analyses (Table 6.1.1.6). There was a urine and/or kidney sample from 26 of the 27 deer, and a blood sample from 25 of the 27 deer. All 21 urine PCR tests, 6 kidney PCR tests, 6 kidney IHC tests, and 24/25 MAT titers were negative (Table 6.1.1.6). One deer had a positive MAT

result with a titer of 1:100 against serovar Pomona. The deer was negative to the other 19 serovars in the 20-serovar panel and was negative via kidney IHC and PCR. This deer did not have a urine sample available to test. Given the borderline-positive titer level, the MAT result could be a false positive. If it is a true positive, it indicates that this deer was exposed to the bacteria, possibly by environmental exposure or spillover from island foxes, which had a large population size and high *Leptospira* shedding prevalence in 2012 when this sample was collected. If the deer population were maintenance hosts of the bacteria and the source of the reintroduced fox exposure, we would expect to see a higher seroprevalence in the MAT results, as well as positive PCR and IHC results showing that the deer have the bacteria in their kidneys and could be shedding. Altogether, given the lack of evidence of kidney colonization or shedding, and only one very low MAT titer detected, the weight of evidence is that the deer are not maintenance hosts of *Leptospira* on Santa Rosa Island and were not the source of *Leptospira* exposure in the reintroduced foxes.



**Figure 6.1.1.12. Locations of the deer mouse kidney samples.**

	<b>Individuals sampled</b>	<b>Urine PCR</b>	<b>Kidney PCR</b>	<b>Kidney IHC</b>	<b>MAT</b>
<b>2012</b>	22	0/21	0/2	0/2	1/22
<b>2013</b>	5	NA	0/4	0/4	0/3
<b>Total</b>	27	0/21	0/6	0/6	1/25

**Table 6.1.1.6. PCR, IHC, and MAT results for mule deer samples.** PCR and IHC values are reported as the number of positive samples / number samples tested.

Island spotted skunks present a different picture. MAT and culture results from the spotted skunks collected in 2010-2012 indicated that skunks are a host of *Leptospira* bacteria, and a potential source of the pathogen into the reintroduced foxes. Serum samples from the 2011 and 2012 seasons show a 42% (95% CI, 25%-61%) and 18% (95% CI, 10%-30%) seroprevalence in the spotted skunks, respectively, and evidence of exposure to *Leptospira* was widespread in skunks across the island (Figure 6.1.1.13). Also 2 of the 8 urine samples collected from skunks at the end of the 2010 season were culture-positive, indicating that the skunks were actively shedding the bacteria in the 2010 season. Variable number of tandem repeats (VNTR)

analysis of pathogen genetics (Zuerner & Alt, 2009) showed a match to isolates collected from foxes in the same sampling trip, indicating likely transmission between the species. MAT cross-reactivity profiles also indicate a match, with significant evidence of the two-clade structure linked to the fox outbreak strain evident in skunk data (Figure 6.1.1.14,  $p=0.014$ ).

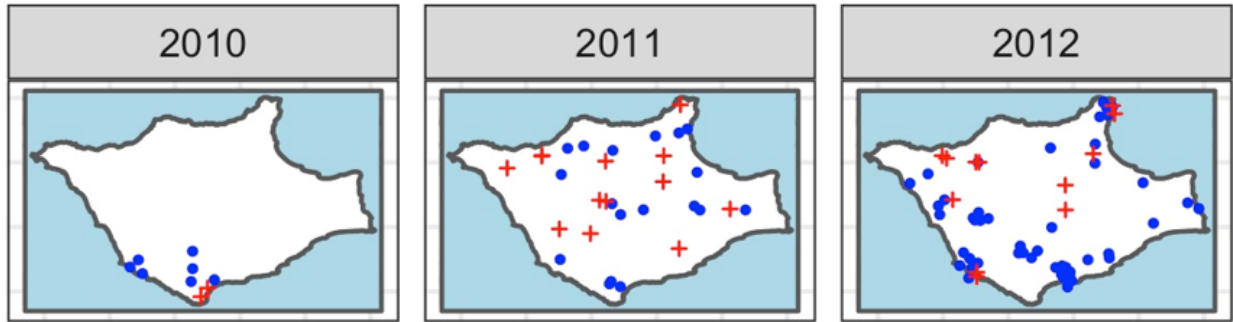


**Figure 6.1.1.13.** Maps of MAT serology results for adult island skunks on Santa Rosa Island, 2010-2012. Blue circles indicate negative MAT results. Red crosses indicated positive MAT results.

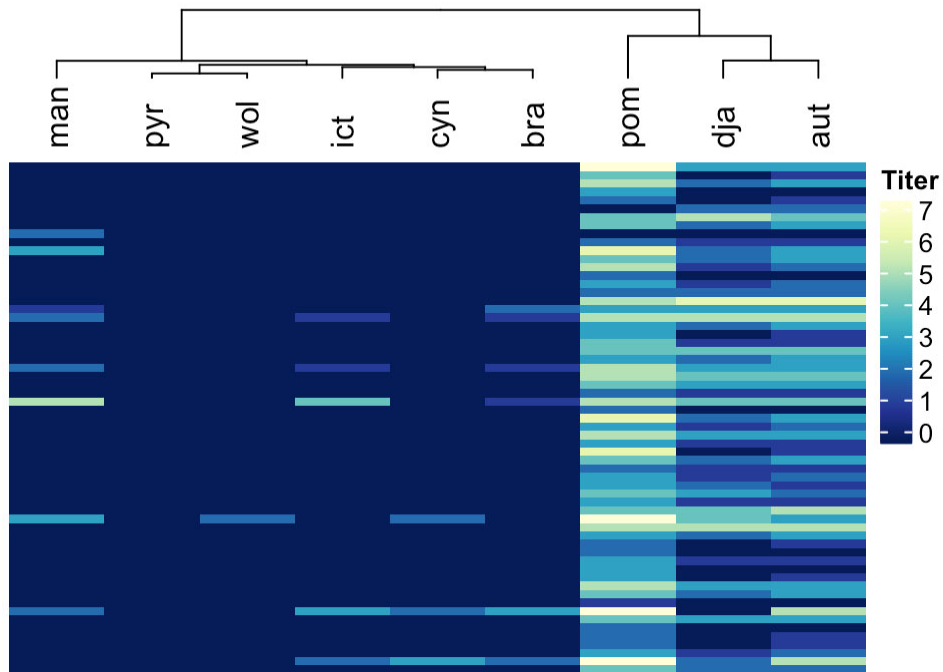


**Figure 6.1.1.14.** MAT cross-reactivity profile for island spotted skunks, sampled 2010-2012. P-value = 0.0138, N=6.

Because biological samples were not collected from island spotted skunks until the end of the 2010 season, we cannot conclude with certainty that they harbored the bacteria while the foxes were in captivity and acted as a source of infection to reintroduced foxes. However, they are a likely source, given that they exhibit high seroprevalence and bacterial carriage, and other

candidates among terrestrial mammals are ruled out. Other alternatives include a possible introduction of *Leptospira* into the Santa Rosa Island ecosystem from a marine reservoir such as California sea lions, though this is not supported by whole genome sequence analysis we recently conducted (unpublished), or that the bacteria persisted elsewhere in the Santa Rosa Island environment (in soil, water, or a non-mammalian host) for the years that the foxes were in captivity, but this greatly exceeds the expected survival time of pathogenic leptospire in the environment (Faine et al., 1999).

Another factor in support of skunks as a possible reservoir for infection is that skunk density on Santa Rosa Island rose to extremely high levels during the 2000s, as they benefited from competitive release while the fox population was absent or at very low abundance (Coonan et al., 2015). Available evidence shows that skunks were abundant across the island. Though trapping locations from 2004 to 2007 do not cover all areas of the island uniformly, skunks were present in all the areas that were trapped (Figure 6.1.1.15). Once the trapping intensity increased in 2008 and grid trapping began in 2009, it was confirmed that skunks were present throughout the island (Figure 6.1.1.15, Table 5.1.1.4). Given the high abundance and widespread distribution of skunks while the foxes were in captivity, and the skunks' known ability to be infected by and to transmit the outbreak strain of *Leptospira*, it is very unlikely that the bacteria would have been present in the environment and not present in the skunks during this period.

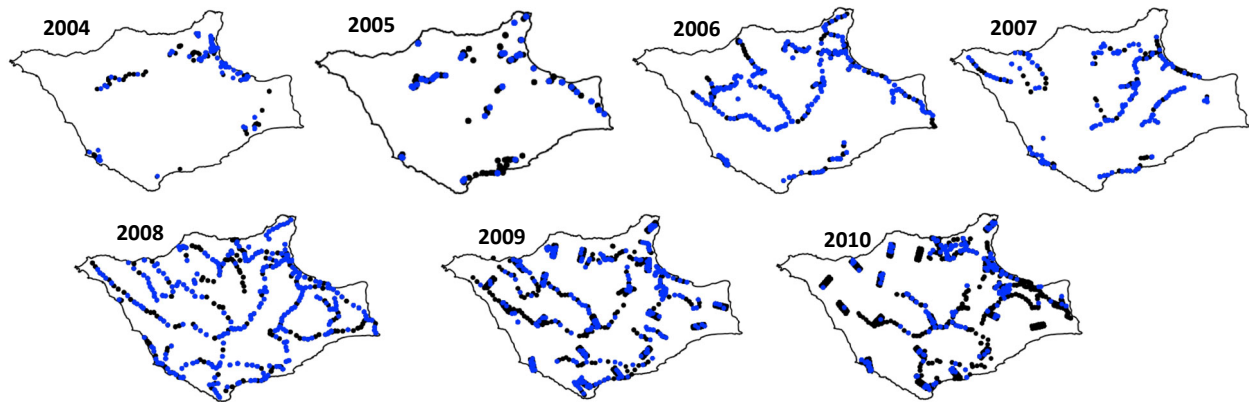


**Figure 6.1.1.15. Maps of trapping locations for island spotted skunks, 2004-2010.** Blue dots indicate a trapping location that had at least one skunk capture during the trapping season. Black dots indicate the trapping locations that did not catch a skunk during the trapping season.

## 6.1.2. Reconstructing the spatiotemporal origins of the SRI outbreak

### *Spatial reconstruction*

Using a generalized additive model with splines, we interpolated the location data through time for individuals with data between 2004 and 2006. By overlaying the cumulative probability that an individual was infected by a given quarter (as summarized in Figure 6.1.1.7), we can visualize where and when the outbreak may have started (Figure 6.1.2.1). By quarter 2 (April - June) of 2005, there were two areas of the island where a fox had a 30% chance of seroconverting. The probability grows in these two areas over the remaining quarters of 2005. By the end of 2005, *Leptospira* infections had clearly occurred in at least two areas of the island. Throughout 2006, there was a greater than 30% chance of infection island-wide with the

probability growing stronger through the year, approaching quarter 3 when the island-wide serosurvey revealed widespread exposure across SRI (Figure 6.1.1.5).

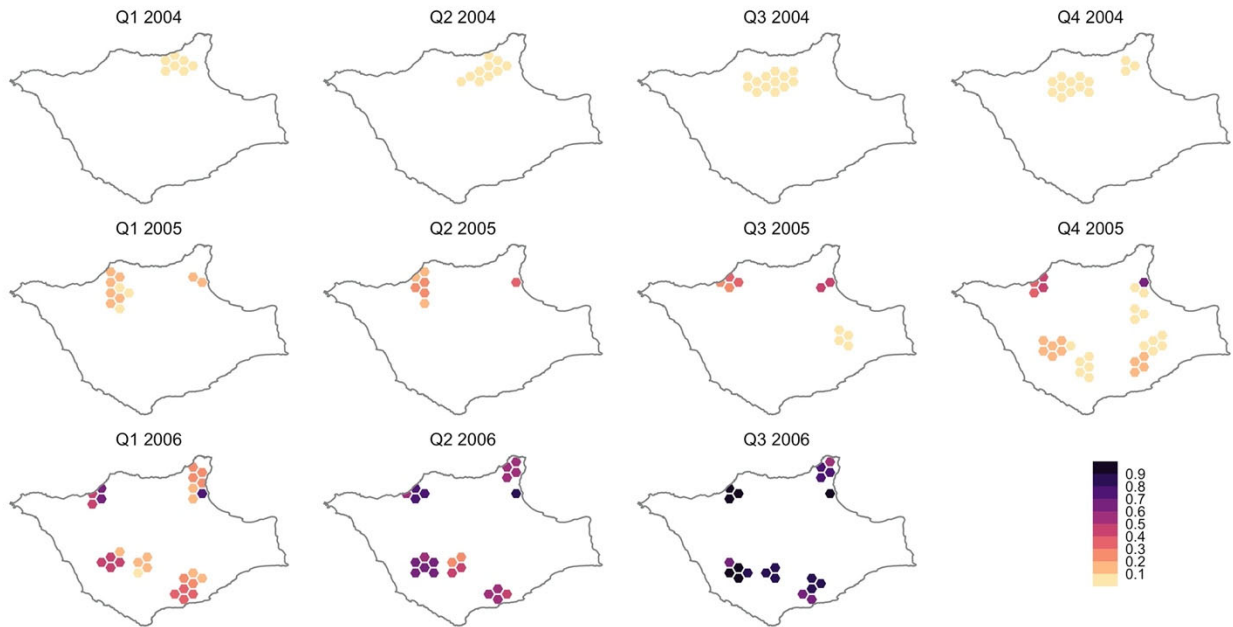


**Figure 6.1.2.1. Spatiotemporal probability of infection for seven foxes between 2004 and 2006.**

Colored grid cells represent the presence of foxes with a non-zero probability of having been infected by that time. The color scale represents the cumulative probability that an individual had been infected by the end of the quarter in question. The darker the color becomes, the higher the probability that an infected fox was present in that cell at that time.

The temporal patterns suggest that the origin of the *Leptospira* outbreak most likely occurred in the second half of 2005. The two individuals with high probability of infection in late 2005 had little to no interaction with each other, so we believe these spatial patterns are most consistent with multiple introductions of *Leptospira* from a reservoir within the island, most likely from skunks.

### 6.1.3. Whole genome sequencing and phylogenetics

#### *Data summary*

Our dataset includes forty-nine bacterial isolates from four host species: island fox, island spotted skunk, California sea lion (CSL), and Northern elephant seal (NES), spanning the years 1988 to 2017 (Table 6.1.3.1).

#### *Multi-locus strain typing (MLST)*

Assembled contigs were scanned against the three *Leptospira* PubMLST typing schemes (Ahmed et al., 2006; Boonsilp et al., 2013; Varni et al., 2014). All forty-nine isolates were found to have the same strain type across the three schemes. Identified strain types and allele IDs can be found in Table A.2.

Host species	1988	2004	2006	2007	2008	2010	2011	2012	2013	2015	2017	Total
CSL	1	3	2	3	1	2	20	2				34
NES							3					3
Island fox							4		3	2	1	10
Spotted skunk							2					2
<b>Total</b>	1	3	2	3	1	2	29	2	3	2	1	49

**Table 6.1.3.1. Frequency of *Leptospira interrogans* serovar Pomona isolates by host species and sampling year.**

*Phylogenetic reconstruction*

The time-calibrated Bayesian phylogeny was constructed with a relaxed lognormal molecular clock and HKY +  $\Gamma$  + I site heterogeneity model. The phylogeny indicates two clearly distinct clades, which are broadly delineated by ecosystem (Figure 6.1.3.1). One clade (Marine1) consists entirely of marine mammals: thirty-three CSL, sampled from 2004 to 2012, and one ES, sampled in 2011. The second clade splits into two subclades: Island and Marine2. The Island subclade contains all terrestrial host isolates and a single CSL isolate (CSL10040), whereas the Marine2 subclade contains two ES isolates and a CSL isolate, which was sampled in 1988.

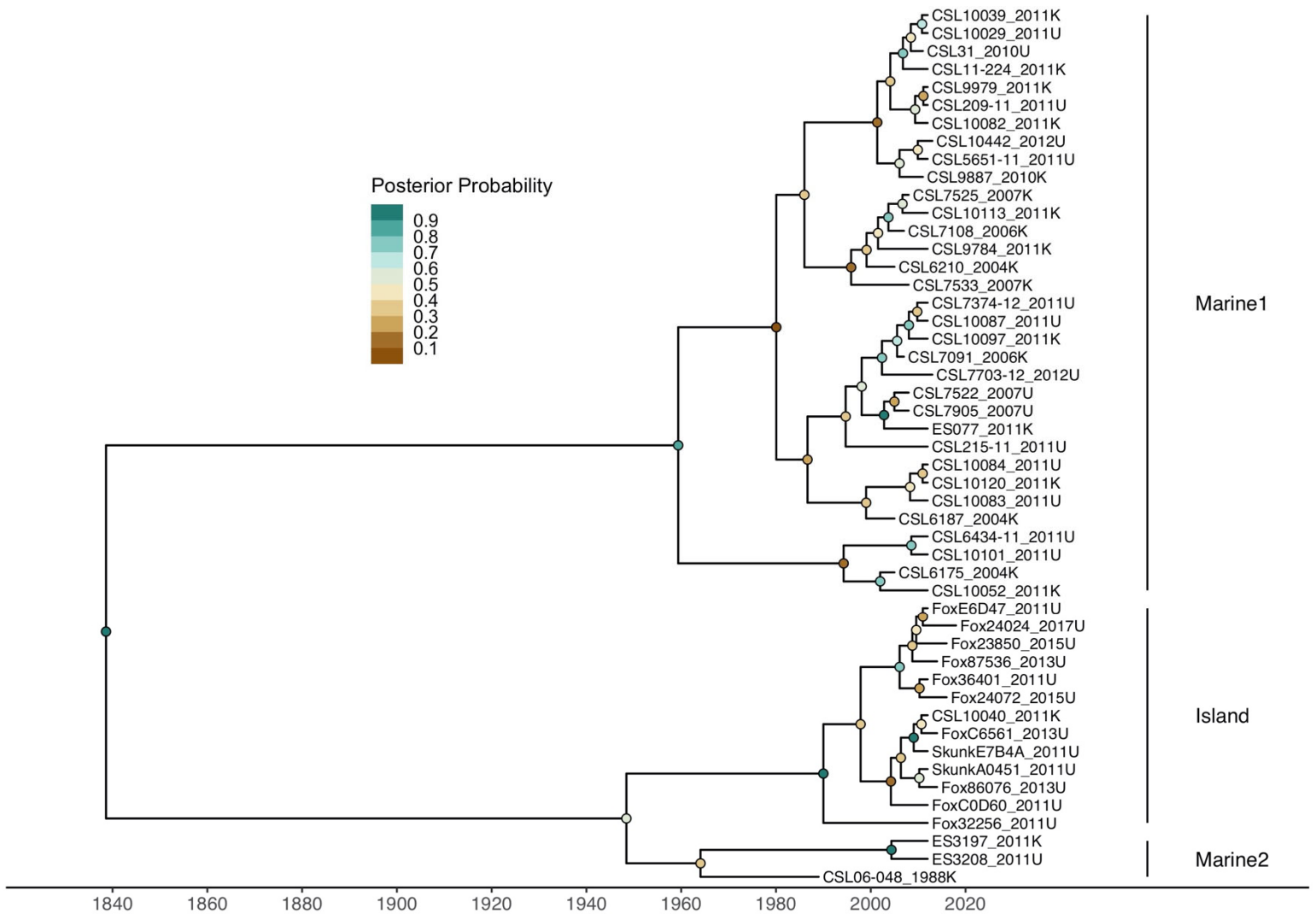


**Figure 6.1.3.1. Time-calibrated maximum clade credibility tree.** Two major clades were identified through Bayesian phylogenetic analysis: Marine1 and Island + Marine2. Interior nodes are labelled with the posterior probability (lower values are brown, higher values are teal). Tips are labeled with host species (CSL = California sea lions, ES = elephant seal), ID number, year, and tissue type (K = kidney, U = urine).

There are three cross-species transmission events directly evident in these phylogenetic reconstructions, but there is more evidence of cross-species transmission when considering the whole tree. The Marine1 clade indicates that transmission occurs between CSL and ES, which makes ecological sense as the two species share haulout and rookery sites and have frequent direct contact. The Island clade contains two types of cross-species transmission: within the terrestrial ecosystem and between the terrestrial and marine ecosystems. The clustering in this clade suggests that island spotted skunks and island foxes had multiple cross-species transmission events prior to 2011. Additionally, there is a single CSL nestled within the island clade, indicating that cross-species transmission can occur from the terrestrial hosts on the island

to the marine ecosystem, most likely from foxes to CSL. Although two elephant seal isolates (ES3197 and ES3208) cluster with the 1988 CSL isolate in the Marine2 clade, we do not believe this is evidence for contemporaneous cross-species transmission, given the interval of time between the sampling dates (23 years). Rather, we believe that there is a separate reservoir that seeded both of these lineages; a minimal interpretation of the Marine2 cluster is that at least one additional substrain has circulated within the broader ecosystem.

The median substitution rate in these genomes was  $1.16 \times 10^{-7}$  substitutions per site per year, which is equivalent to 0.37 SNPs per year per genome. The variation in the evolutionary rate was high with the 95% highest posterior density (HPD) covering  $0.11 - 2.63 \times 10^{-7}$  substitutions per site per year (Table 6.1.3.2). Using this rate, we were able to estimate the date when the different clades diverged or the time to most recent common ancestor (TMRCA). The estimated date for the root of the tree, when isolates from island foxes last shared a common ancestor with the larger Marine1 clade, is 1836 (HPD: 1272-1980). The estimated TMRCA for the Island and Marine2 clades, which represents the last date at which the terrestrial isolates shared an ancestor with the broader marine realm, is 1947 (HPD: 1755-1988). In both instances the uncertainties on the TMRCA are large, due to the limited number of isolates and high variation in substitution rates, but crucially the intervals do not extend to the period after 2000 when the foxes entered captivity.

Parameter	Median (95% HPD)
Clock rate ( $\times 10^{-7}$ )	1.16 (0.11, 2.63)
Coefficient of variation <sup>+</sup>	2.59 (1.60, 4.87)
TMRCA date (root)	1836 (1272, 1980)
TMRCA date (Island + Marine2)	1947 (1755, 1988)

**Table 6.1.3.2. Posterior median estimates of genetic and temporal parameters.** HPD: highest posterior density; TMRCA: time to most recent common ancestor for marine and island lineages. + indicates measure of the variation in evolutionary rate amongst the branches.

The interior nodes of the phylogeny have a wide range of posterior probabilities (PP; Figure 6.1.3.1). Crucially, the branch point at the root of the tree has very high posterior probability (>99%), but subsequent nodes decline in posterior support. This indicates that the separation between isolates circulating in sea lions at the time the SRI outbreak began (i.e. the Marine1 clade) and isolates involved in the SRI outbreak (the Island clade) was almost always present in the posterior set of trees, but the specific branching patterns within the clades were more variable.

Broad clustering patterns within the tree topology suggest that multiple introductions of *L. interrogans* serovar Pomona into the California coastal ecosystem have occurred from an unknown reservoir. These repeated introductions appear to have seeded multiple chains of transmission, which circulated simultaneously in different host species. The island clade most likely had its own introduction from an external reservoir in the early-to-mid 1900s given that its median TMRCA is 1947. It appears likely that the sea lion isolate obtained from CSL06-048 in 1988 was seeded by an introduction independent of the one that seeded the Marine1 clade. Finally, the cluster of elephant seal isolates in 2011 signifies another potential introduction from an unknown reservoir.

In this study, we used *Leptospira interrogans* serovar Pomona isolates to reconstruct host epidemiological linkages within the California coastal ecosystem. Our data suggest that cross-

species transmission occurs primarily within the terrestrial or marine ecosystems but can occur infrequently across ecosystems as well. There is additional evidence that an unknown reservoir may be seeding independent introductions of *L. interrogans* serovar Pomona into multiple host species within the California coastal ecosystem.

## 6.2. *Leptospira* in California Sea Lions

### 6.2.1. Extend long-term time series of leptospirosis in stranded California sea lions

#### *Interannual variation and cyclic outbreaks*

Collaborators at TMMC collected data and samples from 3420 California sea lions that stranded along the central and northern coast of California and were admitted for rehabilitation between January 1, 2015 and December 31, 2020. Of these, 391 were diagnosed with leptospirosis. Samples were analyzed using MAT (N=1373) to assess prior exposure; PCR of urine or kidneys (N=304), or culture (N=634) and *Leptospira* isolation (N=65) from urine and kidney, to assess current infection; and serum chemistry analyses (N=2787) to assess clinical impact of leptospirosis (Table 6.2.1.1). These data allowed us to extend our unique long-term time-series of *Leptospira* circulation to 37 (incidence) and 25 (anti-*Leptospira* antibody seroprevalence) years (Figure 6.2.1.1). This unique long-term dataset, combined with prior work done on the system, provides important insights into the sea lion-*Leptospira* system.

*L. interrogans* serovar Pomona was first detected in the California sea lion population in 1970 (Vedros et al., 1971), but was not detected in the later 1970s or early 1980s, despite systematic surveillance by TMMC since 1975. The pathogen reappeared in CSL in 1984, and from 1984 through 2012 there have been yearly, seasonal outbreaks (Figure 6.2.1.1). During this period, outbreak magnitude varied, with very large outbreaks occurring every 3-5 years (Gulland et al., 1996; Lloyd-Smith et al., 2007). Genetic, serologic, and epidemiologic data suggested endemic circulation until 2013, i.e. sustained transmission of a distinct strain of *L. interrogans* serovar Pomona within the sea lion population (Buhnerkempe et al., 2017; Gulland et al., 1996; Lloyd-Smith et al., 2007; Prager et al., 2013, 2015; Zuerner & Alt, 2009) (also see 6.1.3).

#### *Spontaneous fadeout of Leptospira circulation in the CSL population*

We observed an unprecedented 4-year cessation in leptospirosis strands in CSL from early 2013 to mid-2017, followed by reemergence of the disease in a small outbreak in 2017, then the largest outbreak on record in 2018 (Figure 6.2.1.1). To investigate this pattern and confirm the apparent cessation of endemic transmission (i.e. ‘fadeout’) in the CSL population, we analyzed serologic and infection prevalence data from stranded and wild-caught CSL (Figure 6.2.1.2). During the period that CSL were not stranding with leptospirosis, log<sub>2</sub> antibody titers fell below 6, a level known to be indicative of past infections not current ones (Prager et al., 2020), and were seen only in animals old enough to have been exposed prior to the fadeout, or else titers were so low they suggested either maternal antibodies or false positives. Infection prevalence dropped to zero during this period, with two notable exceptions: one subclinically infected juvenile in 2013 with a low MAT titer (3) that was likely a chronic carrier infected in 2012, and an isolated clinical case of leptospirosis in 2016 that we believe was a failed reintroduction of the pathogen. Together, these data confirm that *Leptospira* stopped circulating in the California sea lion population from early 2013 to mid-2017 when a new strain emerged. This period coincided with an Unusual Mortality Event in 2013 linked to unfavorable

oceanographic conditions, followed by an unprecedented marine heatwave (nicknamed ‘the Blob’) from 2013-2015, which was then followed by an El Niño event in 2015-2016.

Combined with phylogenetic analyses performed on *Leptospira* isolates obtained during this period, as well as previously banked isolates, the stranding time-series confirmed pathogen fadeout and re-emergence of a genetically distinct strain in mid-2017 (Figure 6.2.1.1, Figure 6.2.1.2). These data and those presented in section 6.2.2 also provided the foundation for modeling and empirical efforts to do the following: (i) assess the intrinsic and extrinsic stationarities driving *Leptospira* outbreaks in CSL during the period of endemic circulation (6.2.3.1), (ii) identify the conditions that led to *Leptospira* fadeout, and those that facilitated reemergence (6.2.3.2), and, (iii) in combination with data from the wild free-ranging sea lion population, evaluate the risk of *Leptospira* spillover from CSL to island foxes (6.3.6).

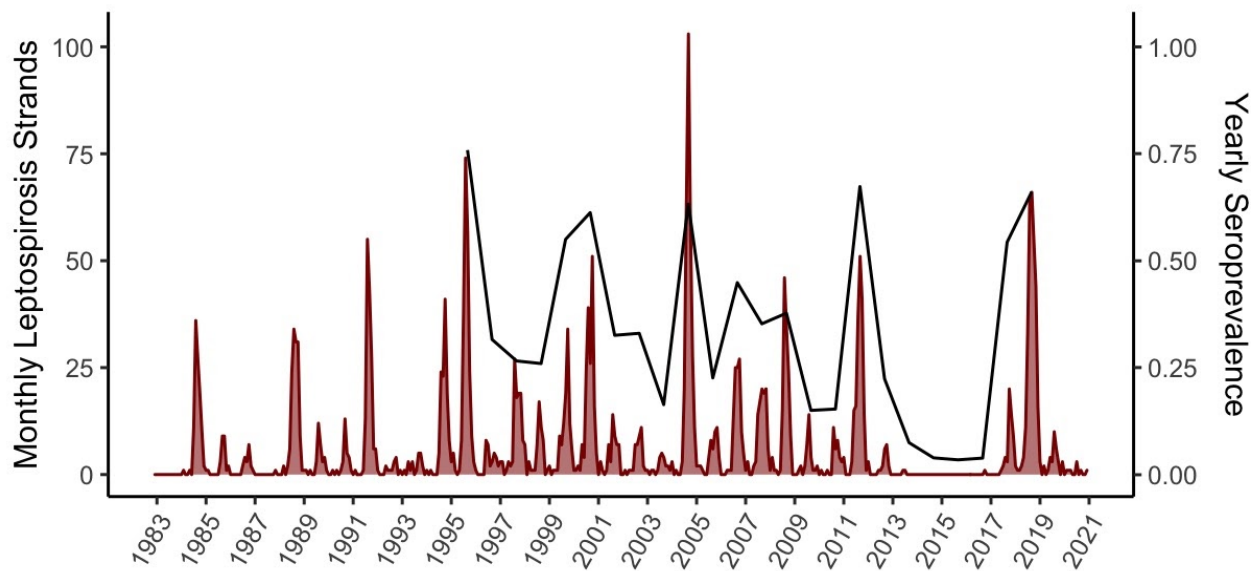


**Figure 6.2.1.1. Stranding and seroprevalence time series.** Number of California sea lions stranding each month at The Marine Mammal Center (TMMC) with leptospirosis (solid) from 1983 to 2021 and annual seroprevalence of anti-*Leptospira* antibodies in animals stranding at TMMC from 1995 to 2019 (black line). Seroprevalence is excluded for 2020 and 2021 because of small sample sizes.

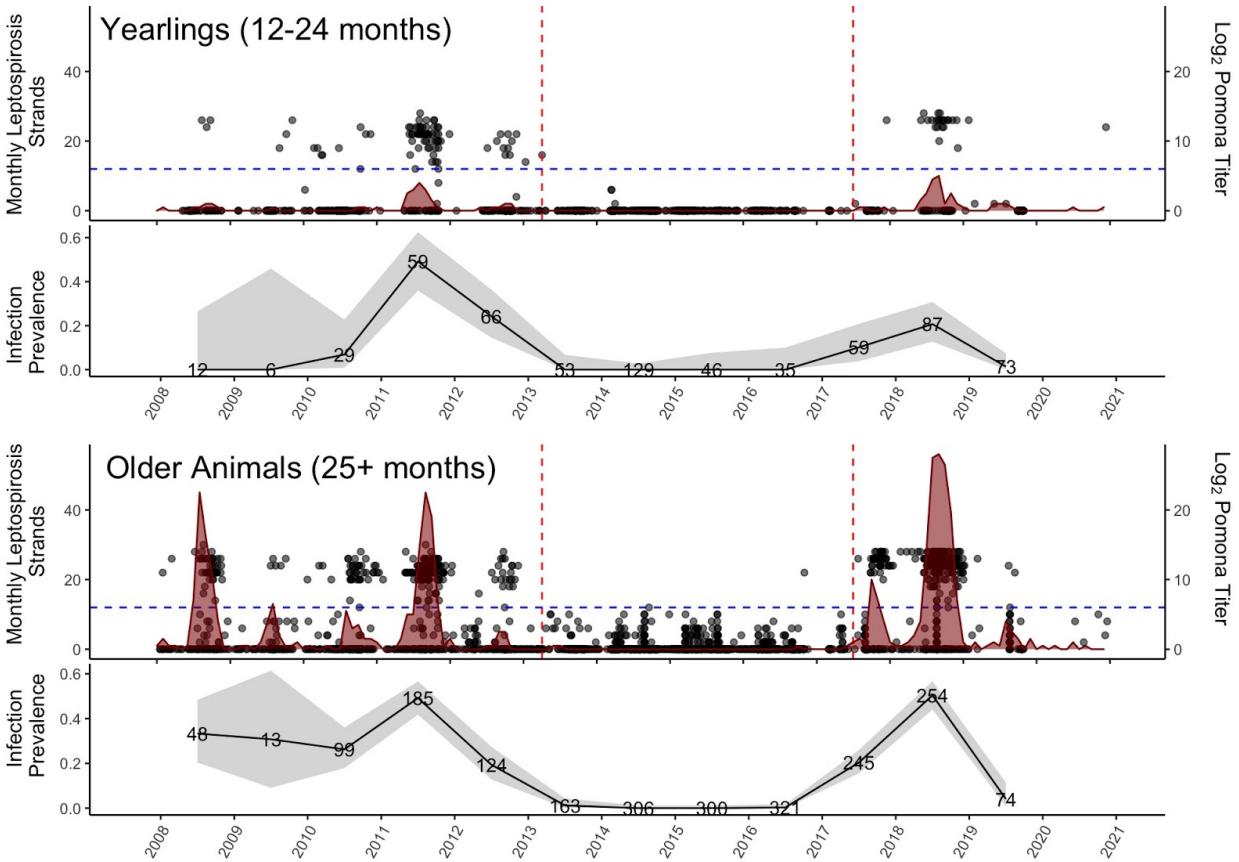


**Figure 6.2.1.2. Stranding, antibody titer, and infection prevalence time-series.** Number of yearling (top) and older – 25 months old and greater – (bottom) California sea lions stranding each month at The Marine Mammal Center (TMMC) with leptospirosis (solid pink) from 2008 to 2020, and log<sub>2</sub> serum anti-*Leptospira* antibody titers (grey circles) from stranded (left) and wild-caught (right) sea lions. Vertical dashed red lines show the beginning and end of the period when *Leptospira* ceased circulating in the CSL population (i.e. the ‘fadeout period’). Antibody titers are plotted as grey circles on the day of sampling; points are transparent and jittered, so darker circles represent multiple animals tested on that day. The horizontal dashed blue line shows the level below which antibody titers correspond to past infections, not current ones. Data from wild-caught CSL are described in section 6.3.6. Infection prevalence (black line) for each age group is plotted in the panels directly below the strand and seroprevalence time-series. Numbers represent total sample size tested and grey bands are the 95% binomial confidence interval surrounding the infection prevalence estimate.

Year	Strands			MAT			PCR			Culture Urine			Culture Kidney		
	L	NL	Total	L	NL	Total	L	NL	Total	L	NL	Total	L	NL	Total
2015	NA	1347	1347	NA	19/553	19/553	NA	0/81	0/81	NA	0/31	0/31	NA	0/33	NA/33
2016	1	451	452	1/1	9/229	10/230	1/1	0/53	1/54	NA	0/24	0/24	NA	0/25	0/25
2017	53	269	322	61/61	4/46	65/107	34/36	2/11	36/47	3/34	0/28	3/62	11/31	0/29	11/60
2018	294	240	534	312/315	29/141	341/456	78/96	5/21	83/117	8/114	0/17	8/131	33/148	0/23	33/171
2019	35	519	554	7/7	4/13	11/20	3/3	0/2	3/5	NA/15	0/60	0/75	2/18	0/4	2/22
2020	8	193	201	2/2	5/5	7/7	NA	NA	NA	NA	NA	NA	NA	NA	NA
<b>Total</b>	391	3019	3410	383/386	70/987	453/1373	116/136	7/168	123/304	11/163	0/160	42/323	46/197	0/114	79/311

**Table 6.2.1.1. Number of California sea lions stranded 2015-2020 and diagnostic tests performed. The number of stranded CSL is separated into those that stranded from leptospirosis (L) and those stranding from other causes (NL). Number of animals that tested positive for antibodies via microscopic agglutination tests (MAT) and *Leptospira* DNA via polymerase chain reaction (PCR) are reported as the number of positive results/the total number tested. *Leptospira* culture results are reported as the total number of successful *Leptospira* isolations/total attempts to isolate *Leptospira* and are separated by sample type (urine or kidney).**

### 6.2.2. Extend long-term time series of CSL demography

Between 2015 and 2018, 1276 pups were branded and weighed on San Miguel Island, and 14821 total resights of 3574 unique sea lion brands were recorded (Table 6.2.2.1, Table 6.2.2.2). These data extended a long-term study of CSL demography and enabled us to estimate the age- and sex-specific survival probabilities of CSL each year from 1976 to 2018 (Figure 6.2.2.1). The results paint a vivid picture of the severe survival impacts of oceanographic non-stationarities, particularly on the youngest age classes of CSL. The new data collected under this project enabled the quantification of severe and sustained drop in survival of 1- and 2-year old sea lions during the marine heatwave (nicknamed “The Blob”) and subsequent El Niño event from 2013-2016.

These survival estimates were combined with pup count data to produce an age- and sex-structured population reconstruction (Figure 6.2.2.2), which reflects how the impacts of oceanographic anomalies propagate through the CSL population. The data from branding were used to estimate mean pup weights at roughly 4 and 8 months-old for each cohort (Table 6.2.2.2). Resighting data from San Miguel Island and Año Nuevo Island were analyzed using a multi-state mark-resight model to determine the proportion of animals remaining on San Miguel in July of each year (Table 6.2.2.3; also see section 6.2.3.2, Figure 6.2.3.12). Such unique, long-term datasets are the foundation from which critical assessments of the impact of oceanographic anomalies on the sea lion population can be made. For example, prior analyses reveal a clear relationship between increases in sea surface temperatures, like those seen during El Niño events or similar anomalies, and decreased population growth (DeLong et al., 2017; Laake et al., 2018). Extension of these time-series further illustrate this trend and show the negative impact of the recent marine heatwave and El Niño event on sea lion survival, especially of the youngest age classes (Table 6.2.2.1).

The age- and sex-structured population reconstruction, when combined with information on *Leptospira*-sea lion dynamics, enabled an age- and sex-structured population reconstruction of *Leptospira*-susceptible sea lions (Section 6.2.3.1; Figure 6.2.3.2). Importantly, when combined with environmental data, these long-term datasets on demography and *Leptospira* susceptibility provide the basis for efforts to understand how intrinsic and extrinsic non-stationarities drive *Leptospira* outbreaks in California sea lions, as described in the next section.

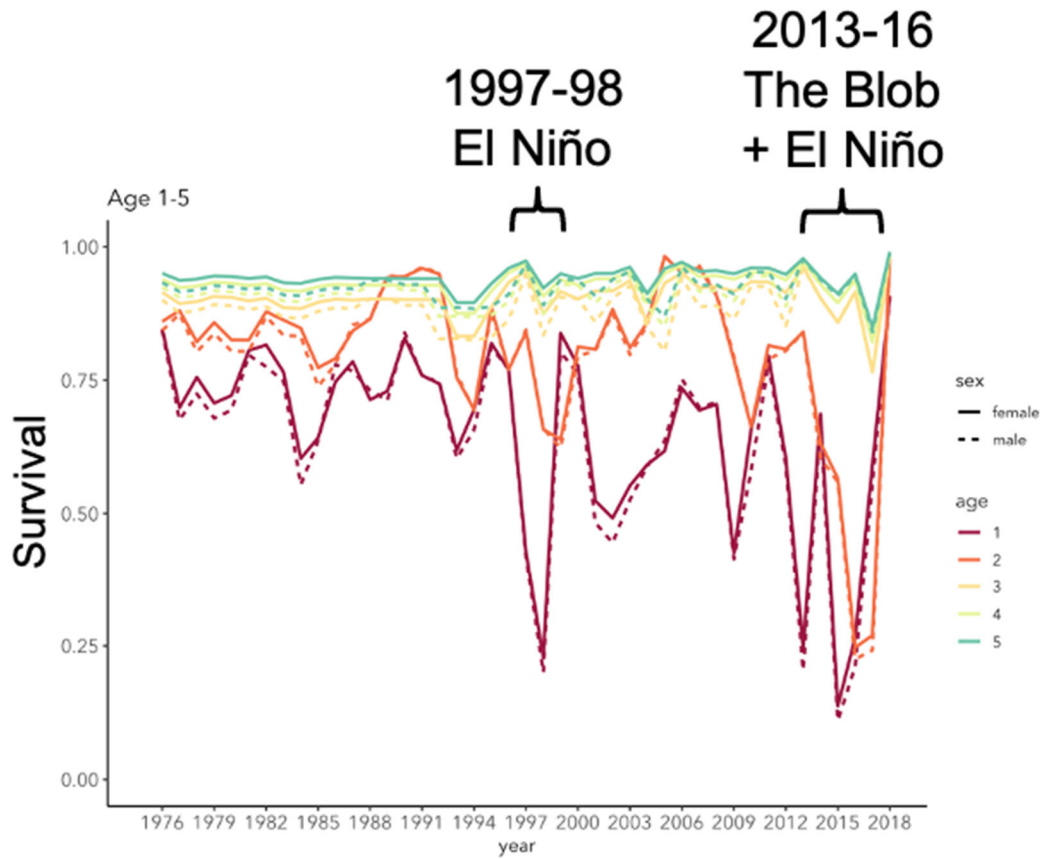


**Figure 6.2.2.1. Age- and sex-specific survival probabilities in California sea lions, 1976-2018.** Survival probabilities for male (dashed line) and female (solid line) sea lions aged 1-5 estimated using mark-resight data as described in 5.2.2. Significant dips in survival, associated with the two most recent El Niño events, can be seen in the population, especially in the youngest age classes.

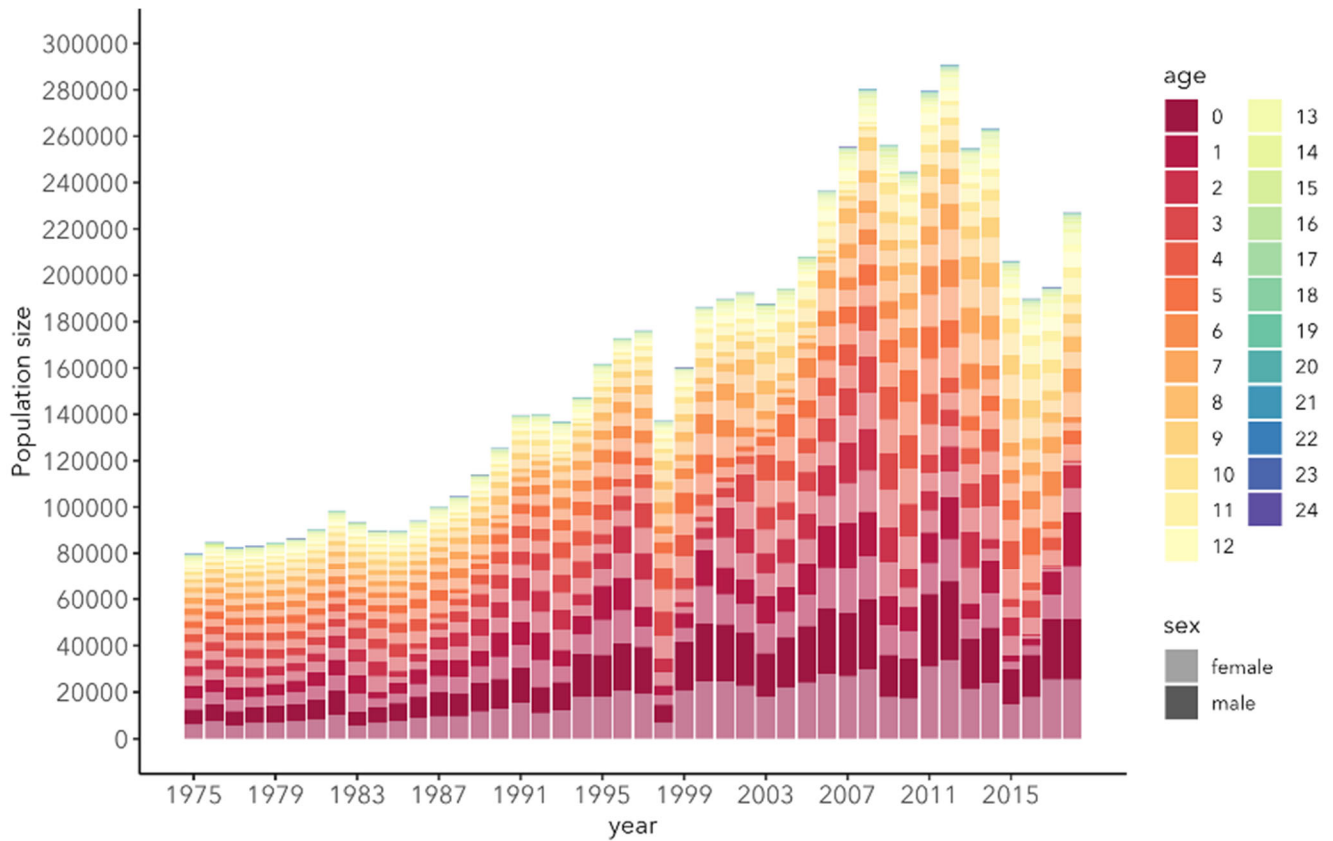


**Figure 6.2.2.2. Age- and sex-structured California sea lion population reconstruction.** Colors go from warm to cold as age increases, and females are distinguished from males by their lighter shade of the same color. The impact of the most recent El Niño events on survival are reflected in the slowed population growth seen in the late 1990s and mid 2010s.

Year	Branded pups		Unique resights		Total resights	
	M	F	M	F	M	F
1996	184	313	166	322	700	1482
1997	185	312	232	549	895	2873
1998	198	302	302	626	1409	3244
1999	199	301	309	586	1527	3345
2000	181	318	452	736	2383	4648
2001	194	306	452	723	2351	4677
2002	183	317	473	781	2683	4911
2003	197	303	335	731	1633	3937
2004	200	300	325	589	1628	3722
2005	199	301	313	867	1305	4794
2006	130	270	396	1031	1923	7414
2007	100	199	437	983	1948	5305
2008	116	184	355	967	1486	4713
2009	104	209	214	815	784	3571
2010	120	124	140	653	665	2927
2011	99	201	284	942	1148	5065
2012	152	148	174	748	652	3027
2013	127	174	326	962	1167	4023
2014	142	158	269	832	900	3736
2015	143	139	265	716	933	2805
2016	117	189	231	655	767	2502
2017	149	161	231	664	917	3843
2018	194	184	211	601	592	2462
2019	146	131	231	662	608	2618
<b>Total</b>	<b>3759</b>	<b>5544</b>	<b>7123</b>	<b>17741</b>	<b>31004</b>	<b>91644</b>

**Table 6.2.2.1. California sea lion pups branded and resighting events of all age classes, 2015-2018.**

Data includes the number of male and female California sea lion pups branded, and total and unique resighting events of branded male and female sea lions of all age classes between 2015 and 2018. These data were used to estimate age- and sex-specific California sea lion survival probabilities.

Year	October				February			
	M		F		M		F	
	N	Mean Weight	N	Mean Weight	N	Mean Weight	N	Mean Weight
1996	184	21.88	313	18.84	0	32.76	0	28.05
1997	194	16.82	347	14.67	33	19.73	27	16.29
1998	293	14.72	409	13.14	25	25.12	34	22.31
1999	200	21.01	302	18.13	31	33.99	38	28.61
2000	183	19.52	324	17.14	27	30.95	31	27.58
2001	206	18.29	329	16.09	27	30.81	33	27.13
2002	180	19.53	334	17.00	32	26.44	29	23.09
2003	275	21.38	393	18.28	24	33.83	32	28.76
2004	201	24.07	305	20.50	32	33.87	25	28.12
2005	200	23.38	305	19.90	28	35.59	32	29.70
2006	231	22.06	275	18.83	36	31.66	36	26.78
2007	204	22.24	308	19.00	36	33.59	45	28.58
2008	115	20.47	195	17.62	23	29.17	38	24.83
2009	216	16.74	298	15.05	27	24.12	32	22.88
2010	190	19.63	234	17.02	41	32.05	41	28.28
2011	108	17.19	239	14.88	0	25.30	0	22.03
2012	183	14.55	237	13.07	31	16.52	36	15.26
2013	155	17.80	188	15.54	40	25.05	58	22.22
2014	177	15.42	203	13.81	102	17.04	106	15.45
2015	245	13.18	262	12.02	56	15.74	55	15.43
2016	172	20.89	251	18.21	34	28.06	40	25.16
2017	155	20.52	172	17.56	36	32.85	33	27.30
2018	194	20.13	184	17.63	45	29.70	29	26.53
2019	146	21.75	131	18.73	39	34.07	21	29.61
<b>Total</b>	<b>4607</b>		<b>6538</b>		<b>805</b>		<b>851</b>	

**Table 6.2.2.2. Number of male and female pups weighed in October and February each year, 2015-2018.** California sea lions are born around June, therefore years indicate cohort year with October weights reflecting the weight of a roughly 4 month-old pup and February weights reflecting those of a roughly 8-month-old pup. These data were used to estimate age- and sex-specific growth rates and mean weights by birth cohort.

Year	Proportion	
	M	F
1996	0.06	0.13
1997	0.11	0.20
1998	0.20	0.35
1999	0.13	0.15
2000	0.14	0.21
2001	0.13	0.17
2002	0.25	0.24
2003	0.10	0.18
2004	0.14	0.11
2005	0.10	0.18
2006	0.23	0.31
2007	0.15	0.24
2008	0.15	0.27
2009	0.03	0.10
2010	0.07	0.12
2011	0.13	0.24
2012	0.26	0.27
2013	0.67	0.63
2014	0.15	0.40
2015	0.59	0.64
2016	0.71	0.69
2017	0.24	0.30
2018	0.08	0.14
2019	0.05	0.19

**Table 6.2.2.3. Proportion of the yearling population on San Miguel Island in July of each year by sex, 2015-2018.**

### **6.2.3. Understand how intrinsic and extrinsic non-stationarities drive leptospirosis outbreaks in CSL**

#### ***6.2.3.1. The endemic period***

##### *Intrinsic and extrinsic drivers of disease dynamics*

A classic unresolved question in ecology is how cyclic dynamics can be driven by interacting intrinsic and extrinsic factors (Bjørnstad & Grenfell, 2001). Intrinsic drivers are those that operate within a biological system, such as fluctuations in population density or immunity, while extrinsic ones are all others that affect system dynamics, such as species interactions or environment. Disease ecology has been at the forefront of this research field, mostly through the study of cyclic epidemics of infectious diseases (Grenfell & Bjørnstad, 2005). Measles research for example has been pivotal to understanding how an intrinsic process (seasonal change in population immunity) can result in regular deterministic cycles (Bjørnstad et al., 2002). Research on cholera (Koelle et al., 2005) and malaria (Rogers et al., 2002) has shown how extrinsic environmental conditions like rainfall can perturb such an intrinsically-driven deterministic

skeleton and cause noisier, less predictable cycles (Finkenstädt & Grenfell, 2000). This perturbing role of environment is expected to be even greater in natural/wildlife systems, which therefore provide excellent opportunities to improve our understanding of the role of intrinsic versus extrinsic processes in ecological cyclic dynamics. Yet surprisingly there do not seem to be any animal systems for which the relative contributions of intrinsic and extrinsic drivers to disease outbreaks have been quantified convincingly, and even for historically well-studied human pathogens examples are rare (notably measles (Bjørnstad et al., 2002), cholera (Koelle et al., 2005), malaria (Rogers et al., 2002), syphilis and gonorrhoea (Grassly et al., 2005)). Here, we leverage a combination of long-term datasets related to pathogen transmission in sea lions and show how the interplay between intrinsic and extrinsic drivers can affect epidemic cycling in a wildlife host.

As described in section 6.2.1, *L. interrogans* serovar Pomona circulates endemically in CSL, causing seasonal outbreaks of leptospirosis and CSL strandings along the coast (F. Gulland et al., 1996). These outbreaks are annual and highly variable, with large outbreaks every 3 to 5 years (Lloyd-Smith et al., 2007) (see section 6.2.1, Figure 6.2.1.1). These patterns are not unlike some human childhood infections (Metcalf et al., 2009), but exhibit more variability. This is likely due to a stronger influence of environment on factors influencing transmission, which is unsurprising for pathogen transmission in wildlife. Ocean conditions impact each aspect of sea lion life history, including foraging, movement, body condition, and survival (DeLong et al., 2017; Lowry et al., 2017; Melin et al., 2008; Peterson & Bartholomew, 1967), resulting in strong variation in the survival of sea lions, particularly when young (Laake et al., 2018) (see section 6.2.2, Figure 6.2.1.1).

Transmission of *Leptospira* typically occurs through the environment after shedding via urine, but because survival of the bacteria in salt water is low (Cilia et al., 2020) transmission between sea lions likely requires close contact, which occurs when they are hauled out together on land. This means that population mixing patterns are likely to drive transmission rates. Movement and mixing are highly dependent on age and sex. Most young animals and lactating females remain near the breeding colonies in the central and southern part of the range year round (Melin et al., 2008; Peterson & Bartholomew, 1967), whereas older males and some non-lactating female adults tend to reside in the north of the sea lion range, with adult males annually migrating to the breeding colonies during the summer reproductive season (Gearin et al., 2017; Maniscalco et al., 2004; Odell, 1981). Local foraging-related movement can vary strongly depending on time of year as well as preceding and current environmental conditions that determine the abundance and location of prey species such as anchovy and sardine (Melin et al., 2008).

#### *Population immunity is a key driver of outbreak intensity*

Population immunity (the proportion of susceptible sea lions) and environment are the main candidate intrinsic and extrinsic drivers of *Leptospira* transmission between sea lions, and the first step in disentangling their contributions is to reconstruct variation in population immunity throughout the study period. We do this for each age- and sex-class, taking into account survival, by expanding on an approach that has been applied to human diseases (Finkenstädt & Grenfell, 2000). Figure 6.2.3.1 shows the reconstruction number of susceptibles (using  $P_{obs} = 0.01$ ) for each age and sex class.

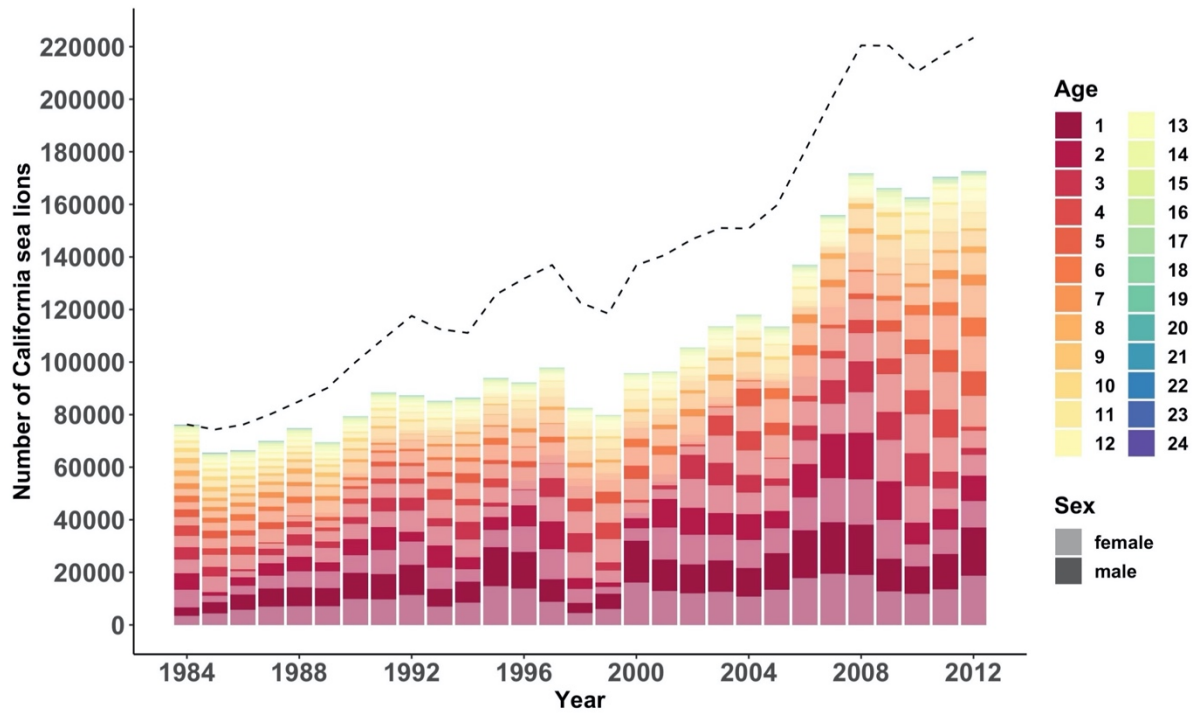


**Figure 6.2.3.1. Reconstructed number of sea lions susceptible to *Leptospira*, structured by age and sex.** Color transparency indicates sex. Dashed line shows annual total population size (using estimates from (DeLong et al., 2017)). Observation probability  $P_{\text{obs}} = 0.01$ .

This reconstruction allows us to answer two pertinent questions: does immunity drive outbreak size, and which demographic groups are the most important? By comparing susceptible reconstructions consisting of different age and sex classes (using generalized additive models and cross-validation tests), we find that immunity in the youngest age groups (yearlings and juvenile males) is the best predictor of outbreak size (22% Deviance explained; Figure 6.2.3.1, Figure 6.2.3.2, Figure 6.2.3.3, Figure 6.2.3.4, Table 6.2.3.1)

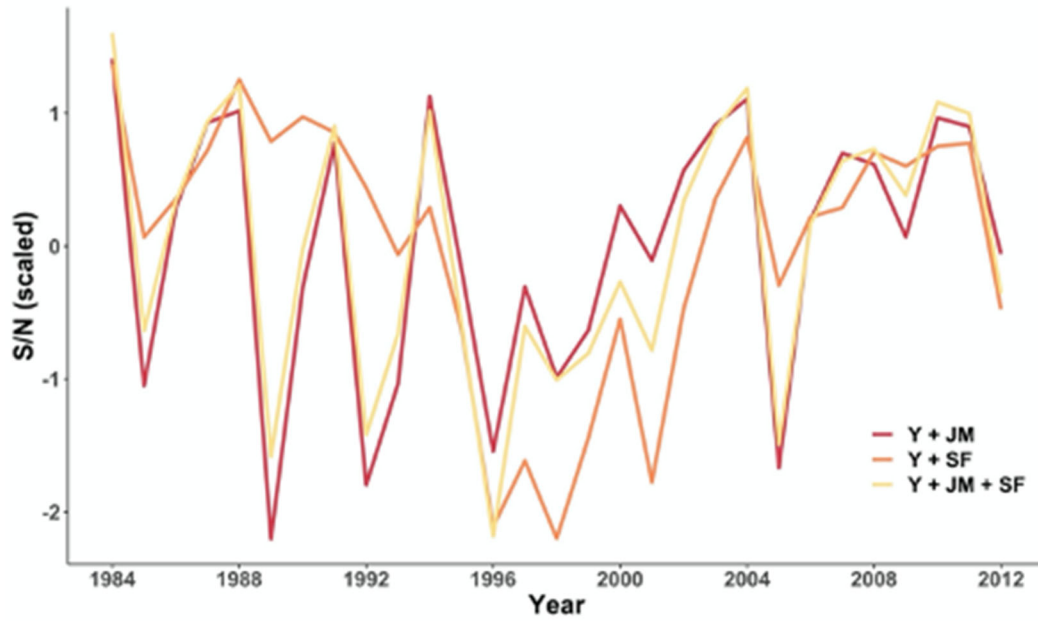


**Figure 6.2.3.2. Reconstructed proportion of susceptibles for a selection of demographic groups.** Values are scaled (mean 0, SD 1). Y = yearlings (male and female), JM = juveniles males, SF = subadult females.

Susceptible Age & Sex Class	Crossvalidation			Full Model					
	Rank	Adj.R <sup>2</sup>	FM	Adj.R <sup>2</sup>	FM	AIC	ΔAIC	Akaike Weight	% Dev
Y + JM	1	0.09	19	0.20	16	-391.1	0.0	0.51	22.4
Y + JM + SF	2	-0.02	21	0.14	17	-388.9	-2.2	0.17	16.7
Y + SF + AF	3	-0.04	22	-0.03	20	-383.3	-7.8	0.01	0.9
Y + JM + SF + AF	4	-0.12	22	0.05	17	-385.8	-5.3	0.04	8.2
Y + JM + SM + AM + SF + AF	5	-0.12	24	0.01	20	-384.6	-6.5	0.02	4.8
Y + JM + SM + SF	6	-0.15	23	0.08	18	-386.8	-4.3	0.06	11.0
Y + JM + SM + SF + AF	7	-0.16	23	0.05	20	-385.9	-5.2	0.04	8.6
Y + JM + SM	8	-0.17	23	0.12	16	-388.1	-3.0	0.11	14.7
Y + JM + SM + AM	8	-0.16	26	0.05	17	-385.7	-5.4	0.03	7.9
Y + SF	9	-0.21	24	0.00	22	-384.2	-6.9	0.02	3.6

**Table 6.2.3.1. Cross-validation and full dataset statistics for models including susceptibles only.**

Compares the reconstructed proportion of susceptibles for different combinations of age and sex classes (Figure 6.2.3.1.2). The same functional demographic groups are used as those in (DeLong et al., 2017b): Y = Yearling, J = Juvenile, S = Subadult, A = Adult, F = Female, M = Male. Green = young sea lions, blue = older sea lions. Adj. R<sup>2</sup> = Adjusted R<sup>2</sup>, FM = Feature Mismatch (explained in the section on model selection). Akaike Weight = AIC-derived measure of relative importance. % Dev = percentage of variation (deviance) explained.

The top models show that susceptible reconstruction based on yearlings and juvenile males results in the best predictions (Table 6.2.3.1). The second-best model is not significantly different from the top model and differs in that it also includes subadult females. However, because the inclusion of subadult females results in worse predictions, and because the model consisting only of yearlings and subadult females performs badly, we conclude that yearlings and juvenile males constitute the demographic group most important for driving transmission. Taken together, these results show that immunity in young animals is an important driver of *Leptospira* transmission in sea lions. We now examine whether the remaining unexplained proportion of variation in outbreak size can be explained by environmental factors.

#### *Environmental conditions further modulate outbreak intensity*

Environmental non-stationarities can affect transmission via two distinct pathways. They can indirectly affect population immunity by affecting the survival of young, mostly susceptible sea lions – this is the susceptible component in classic SIR transmission theory (Anderson & May, 1992). It may also exert a direct effect on sea lion body condition and mixing patterns, which can influence transmissibility and contact rate – two key components of the transmission coefficient ( $\beta$ ) in transmission theory (Anderson & May, 1992).

The importance of the indirect pathway can be tested by creating a second susceptible population reconstruction that uses a version of population size from which annual variation in survival and per capita birth rate is removed through smoothing. This effectively removes the influence of environmental conditions on the proportion of immune individuals, as the environment is known to be highly correlated with sea lion survival (Laake et al., 2018). If the environment were to act strongly on transmission through sea lion survival, the reconstruction based on real survival would correlate more strongly with outbreak size than the smoothed reconstruction. We predicted cases for the top susceptible reconstruction model using the original susceptible reconstruction as well as a ‘smoothed’ version, i.e. one which was calculated using smoothed birth rate and survival estimates to eliminate the indirect effect of environment on these parameters). We found no significant difference between the two susceptible reconstructions, based on any of our metrics of model fit. This indicates that environmental variation did not measurably influence outbreak size via this indirect route (Figure 6.2.3.3).

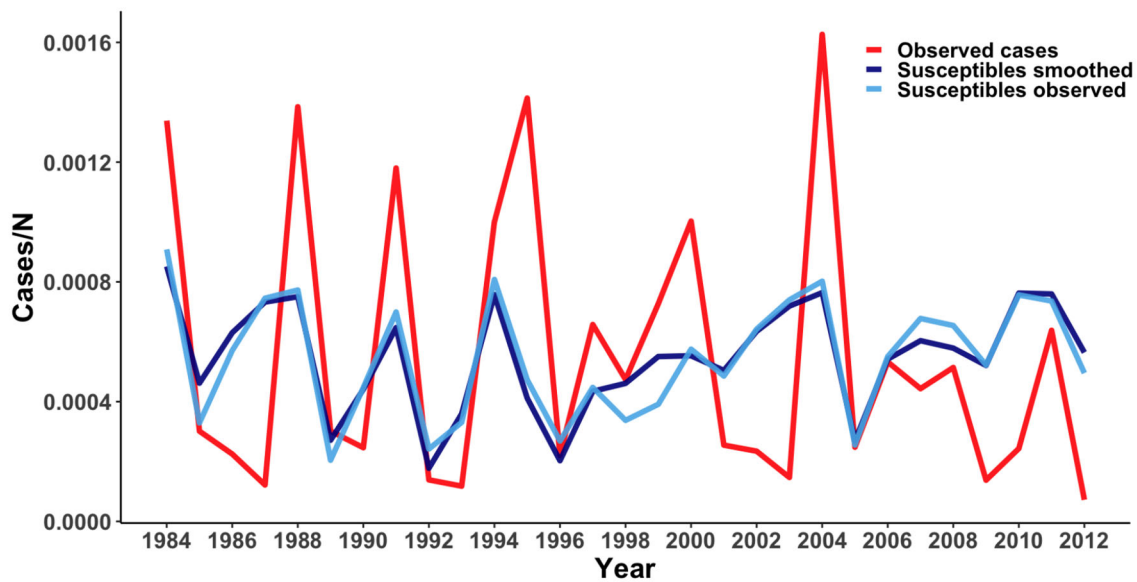


**Figure 6.2.3.3. Predicted cases for the models including reconstructed susceptibles based on observed (light blue) vs. smoothed (dark blue) population data.** The fit of the two models did not differ substantially by any of our fit metrics: Feature Mismatch (smoothed: 17, observed: 16), Adjusted  $R^2$  (smoothed: 0.15, observed: 0.18) or AIC values (smoothed: -369.3, observed: -370.6)

To test for direct impacts of environmental variation on transmission, we used generalized additive models that quantify the relative contributions of immunity and environment to variation in outbreak size. These are fitted to combinations of carefully selected environmental variables (max. 4 in a model) and compared using  $h\nu$ -block cross-validation model fit statistics. Candidate environmental variables were chosen based on existing knowledge of sea lion behavior and biology (DeLong et al., 2017; Melin et al., 2008). Sea surface temperature (SST), coastal upwelling, and spring transition are selected because of the known links with coastal ecosystem productivity and effects on sea lion prey abundance, quality, and

species composition (Bograd et al., 2009). High SST or anomalous (weaker or stronger than normal) upwelling both negatively affect prey availability (Chavez et al., 2002). Spring transition is the time in the year when the upwelling season starts, and a late spring transition generally translates into lower ecosystem productivity throughout the following season. Aside from these abiotic variables, pup and yearling survival are included as biotic indices of preceding environmental conditions affecting the body condition of lactating females and young sea lions.

The explanatory power of the immunity-only model is greatly improved by the addition of environmental variables. The top models show that the key environmental variables are the timing of spring transition of the year preceding the outbreak, upwelling during the increase period of the outbreak, and SST 2-3 months prior to the outbreak (50% Deviance explained; Figure 6.2.3.4, Table 6.2.3.2). These variables affect environmental conditions for sea lions in different ways that matter for pathogen transmission. In an apparent contradiction, we find that outbreaks are *larger* when SST and/or upwelling conditions are good (i.e. suitable for foraging conditions: cool SST and intermediate upwelling), whereas they are *smaller* when spring transition is early and ecosystem productivity is high (Figure 6.2.3.4B). This intriguing difference in the directionality of the relationship between environmental conditions and outbreak size can be explained by the different timescales at which these variables operate and how they are thought to affect different transmission mechanisms.

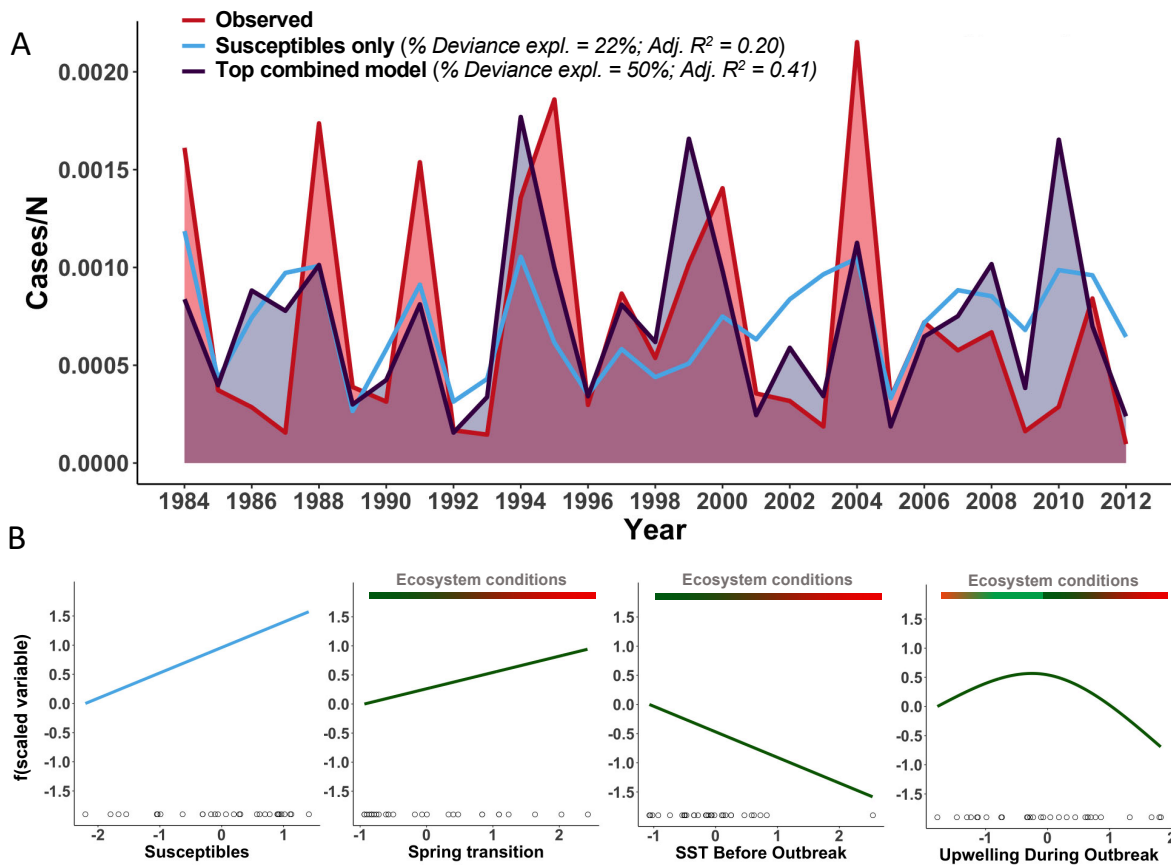


**Figure 6.2.3.4. Outbreak size can be predicted using a combination of intrinsic and extrinsic variables.** (A) Observed (red) and predicted (dark blue: top model; light blue: susceptibles-only model with susceptibles consisting of yearlings and juvenile males) annual leptospirosis cases in stranded California sea lions (normalized by population size). (B) Fitted effect functions for the variables in the top model: proportion of susceptible yearlings and juvenile males, timing of spring transition in the south of the sea lion range, sea surface temperature in the central range prior to the outbreak season, and upwelling conditions in the southern range during the outbreak season. For easy comparison and assessment of the relative contributions of each variable, values are scaled to mean 0 and standard deviation 1 and y-axes are the same. Color bars illustrate typical ecosystem conditions for variable values, from good (green) to bad (red). Points indicate all observed values after scaling; the outlier observed for SST does not affect results.

Variables	Cross-validation			Full model					
	Rank	Adj. R <sup>2</sup>	FM	Adj. R <sup>2</sup>	FM	AIC	ΔAIC	Akaike Weight	% Dev
S + ST <sub>south</sub> + SST <sub>centralJunJul</sub> + UPW <sub>southAugOct</sub>	1	0.18	12	0.41	11	-378.2	-0.1	0.28	0.41
S + ST <sub>south</sub>	2	0.15	16	0.28	15	-373.5	-4.8	0.03	0.28
S + ST <sub>south</sub> + SST <sub>centralJunJul</sub>	2	0.13	15	0.31	14	-374.2	-4.1	0.04	0.31
S + ST <sub>south</sub> + YearlingSurvival + SST <sub>centralJunJul</sub>	2	0.12	14	0.41	11	-378.3	0.0	0.29	0.41
S + ST <sub>south</sub> + SST <sub>centralJunJul</sub> + SST <sub>centralAugOct</sub>	3	0.09	14	0.30	14	-372.9	-5.4	0.02	0.30
S + ST <sub>south</sub> + ST <sub>central</sub> + SST <sub>centralJunJul</sub>	4	0.11	16	0.35	13	-375.4	-2.9	0.07	0.35
S	8	0.09	19	0.19	16	-370.6	-7.7	0.01	0.19

**Table 6.2.3.2. Models and model fit statistics for the top 5 models and the susceptibles-only model.** Rank = model ranking based on cross-validation statistics, Adj. R<sup>2</sup> = Adjusted R<sup>2</sup>, FM = Feature Mismatch, % Dev = proportion of variance (Deviance) explained. Akaike Weight = AIC-derived measure of relative importance

*Putative mechanisms of environmental influence on leptospirosis outbreaks*

The relative importance of each environmental variable over our ensemble of models is calculated using the sum of Akaike weights of the top models in which a variable appears (Table 6.2.3.3). Susceptibility is the most important single driver, indicating that *Leptospira* shows characteristics of other immunizing infections such as measles and smallpox, which also exhibit multi-annual cycles (Anderson & May, 1992). The most important environmental variables are timing of the spring transition, SST, and upwelling.

SST and upwelling have relatively short-term effects on the location of available prey, which determines foraging-related movements of sea lions. This indicates that movement is important for pathogen transmission, likely due to the requirement of close contacts for successful transmission. In general, young sea lions, as well as females nursing pups, have limited flexibility to respond to changes in foraging conditions because they are tied to breeding colonies throughout the year. In contrast, non-reproductive adult sea lions, especially males, can move freely in response to prey movements. We hypothesize that these age- and sex-specific differences in movement potential translate to lower population mixing rates when environmental conditions cause lower prey availability near the breeding colonies and motivate older non-reproductive sea lions to move away from the animals that are tied to the breeding colonies. This may result in lower transmission rates and smaller outbreaks. A preliminary movement analysis using stranding data tentatively supports this hypothesis (see Appendix C for

6.2.3.1), but more in-depth research is needed to uncover the mechanistic links between environmental conditions and population movement and mixing patterns.

In contrast with the short-term effects of SST and upwelling on prey location, spring transition acts on a longer timescale, as nutrient-providing upwelling conditions affect ecosystem productivity cumulatively throughout the longer period leading up to the outbreak season. As spring transition is when ecosystem productivity starts to increase, late spring transition results in a longer period of stressful foraging conditions, with potential negative effects on sea lion health and immunity. We indeed see a significant negative correlation between spring transition timing and body mass index (effect est. =  $-0.5 \pm 0.2$ ,  $F = 49.1$ ,  $df = 8759$ ,  $P < 0.0001$ ). As lower body condition may result in reduced immune system functioning and subsequent increased infection probability, this is a plausible pathway for the effect of spring transition on outbreak size.

Variable	Akaike Importance	Relative importance
S	0.99	0.27
Spring Trans south	0.97	0.27
SST central JunJul	0.73	0.20
Yearling survival	0.38	0.10
UPW south AugOct	0.35	0.10
Spring Trans central	0.10	0.03
UPW central AugOct	0.04	0.01
SST south AugOct	0.03	0.01
Spring Trans north	0.02	0.01
SST central AugOct	0.02	0.01
Pup survival	0.00	0.00
SST south JunJul	0.00	0.00
SST north AugOct	0.00	0.00

**Table 6.2.3.3. Importance of the candidate variables (within the top 20 models).** Akaike importance of a variable is the sum of the Akaike weights of all models that include this variable (ranging from 0 to 1). Relative importance equals Akaike importance of a variable divided by the sum of all Akaike importance values, and can be interpreted as a relative measure of importance. Variables: S = proportion of susceptible yearlings and juvenile male sea lions, Spring Trans = spring transition, SST = sea surface temperature, UPW = upwelling index. South, central, or north indicate variable latitude (south = 36N, central = 39N, north = 42N)

### *Real-time prediction of leptospirosis outbreaks*

The modelling approach in this study and the performance of the top models can be leveraged to make short- and long-term predictions of outbreak size. Real-time predictions would be highly useful for improving the preparedness of wildlife rescue centers, public health agencies and managers of susceptible species of conservation concern such as the island fox, while long-term simulation-based predictions can provide insights into the outbreak patterns that might be expected under climate change.

We test the potential for real-time predictions using an incremental model-fitting procedure in which every year from 1999 to 2012 is predicted using only data from years preceding the year that is being predicted. The models only consider variables that are available prior to the start of the outbreak season. We find that model-averaged predictions using the top models (with key variables susceptibles, yearling survival, and timing of spring transition) are comparable to those of the top model fitted on the entire dataset (Figure 6.2.3.5 and Figure 6.2.3.6). This means that by using demographic and environmental data available before the start of an outbreak, it would be possible to accurately predict the size of an outbreak months in advance. This prediction capability will benefit the preparedness of rescue centers along the US West Coast, and it will allow for improved dissemination of information to target groups such as dog owners about transmission risk from stranded sea lions and land managers in charge of susceptible species of conservation concern.

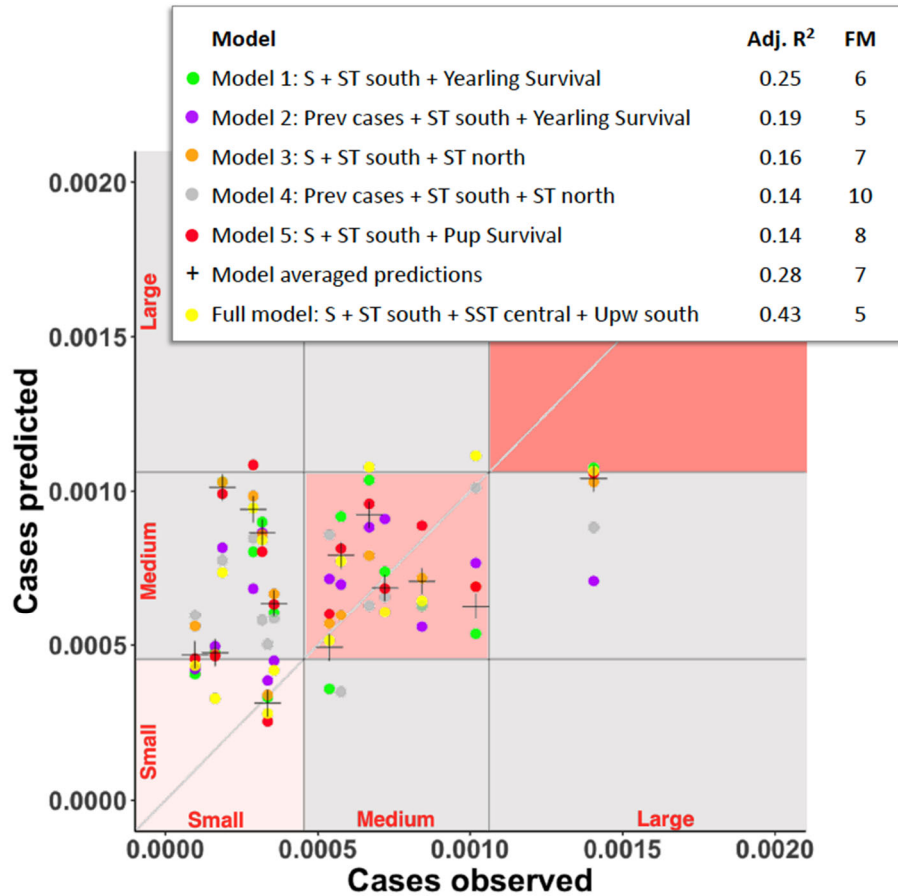


**Figure 6.2.3.5. Real-time predictions of outbreak size.** Real-time prediction results, where outbreak size in year  $t$  is predicted using a model trained on data up year  $t-1$ , and including only variables for which updated information is available prior to the outbreak. S = Susceptibles, ST = spring transition, Prev cases = cases in the previous season, SST = sea surface temperature, Upw = upwelling index.

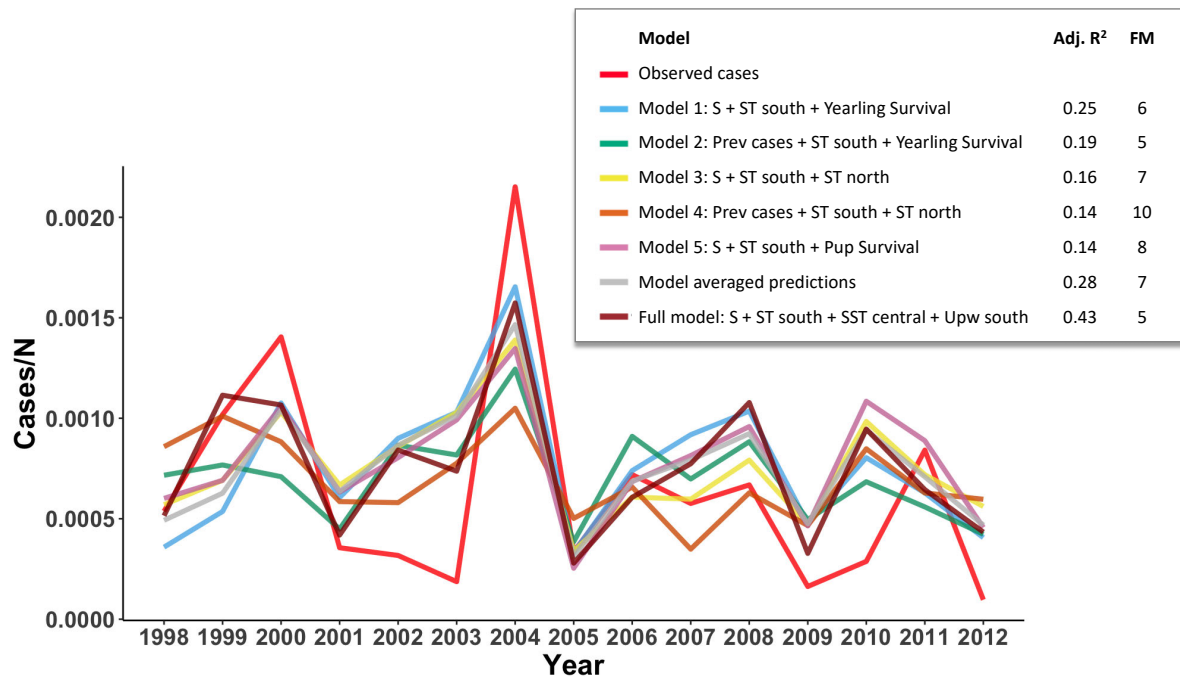


**Figure 6.2.3.6. Prediction of outbreak size using only data available prior to the start of the outbreak year being predicted.** For each prediction year a model is fitted using all available preceding years and is then used to predict the following year. For example, data from 1984 to 1997 are used to fit the model predicting outbreak size in 1998, data from 1984 to 1998 are used to predict 1999, and so on. Abbreviations: S = proportion of susceptibles, ST = timing of spring transition, Y Survival = estimated yearling survival as a proxy for preceding environmental conditions, Prev Cases = cases/N in the previous year, SST = sea surface temperature, Upw = upwelling index, south/central/north = in the southern/central/northern part of the sea lion range, AdjR2 = Adjusted R<sup>2</sup>, FM = Feature Mismatch value.

### *Long-term prediction of climate change impacts on outbreak*

Long-term predictions can be used to gain qualitative information about the potential effects of climate change on leptospirosis outbreaks in California sea lions. We can explore this by fitting simulation models in which the main environmental variables are altered to reflect potential climate change scenarios supported by existing studies on climate change impacts on the California Current system, which includes the California sea lion range (Brady et al., 2017). We use these predictions to generate three scenarios that represent increasingly larger changes in the mean value of these variables (scenarios 1 to 3; Figure 6.2.3.7). Aside from effects on the mean values of climatic variables, climate variability around these means is expected to increase, with potentially large effects on disease transmission (Rodo et al., 2002). We therefore generate another three scenarios that implement increasing magnitudes of variation (scenarios A to C; Figure 6.2.3.8). The two scenario categories are finally combined into scenarios that include both altered mean values and increased variation (scenarios 2A to 2C; Figure 6.2.3.9).

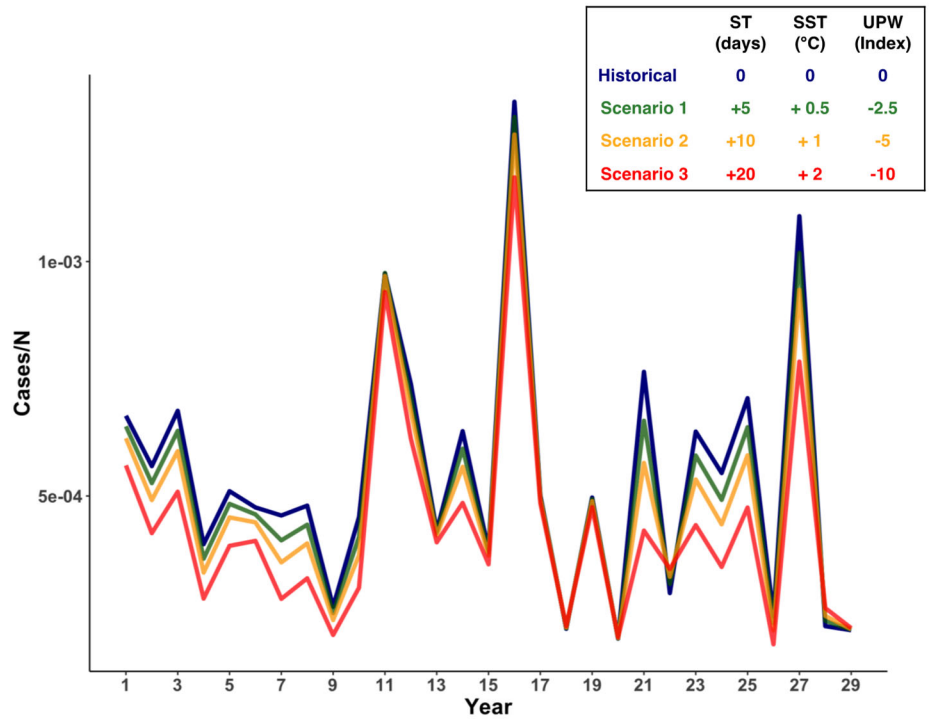


**Figure 6.2.3.7. Predicted cases for different climate change scenarios, effects of altered mean values.** Scenario 1: ST +5 days, SST +0.5°C, Upw -2.5. Scenario 2: ST + 10 days, SST +1°C, Upw -5. Scenario 3: ST + 20 days, SST +2°C, Upw -10. ST = spring transition, SST = sea surface temperature, Upw = upwelling index.

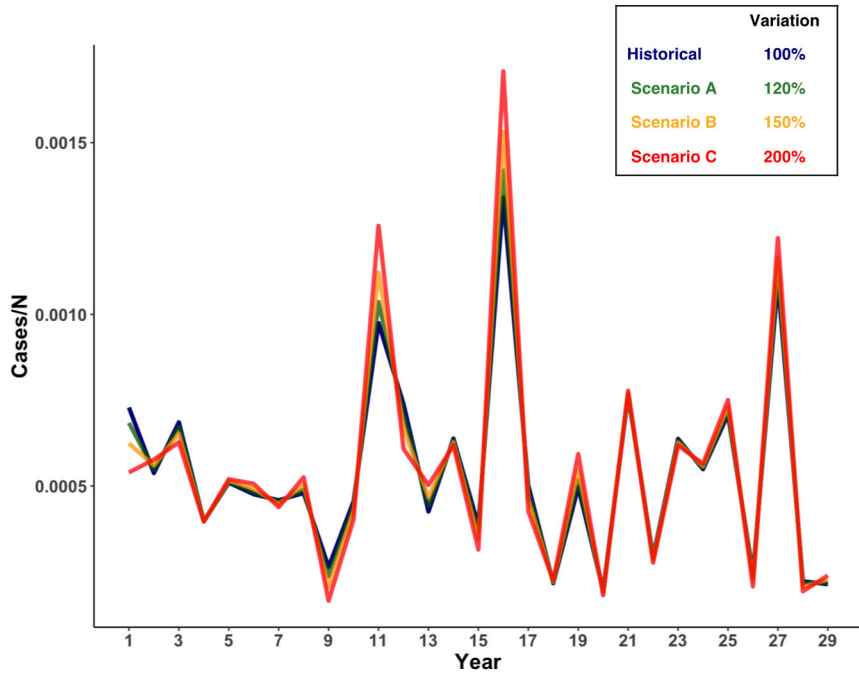


**Figure 6.2.3.8. Predicted cases for different climate change scenarios, effects of increased variation.** Scenario A: variation + 20%. Scenario B: variation + 50%. Scenario C: variation + 100%.

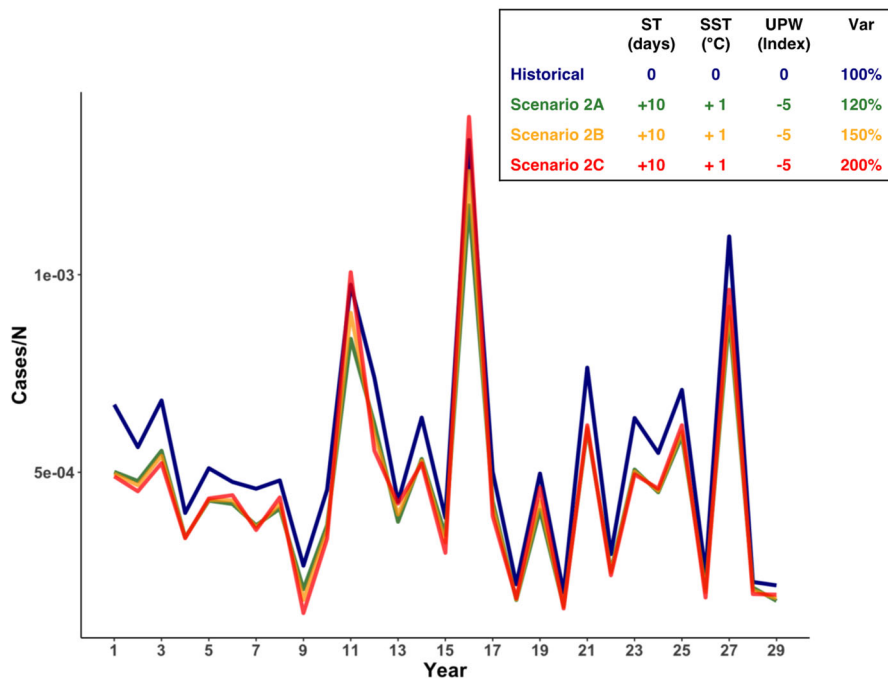


**Figure 6.2.3.9. Predicted cases for different climate change scenarios, effects of altered means and increased variation.** This combines scenario 2 (ST + 10 days, SST +1°C, Upw -5) and the three scenarios with increased variation (A: variation +20%, B: variation +50%, C: variation +100%).

Together, these simulations show that predicted changes in average SST (predicted to increase (Brady et al., 2017)), upwelling (predicted to be weaker (Brady et al., 2017)), and spring transition (predicted to be later (Barth et al., 2007)) should result in outbreaks that are *smaller* on average, but occasionally *more extreme* (larger and smaller) due to increased climatic variability (Figure 6.2.3.10). Even though these predictions are based on explorative simple simulations and do not take into account climate effects on sea lion demography or other factors than environment, they do indicate that the transmission of leptospirosis in sea lions does not follow the controversial general expectation that disease transmission and epidemics will increase under climate change (Lafferty, 2009)

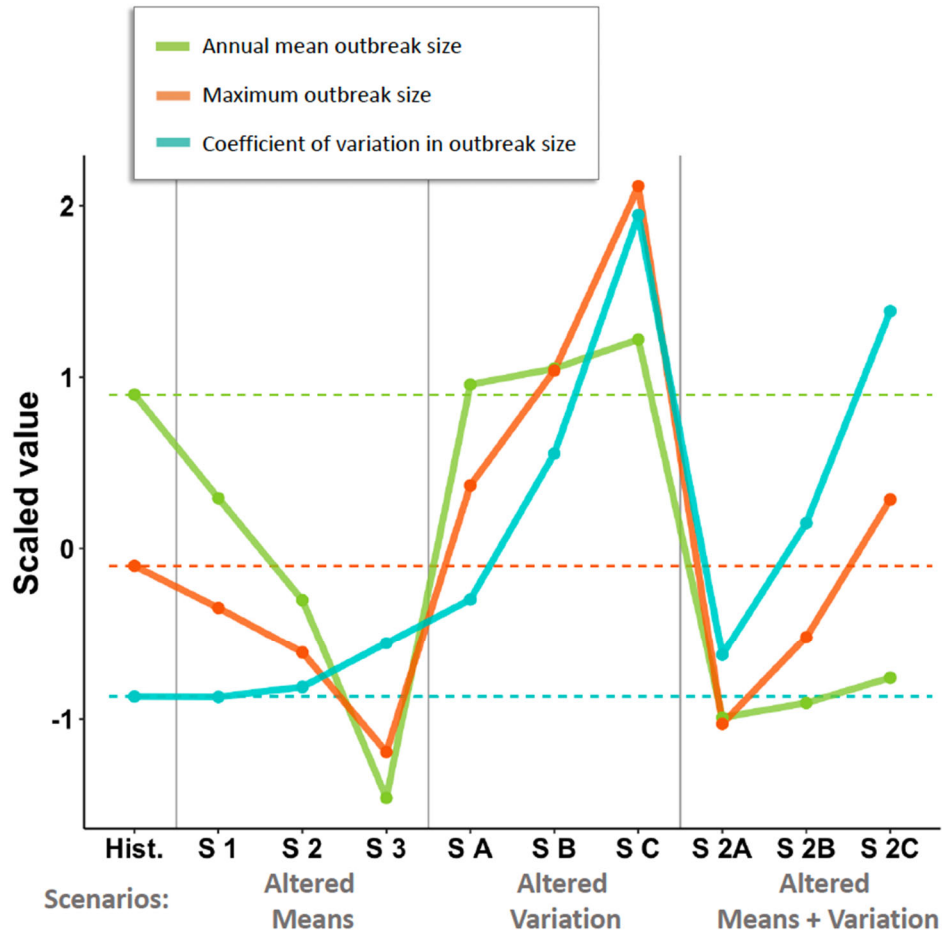


**Figure 6.2.3.10. Long-term predictions of outbreak size.** Summary statistics for different climate change scenarios. Altered means scenarios are those in which the mean values of the different variables are changed up or down based on projected directionality (S1 to S3 = small to large change). Altered variation scenarios are those in which the amount of variation is increased (SA to SC = small to large change). Scenarios S2A, S2B and S2C combined altered means scenario S2 with the altered variation scenarios. Hist. = historical values, for observed data.

*Environmental drivers modulate the natural immunity-driven cycling of Leptospira*

The case of leptospirosis in California sea lions provides fresh insights into the general theory on cyclic dynamics in ecology. Multi-annual cyclicality in outbreak size is always present

to some degree as an intrinsically driven ‘deterministic skeleton’ (Coulson et al., 2004), but we see that its regularity can be perturbed by external environmental forces (Figure 6.2.3.11). In 1995 for example, there would likely have been a small outbreak due to a decrease in susceptibles following the 1994 outbreak, but in fact exceptional environmental conditions conducive to transmission caused the 1995 outbreak to be larger than expected (Figure 6.2.3.11). Yet despite these reverberating effects of extrinsic forcing, the system maintains at least some cyclicity due to the underlying deterministic nature of intrinsic changes in population immunity. This effect of the environment on outbreak size can be interpreted as an external force that alters the threshold proportion of susceptibles needed to trigger a major outbreak. This therefore represents a rare epidemiological case study of how environmentally-driven variation in the transmission coefficient  $\beta$  can alter the proportion of susceptibles needed to confer herd immunity (Grenfell & Dobson, 1995). This advance in epidemiological theory represents a further dimension of the impact of environmental non-stationarities on pathways of pathogen exposure and the dynamics that result.

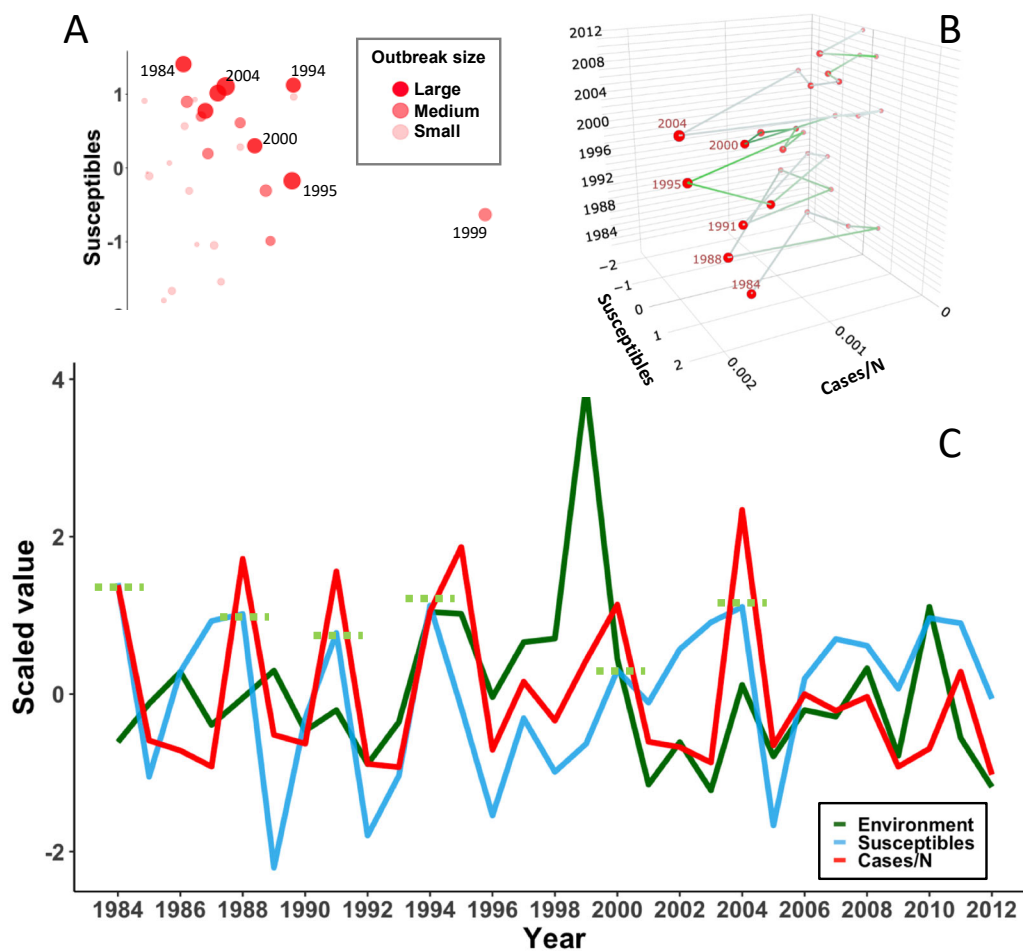


**Figure 6.2.3.11. The interplay between intrinsic and extrinsic drivers of transmission.** (A) Outbreak size in relation to susceptibles and environment (environmental component of the top model). Colors correspond to outbreak category, and circle diameter is scaled proportional to the number of cases that year. (B) Susceptibles vs. cases over time, from 1984 to 2012. Line shades represent the value of the environmental component of the model (low to high). (C) Time series of cases, susceptibles, and the environmental component of the model. Dotted green lines highlight the varying proportion of susceptibles present in the population at the start of a medium/large outbreak, as an illustration of how environment might affect the critical susceptible proportion needed to initiate an outbreak.

### 6.2.3.2. Fadeout and re-emergence

*Leptospira* ceased circulating in the California sea lion population from early 2013 to mid-July 2017 (as described in section 6.2.1, Figure 6.2.1.1, Figure 6.2.1.2). In section 6.2.3.1, we show that during endemic circulation of *Leptospira* from 1984-2012, key demographic and oceanographic factors drove outbreak intensity, with the number of susceptible yearlings and juveniles acting as the strongest driver of outbreak size. Based on epidemiologic and movement data, we hypothesize that the yearly *Leptospira* outbreaks (that occur in the late summer and fall) are sparked in the spring by transmission from older, possibly chronically infected

(Buhnerkempe et al., 2017) sea lions on the California coast to the entirely susceptible yearling population as these young animals leave the rookery islands and travel up the coast (Figure 6.2.3.12).

In 2013, we observed a disruption in the typical movement patterns, with this crucial yearling population remaining almost entirely on the rookeries, instead of migrating to the coast (Figure 6.2.3.13). Furthermore, stranding records show that the few yearlings that did go to the coast did not migrate as far north as usual (Figure 6.2.3.14). At the same time, the yearling population size was anomalously low due to high mortality in the 2012 pup cohort (Figure 6.2.3.13). We propose that this combination of anomalies in CSL movement and demography broke the key link in the transmission chain, preventing the 2013 outbreak from being sparked, and leading to fadeout of *Leptospira* from the CSL population.

This series of events took place in the context of multiple oceanographic anomalies, associated with the onset of the 2013-2015 marine heatwave known as “the Blob” (Fisheries, 2020). Unusual ocean conditions led to shifts in preferred prey species such as sardines and anchovies, which placed nutritional stress on adult females and led to an Unusual Mortality Event being declared beginning in January 2013 (Fisheries, 2021). Pup survival was greatly reduced, and those pups that did survive experienced growth rates that were the lowest on record (Table 6.2.2.2). When movement data were analyzed, the proportion of yearlings leaving the rookeries and migrating north in the fall was much lower than typically seen and was associated with the low weights observed for that cohort (Figure 6.2.3.13), suggesting that these sea lions were too small to travel north. Findings from previous studies suggest similar connections between oceanographic anomalies, such as increased sea surface temperature (SST), and observed changes in sea lion demography and movement (DeLong et al., 2017; Laake et al., 2018; Melin et al., 2010; Melin, Laake, et al., 2012), likely due to the negative impact of increased SST on prey availability (Chavez et al., 2002).

### *Leptospira re-emergence*

In order for *Leptospira* to re-emerge in the CSL population, two conditions must be met. Demographic conditions and movement patterns needed to return to more normal patterns seen during the period of endemic circulation, and *Leptospira* needed to be re-introduced from some external reservoir back into the sea lion population. Notably, a single case of leptospirosis in a sea lion was detected at TMMC in 2016 but did not lead to broader re-emergence of the pathogen. We believe this pathogen re-introduction failed to result in re-emergence due to inadequate environmental and demographic conditions at the time. The Blob had been followed by an El Niño event from 2015-2016 leading to more warm water anomalies, and once again the susceptible yearling population was quite small and of these only a tiny fraction migrated north from the rookery islands (Figure 6.2.3.13). However, in mid-2017, when another such spark must have occurred, conditions were favorable for re-emergence, and by 2018 the susceptible yearling population was the largest seen on record and the majority had followed the traditional northern migration. Thus, conditions were highly favorable for *Leptospira* in 2018, and we observed the largest leptospirosis outbreak on record (Figure 6.2.1.1).



**Figure 6.2.3.12. Depiction of hypothesized link between age- and sex-specific movement patterns and *Leptospira* transmission dynamics.** We propose that a crucial link between fall outbreaks occurs when susceptible yearlings leave the breeding grounds on the islands sometime between April and June and encounter infected, older animals, along the coast. This creates the conditions for *Leptospira* transmission to the entirely susceptible yearling population which act as the necessary ‘fuel’ to start the next fall outbreak cycle.

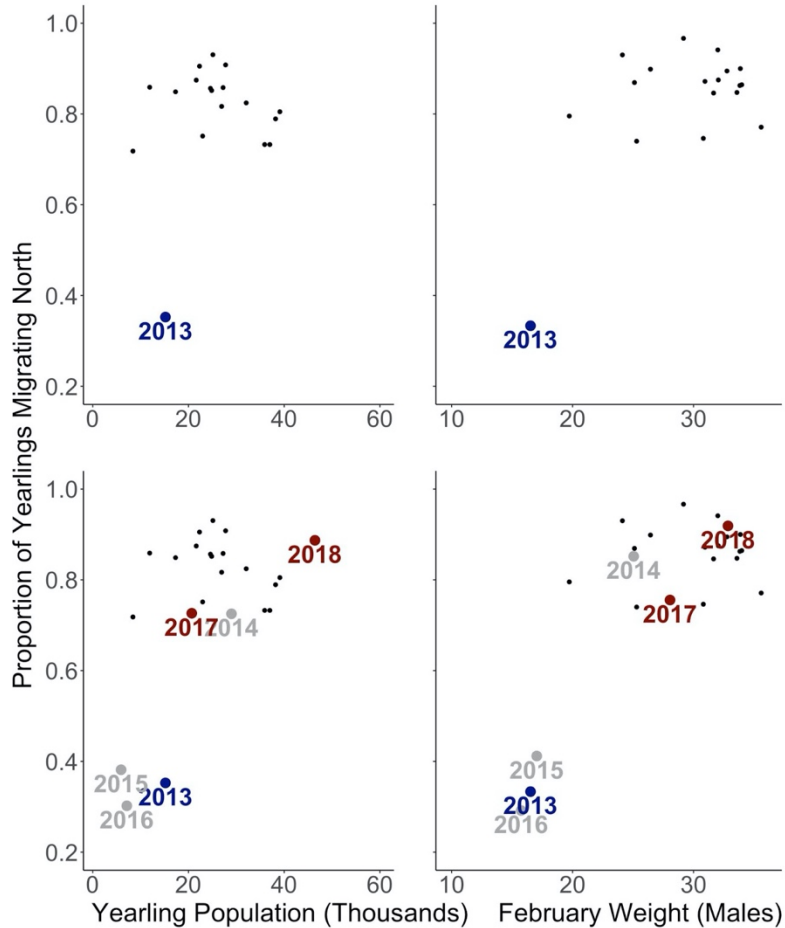


**Figure 6.2.3.13. Fadeout and re-emergence of *Leptospira* in CSL were associated with simultaneous fluctuations in susceptible supply and migratory behavior.** The proportion of the yearling CSL population migrating northward from the rookery islands in July is plotted versus the total yearling population (left) and the mean yearling male weight the February prior to migration (right). Pre- (top) and post-fadeout (bottom) data are separated for clarity. Black points indicate conditions from 1996-2012. The year fadeout occurred - 2013 - is marked in blue, the years between fadeout and reemergence are marked in grey, and re-emergence years are red. In 2013, both the proportion of yearlings migrating north as well as the total yearling population were anomalously low, and the association between the low pre-migration weights (i.e. February weights) and lack of migration, suggests that these animals were too small or lacked sufficient energetic reserves to migrate. Conditions in 2016, the year that a single case of leptospirosis was observed at the Marine Mammal Center, were similar to those seen in 2013, suggesting that they were inadequate to support reemergence. But by 2017 conditions had returned to ‘normal’ and by 2018 they were excellent for *Leptospira* transmission in the sea lion population. Note: only male weights are shown here for clarity, however female weights show the same association with proportion migrating north.

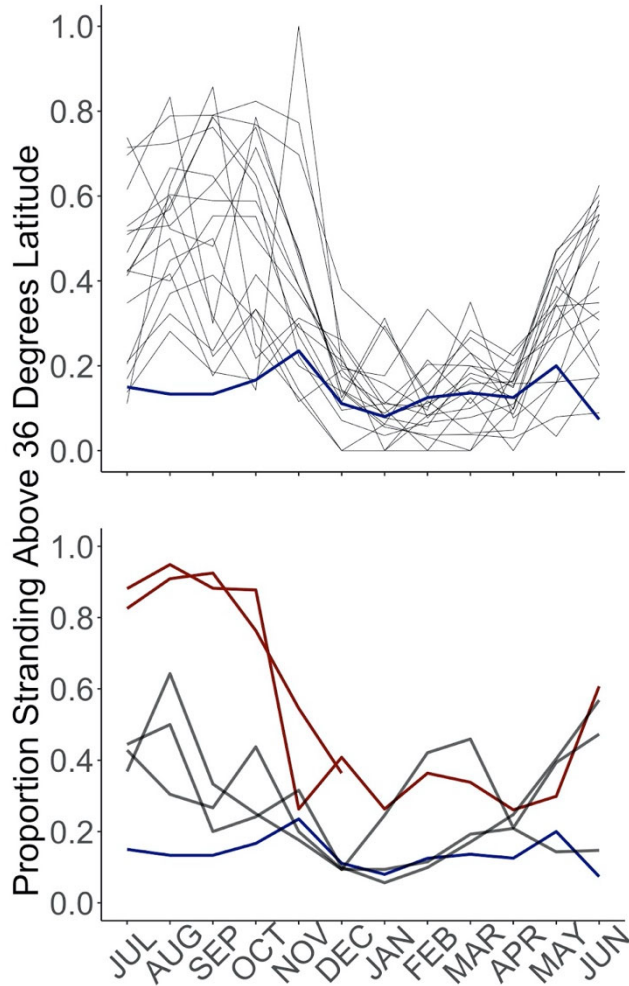


**Figure 6.2.3.14. Proportion of yearling California sea lions stranding above 36 degrees latitude.** Pre- (top) and post-fadeout (bottom) periods are separated for clarity. Grey lines in the top figure indicate years from 1996-2012, and the year that fadeout occurred - 2013 - is indicated in blue. Grey lines in the bottom figure indicate 2014-2016, red lines are for reemergence years - 2017 and 2018 - and 2013 is again shown in blue. These stranding data provide further evidence that yearling sea lions were not following their typical fall pattern of migrating north in 2013, but that they had resumed their historic migratory behavior in 2017, when reemergence occurred.

### 6.3. Understanding the Santa Rosa Island outbreak

#### 6.3.1. Long-term surveillance of the leptospirosis outbreak on Santa Rosa Island

The project extended the long-term surveillance of *Leptospira* in island foxes and spotted skunks on Santa Rosa Island until 2019. Combined with the retrospective sample analyses described in section 6.1.1, our team's surveillance of this outbreak on SRI now entails 17 years of sample collection, with almost 3000 biological samples collected in over 7800 fox captures, and over 400 samples collected in over 3300 skunk captures (see summaries of data collection efforts in section 5.3.1, as well as Table 5.3.1.1, Table 5.3.1.2, Table 5.3.1.3, Table 5.3.1.4). The

extraordinary dataset resulting from these efforts has given rise to powerful insights into the ecology of *Leptospira* in the SRI ecosystem.

### ***The island fox population on SRI has continued to grow***

Despite the outbreak and on-going circulation of *Leptospira* on SRI, the reintroduced fox population has continued to grow (Figure 6.3.1.3). In 2016, the island fox subspecies found on Santa Rosa Island was removed from the federal endangered species list, along with the subspecies on 3 other Channel Islands – a testament to the strong and effective recovery efforts by land managers, scientists, and others in the island fox research and management community. In contrast, the spotted skunk population on SRI has undergone a marked decline (as measured by the best available index of skunk abundance: the total number of skunks captured each year, under roughly constant trapping effort since 2009). This is consistent with the theory that foxes and skunks are competitors on SRI, and that skunk abundance rose markedly during the years that foxes were scarce or absent from the island landscape (i.e. before, during, and after the captive breeding period).

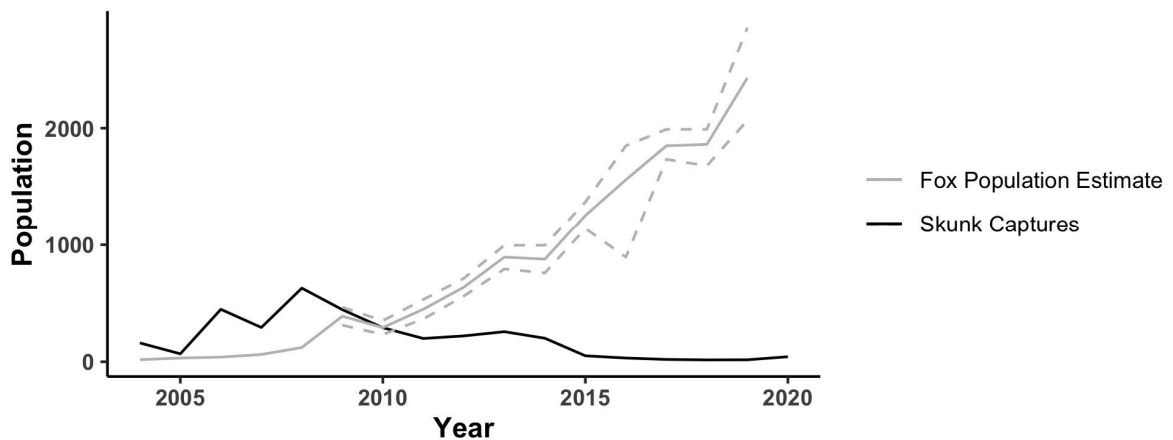


**Figure 6.3.1.1. Fox and skunk population trends on SRI.** Graph shows the estimated population size of island foxes in grey, and the total number of skunks captured (an index of skunk abundance) in black. Fox population estimates are produced by the National Parks Service based on analysis of their trapping grid data, and are plotted with 95% confidence interval since 2009 when the grid trapping program began. Note that skunk captures prior to 2009 are an unreliable index of population abundance because trapping effort was not constant.

### ***Leptospira seroprevalence and prevalence in island foxes over time***

*Leptospira* has circulated continuously in island foxes on SRI since its initial emergence in 2005-2006. Seroprevalence in adult foxes reached a peak of 88% in 2007 following the initial outbreak wave, and since then it has fluctuated but remained high (Table 6.3.1.1, Figure 6.3.1.2). There is a slight downward trend, particularly since 2013, but at no time has adult seroprevalence dropped below 60%. While one contributing factor to the high seroprevalence is that island foxes maintain measurable titers of anti-*Leptospira* antibodies for several years (see below, and section 6.3.2.3), the overall pattern indicates continued infection of susceptible foxes on SRI.

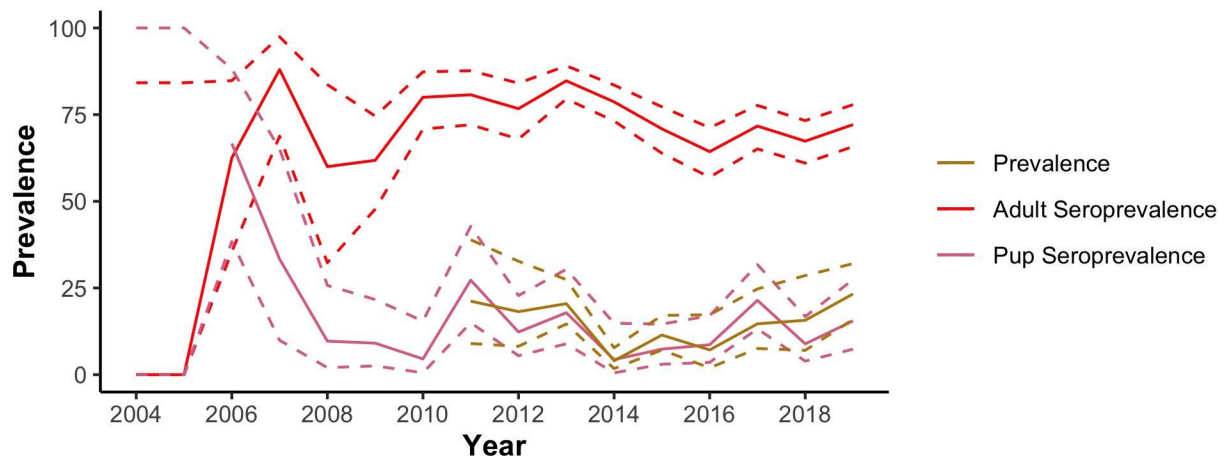


**Figure 6.3.1.2. Fox infection prevalence and seroprevalence over time.** Adult fox seroprevalence (solid red) and fox pup seroprevalence (solid pink) are from MAT results, and combined pup and adult infection prevalence (solid yellow) are from PCR and IHC results, with 95% confidence intervals (dashed lines).

The persistent circulation of *Leptospira* on SRI is corroborated by the pup seroprevalence data and infection prevalence data, both of which maintain lower but consistently non-zero levels over the last decade. These two measures both give insight into the intensity of on-going transmission in a given year, and notably they track each other very closely (Figure 6.3.1.2). Pup seroprevalence is a key indicator of continuing transmission because pups are susceptible when born in March-April each year, so, in order to test positive by the fall, they must be exposed in the intervening months. Infection prevalence data represent the fraction of sampled foxes with detectable signs of *Leptospira* infection. This can be either foxes that are currently shedding or possibly foxes that had been shedding leptospires recently and still have some leptospires (dead or alive) in their urine or tissue. In either case, infection prevalence is a direct measure of the actual source of on-going transmission. *Leptospira* infection prevalence estimates for SRI foxes are unreliable prior to 2011 due to extremely small sample sizes, but, beginning in 2011 when urine collection began, infection prevalence ranges from 4-24% annually through 2019 (Table 6.3.1.3).

Infection prevalence was calculated from samples tested using methods described in Wu et al. (Wu et al. 2014) for samples collected for all years. However, samples collected in 2017-2019 were also tested with a modified protocol that was more sensitive, which showed that the true prevalence is slightly higher than that which is presented in Table 6.3.1.2 and Table 6.3.1.3. Results obtained from the two methods are compared in Appendix C for this section.

Fox Year	All				Adult				Pup			
	Positive	N	SP	95% CI	Positive	N	SP	95% CI	Positive	N	SP	95% CI
2004	0	2	0%	0-84%	0	2	0%	0-84%	0	0	NA	NA
2005	0	2	0%	0-84%	0	2	0%	0-84%	0	0	NA	NA
2006	20	31	64.52%	45-81%	10	16	62.50%	35-85%	10	15	66.67%	38-88%
2007	26	37	70.27%	53-84%	22	25	88%	69-97%	4	12	33.33%	10-65%
2008	12	46	26.09%	14-41%	9	15	60%	32-84%	3	31	9.68%	2-26%
2009	38	99	38.38%	29-49%	34	55	61.82%	48-75%	4	44	9.09%	3-22%
2010	82	144	56.94%	48-65%	80	100	80%	71-87%	2	44	4.55%	0-15%
2011	100	153	65.36%	57-73%	88	109	80.73%	72-88%	12	44	27.27%	15-43%
2012	97	181	53.59%	46-61%	89	116	76.72%	68-84%	8	65	12.31%	5-23%
2013	210	292	71.92%	66-77%	200	236	84.75%	80-89%	10	56	17.86%	9-30%
2014	205	304	67.43%	62-73%	203	258	78.68%	73-84%	2	46	4.35%	1-15%
2015	141	284	49.65%	44-56%	134	189	70.90%	64-77%	7	95	7.37%	3-15%
2016	126	266	47.37%	41-54%	119	185	64.32%	57-71%	7	81	8.64%	4-17%
2017	170	296	57.43%	52-63%	152	212	71.70%	65-78%	18	84	21.43%	13-32%
2018	169	329	51.37%	46-57%	161	239	67.36%	61-73%	8	90	8.89%	4-17%
2019	172	284	60.56%	55-66%	163	226	72.12%	66-78%	9	58	15.42%	7-27%

**Table 6.3.1.1. Seroprevalence of anti-*Leptospira* antibodies in SRI island foxes over time.** Sample size (N), seroprevalence (SP), and 95% confidence intervals for all foxes, adult foxes, and pups, using MAT results per fox year. One sample per individual fox was used per fox year. If a fox had both positive and negative samples within a fox year, it was treated as positive for this calculation.

Fox Year	All				Adult				Pup			
	Positive	N	Prev	95% CI	Positive	N	Prev	95% CI	Positive	N	Prev	95% CI
2004	0	1	0%	0-98%	0	1	1	0-98%	0	0	NA	NA
2005	0	0	NA	NA	0	0	NA	NA	0	0	NA	NA
2006	4	4	100%	40-100%	4	4	100%	40-100%	0	0	NA	NA
2007	2	3	66.67%	9-99%	1	2	50%	1-99%	1	1	100%	3-100%
2008	0	2	0%	0-84%	0	2	0%	0-84%	0	0	NA	NA
2009	0	1	0%	0-98%	0	1	0%	0-98%	0	0	NA	NA
2010	2	2	100%	16-100%	2	2	100%	16-100%	0	0	NA	NA
2011	7	33	21.21%	9-39%	7	29	24.14%	10-44%	0	4	0%	0-60%
2012	8	44	18.18%	8-33%	7	38	18.42%	8-34%	1	6	16.67%	0-64%
2013	34	166	20.48%	15-27%	32	144	22.22%	16-30%	2	22	9.09%	1-29%
2014	8	199	4.02%	2-8%	7	176	3.98%	2-8%	1	23	4.35%	0-22%
2015	20	175	11.43%	7-17%	17	141	12.06%	7-19%	3	34	8.82%	2-24%
2016	4	56	7.14%	2-17%	3	47	6.48%	1-18%	1	9	11.11%	0-48%
2017	8	74	10.81%	5-20%	7	66	10.61%	4-21%	1	8	12.50%	0-53%
2018	7	53	13.21%	5-25%	7	44	15.91%	7-30%	0	9	0%	0-34%
2019	23	118	19.49%	13-28%	21	109	19.27%	12-28%	2	9	22.22%	3-60%

**Table 6.3.1.2. Prevalence of infection with *Leptospira* in SRI island foxes over time.** Sample size, infection prevalence, and 95% confidence intervals for all foxes, adult foxes, and pups, based on positive PCR or IHC results per fox year. One sample per individual fox was used per fox year. If a fox had both positive and negative samples within a fox year, it was treated as positive for this calculation. Culture results were not included, as no fox tested positive for culture without also testing positive via PCR

### *Spatio-temporal distribution of Leptospira exposure and infection in foxes*

Maps of the annual seroprevalence for adult foxes show that exposure to *Leptospira* was widespread across SRI by 2006, and remained widespread and relatively homogeneous throughout the study period (Table 6.3.1.3). Because antibodies persist in foxes for many years, these maps essentially convey the time-integrated history of exposure across the island and reveal that there were no refugia where *Leptospira* exposure did not reach.

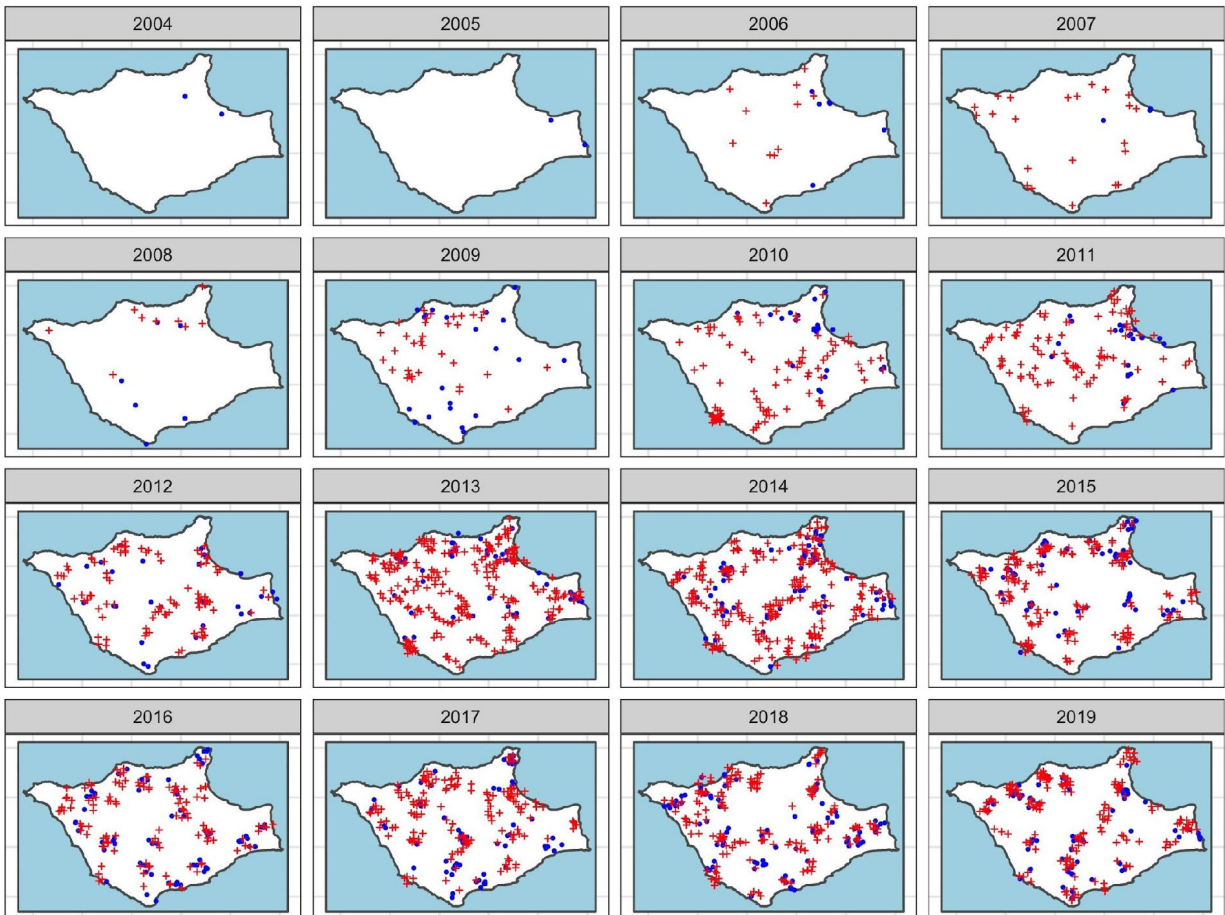


**Figure 6.3.1.3. Spatiotemporal patterns of seroprevalence in adult foxes.** Spatial distribution of MAT positive (red pluses) and negative samples (blue circles) in island foxes for each fox year.

Maps of the annual distribution of pup seroprevalence and infection prevalence are more accurate representations of recent infections, and therefore more precisely describe the spatiotemporal dynamics of transmission (Table 6.3.1.4, Table 6.3.2.1). Both of these series of maps also show widespread distribution of infected foxes, which reach all parts of the island over time. However, there is clear variation among years in spatial patterns. Both the pup seroprevalence maps and the infection prevalence maps show island-wide infections in 2006 and 2013, but in other years there are apparent hot zones of infection and some indications of spatiotemporal waves of infection crossing the island.

An interesting observation from these maps is that while pup seroprevalence and fox infection prevalence track each other very closely in the time series (Figure 6.3.1.2), the spatiotemporal maps of these two data sets align well in some years but not others. For instance, the spatial patterns of pup seropositivity and infection prevalence align well from 2012-2016, but appear to differ from 2017-2019. In 2017, for example, there is a higher density of seropositive pups in the southern part of the island, while PCR-positive foxes appear more concentrated in the northern part of the island. However, the uneven spatial distribution of testing in some years complicates the effort to assess the true spatial patterns, and it is possible that the different time lags, age groups associated with the two data sets, and age-specific ranging behaviors can lead to systematic differences in distribution.

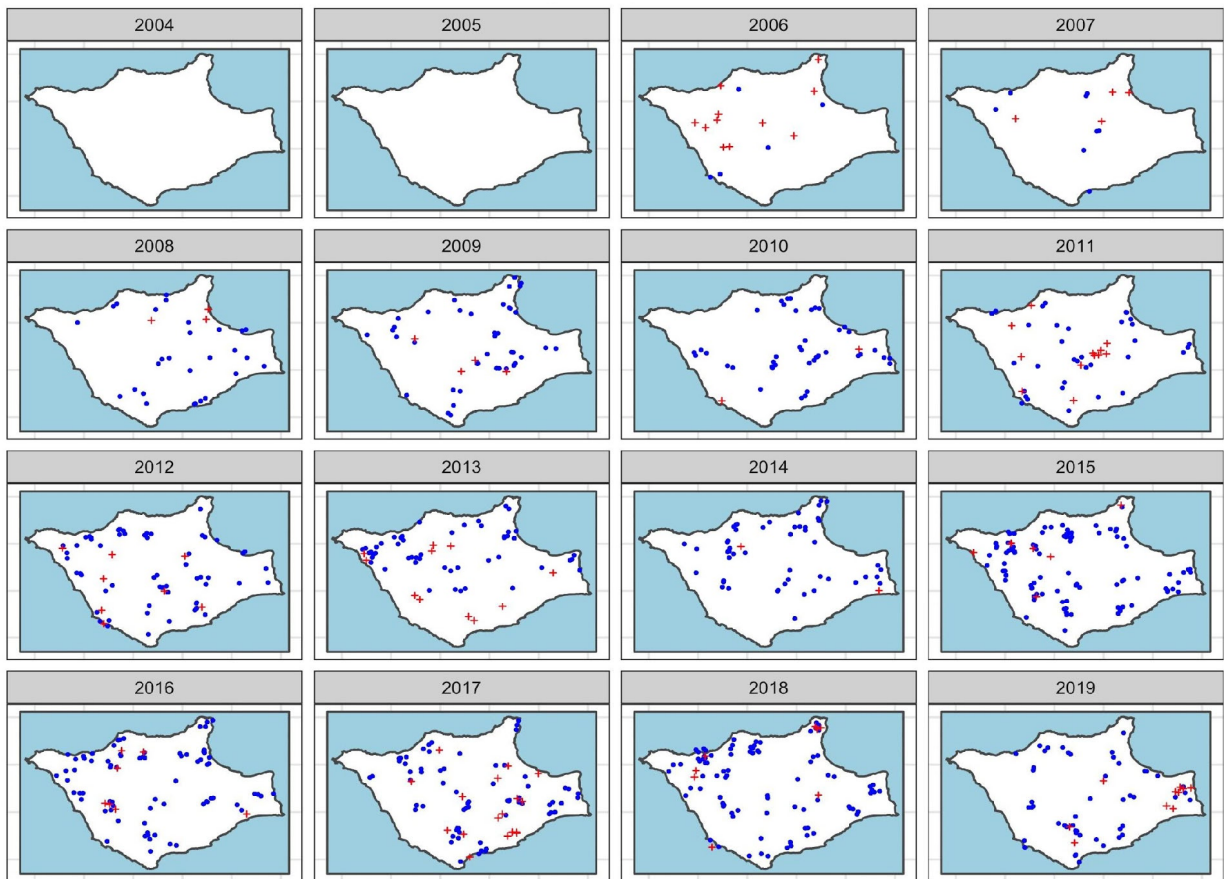


**Figure 6.3.1.4. Spatiotemporal patterns of seroprevalence in fox pups.** Spatial distribution of MAT positive (red pluses) and negative samples (blue circles) in fox pups for each fox year.

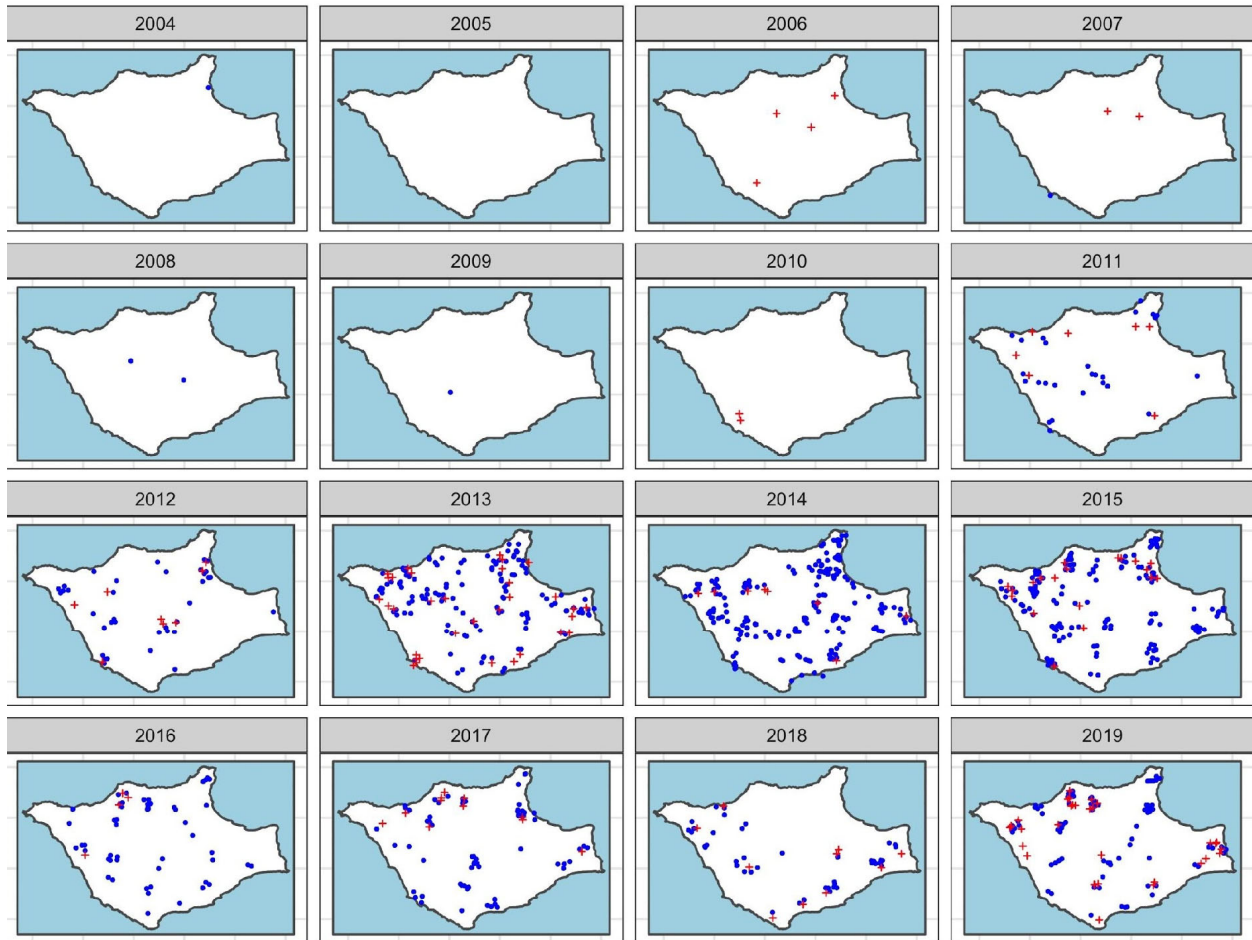


**Figure 6.3.1.5. Spatiotemporal patterns of infection prevalence in island foxes.** Spatial distribution of PCR and IHC positive (red pluses) and negative samples (blue circles) in foxes in each fox year.

### *Leptospira* seroprevalence and prevalence in island spotted skunks over time

Data on island spotted skunks are much more limited. Patterns are consistent with an on-going but declining role in the circulation of *Leptospira* on SRI over the course of our study, but we cannot exclude the possibility of a stable but fluctuating level of on-going exposure. Spotted skunks on SRI were not studied before the end of fox year 2010, when we discovered their potential involvement in the *Leptospira* outbreak. We sampled them intensively for several years, before their declining abundance (and rising fox abundance) severely limited the number of skunks trapped (Figure 6.3.1.1); due to their small size, skunks are always harder to sample, and sample sizes fell to <10 each year (Table 6.3.1.3, Table 6.3.1.4).

Clear patterns of declining seroprevalence and infection prevalence are evident during the period up to 2015 when sample sizes are sufficient to estimate prevalences with confidence (Figure 6.3.1.6, Table 6.3.1.3, Table 6.3.1.4). Seroprevalence was markedly lower from 2012–2015 than its peak of 41% in 2011. After this, estimates drop to 0% for several years before an uptick in 2019, but sample sizes during this period are too small to give a meaningful signal. Mapping the seroprevalence results, it is clear that exposure of skunks to *Leptospira* is

widespread across SRI throughout the years with sufficient sample size, with a possible exception in 2015 when seropositive skunks are more localized (Figure 6.3.1.7).

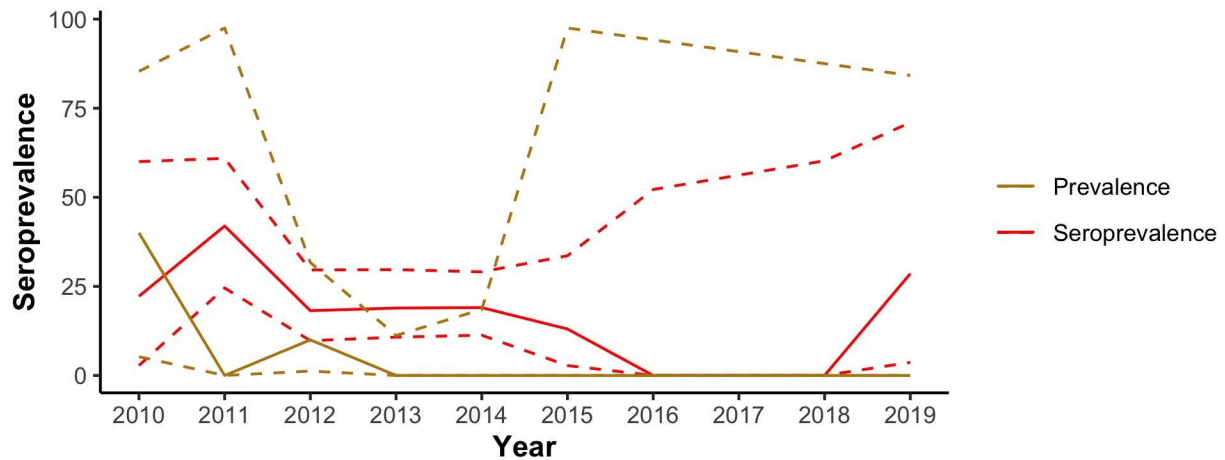


**Figure 6.3.1.6. Skunk infection prevalence and seroprevalence over time.** Figure includes the longitudinal skunk seroprevalence (solid red) from MAT results tested at CDC throughout and skunk infection prevalence (solid yellow) from PCR and culture results with 95% confidence intervals (dashed lines).

Patterns of infection prevalence are less certain. Only 4 SRI skunks have ever tested positive for infection via PCR or culture, the last of which was in 2012 (Table 6.3.1.3). For two years after 2012, we obtained reasonable numbers of samples to analyze by PCR (N=31 in 2013 and 18 in 2014), all of which were negative. From 2015 on, a total of 3 samples could be collected for PCR testing, all of which were negative. These data are insufficient to make any statements on whether or not spotted skunks are still shedding leptospire. Furthermore, the sensitivity of PCR testing in skunks may be lower than in foxes, since only a very small amount of urine can be collected from skunks (typically 0.1-0.5 mL, versus 5-10 mL from foxes), reducing the probability of obtaining a detectable copy number of *Leptospira* genomes.

Fox Year	Positive	N	Prev	95% CI
2010	2	5	40%	5-85%
2011	0	1	0%	0-98%
2012	2	20	10%	1-32%
2013	0	31	0%	0-11%
2014	0	18	0%	0-19%
2015	0	1	0%	0-98%
2016	0	0	NA	NA
2017	0	0	NA	NA
2018	0	0	NA	NA
2019	0	2	0%	0-84%

**Table 6.3.1.3. Prevalence of infection with *Leptospira* in island spotted skunks over time.** Sample size (N), infection prevalence (Prev), and 95% confidence intervals (CI) for skunks using PCR and /or culture results per fox year. One sample per individual skunk was used per fox year. If a skunk had a positive and a negative sample within a fox year the positive sample was used.

Fox Year	Positive	N	SP	95% CI
2010	2	9	22.22%	3-60%
2011	13	31	41.94%	25-61%
2012	12	66	18.18%	10-30%
2013	14	74	18.92%	11-30%
2014	17	84	20.24%	12-30%
2015	3	23	13.04%	3-34%
2016	0	5	0%	0-52%
2017	0	0	NA	NA
2018	0	4	0%	0-60%
2019	2	7	28.57%	4-71%

**Table 6.3.1.4. Seroprevalence of anti-*Leptospira* antibodies in island spotted skunks for samples tested at CDC, 2010-2019.** Sample size (N), seroprevalence (SP), and 95% confidence intervals (CI) for skunks, using MAT results per fox year. One sample per individual skunk was used per fox year. If a skunk had both positive and negative samples within a fox year, it was treated as positive for this calculation.

A further complication in the skunk data arises from inconsistent results between labs. Skunk serum samples from 2016-2019 were sent to ADHC for analysis, after our calibration trials using fox samples showed a strong correlation between MAT results from the CDC and ADHC labs (section 6.3.2.4). However, when seroprevalence estimates were calculated from MAT results of skunk sera run at the two laboratories, a large discrepancy was detected. All 18 skunk samples in the 3 years tested (2016, 2018, and 2019) were reported as MAT-positive by ADHC, yielding a 100% seroprevalence, while CDC MAT results from sera collected in all prior

years yielded seroprevalence estimates of 13-42% (data and maps from ADHC shown in Appendix C, Figure A.2, Figure A.3, Table A.2). Due to this inconsistency, the 16 samples with sufficient volume were retested at CDC, and only 2 were positive. The ADHC MAT did show slightly higher sensitivity relative to that of the CDC with the fox sera, but this discrepancy with the skunk sera is extreme. The reason for this is currently unknown, however current skunk sample numbers and volumes are insufficient to perform additional testing and investigations at this time.

Altogether, we can conclude that island skunks are susceptible to and can shed *Leptospira*, and that they have continued to be infected throughout the duration of this study. When sample sizes were sufficient, the skunks showed signs of exposure in all regions of the island. The quantitative patterns suggest a decline in infection prevalence and seroprevalence from 2010 to 2015, coincident with the marked decline in skunk abundance on SRI. However, the limited sample sizes obtained in later years, and the puzzling discrepancies between results from different certified diagnostic laboratories, prevent a strong conclusion regarding *Leptospira* dynamics in the declining skunk population. Given the continuing widespread circulation of the pathogen in SRI foxes, it is entirely possible that the skunks continue to be infected via cross-species transmission, regardless of continued transmission within their own declining population.

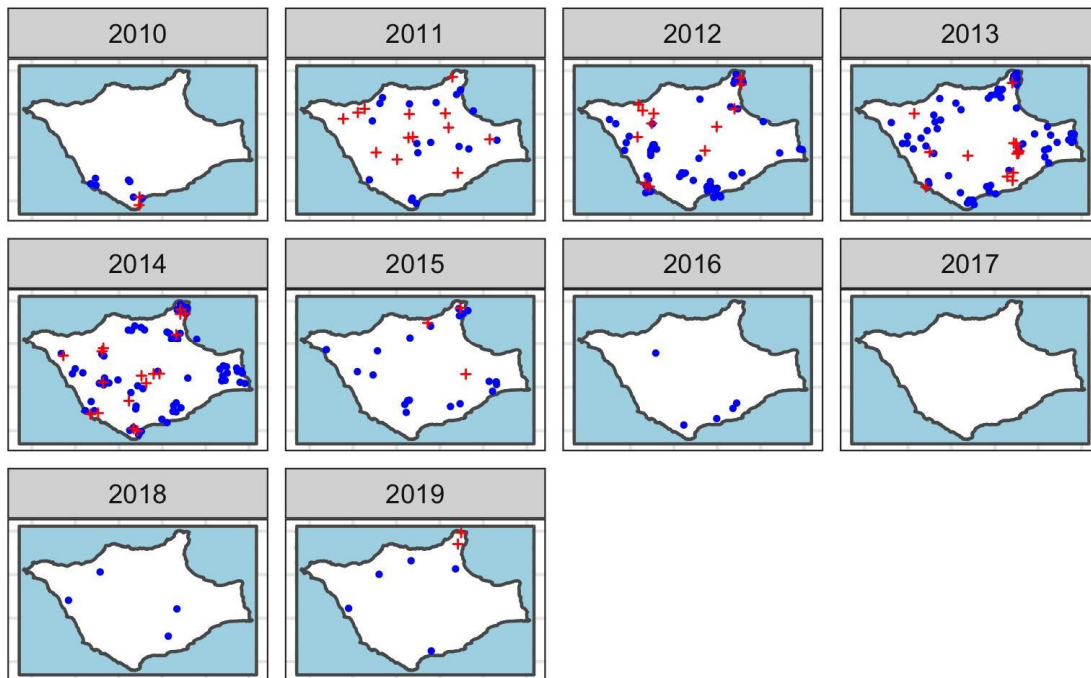


**Figure 6.3.1.7. Spatiotemporal patterns of seroprevalence in island spotted skunks (CDC lab results for all years).** Spatial distribution of MAT positive (red pluses) and negative samples (blue circles) in island spotted skunks for each year. CDC results are shown for all years, for consistency.

## 6.3.2. Analyze data to understand the ecology of leptospirosis in island foxes

### 6.3.2.1. Longitudinal samples

#### *Analysis of longitudinal serology from individual foxes*

Because foxes are often recaptured year after year, and sometimes captured multiple times within a year, we have the rare opportunity to look at longitudinal patterns in individuals. This has enabled us to gain insights into the host-pathogen relationship between island foxes and *Leptospira*, and to develop and calibrate tools to learn more about the ecology and epidemiology of this system. Figure 6.3.2.1 depicts the longitudinal patterns in anti-*Leptospira* MAT antibody titers, where each row of dots represents the history of an individual fox, with time progressing from left to right, and the colors show the antibody titers measured for each serum sample collected. The leading edge of the arc represents the youngest individuals, who typically begin as seronegative, then progress through seroconversion and titer decay. These longitudinal data allowed us to quantify the kinetics of MAT titers through time (section 6.3.2.3) and to study the risk factors for seroconversion (section 6.3.2.4).

It is clear that island foxes maintain antibodies against *Leptospira* for several years. Of the 806 individual wild foxes that ever tested MAT positive for anti-*Leptospira* antibodies, 407 were tested at least twice, 242 were tested at least three times, and so on as shown in Table 6.3.2.1. The timespan between first positive test and last MAT test, which determines the range over which MAT titer kinetics can be studied, ranged from 1 to 11 years (Table 6.3.2.2). The oldest known wild-born foxes on SRI are 11 years old, while mean lifespan is approximately 6 years (NPS, unpublished data), so these longitudinal MAT data give a fair picture of the lifetime titer changes of anti-*Leptospira* antibodies in island foxes.

N Tests	1	2	3	4	5	6	7	8	9	10
N Foxes MAT	806	407	242	131	73	37	17	6	3	1

**Table 6.3.2.1. Distribution of the number of MAT tests per fox of the island foxes that ever tested seropositive.** The numbers shown indicate how many foxes were MAT-tested at least N times, among the group of wild island foxes that ever had a positive MAT result. Repeated sampling events could occur within the same years or in different years.

Years	0	1	2	3	4	5	6	7	8	9
N Foxes	806	411	303	217	150	96	47	22	8	2

**Table 6.3.2.2. Distribution of the time interval between first positive test and last MAT test, for individual foxes that were tested multiple times.** Years represent the number of fox years between the first positive sample and final MAT test for individual foxes. N is the number of individual foxes that had an interval of at least the designated number of years between their first positive test (MAT, PCR, or culture) and final MAT test.

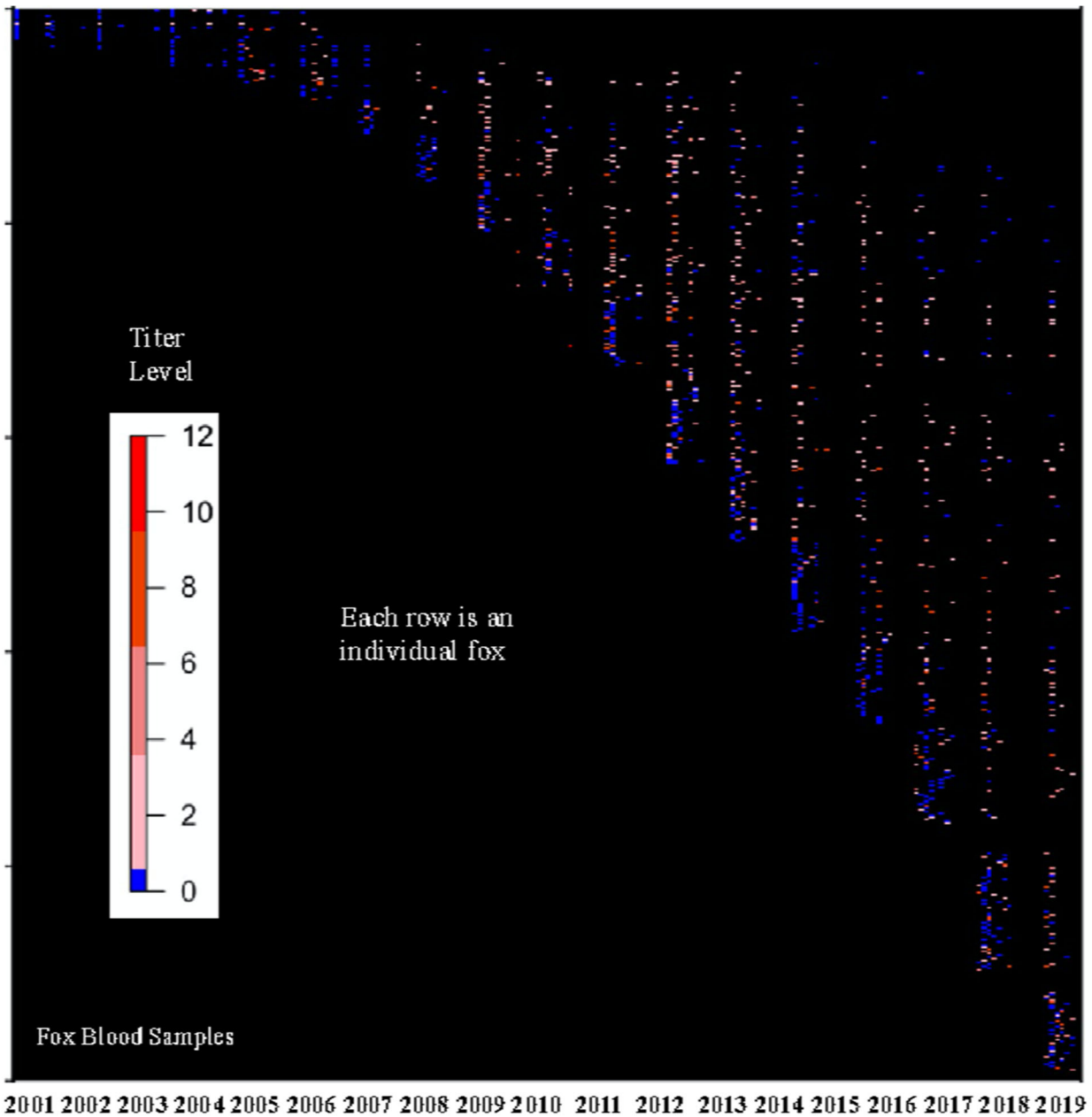


**Figure 6.3.2.1. Longitudinal patterns in MAT anti-*Leptospira* antibody titers from individual foxes.** Each row is an individual fox. The x-axis is time in fox years, with individuals aging from left to right. Individuals are ordered by the season in which they were first tagged, so the leading edge of the arc represents the youngest foxes. Each colored square indicates an MAT test result. A blue square is a negative test, and a square with a red hue is a positive MAT test. The darker the red the higher the titer level, as shown in the colorbar.

We used these extensive longitudinal data to look for serologic signs of reinfection with *Leptospira*, by looking for individuals for which the antibody titer drops over time but then increases rapidly and substantially, presumably representing an anamnestic immune response after reinfection. Of the 407 individuals that ever tested MAT-positive and had two or more tests, only 8 (1.9%) exhibited an increase greater than a 2 two-fold dilution in titer at any point

following their initial positive test. Increases of 1 or 2 dilutions were considered within the error range of the test, and were therefore not classified as boosting.

The MAT anti-*Leptospira* antibody titer trajectories for the 8 foxes that had a greater than two-step increase are shown in Figure 6.3.2.2. Four of them were pups at the time of their first positive test, so the initial positive test may have been due to transient maternal antibodies. Two individuals may have been sampled during the initial stage of infection when their titer was still increasing, as evidenced by the rapid increase from seronegative to a pair of closely spaced positive tests with rising titers. The remaining foxes could represent genuine instances of titer boosting through reinfection, or they could be due to errors in testing or sample handling. Altogether, we conclude that titer boosting reflecting reinfection of island foxes with *Leptospira* occurs rarely, if at all.

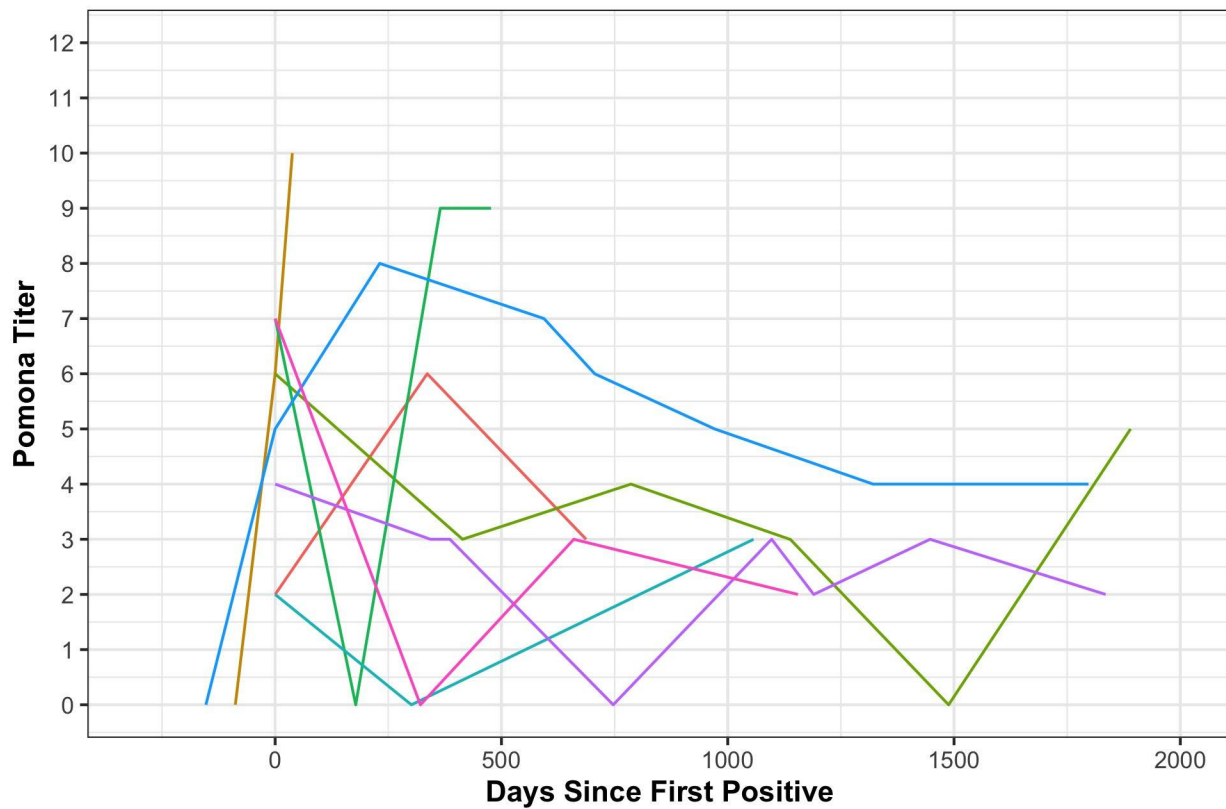


**Figure 6.3.2.2. Titer levels over time for all foxes that ever exhibited boosting.** Each colored line shows the trajectory of anti-*Leptospira* antibody titers (in log<sub>2</sub> units) measured by MAT for an individual fox. These 8 individuals are the only foxes to exhibit titer increases greater than 2 two-fold dilutions. Time is shown relative to the date of each individual’s first positive test for *Leptospira*.

### *Analysis of longitudinal shedding patterns from island foxes*

Analysis of our longitudinal data on urinary shedding of leptospire (leptospiuria) provides important insights into the shedding duration, an important quantity governing transmission dynamics. Of the 598 individual wild foxes that had urine tested via PCR, 116 individuals tested positive at some point. Of these 116 individuals, 57 were tested on 2 or more occasions, and 22 tested positive more than once. The full longitudinal histories of urinary PCR

results for the 57 individuals that had ever tested positive are shown in Figure 6.3.2.3. For the 22 individuals that tested positive more than once, the interval between first and last PCR-positive results ranged from 3 to 755 days. 12 of these 22 foxes had an interval of less than 1 year, 9 foxes had an interval between 1-2 years, and 1 had an interval of just over 2 years (see gold bars in Figure 6.3.2.4 for the complete distribution).

These raw data demonstrate that island foxes can shed *Leptospira* for at least 2 years, but the data are censored so the start and end of the shedding period are not known. We gain further insights by considering that foxes will begin shedding leptospire around the time they seroconvert, so we can use either a positive PCR test or first positive MAT test as the indicator for the onset of shedding. Since many more blood samples were collected than urine samples, including the MAT results increases the size of the usable dataset to investigate shedding duration. This is achieved through an increase in the number of foxes with longitudinal data, and also an increase in the duration of time within which fox shedding may be assessed. By including MAT results, we could estimate a minimum duration of shedding for 50 of the 116 foxes that had ever tested positive via PCR (gold and red bars in Figure 6.3.2.4). These 50 foxes have a range of 1–1057 days between their first positive test and their final positive PCR test. Thirty of these 50 foxes had a minimum shedding duration of between 1 day and 1 year, 15 foxes had a duration of 1-2 years, and 5 foxes had a duration between 2-3 years (Figure 6.3.2.4). Thus, we estimate a lower bound of 3 years for the maximum duration of shedding for island foxes infected with *Leptospira*.

Censoring can also impact observation of the end of the shedding period. If the last observed test is positive, then there is no observed upper bound on shedding duration. If there is one or more negative PCR test at the end of an individual's record, then (barring false negative results) we can infer that the individual stopped shedding. Considering the longitudinal histories in Figure 6.3.1.10, we note that foxes that do not stop shedding will have multiple yellow boxes (denoting positive PCR tests) along their line. The abundance of blue boxes and absence of yellow boxes in the upper right corner of this figure is evidence that foxes tend to cease shedding over time. Figure 6.3.2.4 presents the same data in a different way with the grey bars showing the duration of time that foxes could have been observed to be shedding, given our data set. It is evident that the observed distribution of shedding durations is not truncated by a lack of observations over longer intervals.

There are important caveats to this analysis. We have not fully addressed the censoring issues inherent in estimating shedding duration from widely spaced sampling events. PCR test sensitivity for detecting leptospire via PCR is less than 100%, and urinary shedding could be intermittent or fluctuate in intensity leading to lower test sensitivity. While a positive PCR test indicates that the individual is shedding leptospiral DNA, it does not prove that the leptospire detected are alive and infectious. However, taken together, our work shows that island foxes can shed *Leptospira* for periods up to 3 years or perhaps longer, and that shedding for 1-2 years is common, suggesting that the transmission potential of individual infected foxes can extend for months to years.

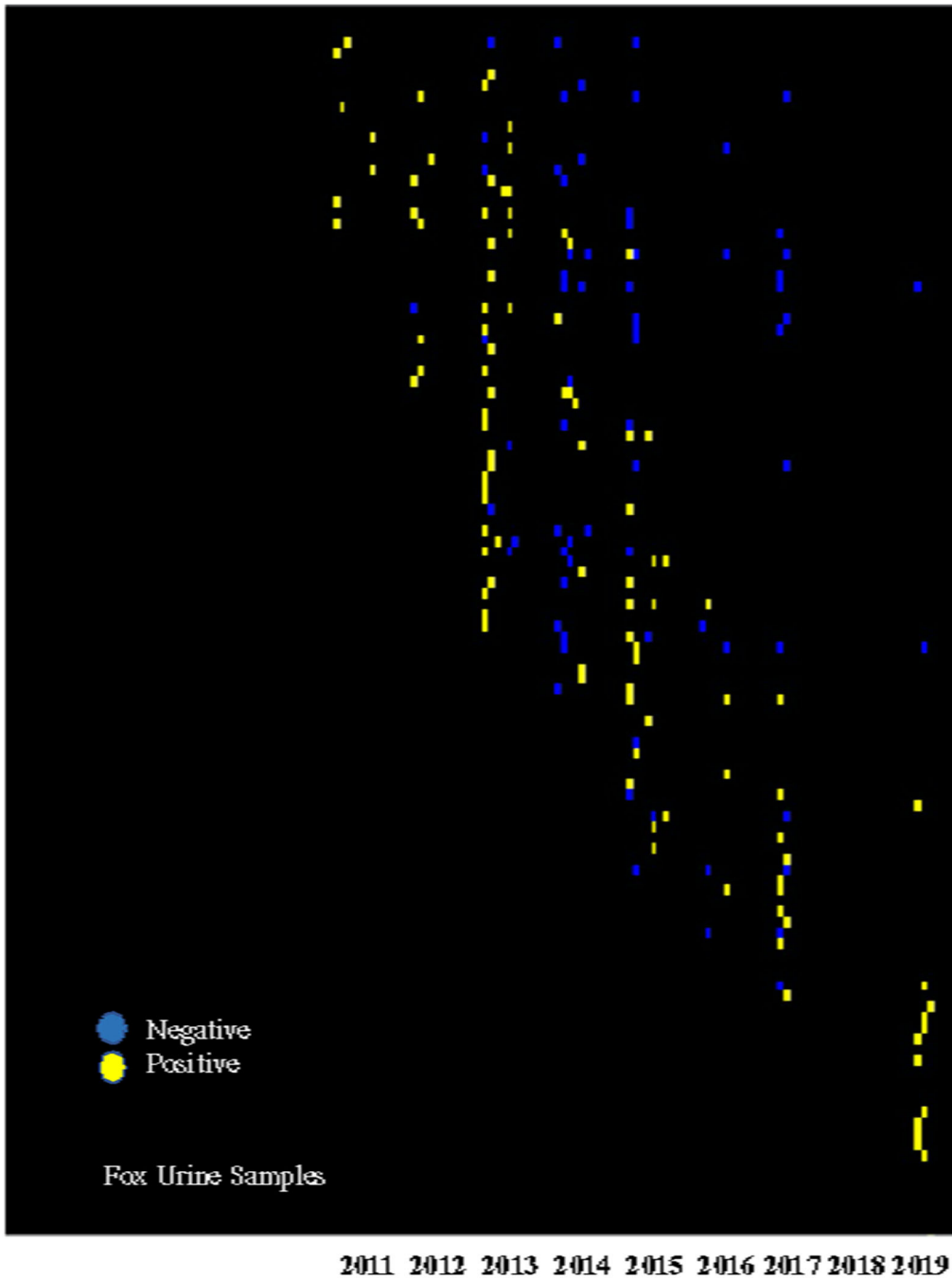


**Figure 6.3.2.3. Longitudinal patterns in PCR results from all individual wild foxes that ever tested positive for *Leptospira* DNA in urine.** Each row is an individual fox and the x-axis is time. Blue boxes indicate a negative PCR test and yellow boxes indicate a positive PCR test. Multiple yellow boxes within a row are evidence for protracted urinary shedding of *Leptospira*, over the time interval spanned by those tests.

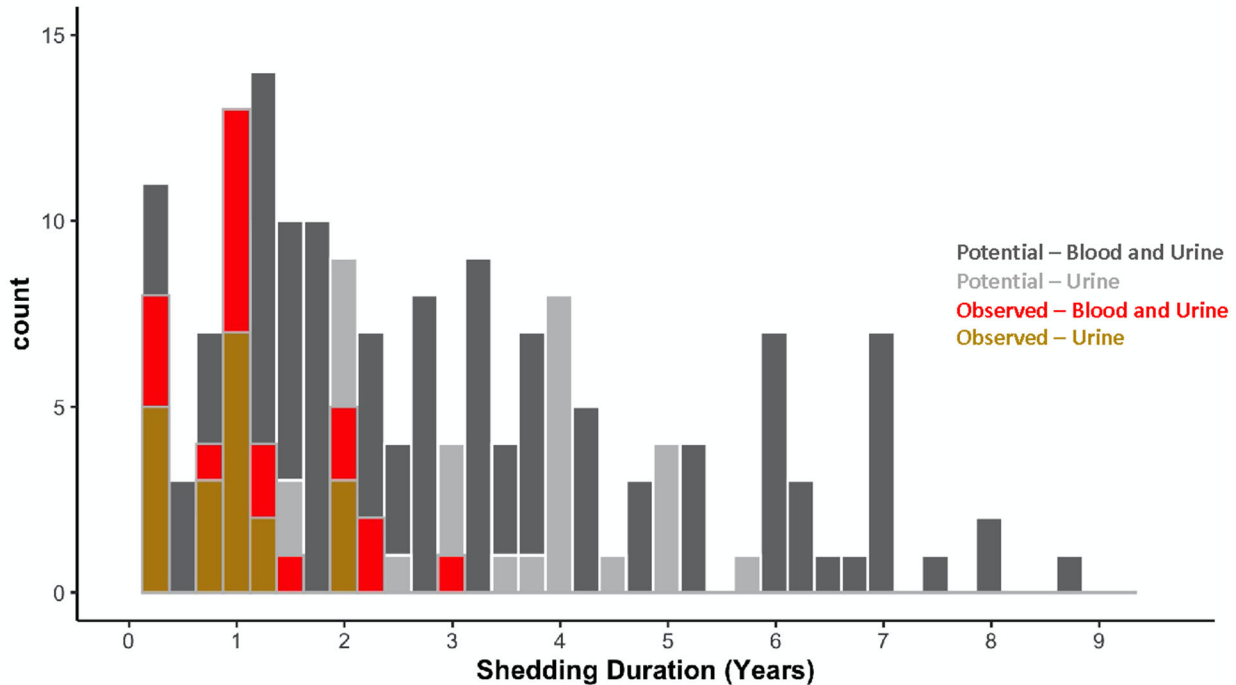


**Figure 6.3.2.4. Observed duration of shedding of *Leptospira* by infected island foxes.** Grey bars indicate the potential duration of shedding that could have been observed, given the samples collected. That is, they show the interval from the first positive test, which is considered the onset of shedding, to the final PCR test that was conducted (regardless of test result). Dark grey bars use the first positive result from any diagnostic test, and light grey bars use only PCR tests to determine the onset of shedding; for both shades of grey, the final PCR test was negative. Gold bars represent the duration of shedding observed using just PCR data, and red bars represent the duration of shedding observed using a positive MAT or PCR result as the onset of shedding; for both gold and red bars, the final PCR test was positive. The width of the bars are 3 months.

### 6.3.2.2. Modeling antibody kinetics to estimate time of infection

#### Model fits

The best fits were observed for the models with more curvature, allowing a faster initial decay that slows with time since peak antibody level, for both serovar Pomona and Autumnalis. The double exponential model had the lowest LOOIC value (LOOIC values: single exponential = 5933, double exponential = 4705, power = 5757). All models were fit to the dataset including both serovar Pomona and Autumnalis, resulting in one overall LOOIC value but separate functions for each serovar. The predicted fitted functions using the population-level posterior means (reported below) are shown in Figure 6.3.2.5A. All further results will be shown for the double exponential model only. The fitted double exponential functions for serovars Pomona and Autumnalis are shown in Figure 6.3.1.2B with the observed data after adjusting the sample times (x-axis) for each individual based on the estimated peak antibody time  $\theta_i$ . The mode (maximum posterior density) was used as the posterior estimate for  $\theta_i$  to accommodate the skewed distributions.

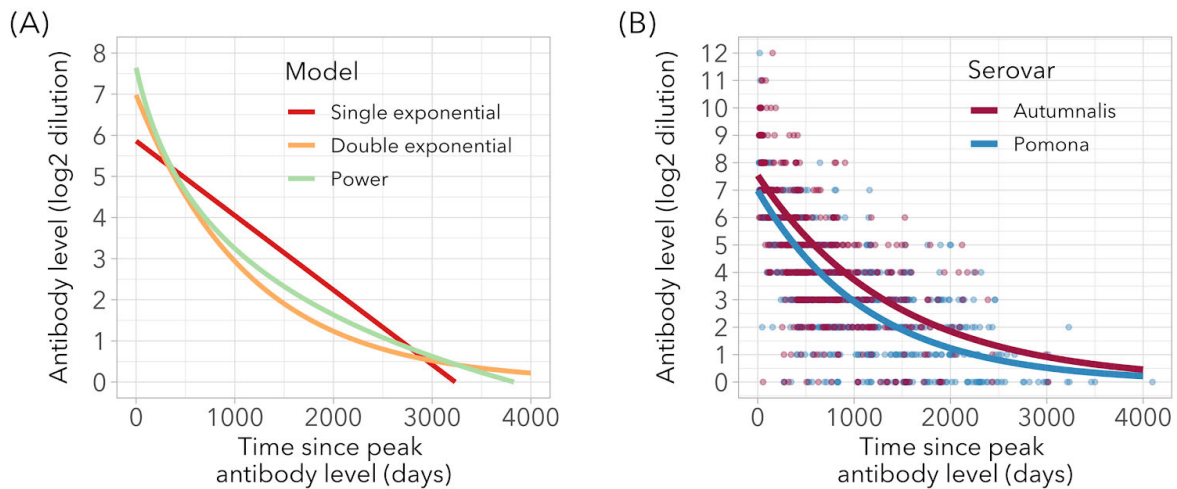


**Figure 6.3.2.5. Models for antibody kinetics and fit to island fox data.** (A) Fitted functions for the three candidate models, using the posterior means for serovar Pomona peak antibody level and decay rate. (B) Fitted double exponential functions for serovars Pomona and Autumnalis, overlaid on observed data for 307 individuals after changing time since first positive sample to estimated time since peak antibody level.

#### Posterior estimates

The posterior estimates for all population-level parameters are provided here. Results for each individual are shown in Figure 6.3.2.8. The population-level posterior means of the peak antibody level distribution parameters for serovar Pomona were  $6.89 \log_2$  units (95% CrI 6.61 to 7.15) for the mean and  $2.00 \log_2$  units (95% CrI 1.79 to 2.24) for the standard deviation. The estimated peak antibody level distribution for serovar Autumnalis was slightly higher, with a mean of  $7.45 \log_2$  units (95% CrI 7.11 to 7.88) and standard deviation of  $2.08 \log_2$  units (95% CrI 1.81 to 2.35) (Figure 6.3.2.6A). Peak antibody levels of individual foxes were estimated to be  $0.67 \log_2$  units (95% CrI -0.38 to 1.24) higher for serovar Autumnalis than for serovar Pomona, with a strong positive correlation (effect estimate = 0.99, 95% CrI 0.90 to 1.14;  $R^2 = 0.99$ , 95% CrI 0.94 to 1.00).

The population-level distribution of decay rate for serovar Pomona had a mean of  $0.00086 \log_2$  units/day (95% CrI 0.00079 to 0.00093) and standard deviation of  $0.00035 \log_2$  units/day (95% CrI 0.00028 to 0.00042). For serovar Autumnalis the mean was  $0.00069 \log_2$  units/day (95% CrI 0.00061 to 0.00078) and the standard deviation  $0.00028 \log_2$  units/day (95% CrI 0.00021 to 0.00037) (Figure 6.3.2.6B). There was no significant correlation between individual peak antibody level and decay rate (posterior mean of the linear regression slope: 90, 95% CrI -456 to 646; Figure 6.3.2.6C).

The mean percentage by which the individual prior peak antibody intervals were reduced after model fitting was 10.8% ( $\pm 0.4$  SE, range 5 to 67%) when using the model that includes both serovars, and 10.8% ( $\pm 0.5$  SE, range 5.9 to 67%) for the model using serovar Pomona only. Mean relative entropy values were 0.100 bits ( $\pm 0.011$  SE, range 0.006 to 1.185) and 0.107 bits ( $\pm 0.014$  SE, range 0.006 to 1.691).

### Correlates of model performance

We found strong individual variation in how much information the model was able to provide about peak antibody time  $\theta_i$ , with peak antibody interval size reductions ranging from 5 to 67%, and relative entropy values from 0.006 to 1.185 bits. To assess whether this variation in information gain was predictable, we tested the correlation between an individual's peak antibody interval reduction and a number of variables: prior peak antibody interval size, number of samples, time range covered by the samples, estimated peak antibody level, and estimated decay rate for serovar Pomona. Correlations were tested using linear models with a log-transformed interval reduction outcome variable. There were positive significant effects of prior peak antibody interval size (effect estimate = 0.14,  $F = 36.9$ ,  $df = 305$ ,  $P < 0.0001$ ), decay rate posterior mean (effect estimate = 0.19,  $F = 81.4$ ,  $df = 305$ ,  $P < 0.0001$ ), peak antibody level posterior mean (effect estimate = 0.08,  $F = 10.6$ ,  $df = 305$ ,  $P = 0.001$ ), and the level of the first positive sample (effect estimate = 0.05,  $F = 5.4$ ,  $df = 305$ ,  $P = 0.02$ ). Model comparison using AIC showed the best fit for a regression model including a combination of decay rate, peak antibody level and peak antibody interval size. Details are in Appendix C.

For a better insight into what individual-level results look like, Figure 6.3.2.7 shows the output for two different individuals.

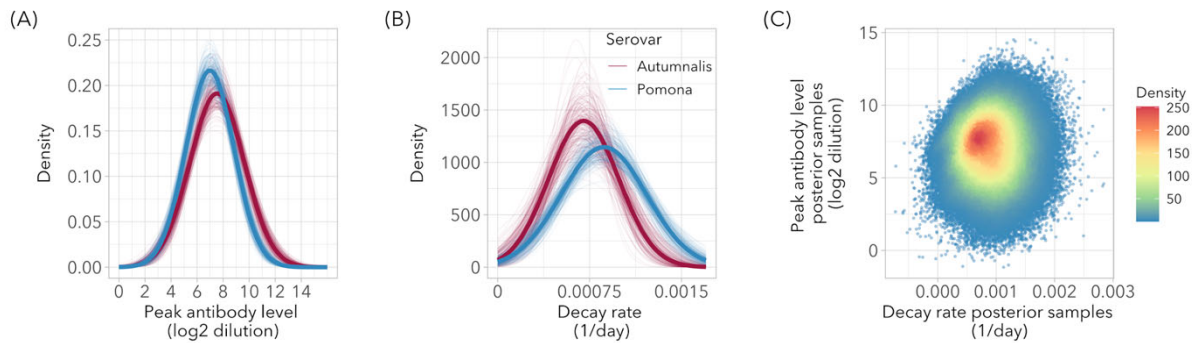


**Figure 6.3.2.6. Estimated population-level distributions of peak antibody level (A) and decay rate (B), for serovars Pomona and Autumnalis.** Bold lines are the distributions based on the posterior means of the mean and the standard deviation of each parameter. Thin lines are drawn from a random selection of 200 MCMC iterations, to show the magnitude of the variation around the posterior mean values. Panel (C) shows posterior samples for peak antibody level and decay rate, with colors depicting the density of points.

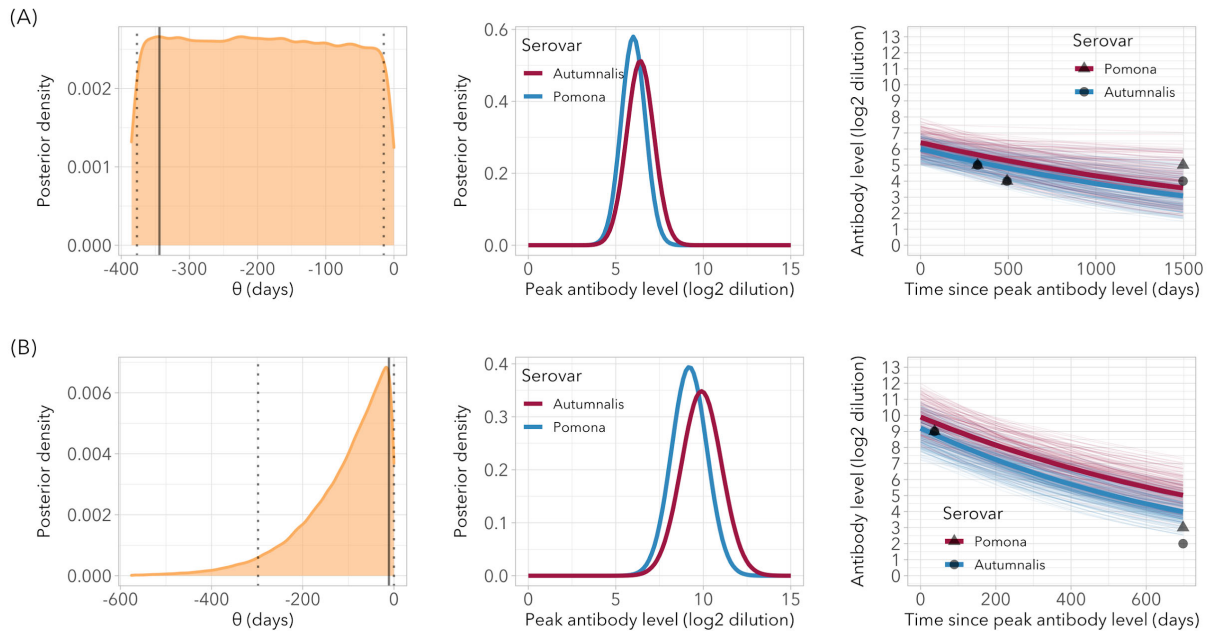


**Figure 6.3.2.7. Posterior results for two individual foxes with low (A) and high (B) gain in information about peak antibody time ( $\theta$ ).** Left: posterior distribution of  $\theta$ , the time between the first positive sample and the estimated peak antibody time, with maximum density and 95% CrI indicated by bold and dotted lines. Center: posterior density for peak antibody level. Right: fitted functions using posterior estimates (bold lines) overlaid on 200 randomly selected iterations to show the distribution; black points are the observed samples

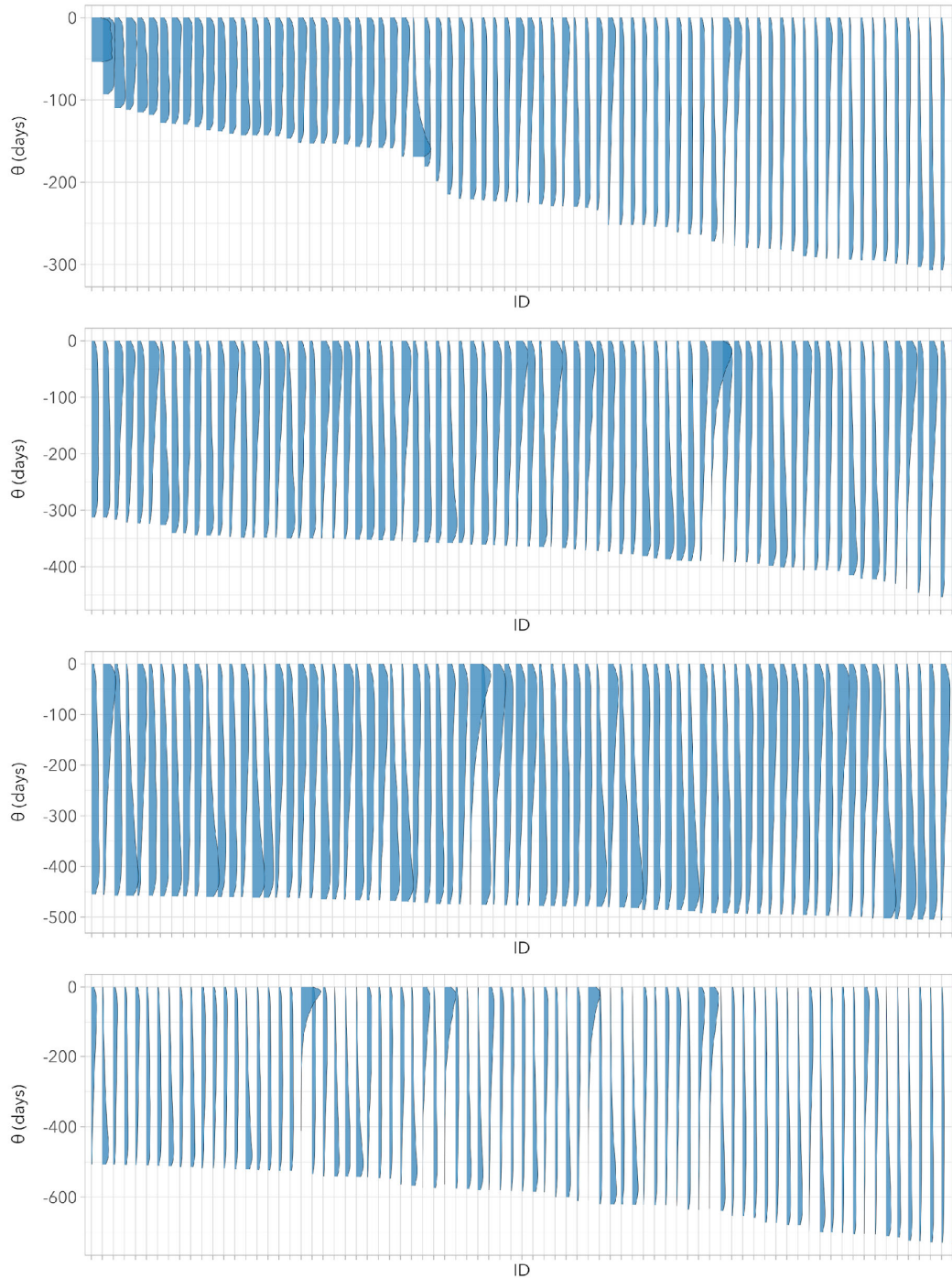


**Figure 6.3.2.8. Posterior densities of peak antibody time ( $\theta$ ) for all foxes.** Densities were plotted along the y-axis to enable showing all individuals, ordered along the x-axis by prior peak antibody interval size.

### Simulation results

The models fitted to simulated data were always able to estimate the population-level parameters precisely ( $\beta_0$ ,  $\sigma_{\beta_0}$ ,  $\lambda_0$  and  $\sigma_{\lambda_0}$ ), showing that the modeling approach works well. The estimation of parameter values at the individual level was good overall, but performance declined with more extreme values of the “real” individual peak antibody level (i.e. when the real simulated level was much lower or higher than the population mean; Figure A.6, Figure A.7, Figure A.8).

Of broader relevance to biomarker dynamics in general, we found that model performance was strongly dependent on both decay rate and peak antibody level variation (sd). There was a strong positive correlation between decay rate and model performance (measured as peak antibody interval reduction), while there was a negative correlation between standard deviation of peak antibody level and model performance (Table 6.3.2.3). Figure A.11 illustrates how the estimation of peak antibody time  $\theta_i$  will be more accurate when decay rates are high, and how a faster decay and/or smaller variation in peak antibody values in the population would result in better inference (Table 6.3.2.3).

Peak antibody interval reduction (%)				
Peak Ab SD (log <sub>2</sub> units)	Decay rate (log <sub>2</sub> units/day)			
	0.005	0.001	0.0005	0.0001
0.5	49	52	39	10
1.0	48	40	27	8
2.0	41	30	17	7
3.0	37	21	13	6

**Table 6.3.2.3. Model performance on individual peak antibody time ( $\theta_i$ ).** Gained information on peak antibody time relative to the prior knowledge, a uniform interval bound by the last negative and first positive samples. Values show the percentage by which the peak antibody interval size was reduced, where the 95% CrI of the posterior distribution was taken as the new interval. Results were similar when using relative entropy.

### Broader implications

One of the outstanding challenges in quantitative serology is how to model biomarker dynamics when infection times are unknown (Borremans et al., 2016; Pepin et al., 2017). By integrating data from different sources using a Bayesian approach, we were able to model antibody decay despite imprecise knowledge about when individuals were infected. Two key sources of prior information were used in the model. The first is information about possible peak antibody levels provided by a subset of foxes known to have been infected relatively recently. The second is an interval that bounds each individual’s possible times at which antibody levels must have peaked, provided by a negative sample preceding the first positive one. Additionally, the Bayesian approach enabled leveraging data from multiple biomarkers, in this case antibody level data on *Leptospira interrogans* serovar Autumnalis in addition to serovar Pomona.

Model fit statistics showed a clear preference for the two models in which decay slows down with time, and of those the most parsimonious double exponential model received the highest level of support. For the double exponential model, the antibody half-lives on the log-scale were estimated to be 889 days for serovar Pomona and 1005 days for serovar Autumnalis.

As these half-lives are for the log-transformed dilutions, this means that the actual decay in original dilution units gradually slows down with time since peak antibody (e.g. from an initial serovar Pomona antibody dilution of 1:6400 it would take 198 days to decay to 1:3200, 431 days to 1:1600, 718 days to 1:800, and 2495 days to 1:100). Initially rapid antibody decay followed by a slow phase seems to be relatively common, and has for example been observed for leptospirosis in California sea lions (Prager et al., 2020), *Bordetella pertussis* in humans (Teunis et al., 2016) and arenavirus in multimammate mice (Borremans et al., 2015). It has been suggested that this may be a consequence of the heterogeneous dynamics of antibodies produced at different sites in the body, at different rates and driven by different mechanisms, resulting in the overall pattern observed here (Teunis et al., 2016; Traggiai et al., 2003).

There was a strong correlation between antibodies against serovars Pomona and Autumnalis, especially peak antibody levels. This meant that the information gained by the addition of data on serovar Autumnalis was limited, as that information was for the most part already provided by serovar Pomona. We indeed found that the reduction in peak antibody interval size was not much better when integrating data on both serovars than when only using serovar Pomona. This is a useful general insight into what to expect when considering incorporating multiple biomarkers for quantitative serology and suggests that a useful strategy would be to prioritize biomarkers that do not correlate strongly. For instance, combining antibody data with data on the presence of a pathogen (or its genetic material) is likely to be much more informative than data on an antibody exhibiting the same dynamics, as shown for arenavirus infection in the rodent *Mastomys natalensis* (Borremans et al., 2016), *Leptospira interrogans* infection in California sea lions (Prager et al., 2020) and influenza A in swine (Strelhoff et al., 2013).

We found that population-level estimates of peak antibody level and decay rate could be reproduced well in simulations, and while most individual-level estimates were close to the (simulated) values, some were not as good. Closer inspection showed that this happens when an individual's peak antibody level was much lower or higher than average. Because the model assumes that individual levels are a sample of the population-level distribution, values closer to the mean will have a higher likelihood. This “pulls” the individual estimates towards the population means, which is generally not problematic unless the real individual peak antibody value is much lower or higher. This is by definition rare when peak antibody levels or decay rates are assumed to be distributed normally.

Model performance correlated strongly with a number of individual variables. The reduction in individual peak antibody time intervals increased with higher decay rate, higher peak antibody level, higher level of the first positive sample and the size of the prior interval. The latter can be explained by the fact that when the prior interval is wider, larger improvements are possible given the fact that decay rate and peak antibody level are restricted to the normal distribution around their population-level mean. The improved performance with higher decay rates is a consequence of the smaller posterior distribution for the peak antibody time interval when the change in antibody level happens in a shorter time period (Table 6.3.2.3, Figure A.11). The effect of a higher level of peak antibody or first positive sample results from the fact that decay is faster at higher levels, which results in smaller possible time windows for peak antibody time as explained above. Last, through simulations we also observed that a broader distribution of possible peak antibody levels directly translates into a broader distribution of possible peak antibody times, which means that lower individual variation will result in better estimates of peak antibody time (Table 6.3.2.3).

These characteristics related to model performance are intrinsic to a pathogen-host system, and will determine the upper level of performance of any model. Here we found that the decay of antibodies against *L. interrogans* serovar Pomona in Channel Island foxes is slow, and that there is considerable variation in peak antibody level, which means that the information gained from using antibody level data is relatively limited. Indeed, the estimated decay rate of 0.0009  $\log_2$  units/day results in a peak antibody time window of 320 days between peak antibody levels 6 and 8  $\log_2$  units. In the simulations we observed an 8% peak antibody interval reduction for a decay rate of 0.0001 and peak antibody standard deviation 1, while for the same standard deviation but a faster decay of 0.005, the reduction increased to 48%. This means that for other systems such as *L. interrogans* serovar Pomona infection in California sea lions (*Zalophus californianus*) where antibody decay can be as fast as 0.058 (Prager et al., 2020), a similar model would be expected to add much more information about peak antibody time. Despite this restriction however there were still foxes for which the reduction in the peak antibody interval exceeded 60%.

Regardless of system characteristics and data quality, there will always be a certain amount of uncertainty due to biological variation and observational noise. Another major benefit of using a Bayesian MCMC approach is the fact that it explicitly integrates all sources of variation and uncertainty, resulting in a probability distribution of all parameter estimates instead of a single point estimate with a standard error when using frequentist methods. All uncertainty is therefore acknowledged in the posterior distributions. Another advantage of the Bayesian approach is that it enables the use of information from widely varying sources (Figure 5.3.2.1). We have for example shown here that it is possible to incorporate an additional biomarker (antibodies against *L. interrogans* serovar Pomona). Other candidate data sources to include would be variables such as individual age, sex, or body condition. For example, we tested whether any of these three variables correlated with the antibody level of the first positive sample of recently infected individuals (see Appendix C). None of the correlations were significant, but if they were then that correlation could be included in the model as prior information for peak antibody level. The strength of the combined use of different sources of information can be seen for the estimation of the time of infection in multimammate mice infected with an arenavirus, where the incorporation of antibody level, virus RNA presence, individual age and encounter probability resulted in large increases in model performance (Borremans et al., 2016).

Once a model to estimate infection time (or peak antibody time) has been constructed using an informative dataset of individuals, it can be applied to new/future data. These data can be of lower resolution and sparser, and can even consist of a single result per individual. This enables the application of these back-calculation methods to cross-sectional data. A further advantage of the Bayesian approach is that it is trivial to improve the model when new informative data become available, as the same model can be fitted using the expanded dataset (Bolker, 2008).

Quantitative serology is a growing field with incredible potential (Gilbert et al., 2013; Held et al., 2019; Pepin et al., 2017; Teunis et al., 2012; Wilber et al., 2020), but its broad adoption has been relatively limited. While this may partly be due to a lack of exposure, it is likely that a number of outstanding challenges are keeping scientists from applying these methods. One of these challenges, especially for wildlife systems with sparse sampling, is the difficulty in constructing biomarker models when there are no experimental data and when infection times are unknown. As most biomarker models are specific to a host-pathogen system,

they need to be constructed for each system before they can be used to estimate time of infection. Here, we have provided a complete approach to constructing biomarker models when data are sparse and infection times unknown, using a hierarchical Bayesian framework that enables leveraging multiple sources of information and multiple types of data (Figure 5.3.2.1). This addresses a major challenge in quantitative serology and time-of-infection estimation that has been one of the key barriers for application to wildlife systems. Other remaining challenges include incidence reconstruction with proper error propagation, anamnestic immune response following re-exposure (boosting), dealing with antibody cross-reactivity, integration of infection time estimation and transmission modeling, and software development for easy integration of data sources and incidence reconstruction.

### 6.3.2.3. Risk factors for infection

#### Univariate models

Clear patterns arose within each category in the univariate analysis (Figure 6.3.2.9, Table 6.3.2.4). Twelve- and twenty-four-month cumulative precipitation appear to increase the risk of infection by 6% and 12%, respectively, with every increase in one standard deviation (4.53 and 5.67 inches, respectively). One-month precipitation and monthly average temperature and relative humidity showed weak trends but were not significant predictors of risk.

Covariate description	Mean	SD	HR*	95% Interval
<b>Individual level</b>				
Sex (Male)	n=647 (52.8%)		1.04	(1.00, 1.10)
<b>Abiotic environmental</b>				
1-month cumulative precipitation (precip1)	0.90	1.46	1.03	(0.93, 1.13)
12-month cumulative precipitation (precip12)	10.70	4.53	1.06	(1.01, 1.11)
24-month cumulative precipitation (precip24)	20.64	5.67	1.12	(1.07, 1.17)
Monthly average temperature	56.68	4.78	0.98	(0.89, 1.06)
Monthly average relative humidity	73.11	11.95	0.97	(0.92, 1.04)
<b>Biotic environmental</b>				
Fox abundance	812.56	763.40	0.93	(0.91, 0.96)
Skunk abundance	16.69	14.68	1.11	(1.06, 1.15)
Pup seroprevalence	0.15	0.16	1.28	(1.21, 1.34)

**Table 6.3.2.4. Potential factors affecting *Leptospira* infection risk in 1226 foxes between 2004 and 2019.** Descriptive statistics are given for the unscaled covariates. Hazard ratios and the center 95% intervals are shown for the set of univariable models. \*HR = Median hazard ratio.

All biotic environmental variables had significant relationships with the risk of infection in univariate analyses. Fox abundance decreases the risk of infection as the population increases, whereas skunk abundance has the opposite effect. However, these two covariates are strongly negatively correlated, and there are major biases in the skunk abundance data, so the fox

abundance was maintained for further analyses. Pup seroprevalence had the largest effect size of any covariate. For a 16% increase in pup seroprevalence, the individual risk of infection increases by 28%.

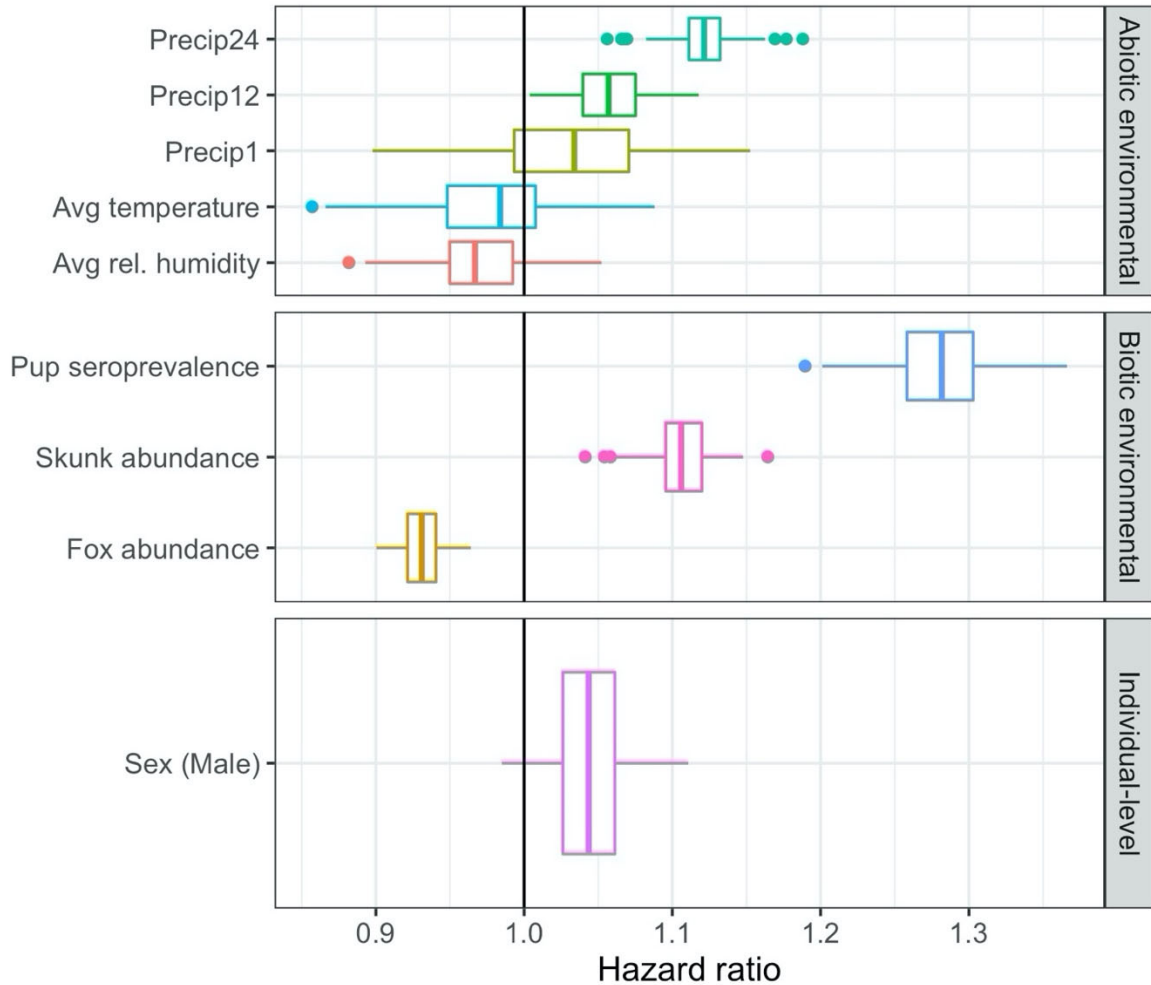


**Figure 6.3.2.9. Distribution of hazard ratios estimated by univariate Cox proportional hazards model with imputed time of infection estimates.**

### *Multivariate model*

Across the three categories of covariates, we wanted to capture the trends in environmental covariates while controlling for individual-level differences. Thus, our multivariable model included sex, fox abundance, and 24-month cumulative precipitation (precip24). We also tested the inclusion of monthly average temperature and relative humidity, but neither covariate added significant contributions to the model fit (Table 6.3.2.5).

<b>Model</b>	<b>Median AIC</b>
Sex	8202.138
Sex + Fox abundance	8199.406
Sex + Fox abundance + Precip24	8188.088
Sex + Fox abundance + Precip24 + Mean temperature	8186.117
Sex + Fox abundance + Precip24 + Mean rel. humidity	8185.707
Sex + Fox abundance + Precip24 + Pup seroprevalence	8177.671

**Table 6.3.2.5. Median Akaike information criterion (AIC) for multivariate Cox proportional hazards models across 100 bootstrap runs.** Lower AIC values indicate models that achieve superior balance of parsimony and goodness of fit, with AIC differences of 10 or more providing a strong basis for model selection.

In the multivariate model, we detected enhanced effects of those observed in the univariate models (Figure 6.3.2.10). After controlling for individual level variation, 24-month cumulative precipitation exhibited a stronger effect of increasing infection risk (median HR = 1.15) and fox abundance exhibited a stronger protective effect (median HR = 0.90). These effects are qualitatively robust but diminished in magnitude when pup seroprevalence is included in the model (Table 6.3.2.6). Pup seroprevalence has a median hazard ratio of 1.21 after controlling for sex, precipitation, and fox abundance, which means that the risk increases by 21% with every one standard deviation increase in pup seroprevalence.

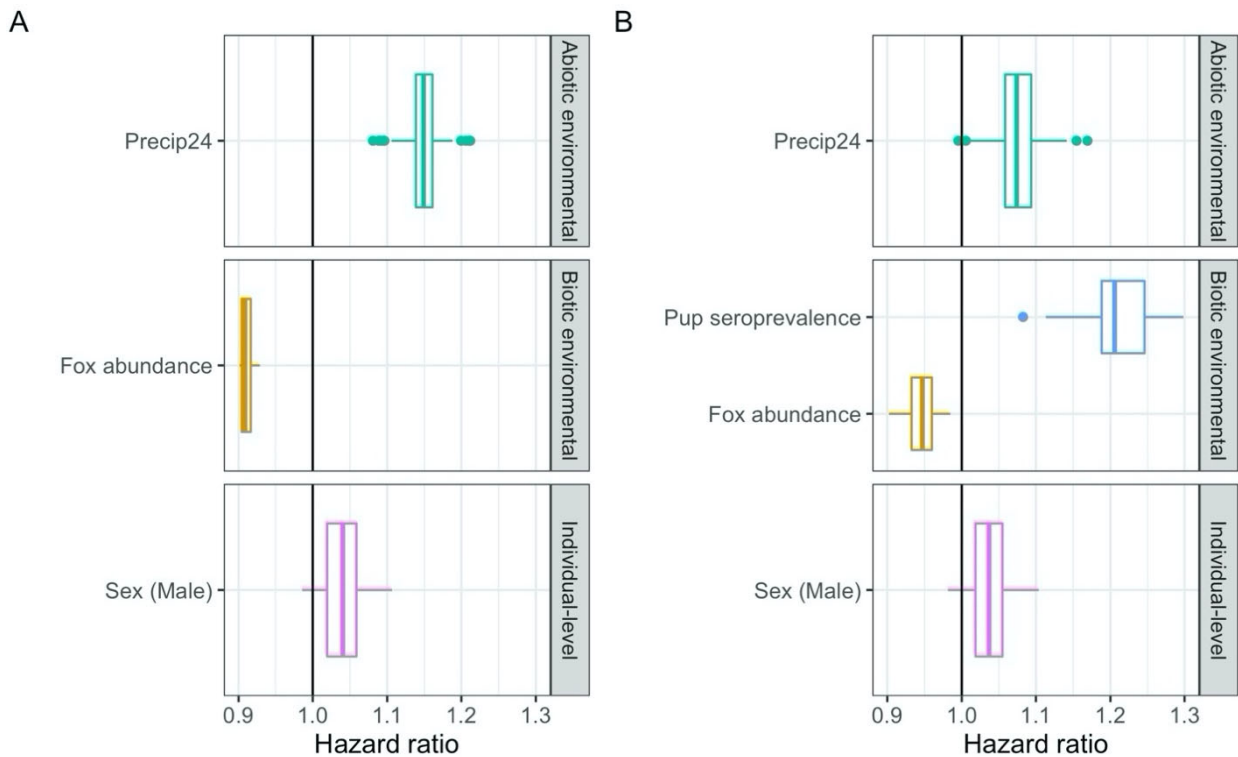


**Figure 6.3.2.10. Distribution of hazard ratios estimated by multivariable Cox proportional hazards model with imputed time of infection estimates.** Panel A shows the final multivariable model, which includes sex, yearly fox abundance, and 24-month cumulative precipitation. Panel B shows the same model with the inclusion of yearly pup seroprevalence.

	Without pup SP		With pup SP	
	HR*	95% Interval	HR*	95% Interval
<b>Individual level</b>				
Sex (Male)	1.04	(1.00, 1.09)	1.04	(0.99, 1.09)
<b>Abiotic environmental</b>				
24-month cumulative precipitation (precip24)	1.15	(1.09, 1.20)	1.07	(1.01, 1.14)
<b>Biotic environmental</b>				
Fox abundance	0.90	(0.87, 0.93)	0.95	(0.90, 0.98)
Pup seroprevalence			1.21	(1.12, 1.30)

**Table 6.3.2.6. Estimates of median hazard ratios of multivariable Cox proportional hazards model with imputed times of seroconversion.** \*HR = Median hazard ratio.

### *Time-to-seroconversion curves*

We compared median time-to-seroconversion (the time corresponding to a 0.5 probability of seroconverting) for males and females at varying levels of fox abundance and 24-month cumulative precipitation. The low, medium, and high levels of fox abundance and 24-month cumulative precipitation were defined by the 10th, 50th, and 90th percentiles of each covariate. Regardless of stratification level, most median time-to-seroconversion estimates are greater than one year (Figure 6.3.2.11). Females have 2- to 4-week longer times than those of males across all levels of abundance and rainfall. The shortest median times (males: 345 days; females: 360 days) occur when foxes are at low abundance with high precipitation.

We also compared the model's predictions for the probability of infection during the different periods of time at risk on the island, under different conditions. After the first year at-risk, male foxes have, at most, a 53% chance of seroconverting (Table 6.3.2.8). If the first year of life occurred during less ideal conditions for infection (i.e. high fox abundance and low cumulative precipitation), the probability of seroconverting could be as low as 32%. After 2 years at-risk, the probability of seroconverting is greater than 58% under all abundance and precipitation conditions for both sexes.

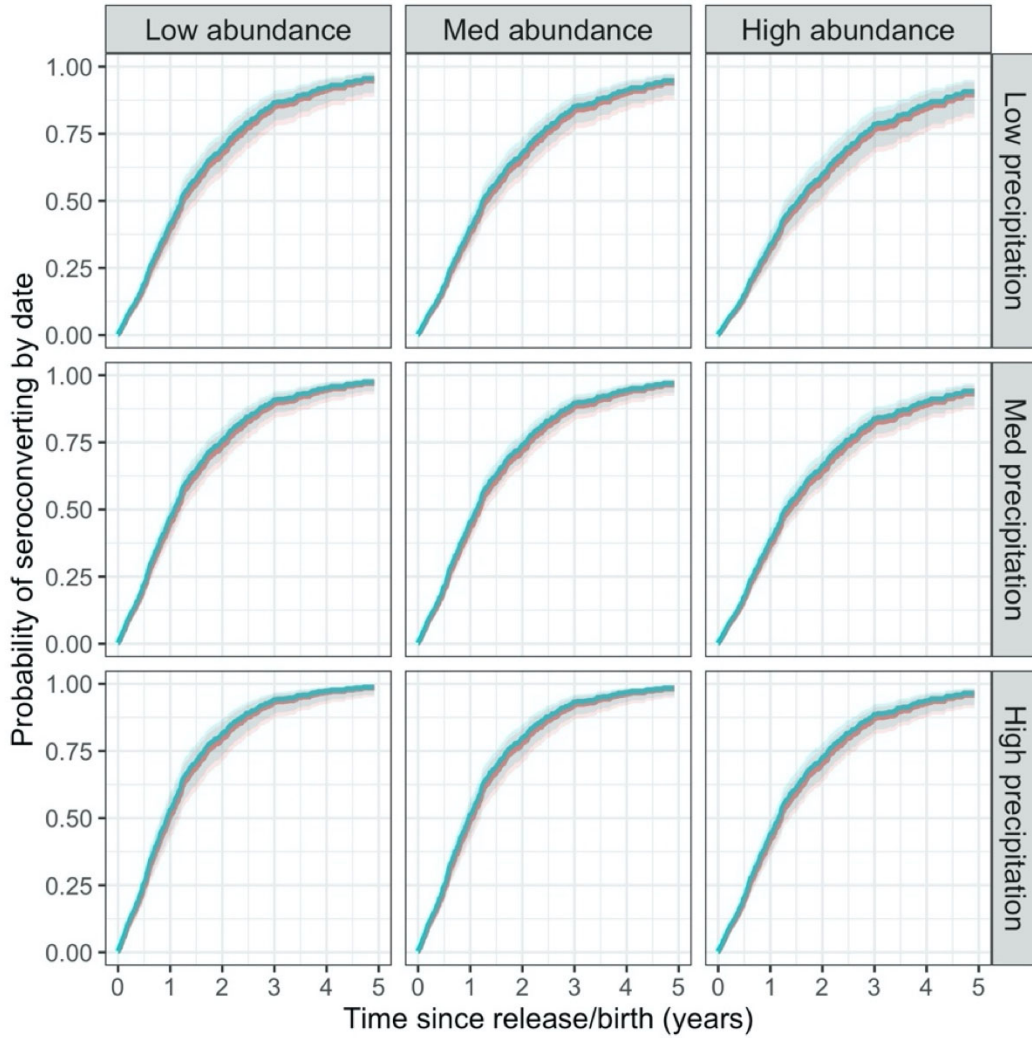


**Figure 6.3.2.11. Time-to-infection curves for low, medium, and high levels of fox abundance and 24-month cumulative precipitation when stratified by sex.** Low, medium, and high levels of abundance and precipitation are defined by the 10<sup>th</sup>, 50<sup>th</sup>, and 90<sup>th</sup> percentiles of each covariate. Within each subplot, the curves are stratified by sex (males = blue; females = coral).

	<b>Low abundance</b>	<b>Medium abundance</b>	<b>High abundance</b>	
<b>Female</b>	458	477	595	<b>Low precipitation</b>
<b>Male</b>	444	456	568	
<b>Female</b>	416	430	501	<b>Medium precipitation</b>
<b>Male</b>	398	415	471	
<b>Female</b>	360	379	442	<b>High precipitation</b>
<b>Male</b>	345	359	425	

**Table 6.3.2.7. Median survival times (days) given sex, 24-month cumulative precipitation, and fox abundance.** The median survival time is the time corresponding to a 50% probability of seroconverting.

		Low abundance	Medium abundance	High abundance	
1-year	Female	0.40	0.38	0.32	Low precipitation
2-year		0.67	0.66	0.58	
1-year	Male	0.41	0.40	0.34	
2-year		0.70	0.68	0.60	
1-year	Female	0.45	0.43	0.37	Medium precipitation
2-year		0.74	0.72	0.64	
1-year	Male	0.47	0.45	0.38	
2-year		0.76	0.74	0.66	
1-year	Female	0.51	0.49	0.42	High precipitation
2-year		0.80	0.78	0.70	
1-year	Male	0.53	0.51	0.44	
2-year		0.81	0.80	0.72	

**Table 6.3.2.8. Probability of seroconverting when stratified by sex, fox abundance, and 24-month precipitation after 1 and 2 years at risk.**

*Implications for risk analysis*

We have applied a Cox proportional hazards model to evaluate factors that influence the hazard rate of infection with *Leptospira* for island foxes on SRI. We found that greater precipitation over the preceding 24-month period increases the risk of exposure, while monthly precipitation, temperature, and relative humidity had little effect. This indicates that multi-annual trends in precipitation and, notably, the previous two rainy seasons are more important in driving exposure risks than current climate conditions. Thus, under a changing climate, the long-term effects on the island’s water table will be more important in driving new infections than short-term fluctuations. We postulate that this effect may be governed by changes in the distribution of standing water on the island, but further research is needed.

Additionally, and somewhat counter-intuitively, we found that greater fox abundance has a protective effect against *Leptospira* exposure. Throughout the study period, fox abundance is steadily increasing, and thus this effect could be confounded with other temporal trends. In particular, we were concerned about confounding with the high risk from the initial large outbreak wave in 2006-8, compared to the lower risk as the pathogen transitioned to endemic circulation on the island. However, the effect remained in the model when pup seroprevalence was added as a proxy for overall prevalence of active infections on the island. Instead, we believe that this negative density dependence of risk may arise from the stabilization of island fox social structure as the reintroduced population became established on the island. As the population grew, foxes were less likely to move outside their home ranges and disperse across the island (Figure 6.3.4.3). This reduced overall mixing in the fox population, despite the larger population, which decreased risk of new infections.

The shortest median times-to-seroconversion occurred at low fox abundance and high 24-month cumulative precipitation. These conditions were met during the early phase of fox reintroduction in 2005 and 2006. In the winter months of 2005, the water table was at a peak with more than 30 inches of cumulative precipitation in the previous two years (more than 1.5

standard deviations above the average 24-month cumulative precipitation) while there were fewer than 40 foxes on the island. These combined conditions were highly conducive to *Leptospira* transmission according to our model and may have driven the initial outbreak of *Leptospira* in the population.

As expected, including a measure of the level of infection on the island through pup seroprevalence significantly improved model fit and moderated the effects of fox abundance and 24-month cumulative seroprevalence. It follows that having more disease present on the island would increase the risk of seroconverting and decrease the time required to seroconvert. However, in most systems and on other islands, this information would be unavailable at the beginning of an outbreak and would require intense monitoring to have accurate estimates throughout the study period. Thus, we excluded it in our primary multivariable model to evaluate what conditions would be ideal when disease-related information were unavailable.

In conclusion, we found strong effects of fox abundance and 24-month cumulative precipitation on the risk of seroconverting. We believe that the precipitation effect reflects the transmission ecology of *Leptospira* in the Channel Island habitat, while the fox abundance effect is likely a proxy for stability of fox social structure and frequency of large movements across the island. Thus, if *Leptospira* were introduced on other islands, the risk of transmission would be greatest after a multi-year rainy period with a destabilized population.

#### ***6.3.2.4. Analysis of host species effects and laboratory effects on serological reactivity profiles***

##### *Highest MAT titer does not reliably indicate the infecting serovar*

All host species exhibited strong antibody cross-reactivity against the five *Leptospira* serovars included in the MAT panel. The serovar against which the highest antibody titer was mounted differed amongst the three host species, despite sharing the same infecting strain (Figure 6.3.2.12). The highest antibody titer detected in the majority of California sea lion (89.9%) and spotted skunk (100%) samples was against serovar Pomona, but the highest antibody titer detected in island fox samples was most often against serovar Autumnalis (69.5%). This vividly illustrates that the serovar against which the highest titer is detected should not be assumed to be the infecting serovar, as is still done in many studies and reports.

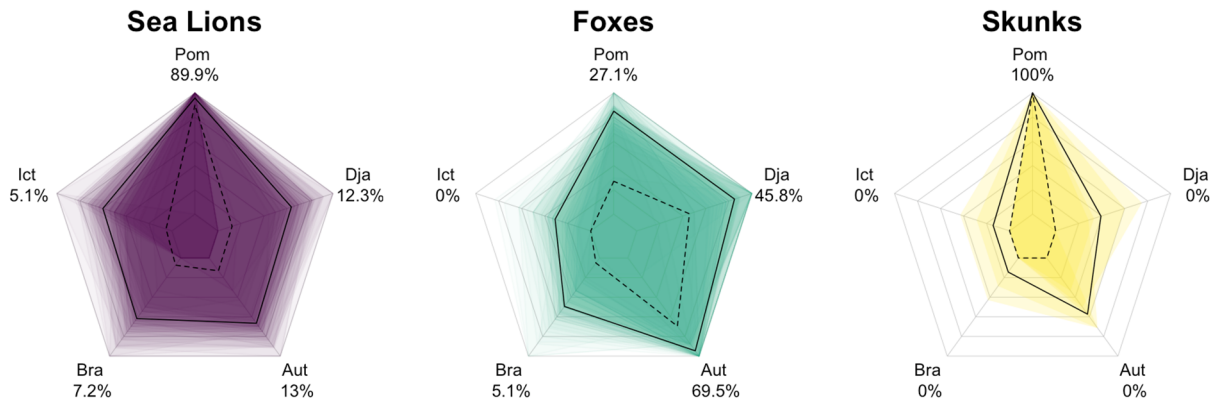


**Figure 6.3.2.12. Host-specific patterns of relative MAT antibody titers detected against five *Leptospira* serovars when the infecting serovar is *L. interrogans* serovar Pomona.** Each plot shows the relative antibody titer levels (antibody titer against one serovar divided by the highest antibody titer detected against any serovar in the 5-serovar MAT panel run for that sample) for California sea lions (left; purple; n=56), Channel Island foxes (middle; cyan; n=56), and spotted skunks (right; yellow; n=4). The shaded regions on each plot are a representative subsample of overlaid polygons linking the values for an individual sample. The continuous black line shows the standardized antibody titer level for each sample (sample titer/maximum sample titer) averaged across all samples for each serovar for that species. The dashed black lines and the percentages associated with each serovar indicate the proportion of samples for which that serovar has the highest titer out of all serovars in that individual's panel, regardless of the actual titer. The numbers add up to more than 100% since multiple serovars can have the highest titer for any given sample (e.g. the highest antibody titer detected in the 5-serovar panel for that individual is both Pomona and Icterohemorrhagiae, with titers of 1:6400).

*Absolute magnitudes of MAT titers vary among host species*

We detected a clear difference in the absolute magnitude of anti-*Leptospira* antibody titers across the three host species (Figure 6.3.2.13). Across four of the five serovars, sea lions exhibit consistently higher antibody titers relative to foxes and skunks. The exception was serovar Autumnalis, against which similar antibody titer magnitudes were detected in sea lions and foxes (Figure 6.3.2.13, inset). Meanwhile, antibody titers detected in skunks were consistently lower than those in the other host species. This indicates that the common practice of using particular MAT titer levels as indications of current or recent infection must be undertaken with care and in light of species-specific data. If such inferences are desired, it is essential to develop datasets and models for each species, as we have done for island foxes (section 6.3.2.3).

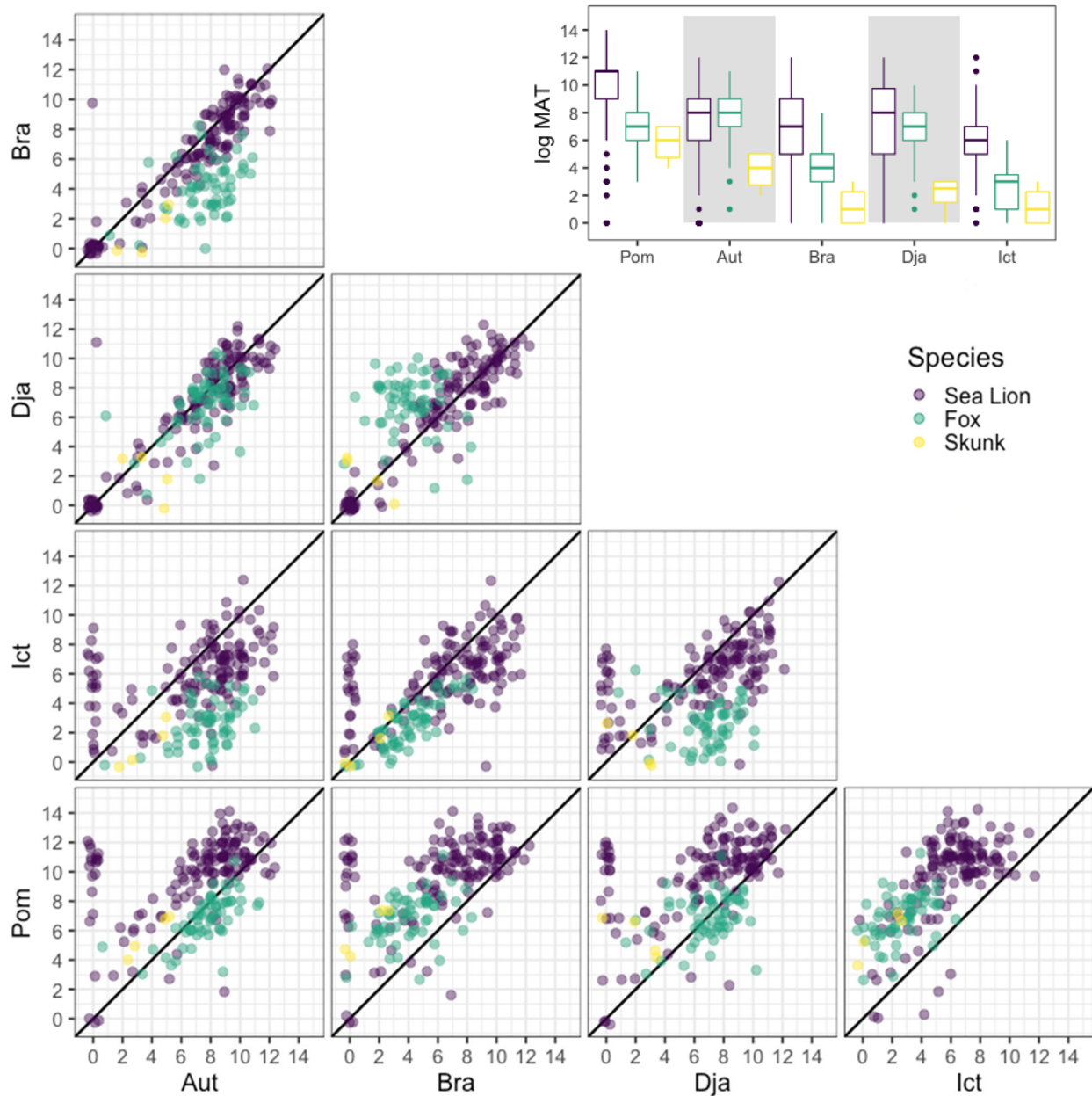


**Figure 6.3.2.13. Pairwise antibody titer levels against *Leptospira interrogans* serovars Pomona, Djasiman, Autumnalis, Bratislava, and Icterohaemorrhagiae in three host species.** Each plot shows the pairwise endpoint MAT results on a log-scale for California sea lions (purple), Channel Island foxes (teal), and spotted skunks (yellow), all presumed to be infected with the same strain of serovar Pomona. The colors aggregate in a distinct pattern, showing that the serovar reactivity pattern is affected by the host species and that absolute titer magnitude differs among species. The black diagonal line corresponds to perfect equivalence between different serovars. Jitter has been added to the points to aid visualization. Inset: differences among host species in magnitude of MAT titer against each serovar.

Individual-level longitudinal fox data spanning 2009-2019 allowed us to examine titer dynamics and changes in the cross-reactivity profile through the course of infection and recovery. One fox, in particular, illustrates a course of infection during which the titer against the infecting serovar (Pomona) declined to zero through time while the titer against the non-infecting serovar (Autumnalis) remained positive and consistently higher than that against Pomona (Figure 6.3.2.14). Although this is the clearest case study in our dataset, other individuals have similar courses of infection where their highest titer is against a non-infecting serovar (Figure A.13)

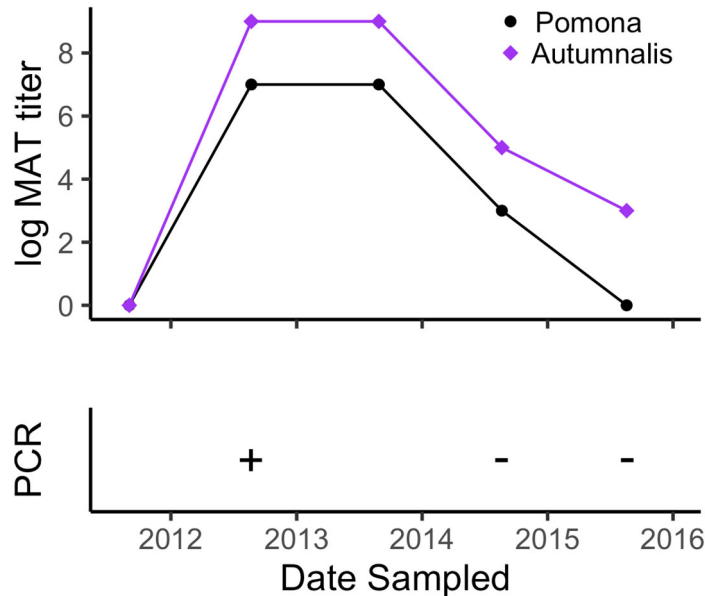


**Figure 6.3.2.14. Selected example of longitudinal antibody titer dynamics in a Channel Island fox.** The top panel shows antibody titers against *L. interrogans* serovars Pomona and Autumnalis from longitudinally collected serum samples from one fox. The bottom panel indicates the PCR test result from urine samples taken at the same time as serum collection.

These longitudinal data highlight a number of challenges. This individual was infected with serovar Pomona, but at every sampling event its MAT titer against serovar Autumnalis was higher than that for serovar Pomona. At the final sampling event, the individual no longer exhibited a positive MAT result against serovar Pomona, but was still seropositive for serovar Autumnalis. If the individual had been sampled only once, at this point in time, the natural interpretation would be that it had been exposed to serovar Autumnalis, not serovar Pomona as was actually the case.

*Both absolute and relative titer magnitudes can vary among certified laboratories*

Analysis of 46 fox serum samples at three different labs showed that both absolute and relative serovar Pomona and Autumnalis titer levels varied systematically across labs (Figure 6.3.2.15). When comparing absolute antibody titer magnitude against serovar Pomona, the median titer was lowest from Lab A and highest from Lab C (Figure 6.3.2.15B) with titers detected against serovar Pomona roughly one dilution greater at Lab B than Lab A, and more than three dilutions greater at Lab C than Lab A (Figure 6.3.2.15B). Endpoint titers against

serovar Autumnalis were not run for all samples at all three labs, so comparisons were not possible at log<sub>2</sub> titer levels greater than 7. When assessing relative titer magnitude between labs, we found that at Lab A, antibody titers against serovar Autumnalis were generally higher than those against serovar Pomona (Figure 6.3.2.13), whereas at Labs B and C, antibody titers detected against serovar Autumnalis were generally equal to (Lab B) or less than (Lab C) those against serovar Pomona (Figure 6.3.2.15A, Figure A.14).

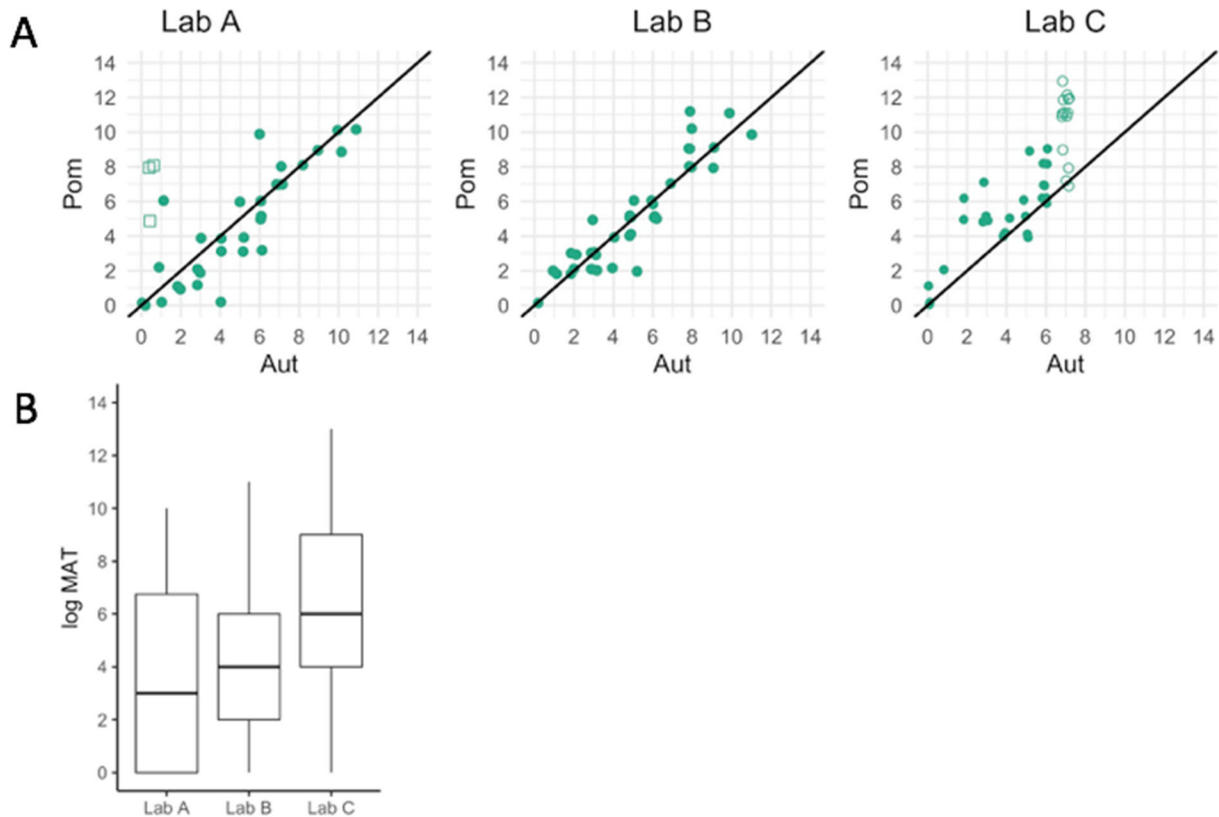


**Figure 6.3.2.15. Comparison of antibody titer results for fox serum samples evaluated at three testing labs.** Island fox serum samples (n=46) were tested in three different certified testing laboratories. The MAT antibody titers for serovars Pomona and Autumnalis are shown. All Pomona titers were run to endpoint dilution. In Panel A, open circles indicate non-endpoint Autumnalis titers at 1:6400 (log MAT titer 7) whereas open squares denote samples that were positive against serovar Autumnalis at 1:100, but no dilutions were performed. Jitter has been added to the points to aid visualization. Panel B represents the difference in antibody titer magnitude for a subset (n=32) of samples that were run to endpoint for serovars Autumnalis and Pomona at all three labs.

#### *Implications for Leptospira ecology and epidemiology*

Through the comparison of antibody results from a 5-serovar MAT panel used to test sera from three host species at three different testing laboratories, we find that host factors influence MAT antibody cross-reactivity patterns, despite infection with the same causative agent. We also show that the highest detected antibody titer is not necessarily against the infecting serovar, and that the relative and absolute antibody titer magnitudes detected against different serovars can vary by diagnostic lab. MAT titers and cross-reactivity patterns are frequently used to infer *Leptospira* epidemiology, with some studies proposing without further evidence that the

infecting serovar is that against which the highest MAT antibody titer is detected (Bharadwaj et al., 2002; Bishara et al., 2002; Panaphut et al., 2002; Santos et al., 2016; Sehgal et al., 1995; Tunbridge et al., 2002), and interpreting high MAT antibody titers against multiple serovars as proof of multiple circulating strains (Pedersen et al., 2015).

Our results highlight the fact that such interpretations can lead to inaccurate conclusions regarding the epidemiology of *Leptospira* transmission dynamics within and between host species. Our findings in sections 6.1.1 and 6.3.2.3 indicate that serologic data can be used to gain robust, high-resolution insights into *Leptospira* dynamics, and indeed that cross-reactivity patterns include additional information that can advance this goal. However, it is essential to account for host species effects, which requires development of suitable data resources and models.

### **6.3.3. Impacts of *Leptospira* on the demography of island foxes**

#### ***Early mortalities associated with leptospirosis***

In the initial years of the reintroduction program, many of the released foxes died shortly after their reintroduction. While biological sampling and testing of the released foxes was limited, these high-resolution data give valuable insight into the early demographic impact of leptospirosis in the island fox population. Table 6.3.3.1 lists the fates of the foxes released from captivity between 2003 and 2006, showing that many foxes died or went missing soon after reintroduction. Here we briefly describe key findings:

- Of the 12 foxes released in 2003, 5 were returned to captivity within 1-3 months due to rapid weight loss post release, two other foxes died of predation and trauma, and three went missing in 2005 or 2006.
- Of the 13 foxes released in 2004, 6 died of predation and another 2 went missing within 1 year of their release.
- Of the 14 foxes released in 2005, 2 died of predation, 1 died of unknown causes, and 2 others went missing within 1-3 months of their release. Six more foxes died within 1 year of being released, and two of these foxes, with deaths occurring in March and September of 2006, had kidney samples available for testing, and are the earliest confirmed cases of *Leptospira* infection in post-release foxes on Santa Rosa Island.
- Of the 8 captive-born foxes released in 2006, five died rapidly following release, but, notably, unlike in prior year release cohorts, none were predation related. One fox died due to trauma, while the other 4 were listed as unknown. Two of these five foxes, which died 28 and 49 days post-release, had kidney samples available for testing, and both were positive for *Leptospira*.

This close examination of the fates of the earliest released foxes suggests that *Leptospira* was having a significant impact on the foxes by 2006, and that the cause of death in early released foxes shifted from mainly predation mortalities to mainly unknown-cause mortalities. Where banked samples existed to allow testing, several of these early unknown-cause deaths were confirmed to be *Leptospira*-positive, including one individual that died in March 2006.

Year	# Released	Fate post Release
2003	12	5 Returned to captivity within 1-3 months
		<i>1 Died 39 days post release, predation</i>
		<i>1 Died 382 days post release, trauma</i>
		<i>2 foxes went missing in 2005</i>
		<i>1 fox went missing in 2006</i>
		2 had their first post release MAT test in 2006 and were positive
2004	13	5 died within 1-3 months - all predation
		<i>1 went missing within 1-3 months</i>
		<i>1 died within 1 year, predation</i>
		<i>1 went missing within 1 year</i>
		<i>2 died within 2 years (1 of which was tested MAT just prior to death and was positive)</i>
		<i>1 went missing within 2 years and tested positive prior to going missing</i>
		2 went missing in 2009 and 2010 both tested negative multiple times
2005	14	3 died within 1-3 months (2 predation, 1 unknown)
		<i>2 went missing within 1-3 months</i>
		<i>6 died within 1 year (2 tested via PCR and were positive - Earliest known post reintroduction positives).</i>
		<i>1 died in 2010 (tested MAT positive in 2006)</i>
		<i>1 died in 2011 (tested MAT positive in 2006)</i>
		<i>1 died in 2012 (tested MAT negative in 2006 and MAT positive in 2007)</i>
2006	8 captive-born	<b>5 died within 1-3 months (1 trauma, 4 unknown, 2 tested via IHC and were positive)</b>
		<i>1 missing within 2 years (tested MAT positive within 2 months)</i>
		<i>1 died in 2012 (tested MAT positive in 2008)</i>
		<i>1 went missing in 2014 (tested MAT positive in 2007)</i>

**Table 6.3.3.1. Fates of foxes released from captivity between 2003-2006.** This table lists the number of foxes initially released in each year and details the fates of those individuals. Foxes in italics indicated foxes that could have died from leptospirosis. N.B. 6 seropositive founder foxes released in 2006 are not shown, due to presumed antibody protection from *Leptospira* infection.

Survival rate and causes of mortality could be determined from radio-collared foxes (Figure 6.3.3.1, Table 6.3.3.2). This analysis combines the fates of both the released and wild-born foxes, whereas prior work considered only the fates of the released foxes. Kaplan-Meier survival estimates were 69% (95CI, 47%-90%) in 2004 and 71% (95CI, 57%-85%) in 2005, which then dropped to 45% (95CI, 33%-57%) in 2006 before increasing to range between 67%-91% in the 2007-2011 seasons. As shown in Figure 6.3.3.1, many of the mortalities that occurred between 2004-2010 were due to predation, a few were due to trauma, and, for many others, the cause of death was unknown. In 2006, when the survival rate was at its lowest, there was a large

spike in the percentage of mortalities due to unknown causes. This spike in unknown-cause mortalities continued into 2007, while, in all other years between 2004-2010, predation was the primary cause of mortality. Notably, this spike in unknown-cause mortalities coincides with the timing of the initial wave of the *Leptospira* outbreak in SRI foxes (sections 6.1.1 and 6.3.2).

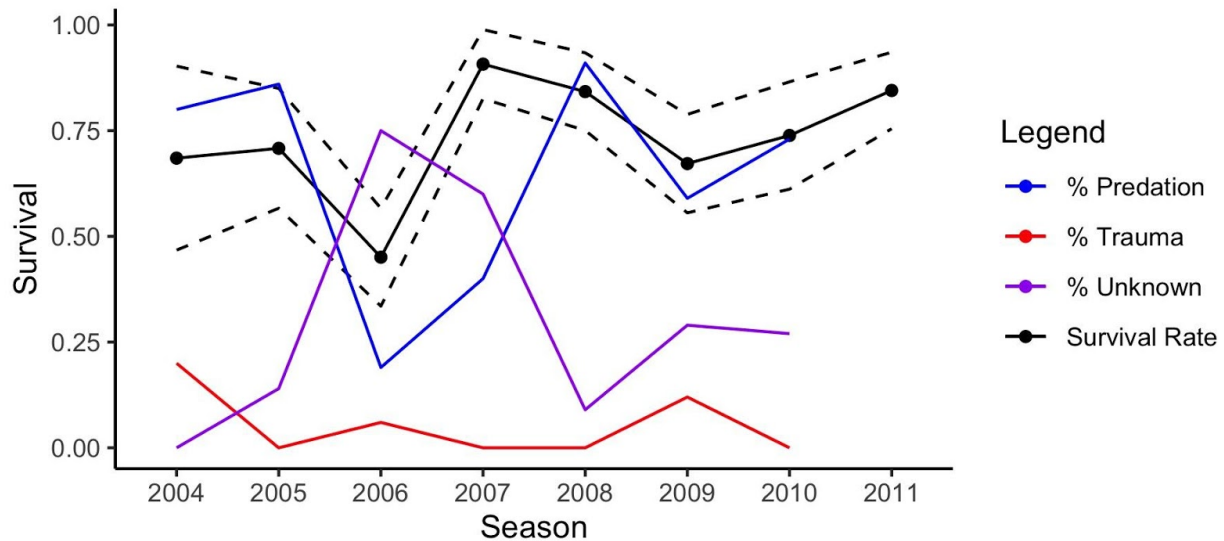


**Figure 6.3.3.1. Survival rate and causes of death of collared foxes by season.** Kaplan-Meier survival estimates with 95% confidence interval in black and percentage of mortalities that were predation (red), trauma (purple) and unknown (blue).

Retrospective testing allowed us to reassess some of these unknown early mortalities. Despite telemetry efforts, many carcasses were not found until they were too decayed for necropsy; therefore, only a small number of the unknown-cause mortalities were necropsied, and even fewer had recoverable kidney tissue to assess possible *Leptospira* infection. Altogether, we were able to test kidney samples from 12 foxes that died between 2004-2010 (Table 6.3.3.1). Ten died of unknown causes, but two died of known causes. Of these, one died in 2004 after being stuck in a pipe, while the other died of predation in 2008; kidneys from both of these foxes tested negative.

Of the ten foxes with available kidney tissue but unknown cause of mortality, 6 were released captive-born foxes (4 from 2006, 1 from 2007 and 1 from 2008) and 4 were foxes born in the wild post-reintroduction (1 from 2007, 1 from 2009 and 2 from 2010). The kidneys were tested via IHC, PCR or both. The foxes that died in the 2008 and 2009 seasons both tested negative via PCR and IHC. All the other foxes, namely those that died in 2006, 2007, and 2010, tested positive via IHC or PCR. Figure 6.3.3.2 shows the detailed individual histories of the 9 tested foxes that were born or released between 2003-2007. Five of the positive individuals were captive-born foxes with multiple negative MAT tests prior to release, and all became infected and died within 1 year of release. Two of these died 28 and 49 days after their releases in October and November 2006.

Focusing on the period when unknown-cause mortalities spiked, of the 6 foxes that died of unknown causes in 2006 and 2007 and were tested for *Leptospira* infection, 100% tested positive. This is direct evidence of the lethal impact *Leptospira* can have on island foxes.

Another 8 foxes died of unknown causes in 2006 but could not be tested; it is plausible that most of these had leptospirosis as well, in which case the disease killed roughly one quarter of the fragile establishing population. Taken together, it is clear that *Leptospira* had a dramatic negative impact on the demography of the SRI foxes during this early period.

Season	Active Collars	Pop Estimate	Morts	Collared Morts	Collars Perm went Missing	Returned to Captivity	Predation Morts	Trauma Morts	Unknown Morts	Unknown Lepto Tested	Unknown Lepto Test Positive
2003	12	12	1	1	0	5	1	0	0	0	NA
2004	23	24	5	5	1	1	4	1	0	0	0
2005	38	41	7	7	5	0	6	0	1	0	NA
2006	55	58	16	16	4	0	3	1	12	4	4
2007	63	64	5	4	1	0	2	0	3	2*	2
2008	92	122	11	9	7	0	10	0	1	1	0
2009	72	313-466	17	15	12	0	10	2	5	1	0
2010	63	233-351	11	11	7	0	8	0	3	2	2

**Table 6.3.3.2. Table of released and wild born radio collared foxes and of all wild fox mortalities.** The table provides the number of active radio collars, the population estimate, the total number of mortalities, the number of mortalities that were radio collared, the number of radio collared foxes that went missing, the number of foxes that were returned to captivity, the number of mortalities that were due to predation, trauma or unknown cause, the number of unknown cause mortalities that were tested for *Leptospira*, and the number of those that tested positive in a given fox year. \*A third fox of unknown mortality cause was tested in 2007 and was negative, however this fox was excluded from this table as it was a founding fox known to have been previously exposed and not therefore likely not susceptible to *Leptospira* infection



### *Preliminary results on demographic impacts - later phase (2009-2020)*

Our analyses of further demographic impacts of *Leptospira* infection are still underway, owing to sample analysis delays triggered by the COVID-19 pandemic and other challenges faced by the responsible team member. Here we summarize results to date, which we will continue refining in the course of on-going dissertation research.

Preliminary analyses of survival impacts, achieved by analyzing grid capture data using multi-state robust design capture-mark-recapture models, have yielded null results indicating no reduction in apparent survival probability associated with *Leptospira* infection. Importantly, these analyses have not yet incorporated spatial movements, so true mortalities are confounded with fox movements away from their original trapping grids. Furthermore, there are potential challenges arising from the rapid progression to death observed in some of the early mortality records. If an uncollared fox gets infected and dies within a few months, we are unlikely to detect its infection using an annual trapping design; the known fates analysis of radio-collared foxes may shed more light on this point. Given the direct evidence of *Leptospira*-associated mortalities of otherwise healthy foxes, and the population-wide decrease in survivorship during the initial outbreak wave (described above), we believe that *Leptospira* infection probably does impact fox survival, but perhaps at too subtle a level to detect using annual trapping.

Preliminary analyses of data on reproductive status indicate a possible impact of recent *Leptospira* infection on reproductive success. We examined records of 222 adult female foxes that were classified as Recent or Prior infections, and could be classified clearly as lactating or not lactating (which indicates whether they had a surviving pup). Females with recent infections had significantly lower probability of exhibiting signs of successful reproduction (0/21 vs 35/166, one-tailed Fisher's exact test,  $p=0.02$ ); this is consistent with known effects of *Leptospira* in some other host species, where it is associated with abortion (Faine et al., 1999). We are working to test this finding using a larger database and using the alternative metric of pups per adult female on each grid.

#### **6.3.4. Transmission dynamics model for *Leptospira* in island foxes on SRI**

The stochastic simulation model for *Leptospira* transmission among SRI foxes was fitted to our observed data, then used to investigate the ecology of the system and assess management strategies. We first describe the results of model fitting, then summarize findings from the model simulations.

##### ***Demographic parameters***

The models with year-specific survival resulted in the best fit to data (Table 6.3.4.1). Based on these results, we used the estimates for year-specific fertility and survival as the demographic parameters of the transmission model (Figure 6.3.4.1), with overall mean fertility  $\hat{F}_t = 1.4$ , mean  $\hat{\phi}_{P,t} = 0.8$  and mean  $\hat{\phi}_{A,t} = 0.8$ .

Model	DIC
$F_t + \phi_{P,t} + \phi_{A,t}$	299.2
$F_t + \phi_P + \phi_A$	317.0
$F_t + \phi_{P,t} + \phi_A$	318.2
$F_t + \phi_P + \phi_{A,t}$	299.4

**Table 6.3.4.1. DIC values for demographic models.** Parameters:  $F$  (fertility),  $\phi_P$  (pup survival),  $\phi_A$  (adult survival). Indexing by  $t$  indicates year-specific values (vs. constant across all years).

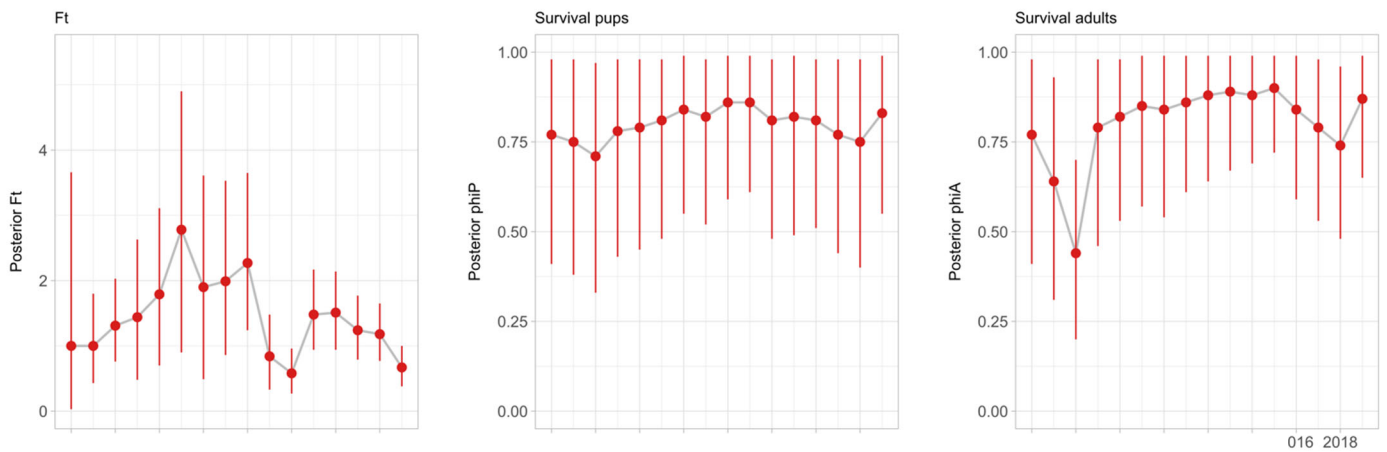


**Figure 6.3.4.1. Posterior estimates (means and 95% credible intervals) of demographic parameters through time.** These parameters include fertility, pup, and adult survival (model  $F_t + \phi_{P,t} + \phi_{A,t}$ )

### *Movement parameters*

The probability of moving differed significantly between seasons (Likelihood ratio chi-squared test of generalized linear models with logit link function and binomial error distribution: Chi-sq = 8.8, df = 3, P = 0.03). Movement exhibited clear seasonality where foxes were more likely to move between functional patches between December and May (Figure 6.3.4.2).

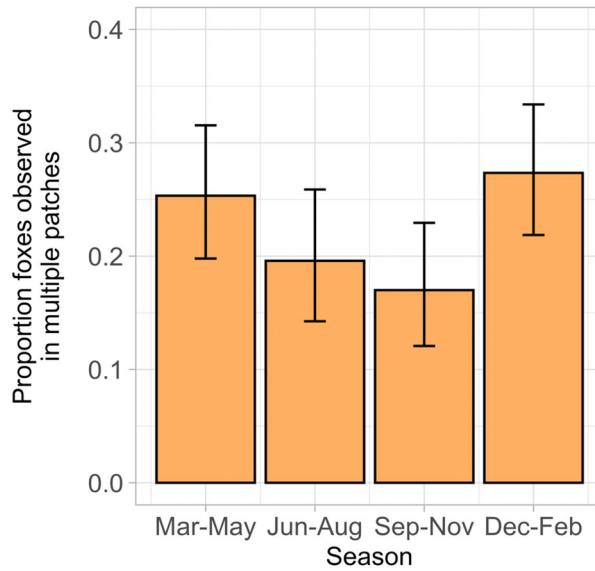


**Figure 6.3.4.2. Movement probability in different seasons.** Proportion of foxes that were observed in multiple patches within the same season, out of foxes that were observed at least twice. Error bars show 95% binomial exact confidence intervals.

Movement distances were relatively small, with most movements being to a neighboring patch (Figure 6.3.4.3). This is consistent with the observations that island foxes tend to remain near their home range, with only periodic dispersal events, and that dispersal distances are short. Comparing movement patterns across different time periods revealed a clear pattern, where movements were more frequent and spanned longer distances during the early years of the reintroduced population (2004-2006 and 2007-2009). The probability of not moving was highest during the most recent period assessed, from 2013-2016. These patterns are consistent with the fact that the reintroduced population was less settled during the early years, potentially facilitating spread of the pathogen.

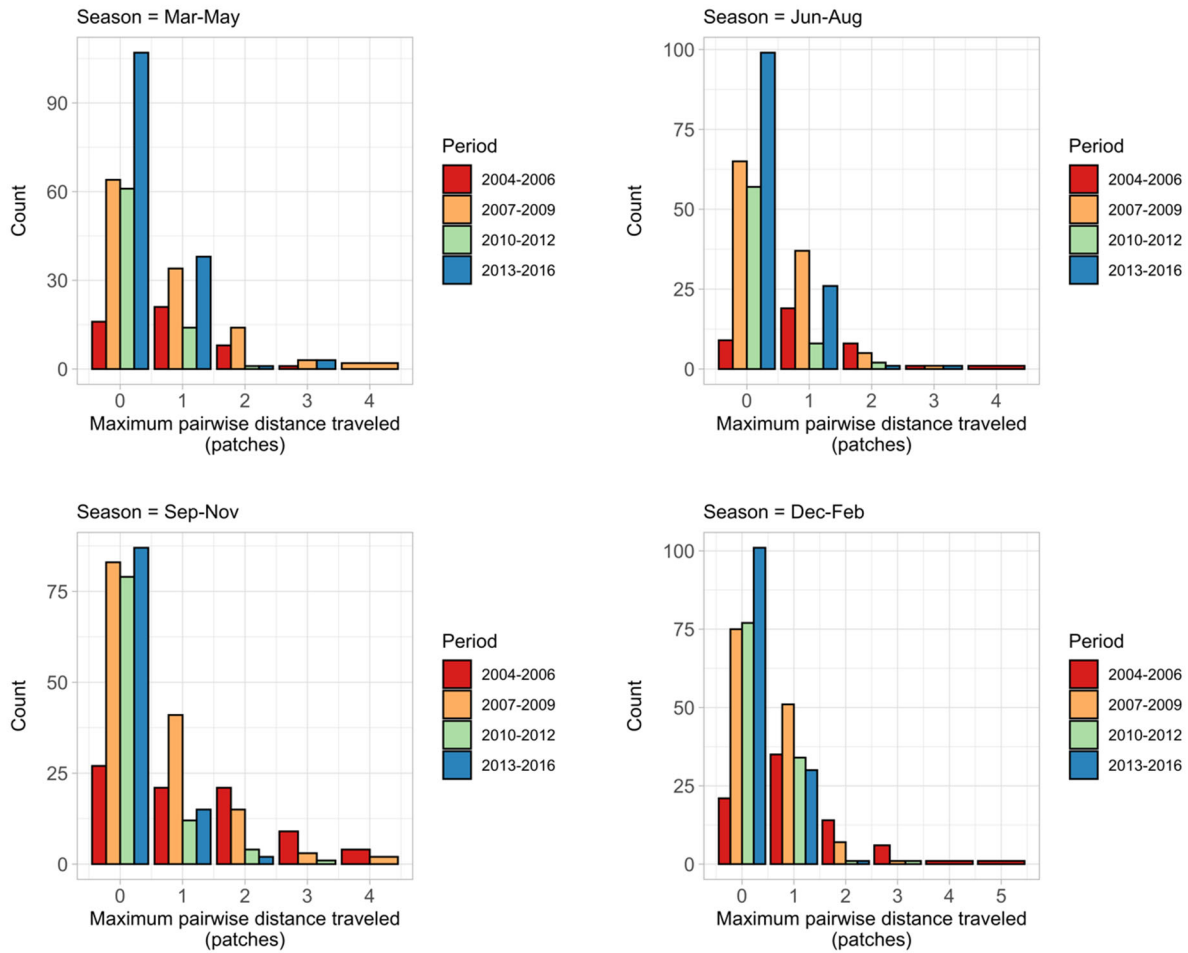


**Figure 6.3.4.3. Movement distance frequency distribution in different seasons, for different time periods.** The maximum pairwise distance observed was 5. Distances of zero patches indicate no movement.

Movement patterns between pairs of patches were highly non-random and asymmetrical, with particular patches much more likely to serve as destinations (Figure 6.3.4.4).

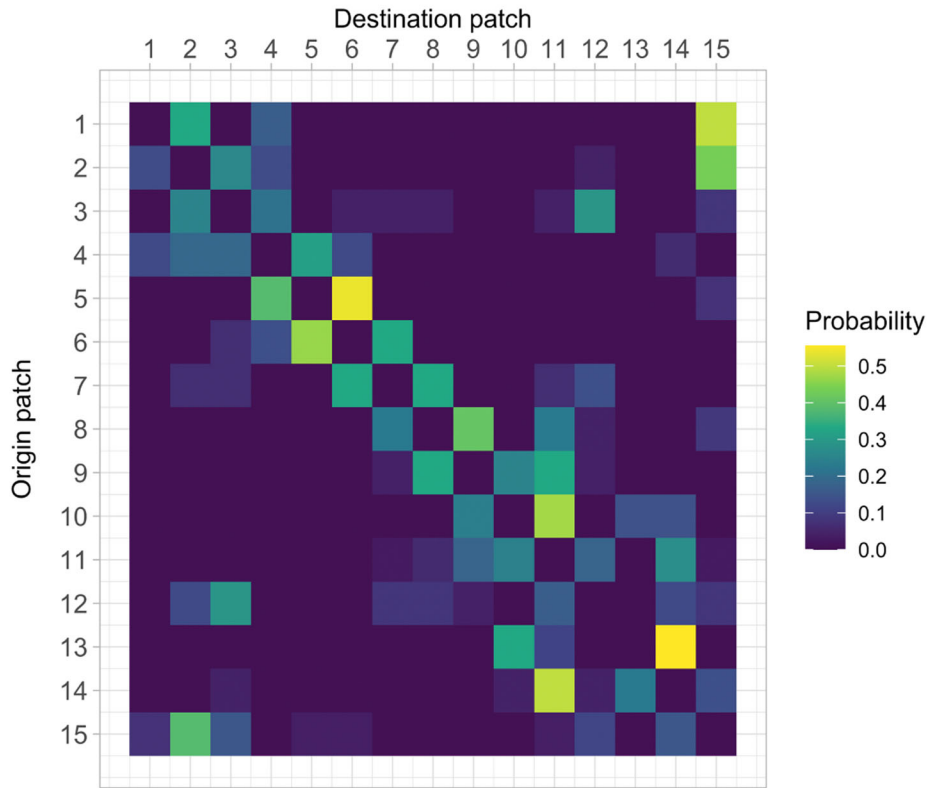


**Figure 6.3.4.4. Pairwise movement probability showing the relative proportion of movements from an origin patch to all other patches.** Each row represents all movements observed from a certain patch to all other patches as proportions, with each row adding up to one.

### *Infection parameters*

We found a marked difference in the distribution of antibody titer levels between PCR-negative and PCR-positive samples (Figure 6.3.4.5). While PCR-negative samples rarely have antibody levels higher than 5, most PCR-positive samples have antibody levels of 6 or higher.

Similarly, we observed a clear difference in the distribution of estimated times of infection, where the time between infection and the sample tended to be much longer for PCR-negative samples than for PCR-positive samples (Figure 6.3.4.6). Given the reasonable assumption that PCR-positive urine is a proxy for infectiousness, we used these patterns to (1) choose infection states and (2) fit the relative simulated proportions of infection states to observed data. Because the number of fox sampling events for which there is a MAT result is much greater than that for which there are PCR results, we fit the model to patterns in MAT data alone, using the following mapping between infection states and titer levels: susceptibles (S: antibody level = 0), infectious (I: antibody level > 5) and recovered (R: antibody level > 0 and ≤ 5). The distribution of infectious periods ( $1/\gamma$ ) was estimated by fitting an exponential distribution ( $e^{-\gamma*t}$ ) to the distribution of estimated time since infection for PCR-positive samples, with fitted  $\gamma = 0.0024$ , resulting in a mean infectious period of  $1/\gamma = 422$  days.

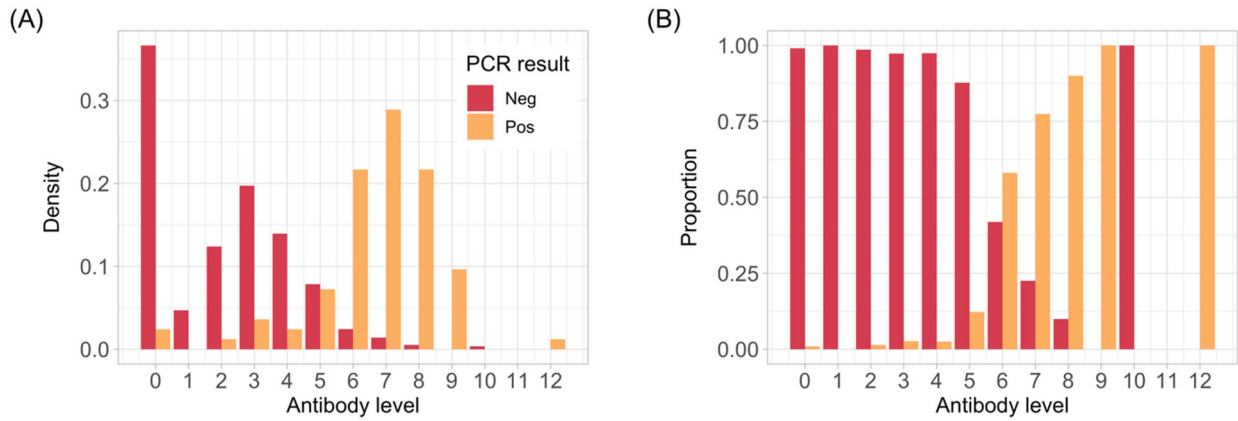


**Figure 6.3.4.5. Antibody titer distributions for island foxes with PCR-negative and PCR-positive samples.** (A) Normalized density distributions. (B) The proportion of PCR-negative and PCR-positive samples for each antibody level. Note that the sample size was 1 for both antibody levels 10 and 12, and 0 for antibody level 11, which gives disproportionate visual weight to a single PCR-negative animal with high titer.

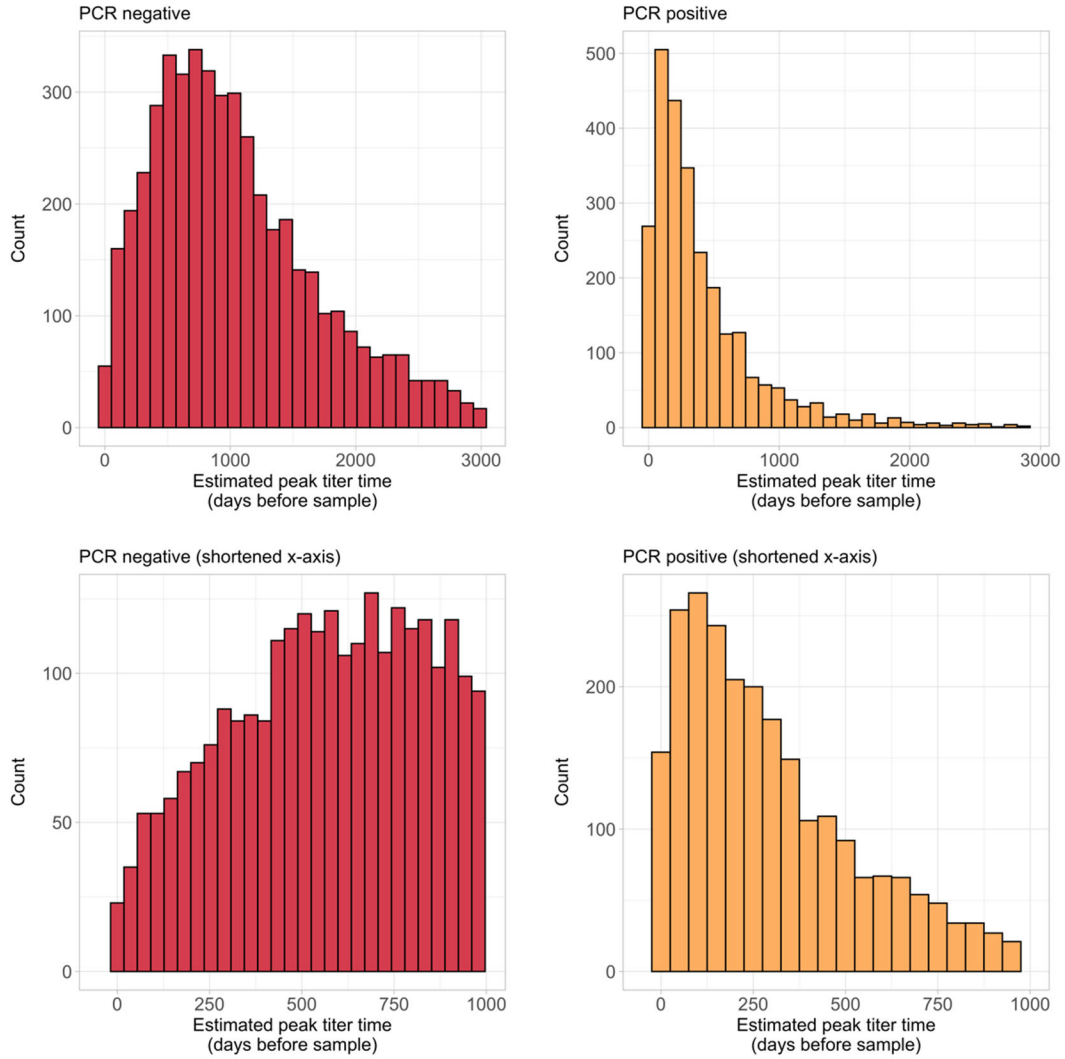


**Figure 6.3.4.6. Distribution of possible times since infection for PCR-negative (left) and PCR-positive (right) samples.**

***Model transmission parameters***

ABC model fitting resulted in the following posterior means (Figure 6.3.4.7) for the different transmission parameters:

$$\beta_i = 0.08$$

$$\beta_{skunk} = 0.004$$

$$q = 0.94$$

$$1/\gamma = 370$$

These parameter estimates were used for all ensuing simulations used for different scenarios, unless otherwise noted.

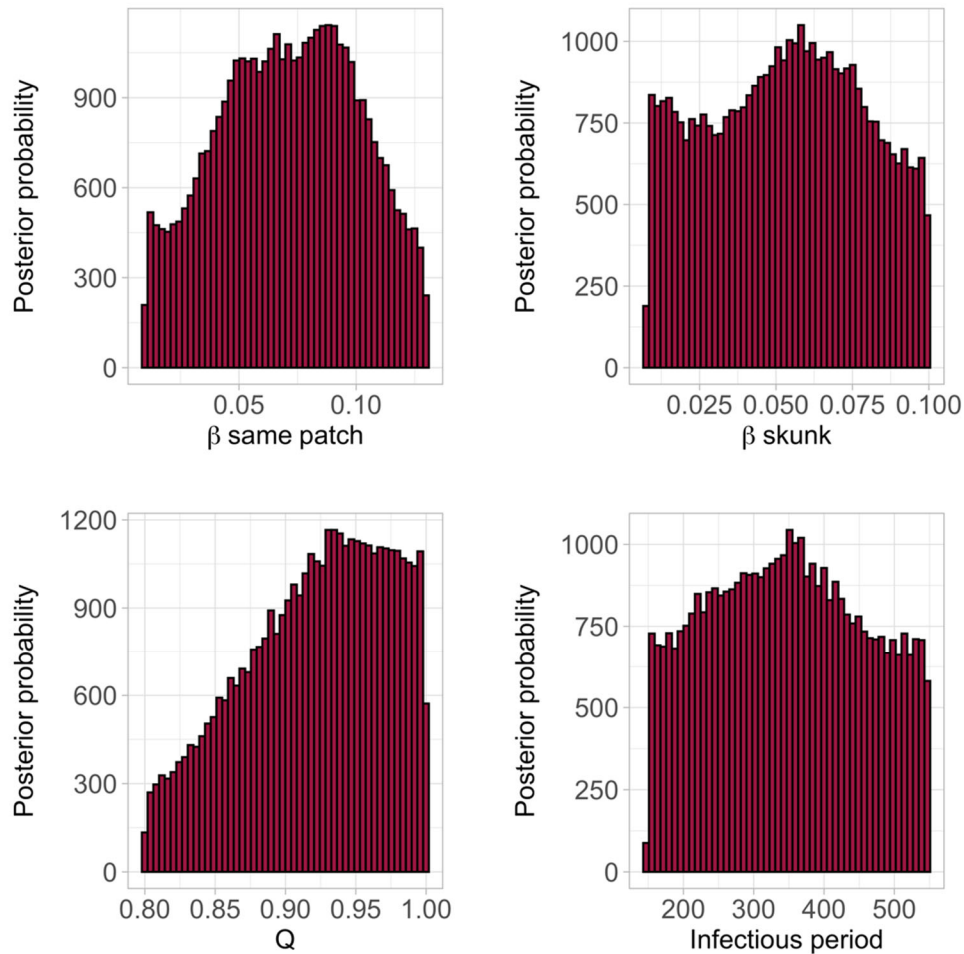


**Figure 6.3.4.7. Posterior estimates for transmission parameters fitted using Approximate Bayesian Computation.**

### *Invasion, persistence, and monitoring*

We used our transmission model for *Leptospira* on SRI to predict the probability of endemic persistence of the pathogen under a range of demographic and environmental conditions. We found that the pathogen persisted in 100% of simulations (out of 500 per scenario) under normal rainfall and average demographic parameters, as well as for scenarios entailing three years of increased or decreased rainfall, or decreased fertility and survival (Table 6.3.4.2). This strong tendency to circulate persistently is an expected consequence of the long infectious periods we have measured, combined with the annual influx of susceptible foxes following the birth season.

We also simulated the probability that *Leptospira* could successfully invade the island, if a single fox gets infected by spillover in an otherwise fully susceptible fox population. Under a

range of demographic and environmental scenarios, the probability of invasion was always greater than 60%, and could be as high as 80% under increased rainfall conditions (Table 6.3.4.2). Successful invasion was more likely when there had been elevated rainfall within the last 2 years, and also more likely when the fox population was smaller. We also investigated the impact of the seasonal timing of pathogen introduction, and we found that invasion success was lowest when an infected fox was introduced in the third quarter (Sep-Nov) and highest in the first quarter (Jan-Mar). Variation in invasion success is likely linked to the seasonal variation in movement patterns, which is lowest in the third quarter and highest in the first and fourth quarters, closely matching the seasonal patterns of invasion success.

Scenario	Persistence (%)
Persistence, normal conditions	100
Persistence, with 3-year drought	100
Persistence, with 3-year increased rainfall	100
Persistence, with 3-year low demographic rates	100
Invasion, with introduction in 1st quarter	75
Invasion, with introduction in 2nd quarter	65
Invasion, with introduction in 3rd quarter	61
Invasion, with introduction in 4th quarter	71
Invasion, half population size	76
Invasion, with 3-year drought	72
Invasion, with 3-year increased rainfall	80

**Table 6.3.4.2. Probabilities of *Leptospira* persistence and invasion under different scenarios.**

Probability of persistence was defined as the proportion of simulations in which at least one infected fox was present at the start of year 10, after initializing the system with 20% of foxes infected and 55% of foxes recovered. Probability of invasion was defined as the proportion of simulations in which at least one infected fox was present at the start of year 10, after initializing the system with 1 infected fox in an otherwise completely susceptible population.

We investigated the efficacy of different fox monitoring strategies by characterizing the time delay before the first detection of an infected fox, for different sample sizes and periodicities of sampling, and for endemic and invasion scenarios. When transmission was endemic, detection was near-certain with a sample size of 5 or more foxes captured during a single month-long sampling session, regardless of the timing of this month (Figure 6.3.4.8). In an invasion scenario when an outbreak is just beginning, the time to detect the presence of the pathogen depends more strongly on the surveillance design. For all periodicities of sampling, the mean time to first detection was greater than a year for sample sizes of 20 foxes or lower (Figure 6.3.4.8). For larger sample sizes, the average detection time could be brought down to 6 months or less under quarterly or semi-annual sampling. Under the annual sampling schemes currently used on the Channel Islands, typical first detection times were 1-2 years after introduction of the pathogen, with an increasing chance of detection in the year of introduction for sample sizes of 40 foxes or more.

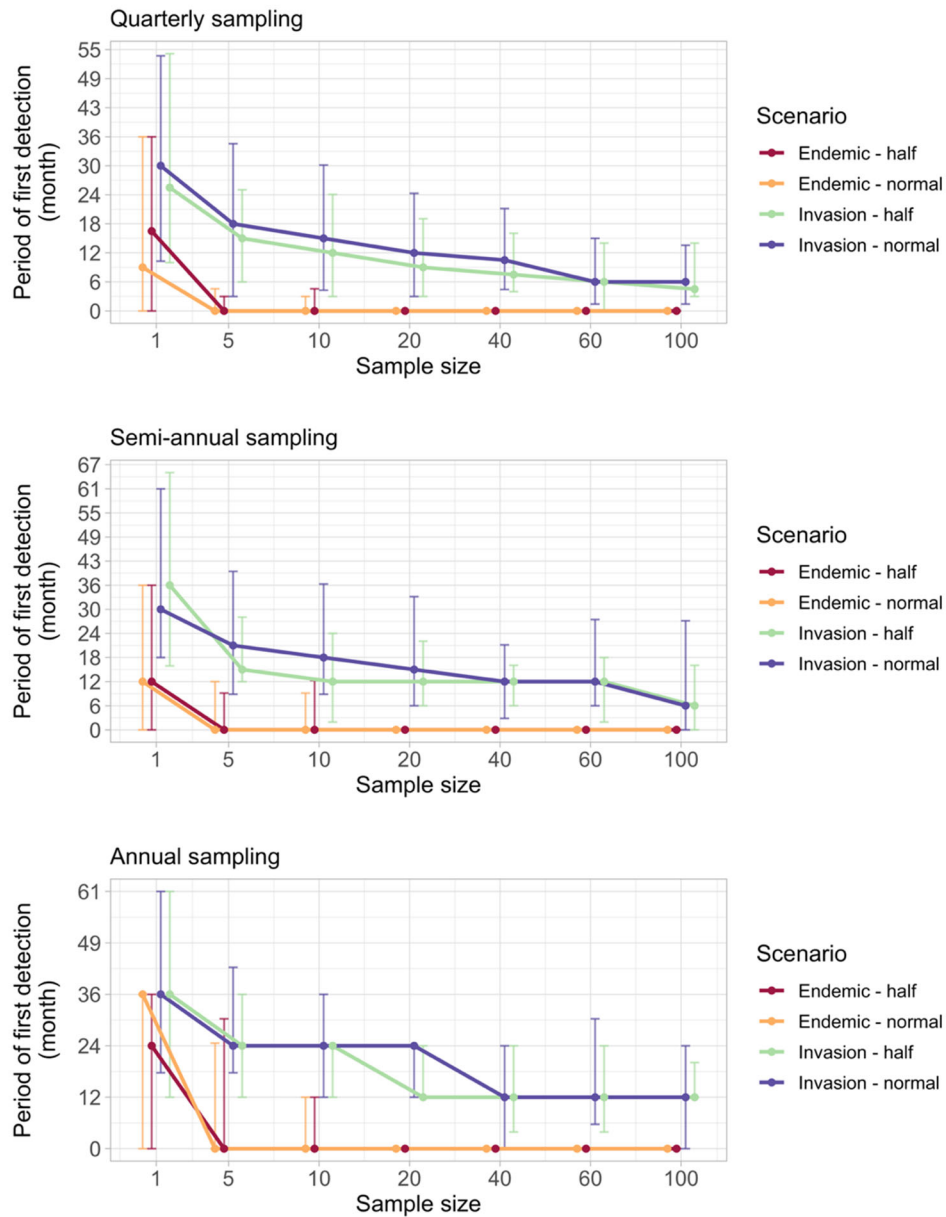


**Figure 6.3.4.8. Timing of first detection of an infected fox, for different sampling regimes and simulation scenarios.** Sampling was always done within one month, and spaced quarterly (every 3 months), semi-annually (every 6 months) or annually (every 12 months). Simulated scenarios were for endemic transmission (starting with 20% infected foxes and 55% recovered foxes) and invasion (starting with 1 infected fox and no recovered foxes), and for population sizes near carrying capacity ("normal") and at half carrying capacity ("half"). Dots show the median time until detection, error bars indicate 2.5% and 97.5% quantiles.

### 6.3.5. Transmission dynamics model for *Leptospira* in island foxes on San Clemente Island

We also characterized the probability of invasion and time to first detection using our independent model of *Leptospira* transmission on San Clemente Island, built using a completely

different set of assumptions for fox distribution and contact. We found that invasion of *Leptospira* following the introduction of one infected fox on San Clemente Island had a success rate of 91% in a population at normal population size, and 87% at half the normal population size, when the population is fully susceptible. Time to first detection following invasion was highly dependent on sample size and frequency, and the time between invasion and detection range from 3 to 21 months depending on sample size. For the annual sampling intervals actually employed on SCL and other islands, the first detection occurred after one year on average, for all sample sizes, with an increasing chance of detection in the year of introduction as sample size grew.

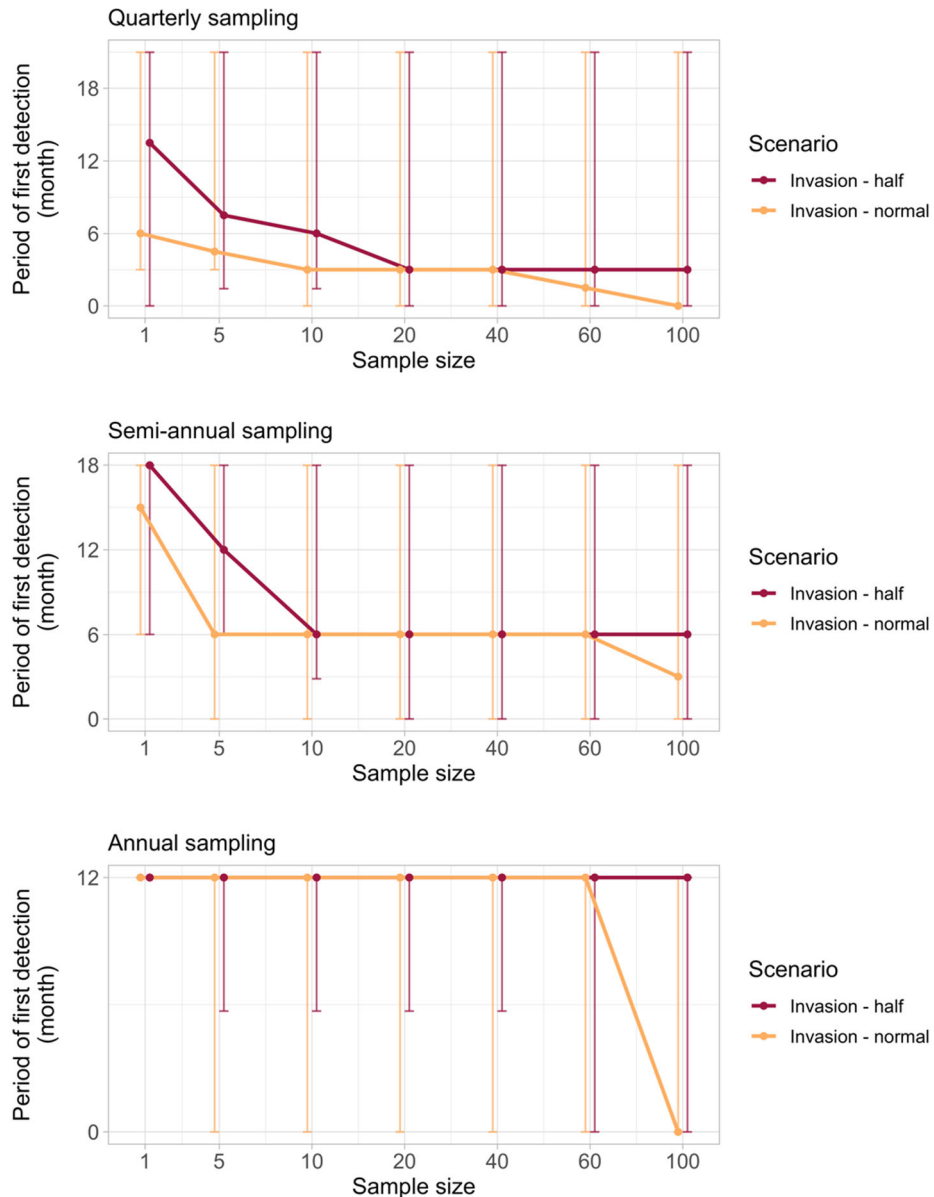


**Figure 6.3.5.1. Timing of first detection of an infected fox on San Clemente Island, for different sampling regimes and simulation scenarios.** Dots show the median time until detection, error bars indicate 2.5% and 97.5% quantiles.

### 6.3.6. Determine when infected CSL are found on the islands, during and after a major outbreak

We used data on *Leptospira* from stranded sea lions at TMMC and from wild-caught, free-ranging sea lions to determine when, relative to *Leptospira* outbreaks occurring along the central California coast, infected sea lions are found on the Channel Islands, where they pose a potential infection risk to naïve island fox populations. As mentioned in 6.2.1, prior fieldwork revealed that during the outbreak cycle immediately preceding fadeout (i.e. 2010-2012), no *Leptospira* shedding was detected in CSL on San Miguel Island in the year before or during the large 2011 outbreak, but low shedding rates were detected in September 2012. This is consistent with the known migratory behavior of CSL, if a chain of transmission begins on the coast in the fall and continues through the animals' northward migration in winter as well as their return migration to the islands in spring. This finding suggested that spillover risk to island fox populations on this and other rookery islands may peak in the year following major outbreaks.

Data collected through a full 3-year outbreak cycle (pre-, during, post-outbreak years) in 2017-2019 revealed a very different pattern (Table 6.3.6.1, Figure 6.3.6.1). We detected no shedding and no evidence of prior exposure (i.e. anti-*Leptospira* antibodies) in sea lions captured on San Miguel Island during this entire outbreak cycle. Thus, the 2017-2019 outbreak cycle did not repeat the pattern observed in 2010-2012, though it is possible that the recent cycle was atypical since it followed immediately after the 2017 reemergence of *Leptospira* in sea lions. Taken together, our observations on San Miguel Island indicate that infected CSL can bring *Leptospira* to the Channel Islands, but the pattern of infected CSL appearing the fall after a major outbreak was not reproduced.

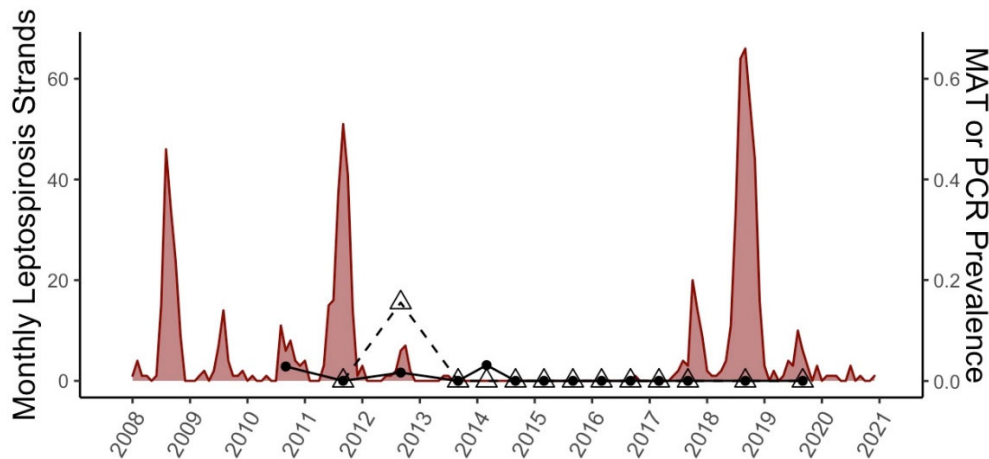


**Figure 6.3.6.1. *Leptospira* exposure and infection prevalence in sea lions on San Miguel Island.** Prevalence of anti-*Leptospira* antibodies indicating prior exposure (solid line and circle) and of leptospire shedding (as measured by PCR of urine; dashed line and hollow triangle) in California sea lions sampled in the spring and fall on San Miguel Island (SMI). These data are plotted over the time-series of the monthly number of stranded sea lions diagnosed with leptospirosis at the Marine Mammal Center (solid pink). SMI sea lion seroprevalence and shedding prevalence increased in 2012, the year after a major outbreak in 2011. In contrast, both measures remained at zero after reemergence and the major outbreak in 2018.

Year	Season	ANI			SMI			SNI			OR.WA		
		Total	PCR	MAT	Total	PCR	MAT	Total	PCR	MAT	Total	PCR	MAT
2008	Non-outbreak	-	-	-	-	-	-	-	-	-	-	-	-
	Outbreak	16	-	1/16 (0.06)	-	-	-	-	-	-	-	-	-
2009	Non-outbreak	-	-	-	-	-	-	-	-	-	-	-	-
	Outbreak	-	-	-	-	-	-	-	-	-	-	-	-
2010	Non-outbreak	-	-	-	-	-	-	-	-	-	-	-	-
	Outbreak	52	7/47 (0.15)	6/52 (0.12)	35	-	1/35 (0.03)	-	-	-	-	-	-
2011	Non-outbreak	-	-	-	-	-	-	-	-	-	-	-	-
	Outbreak	51	28/51 (0.55)	25/51 (0.49)	55	0/46 (0)	0/55 (0)	-	-	-	-	-	-
2012	Non-outbreak	-	-	-	-	-	-	-	-	-	26	1/26 (0.04)	11/24 (0.46)
	Outbreak	55	18/54 (0.33)	4/55 (0.07)	61	7/45 (0.16)	1/61 (0.02)	-	-	-	1	0/1 (0)	-
2013	Non-outbreak	-	-	-	-	-	-	-	-	-	-	-	-
	Outbreak	58	0/56 (0)	1/57 (0.02)	27	0/22 (0)	0/27 (0)	67	0/59 (0)	0/67 (0)	-	-	-
2014	Non-outbreak	-	-	-	64	0/64 (0)	2/64 (0.03)	62	0/60 (0)	2/62 (0.03)	27	0/24 (0)	12/27 (0.44)
	Outbreak	60	0/57 (0)	1/58 (0.02)	60	0/59 (0)	0/60 (0)	61	0/60 (0)	0/61 (0)	34	0/33 (0)	19/34 (0.56)
2015	Non-outbreak	-	-	-	53	0/49 (0)	0/53 (0)	-	-	-	63	0/60 (0)	25/60 (0.42)
	Outbreak	67	0/62 (0)	0/66 (0)	22	0/20 (0)	0/22 (0)	-	-	-	50	0/50 (0)	19/50 (0.38)
2016	Non-outbreak	-	-	-	62	0/58 (0)	0/60 (0)	-	-	-	92	0/90 (0)	19/90 (0.21)
	Outbreak	46	0/44 (0)	0/35 (0)	62	0/59 (0)	0/62 (0)	-	-	-	41	0/40 (0)	8/40 (0.2)
2017	Non-outbreak	-	-	-	67	0/62 (0)	0/64 (0)	-	-	-	24	0/23 (0)	9/23 (0.39)
	Outbreak	38	6/24 (0.25)	1/37 (0.03)	60	0/56 (0)	0/60 (0)	-	-	-	41	0/39 (0)	11/40 (0.28)
2018	Non-outbreak	-	-	-	-	-	-	-	-	-	27	0/27 (0)	17/27 (0.63)
	Outbreak	63	1/60 (0.02)	3/63 (0.05)	60	0/53 (0)	0/60 (0)	-	-	-	34	4/30 (0.13)	19/30 (0.63)
2019	Non-outbreak	-	-	-	-	-	-	-	-	-	49	0/19 (0)	15/30 (0.5)
	Outbreak	64	0/59 (0)	1/64 (0.02)	61	0/60 (0)	0/61 (0)	-	-	-	23	0/23 (0)	16/23 (0.7)

**Table 6.3.6.1. Shedding and seroprevalence data from free-ranging CSL.** PCR and MAT test results (positive/total (prevalence); TOTAL – total animals sampled; P – results are pending) from samples collected from free-ranging California sea lions by site (Año Nuevo Island – ANI, San Miguel Island – SMI, San Nicolas Island – SNI, and Oregon and Washington – OR.WA), year and time of year (January – June is spring/non-outbreak season, July – December is fall/outbreak season).

### 6.3.7. Analysis of San Nicolas Island

#### *Serology results show evidence of low but rising exposure to Leptospira*

The island fox population on SNI has declined sharply since 2009, for unknown reasons (US Navy, unpublished data, Sept 2018). To test whether exposure to *Leptospira* may have played a role in this decline, we conducted MAT analysis on 245 serum samples from SNI between 2010 and 2015 (Table 6.3.7.1), which included samples from 221 adults and 24 pups.

When we apply the same criteria for seropositivity as used on Santa Rosa Island (i.e. positive to any of Pomona, Bratislava, Autumnalis, Icterohaemorrhagiae, and Djasiman), 7 out of 245 samples were positive: one from each season from 2011-2014, and 3 from the 2015 season. Only one sample was positive to serovar Pomona, at a low titer of 1:200. Among the remaining samples, 7 other foxes were positive only to serovar Tarassovi, which is a serovar that has never been positive in SRI foxes in the 461 times it has been tested with SRI fox sera. Only one SNI fox sample had positive results to both serovar Tarassovi and one of the focal serovars from the SRI analysis; in particular, this fox was positive to both Tarassovi and Djasiman. All SNI pup samples were negative to all serovars.

Taking the broadest definition of seropositivity (i.e. positive to any serovar), adult fox seroprevalence ranged between 0% (95%CI, 0%-23%) in 2010 to 13% (95%CI, 5%-29%) in 2014 (Figure 6.3.7.1). Seroprevalence increased significantly over time. A chi square test was done to test if numbers of positive foxes varied in pairs of seasons, 2010-2011, 2012-2013, and 2014-2015, which indicated a significant departure from the null hypothesis of no relation between seroprevalence and time across the 3 by 2 table ( $\chi^2=6.61$ ,  $df=2$ ,  $p=0.04$ ). Pairwise testing was also performed among these time periods, with a significant increase detected between the earliest and latest pairs of seasons 2010-2011 and 2014-2015 ( $\chi^2=3.79$ ,  $df=1$ ,  $p=0.05$ ). Thus, seroprevalence of antibodies against any serovar of *Leptospira* increased over the period of the recent SNI fox decline.

*Leptospira* serology results were plotted on a map of SNI and results show a west to east movement of detected seropositive foxes across the island over time (Figure 6.3.7.1). The first foxes with evidence of exposure to *Leptospira* were on the western portion of the island in 2011-2013, and, beginning in 2014, seropositive foxes were also detected in the eastern portion of the island.

Season	All Samples				Adults Only				Pups Only			
	Pos	N	SP	95% CI	Pos	N	SP	95%CI	Pos	N	SP	95%CI
2010	0	15	0%	0%-25%	0	13	0%	0%-23%	0	2	0%	0%-66%
2011	1	47	2%	0%-11%	1	47	2%	0%-11%	0	0	NA	NA
2012	2	46	4%	1%-15%	2	42	5%	1%-16%	0	4	0%	0%-61%
2013	2	49	4%	1%-14%	2	44	5%	1%-15%	0	5	0%	0%-54%
2014	4	39	10%	4%-24%	4	31	13%	5%-29%	0	8	0%	0%-32%
2015	5	49	10%	4%-22%	5	44	11%	5%-24%	0	5	0%	0%-54%

**Table 6.3.7.1. Seroprevalence of foxes on San Nicolas island by age class, 2010-2015.**

Table includes San Nicolas Island fox serum samples tested for anti-*Leptospira* antibodies via a 20 serovar panel MAT analysis. Results are shown for all foxes, adults only, and pups only. N indicates the number of samples analyzed for each age group in each year. SP indicates the seroprevalence estimate, and 95% CI shows the 95% confidence interval around the seroprevalence estimate. Foxes were categorized as positive (Pos) if they had an antibody titer greater than or equal to 1:100 for any serovar. Time frames indicated are fox seasons March – February.

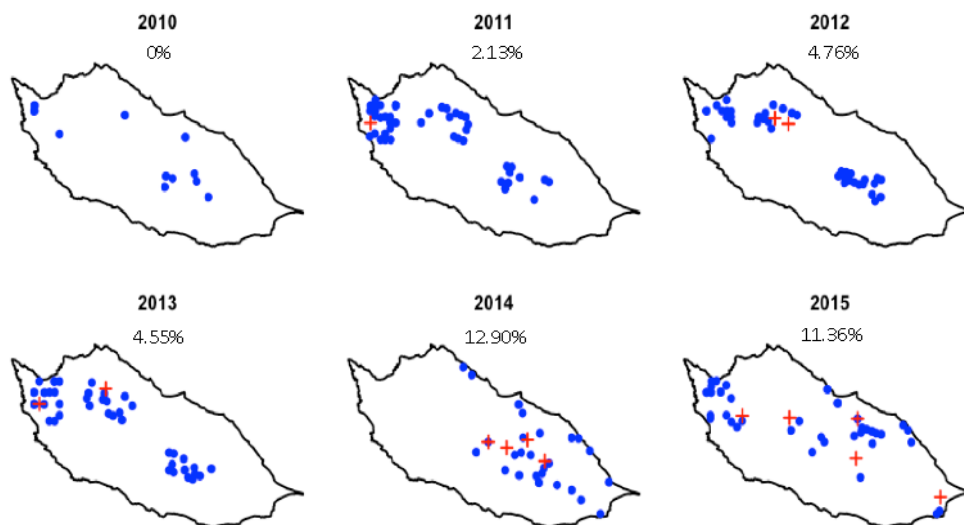


**Figure 6.3.7.1. SNI Adult Fox Seroprevalence Maps.** Annual maps of adult SNI fox *Leptospira* MAT results. Blue dots are negative results and red crosses are positive results. Time frames indicated are fox seasons March – February. Percentages indicate the prevalence of positive MAT results for the given year.

***MAT reactivity patterns do not match those seen on Santa Rosa Island***

At face value, the MAT profiles of SNI foxes do not resemble those from SRI foxes. Only one SNI fox showed any MAT reactivity against serovar Pomona, which is the strain causing the outbreak on SRI. As a further test of whether MAT results from SNI and SRI could reflect exposure to the same strain of *Leptospira*, we compared the titer levels and serovar cross-reactivity pattern of the MAT results on the two islands. Positive MAT results from foxes on SNI have much lower titers than those from foxes on SRI: the highest SNI titers were 1:200, which is only one dilution above the cutoff to be considered positive, while SRI titers ranged as high as

1:204,800. Furthermore, the serovar reactivity patterns in SNI fox samples do not match the cross-reactivity profile seen for SRI foxes (Figure 6.3.7.2, Figure 6.3.7.3). Our permutation test yielded an insignificant p-value of 0.32, indicating that the SNI data show no more evidence of the two-clade pattern associated with the SRI outbreak strain than the randomly permuted data.

These differences are evident from inspection of the MAT reactivity patterns (Figure 6.3.7.2., Figure 6.3.7.3). While the SRI strain has been genetically confirmed to be *L. interrogans* serovar Pomona, SRI foxes have shown cross-reactivity to 14 of the 20 serovars tested, with individual foxes reacting from 1 to 10 different serovars. Overall, SRI foxes react most frequently to serovars Autumnalis, Pomona, and Djasiman. In sharp contrast, seropositive SNI foxes showed reactions to a total of 6 serovars, with most individuals reacting to only one serovar, two reacting to two serovars, and one reacting to three serovars. SNI foxes reacted most frequently to serovar Tarassovi, a serovar to which no SRI fox has ever tested positive.

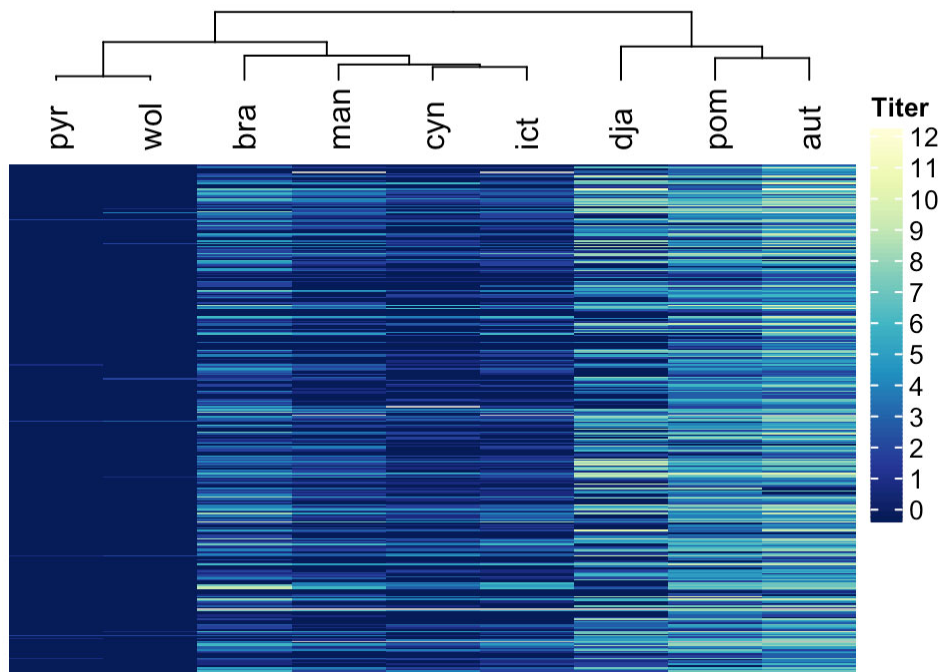


**Figure 6.3.7.2. MAT cross-reactivity profile for SRI foxes sampled during the outbreak, between 2006 and 2013.** Each row represents an individual fox, and the colors show the MAT titer against the serovar shown in the column header (titers range from 1=1:100 to 12=1:204,800; titer 0=negative). The dendrogram shows the serovar clustering pattern of the cross-reactivity profile. Serovars are abbreviated as follows: aut=Autumnalis, bra=Bratislava, cyn=Cynopteri, dja=Djasiman, ict=Icterohaemorrhagiae, man=Mankarso, pom=Pomona, pyr= Pyrogenes and wol=Wolffi.

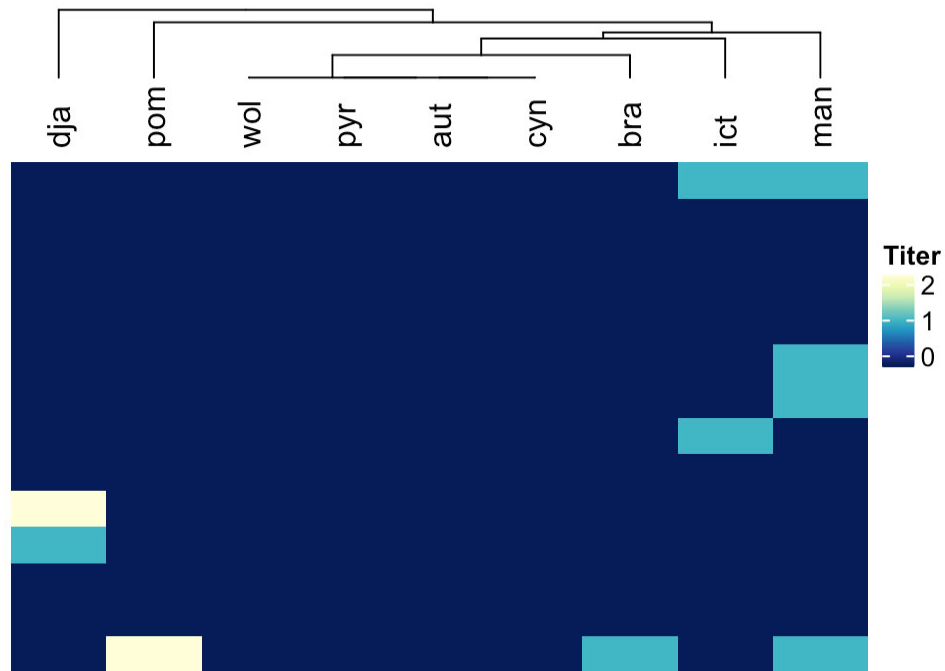


**Figure 6.3.7.3. MAT cross-reactivity profile for SNI foxes, 2010-2015.** Each row represents an individual fox, and the colors show the MAT titer against the serovar shown in the column header (titers range from 1=1:100 to 2=1:200; titer 0=negative). Rows that are entirely dark blue represent individuals who tested positive only to a serovar outside the core set of 9 serovars considered in this analysis. The dendrogram shows the serovar clustering pattern of the cross-reactivity profile. Serovars are abbreviated as follows: aut=Autumnalis, bra=Bratislava, cyn=Cynopteri, dja=Djasiman, ict=Icterohaemorrhagiae, man=Mankarso, pom=Pomona, pyr= Pyrogenes and wol=Wolffi.

### *Exploring the association between mortalities and *Leptospira* exposure*

Given the increase in *Leptospira* seroprevalence during the time frame of the recent population decline of SNI foxes, we analyzed mortality data to look for possible associations with *Leptospira* exposure. Figure 6.3.7.4 shows the number of non-anthropogenic mortalities through time in the SNI mortality database. The inconsistency in monitoring practices prevents any formal analysis of mortality counts across years, but there is an apparent increase in mortalities from the first round of telemetry monitoring in 2006-2009 to the second round of telemetry monitoring in 2014-2017. Figure 6.3.7.5 shows locations of these mortalities for the 2010-2015 seasons.

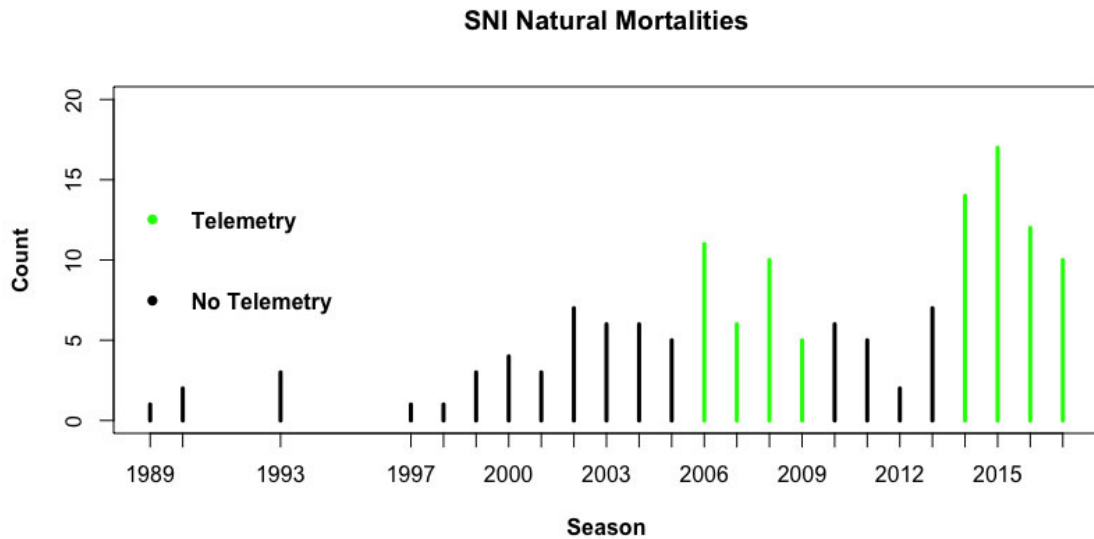


**Figure 6.3.7.4. Natural mortalities of island foxes on SNI, 1989-2017.** Graph of numbers of non-anthropogenic island fox mortalities on SNI per season. Green bars indicate seasons where foxes were collared with VHF collars with mortality sensors and tracked regularly via radio telemetry. Mortality detection rate is expected to be higher in seasons where foxes were collared and tracked via telemetry.

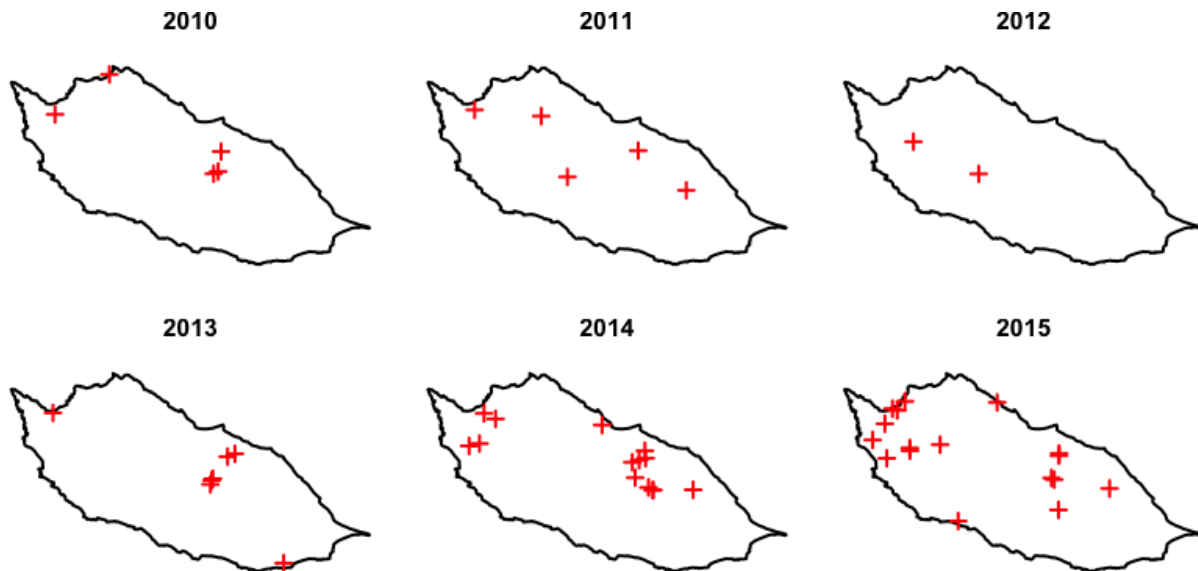


**Figure 6.3.7.5. Maps of natural mortalities of island foxes on SNI, 2010-2015.** The locations of non-anthropogenic island fox mortalities on SNI are mapped, for the 2010 through 2015 seasons.

*Spatiotemporal analysis*

Seroprevalence data and mortality data were combined to test for a relationship between SNI fox mortalities and anti-*Leptospira* antibody seroprevalence through space and time. Negative binomial regression showed no significant relationship between unexplained mortality

counts and seroprevalence in either the 4-segment ( $p=0.13$ ) and 3-segment analysis ( $p=0.28$ ) (Figure 6.3.7.6, Figure 6.3.7.7, Table 6.3.7.2, Table 6.3.7.3). Both analyses show signs of a positive correlation, but the scarcity and irregular distribution of the data limit our power to detect a significant relationship.

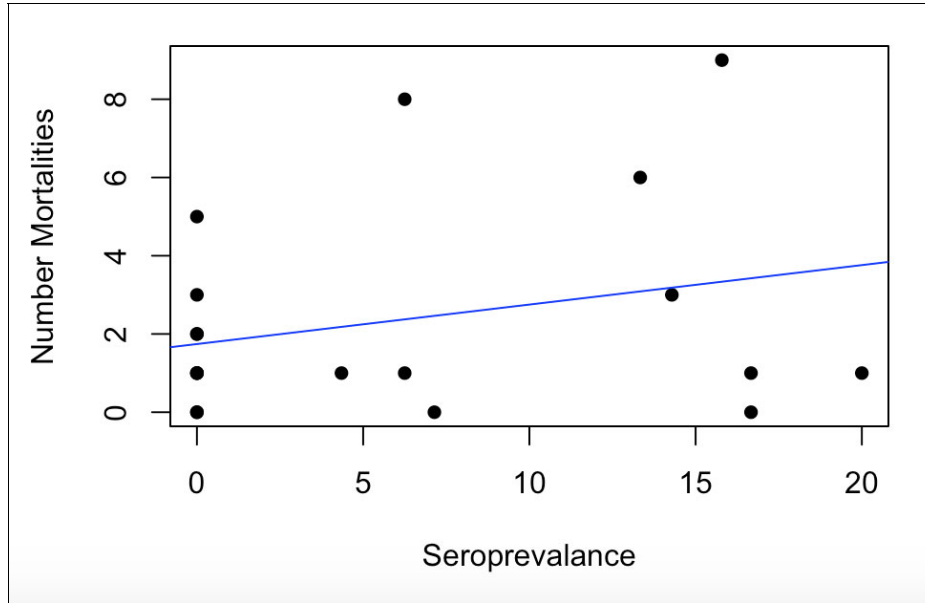


**Figure 6.3.7.6. Analysis of relationship between fox mortality and seroprevalence, 4-segment model.** The plot shows mortality counts versus estimated seroprevalence for each year-by-segment data point, for the analysis where SNI was divided into 4 segments. The fitted relation from negative binomial regression is shown in blue.

Coefficients	Estimate	Std. Error	Z Value	Pr (>  Z )
Intercept (Morts)	1.74248	0.62949	2.768	0.00564**
Seroprevalence	0.10092	0.09309	1.084	0.27832
Null deviance: 21.321 on 18 DF		Residual deviance: 20.154 on 17 DF		AIC: 82
Theta: 1.390		Standard Error: 0.764		

**Table 6.3.7.2. Negative binomial regression results for the analysis of the relationship between fox mortality and seroprevalence, 4-segment model.** The table includes the outputs for the negative binomial regression of mortality counts versus estimated seroprevalence for each year-by-segment data point, with the fitted relation shown as a blue line above.

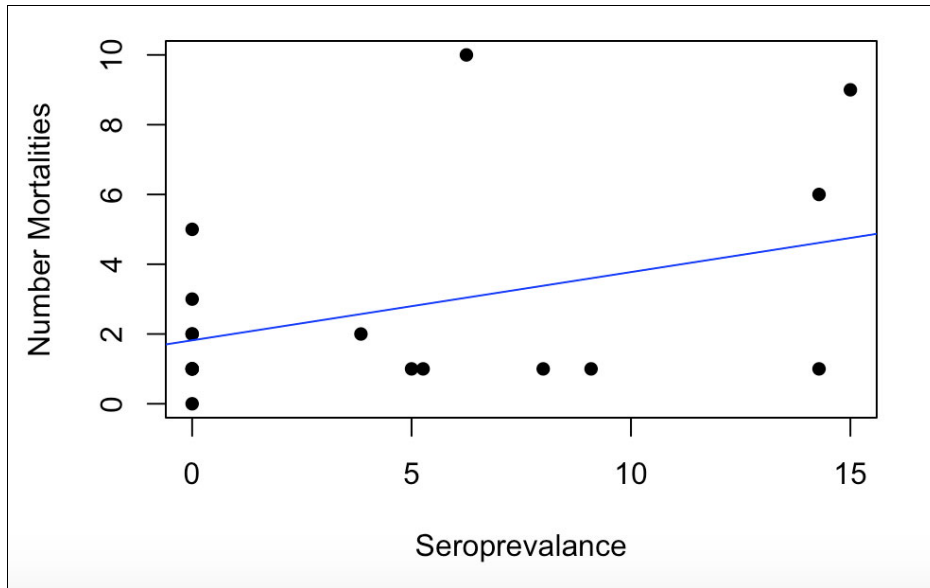


**Figure 6.3.7.7. Analysis of relationship between fox mortality and seroprevalence, 3-segment model.** The plot shows mortality counts versus estimated seroprevalence for each year-by-segment data point, for the analysis where SNI was divided into 3 segments. The fitted relation from negative binomial regression is shown in blue.

Coefficients	Estimate	Std. Error	Z Value	Pr (>  Z )
Intercept (Morts)	1.8189	0.6055	3.004	0.00266**
Seroprevalence	0.1959	0.1285	1.525	0.12738
Null deviance: 19.492 on 16 DF		Residual deviance: 19.194 on 15 DF		AIC: 75.81
Theta: 2.42		Standard Error: 1.53		

**Table 6.3.7.3. Negative binomial regression results for the analysis of the relationship between fox mortality and seroprevalence, 3-segment model.** The table includes the outputs for the negative binomial regression of mortality counts versus estimated seroprevalence for each year-by-segment data point.

*Individual-level data on serology before death*

We examined records for 13 individual foxes on SNI that were known mortalities between 2010 and 2015 and had serum samples included in our study (Table 6.3.7.4). Most of the individuals' serology tests were well before their date of death, and for all but one fox the MAT results were negative. One individual did have a 1:100 MAT titer to serovar Tarassovi, in a sample drawn over a year before its death. This positive result occurred in August 2014 and the fox died in November 2015. If this MAT result is a true positive, reflecting exposure to some strain of *Leptospira*, then these data show that in 2014 this exposure was not necessarily lethal to SNI foxes.

<b>PIT tag</b>	<b>MAT Date</b>	<b>MAT Result</b>	<b>Mortality Date</b>
	10/31/12,	Neg	
<b>01795</b>	09/02/13	Neg	9/12/15
<b>01839</b>	08/30/13	Neg	3/6/15
<b>16248</b>	08/28/11	Neg	<11/23/12
<b>21440</b>	08/29/11	Neg	<<<8/24/14
<b>38057</b>	08/08/15	Neg	<12/21/15
	08/27/11	Neg	
	09/29/12	Neg	
<b>40530</b>	08/30/13	Neg	8/8/15
	11/01/12	Neg	
	09/01/13	Neg	
<b>60001</b>	07/26/14	Neg	1/27/15
<b>70B11</b>	08/09/14	Tarassovi 1:100	11/4/15
<b>99103</b>	08/04/14	Neg	8/21/14
	09/29/12,	Neg	
<b>B1D0E</b>	08/09/15	Neg	12/9/15
<b>B7579</b>	11/19/11	Neg	10/30/12
<b>B782F</b>	09/02/13	Neg	12/30/15
<b>E104E</b>	07/04/10	Neg	<<<9/24/13

**Table 6.3.7.4. MAT results for 13 SNI foxes with known mortality between 2010 and 2015.** The symbol < indicates that the carcass was decayed, since the fox died prior to the date the carcass was found. <<< indicates the carcass was significantly decayed, since the fox died long prior to the carcass being found.

#### *Necropsy Report Analysis*

Necropsy reports of all SNI mortalities from 1980-2017 from both anthropogenic and natural causes were reviewed to look for signs of kidney disease possibly caused by leptospirosis. Results were pooled by decade to assess whether kidney disease rates rose during the period of the population decline, when anti-*Leptospira* antibody seroprevalence also rose.

There are no apparent differences in the proportion of carcasses presenting with kidney disease or abnormalities in the decades beginning in 1990, 2000, and 2010, each of which show kidney abnormalities in 48-56% of cases analyzed (Table 6.3.7.5). All of these do differ from the 5% (95% CI, 1%-25%) of kidney abnormalities reported in the earliest available necropsy reports from 1980-1989. We note that reporting methods and pathologists have changed over time, and there is unknown potential for bias in the selection of mortalities for necropsy. In the key time frame around the population decline from 2009-2012, very few carcasses were necropsied (just 15 of at least 86 known mortalities). All these issues complicate comparisons of the frequency of kidney disease over time and could obscure actual changes.

Seven SNI foxes that died between 2011 and 2016 had kidney tissue tested for *Leptospira* antigens via IHC, and all were negative. PCR testing for *Leptospira* DNA was not performed.

Decade	Necropsy Reports	Kidney Abnormalities	Percent	95% CI
1980-1989	19	1	5%	1%-25%
1990-1999	32	17	53%	35%-70%
2000-2009	71	34	48%	37%-59%
2010-2017	39	22	56%	41%-71%

**Table 6.3.7.5. Frequency of kidney abnormalities in SNI foxes, by decade of mortality.**

### ***Comparison to earlier serosurveys on San Nicolas Island and other Channel Islands***

This study marks the first detection of antibodies against *Leptospira* in SNI foxes. Two previous serostudies that included MAT testing for anti-*Leptospira* antibodies were conducted on SNI foxes. Garcelon *et al* (Garcelon et al., 1992) tested 46 SNI fox serum samples from 1988 via MAT against 2 serovars (Canicola and Icterohaemorrhagiae), and no anti-*Leptospira* antibodies were detected. Clifford *et al* (Clifford et al., 2006) tested 45 SNI fox serum samples from 2001 and 2002 via MAT against 6 serovars (Bratislava, Canicola, Hardjo, Grippotyphosa, Icterohaemorrhagiae, and Pomona) and no anti-*Leptospira* antibodies were detected. Samples in the Garcelon *et al* study were tested at the Washington Animal Disease Diagnostic Laboratory, and those in the Clifford *et al* study were tested at the Animal Health Diagnostic Laboratory at Cornell University. Direct comparison of samples tested at both CDC and Cornell, using serum samples from SRI foxes, has indicated that the CDC testing is more sensitive (unpublished data).

However, these prior surveys also tested sera from island foxes on five other Channel Islands, and results from these same labs did detect anti-*Leptospira* antibodies in these other island fox populations. In 1988, Garcelon *et al* detected anti-*Leptospira* antibodies only on Santa Cruz Island at 48% seroprevalence. In 2001 and 2002, Clifford *et al* detected anti-*Leptospira* antibodies in island foxes on four of six islands with island fox populations (SCZ, SCA, SCL and SRI), with seroprevalences from 7.1% to 21.4%. Neither study published information on MAT titer levels, but merely indicated seroprevalence and stated that any titer at or above 1:100 was considered positive. As shown in sections 5.1.1. and 6.1.1. of this report, the recently detected outbreak impacting foxes on SRI has adult seroprevalences above 80% in some years, with peak MAT titers of 1:204,800. The seroprevalence we have detected on SNI agrees more with the lower seroprevalences observed over the year on the other islands, rather than the elevated level seen in the context of the SRI outbreak.

### ***Interpretation of MAT reactivity profile in SNI foxes***

Serovar reactivity patterns and titer levels differ sharply between SNI and SRI foxes. The low titers and unusual serovars in the SNI data could be interpreted as false positives, though the non-random patterns of exposure through time and space argue against this interpretation. Another likely explanation is that SNI foxes are being exposed to one or more different strains of *Leptospira* than the SRI outbreak strain, with unknown epidemiological and disease-causing traits. However, another explanation could be variation in immune response between SNI and SRI foxes. We see substantial individual variation in cross-reactivity patterns on SRI, where all evidence suggests that the only strain circulating is *L. interrogans* serovar Pomona. As SNI foxes have extremely low genetic variation (Robinson et al., 2016), it is possible that the immune

response of the SNI foxes varies greatly from that of the other island fox subspecies. It is plausible that some dimensions of the immune response could differ in SNI foxes, as Aguilar (Aguilar et al., 2004) concluded that the SNI population went through an extreme population bottleneck, resulting in genetic monomorphism at neutral loci, but that 5 loci on the immune-related MHC genes experienced balancing selection with unprecedented selection coefficients. It is conceivable, if unlikely, that strong divergence in immune-related genes could lead to very different serologic responses to the same infecting strain.

Overall there is no evidence that the SNI foxes are infected with the same strain that is impacting the SRI foxes. There is some evidence that exposure of SNI foxes to some strain of *Leptospira* has increased in the last decade, and some hints that this could be associated with SNI fox mortalities. If the US Navy is interested in learning the possible connections to the SNI fox decline more definitively, a more thorough investigation is needed. The first steps in moving forward would be to send the remaining carcasses from 2008 onward for necropsy and to test those carcasses, as well as past necropsied foxes, for the presence of *Leptospira* DNA via PCR and, if any kidney abnormalities are noted, also IHC. Further collection of serum samples and MAT analysis would enable more robust testing of the statistical relationships described above. Ultimately, only a culture isolate could identify what strain(s) of *Leptospira*, if any, are infecting SNI foxes, so efforts to culture kidney samples from fresh carcasses could also be undertaken.

## 7. Conclusions and Implications for Future Research/Implementation

Our project set out to characterize the ecology of *Leptospira interrogans* serovar Pomona in the California coastal ecosystem, and to understand how non-stationary conditions have impacted the transmission dynamics and disease impacts of this pathogen in island foxes and California sea lions (CSL). In particular, we aimed to understand a dramatic outbreak of leptospirosis in the reintroduced island fox population on Santa Rosa Island (SRI), in the context of long-term circulation of the pathogen in California sea lions that share the coastal environment, and to extract useful insights to guide future management of the system.

Our project proposal included the following summary of the major objectives of our work, showing what was known, what we hoped to learn, what non-stationary conditions might affect disease dynamics, and how our project could support future disease control and management. We have succeeded in addressing all major questions set out in our proposal, and our work has yielded further unanticipated benefits – in part arising from unprecedented environmental perturbations and their consequences.

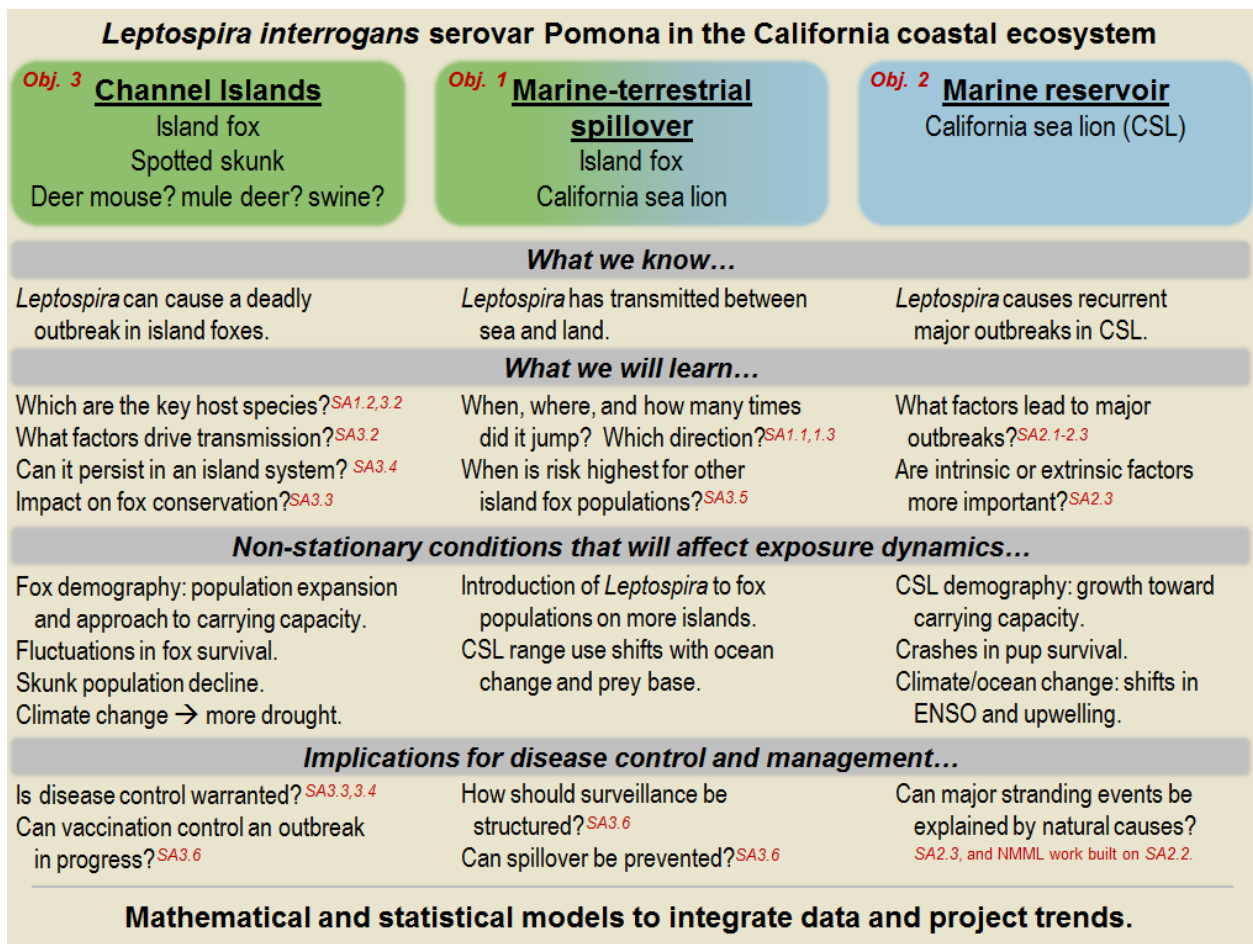


Figure 6.3.7.1. Summary of project goals, as included in our project proposal.

For one or two project outcomes, our current results are still preliminary, and we will continue work to refine and extend them. This is largely due to the impacts of the COVID-19 pandemic, which was a major disruption to the final 18 months of our project, delaying lab analyses and imposing unforeseen personal and professional commitments on key team members. Owing to our team's expertise in zoonotic pathogen emergence and dynamics, including new capabilities developed under this project (e.g. quantitative analysis of antibody kinetics), we were called to aid the national and global response to the pandemic. SERDP leadership was supportive of these activities, which led to a number of impactful contributions which credited SERDP support (Borremans et al., 2020; Fischer et al., 2020; Gostic et al., 2020; Morris et al., 2021; Mummah et al., 2020; Van Doremalen et al., 2020; Vespignani et al., 2020).

## Conclusions and Major Findings

### ***Objective 1: To identify the source of the current *Leptospira* outbreak in the endangered Santa Rosa Island fox.***

Based on information available when we proposed this work (namely: apparent lack of disease on SRI before 2000 when foxes entered captivity, lack of disease in captive foxes, widespread exposure of reintroduced foxes by 2010, and genetic similarity between the SRI outbreak strain and the CSL strain), we hypothesized that the pathogen strain causing the outbreak had been transmitted from CSL between 2004 and 2008. Our research on this project has proven this hypothesis to be incorrect; instead our findings aligned fully with an alternative hypothesis from the proposal (reproduced in Table 4.1) that the pathogen was introduced from other terrestrial hosts on the island. Our key findings on this objective include:

- *Leptospira* was present on SRI in the 1980s and 1990s, and the wild foxes that founded the captive population had been exposed. Our analysis of serological cross-reactivity profiles indicates that this was the same strain that is causing the on-going outbreak on SRI, but we do not have pathogen isolates from before the captive period so we cannot use genetic methods to reach a definitive conclusion on strain identity.
- *Leptospira* did not persist in the captive fox population. Thus captive-born foxes reintroduced from 2003 onward were naïve to *Leptospira*.
- *Leptospira* rapidly re-emerged and caused widespread exposure and disease in the reintroduced fox population on SRI. By fall 2006, the first year with a substantial number of serum samples available, signs of exposure to *Leptospira* were present in the majority of adult foxes over most of the island's area.
- Island foxes were absent from the SRI landscape from May 2001 (last animal captured) to November 2003 (first release from captivity), and were present in extremely low abundance (<10 animals) for a year before and after this period, so another host species must have maintained circulation of the pathogen. To understand how the pathogen persisted in the SRI ecosystem while foxes were absent, we studied evidence of infection in all species of terrestrial mammal on SRI. Feral pigs showed evidence of exposure in 1987, but were eradicated before 2001. Island spotted skunks have been involved in the on-going outbreak, at times showing high seroprevalence and infection rates, and shedding viable *Leptospira* organisms. Among the three other species of terrestrial mammal present on SRI during the period of fox captivity, data from deer mice and mule deer do not support a role for these species in maintaining the pathogen, and no samples are available from elk to assess their role. Integrating all evidence, we conclude that

spotted skunks are the most likely reservoir in which the pathogen persisted while foxes were absent, and hence the likely source of exposure to the reintroduced fox population.

- We reconstructed the spatiotemporal origin of the outbreak with unprecedented resolution for a wildlife disease emergence event, pinpointing the first cases to a period in mid-late 2005 and a region on the northern shore of the island. We accomplished this despite a lack of banked samples from this time period, by developing a model of serum antibody kinetics to estimate the time of infection of the earliest cases, and intersecting these times with reconstructed movement trajectories of the early foxes created by interpolating telemetry data. These findings tentatively support multiple introductions of *Leptospira* into the fox population, with no signature of proximity to marine mammal haul-outs, lending further support to our conclusion that island skunks were the likely source.
- Analysis of whole genome sequences of 49 *Leptospira* isolates taken from island foxes, spotted skunks, CSL and elephant seals provides independent corroboration of these conclusions. The genome sequence data are inconsistent with our original hypothesis that the outbreak was triggered by spillover from CSL. Our phylogenetic reconstructions show a nested clade structure, with deep separation between the SRI outbreak isolates from foxes and skunks and a distinct clade containing the isolates circulating in CSL at the time the SRI outbreak originated. Using ‘molecular clock’ assumptions, we estimated that these two clades diverged tens or hundreds of years ago, well before the SRI foxes were taken into captivity.
- Our phylogenetic analysis reveals multiple instances of cross-species and cross-ecosystem transmission of *Leptospira*. Most remarkably, we detected direct evidence of terrestrial-to-marine spillover, as an isolate taken from a CSL on the California coast mapped unambiguously within the clade of SRI outbreak isolates from foxes and skunks. Additionally, and less surprisingly, the phylogenies show instances of cross-species transmission between CSL and elephant seals, and between foxes and skunks. The deeper clade structure of the phylogenies implies other past transmission events between terrestrial and marine ecosystems. We postulate that an as-yet-undiscovered reservoir of *Leptospira*, perhaps in a terrestrial host on the California coast, has seeded multiple lineages in marine mammal and island communities.

*Conclusion:* The source of the outbreak in reintroduced Santa Rosa Island foxes was spillover from another terrestrial host species on the island, almost certainly island spotted skunks. The captive-bred foxes were reintroduced into a ‘hot’ landscape with undetected *Leptospira* already present, and by mid-late 2005 the pathogen had transmitted into foxes and initiated the outbreak. At the same time, genomic data indicate that *Leptospira* transmission can and does occur between the terrestrial and marine realms, so spillover between island species and marine mammal species is a continuing possibility (although sea lion to island fox transmission remains a hypothetical risk).

***Objective 2: To understand how non-stationary drivers shape *Leptospira* dynamics in the CSL population, and formulate a model capable of short-term outbreak prediction and long-term trend projection.***

For three decades since 1984, *Leptospira* caused annual seasonal outbreaks in the CSL population, as captured by a remarkable long-term dataset from stranded sea lions collected by our collaborators at The Marine Mammal Center. These outbreaks show strong interannual

variability, with an apparent tendency toward 3-5 year cycles. We hypothesized that the intensity of annual leptospirosis outbreaks in CSL is governed by non-stationary host demography, past disease exposures and prevailing environmental conditions. Our research on this project has proven this hypothesis correct, while also showing that extreme environmental anomalies can knock the system into a qualitatively different regime. In addition, we gained important new insights into the ecology of the CSL/*Leptospira* interaction. Our major findings on this objective include:

- We extended the long-term time series of *Leptospira* dynamics in the CSL population, and documented an unprecedented 4-year cessation in leptospirosis strands in CSL from early 2013 to mid-2017, followed by reemergence of the disease in a small outbreak in 2017, then the largest outbreak on record in 2018. We investigated this apparent ‘fadeout’ of infection using extensive serologic and PCR testing of samples from stranded and wild-captured CSL, and confirmed that all evidence is consistent with a spontaneous break in the endemic circulation of the pathogen after 30 years of uninterrupted annual outbreaks in CSL, followed by reintroduction of the pathogen 4 years later.
- We extended the long-term demographic study of CSL, and estimated age- and sex-specific survival probabilities each year using a mark-resight model. We integrated these with pup count data using a mathematical model, to develop an age- and sex-structured reconstruction of the CSL population for the period 1975-2018. We quantified severe impacts to the survival of young sea lions during a major marine heatwave in the Eastern Pacific Ocean from 2013-2016 (nicknamed “the Blob”), as well as the rebound of the CSL population after ocean conditions returned to normal.
- We developed a novel algorithm to combine the long-term datasets on *Leptospira* incidence and CSL demography, to reconstruct the size and age structure of the population of susceptible CSL, i.e. how many sea lions were available to be infected by *Leptospira* each year. The susceptibility of the population varies markedly among years, due to environmentally-induced cohort failures and sporadic major outbreaks of leptospirosis which confer protection against *Leptospira* for those sea lions that survived infection.
- We analyzed 30 years of annual leptospirosis incidence data prior to 2013 (when the fadeout occurred), and found that outbreak intensity is jointly driven by susceptible supply and variation in environmental drivers. We found that *Leptospira* transmission in CSL is driven most strongly by the supply of susceptible yearlings (of both sexes) and juvenile males. The most important environmental drivers relate to oceanographic conditions preceding and during the fall outbreak season, including the timing of the ‘spring transition’ in upwelling (which is known to drive ecosystem productivity and CSL prey availability), sea surface temperature off the central coast of California during the summer, and the intensity of upwelling during the fall. We propose biological mechanisms for these effects, based on CSL foraging and migration behavior and the potential for poor feeding conditions to weaken CSL immune function, but further research is needed to test these proposals. Our best model explains 50% of the interannual variability in outbreak intensity, based on non-stationary demographic and environmental drivers.
- We tested the ability of this model framework to make real-time predictions of outbreak intensity, using data that could be obtained by mid-summer each year (i.e. several months before the outbreak ramps up). Real-time predictive accuracy approached that of the

retrospective model, though the real-time model struggled to accurately predict extreme outbreak sizes. Through simulations we also found that climate change is expected to result in lower average outbreak sizes, but with more extreme peaks and troughs. Together, these findings show how a combination of intrinsic and extrinsic drivers can affect disease outbreaks in animals, contributing a powerful wildlife disease case study to a classical theme in population ecology.

- The fadeout of *Leptospira* from the CSL population provided an unexpected demonstration of the extreme outcomes possible when environmental conditions deviate too far from normal. Using serologic, molecular, demographic, and ecological data and samples collected between 2010-19, we showed that *Leptospira* disappeared from the CSL population in 2013 and re-emerged in 2017. We provide multiple lines of evidence that perturbations in both host demography and seasonal movement patterns – both driven by oceanographic anomalies – caused pathogen fadeout in the system. When ocean conditions returned to normal after the Blob and 2016 El Niño event, the CSL population recovered and *Leptospira* was reintroduced and reestablished annual outbreaks. This is the first recorded example of spontaneous fadeout of an endemically circulating pathogen from a large, robust host population. These findings complement the conclusions of our outbreak intensity analysis, demonstrating the powerful influence of non-stationarities in climatic and intrinsic host factors on pathogen transmission and persistence in a natural system.

*Conclusion:* Long-term studies of California sea lions and their interactions with *Leptospira* have enabled us to dissect the interplay of intrinsic and extrinsic forces that govern leptospirosis outbreaks in this host population. Oceanographic anomalies have strong impacts on CSL demography, and also moderate the transmission of *Leptospira* via their impacts on foraging and migratory behavior. Extreme fluctuations in environmental conditions are predicted to generate more extreme variation in outbreak intensity, as evidenced by the spontaneous fadeout of *Leptospira* from 2013-2017 and the largest outbreak on record in 2018.

***Objective 3: To characterize the ecology of Leptospira in island foxes, and develop a data-driven model to project impacts and assess prevention and control strategies under changing conditions.***

Discovery of the leptospirosis outbreak on SRI prompted concerns about its long-term impact on the island's fragile ecosystem, and on the potential risks posed to threatened and endangered island fox subspecies on other Channel Islands. Based on the observation that the pathogen had circulated for multiple years before our project began, and exposure in adult foxes was widespread, we hypothesized that *Leptospira* could establish persistent circulation in the fox population on SRI. Based on anecdotal observations of fox mortalities tied to *Leptospira* infection, and on the fact that SRI's population growth lagged that of other islands, we postulated that the disease could also cause significant demographic impacts. Finally, we hypothesized that we could gain sufficient insight into the ecology of *Leptospira* in island foxes to understand risks to other island fox populations, and to provide evidence-based guidance regarding if, when and how to take actions to prevent *Leptospira* from invading naïve island fox populations on other islands. At the request of the US Navy, we investigated the possible role of *Leptospira* in an unexplained population decline of island foxes on San Nicolas Island (SNI). Our major findings on this objective include:

- By extending surveillance of the SRI outbreak until 2019, and analyzing banked samples to reconstruct the origins of the outbreak, we built a unique long-term dataset describing the progression of the outbreak from the first cases, through the initial epidemic wave, to an endemic state of continued circulation on the island. The dataset is comprised of almost 3000 biological samples collected in over 7800 fox captures, and over 400 samples collected in over 3300 skunk captures. A dataset of this depth, duration and resolution is unprecedented for a wildlife disease system, and enables us to learn a great deal about the ecology of *Leptospira* in the island ecosystem and, more generally, about the dynamics of infectious disease in a population recovering from near-extinction.
- Following the initial wave of infection in 2006-7, *Leptospira* has become established in the SRI ecosystem. Since 2011 it has infected 4-27% of island fox pups each year, indicating an on-going (if fluctuating) hazard of infection on the island. Seroprevalence in adult foxes has remained near 75%, indicating that most foxes get infected sometime in their life. Spatiotemporal mapping of our data shows that hot spots of infection move around from year to year, but seroprevalence shows that the pathogen reaches foxes found across the island.
- Crucially, the island fox population on SRI has continued to grow despite the continuing circulation of *Leptospira*. A closer examination of mortalities during the initial outbreak wave showed that the pathogen had a major, undetected impact on the reintroduced population, with a spike in ‘unknown-cause’ mortalities in 2006-7 apparently attributable to leptospirosis. Evidence of demographic impacts are harder to discern in later data, possibly because of longer sampling intervals as the fox population grew; in addition to the direct mortalities observed, there are signs that *Leptospira* may reduce reproductive success as well, but further analyses are needed. The potential interactions of *Leptospira* with other stressors, such as drought, is an important avenue for future research.
- Island spotted skunks played a crucial role in sparking the outbreak in foxes, but their importance to outbreak dynamics has diminished over the last decade as their population has declined. After 2015, data are sparse since very few skunks were captured, but it is clear that skunks continue to be exposed and infected on SRI. Demographic impacts of *Leptospira* on spotted skunks are unknown.
- We were able to recapture and resample many foxes, giving rise to precious longitudinal data. Analyses of longitudinal antibody titer data showed that reinfection and titer boosting of foxes is very rare, if it happens at all. We identified systematic patterns of antibody titer kinetics in wild foxes, and developed a Bayesian model to estimate the time of infection of individual foxes from their antibody levels. This is a novel tool in wildlife disease ecology since previous models of this kind relied on laboratory exposure data to characterize titer kinetics.
- Longitudinal PCR data showed direct evidence of urinary shedding of *Leptospira* for up to 3 years after infection, with a high proportion of individuals shedding for 1 year or more. Due to unavoidable censoring of data derived from widely-spaced fox capture events, these observed shedding durations are lower bounds on the actual shedding duration by individual foxes. However, we showed that our samples were sufficient to detect longer durations of shedding, if these occurred, so we are confident that our results approximate the true distribution of this crucial epidemiological parameter.
- We used survival analysis to study the risk factors for *Leptospira* infection in SRI foxes, leveraging our longitudinal data and the time-of-infection estimates derived from our titer

kinetics model. Results showed clear dependence on non-stationary environmental factors, as infection risk was positively associated with cumulative precipitation over the past 24 months, and negatively associated with fox abundance. We believe that the precipitation effect reflects the role of standing water and moist soil in spreading this environmentally transmitted pathogen, while the fox abundance effect is likely a proxy for greater stability of fox social structure as the growing population began to saturate the island habitat. Thus, if *Leptospira* were introduced on other islands, the risk of transmission would be greatest after a multi-year rainy period with a destabilized population. (We note that these conditions describe SRI in 2005, when the current outbreak began.)

- We developed a spatial, stochastic transmission model to represent the introduction and on-going dynamics of *Leptospira* spread on SRI. By fitting the model to our long-term surveillance data from the island, we corroborated and refined our knowledge of key epidemiological parameters. Notably, the model fitting estimated the infectious period of *Leptospira* to be exponentially distributed with a mean of 370 days, which closely matches the patterns discerned from our longitudinal shedding data.
- We used the transmission model to predict future dynamics of *Leptospira* on SRI under baseline conditions and a range of non-stationary conditions. The model predicts that the pathogen will maintain persistent circulation with near certainty, in all scenarios examined. This is a logical consequence of the fact that island foxes exhibit such lengthy infectious periods for this pathogen; such chronic shedding enables persistent circulation even in small host populations, as we demonstrated in a separate analysis of *Leptospira* in CSL (Buhnerkempe et al., 2017).
- We used our transmission model as a platform to examine the probability that *Leptospira* could invade a naïve island fox population, if introduced under different conditions of fox population abundance and precipitation. We found that the pathogen had greater than 60% probability of invading successfully under all circumstances examined, with higher probabilities associated with high-rainfall scenarios and with fall and winter introductions, when fox movements were more frequent. We also modeled the time delay before an incipient *Leptospira* outbreak would be detected, under a range of potential designs for surveillance and monitoring programs. We found that delays of 12 to 24 months are likely under annual passive surveillance programs currently utilized on most islands; further scenarios will be explored in consultation with population managers.
- To generalize our guidance for island fox managers, we developed a parallel model for San Clemente Island (adapted from a published model of viral epidemics on that island (Sanchez & Hudgens, 2020)). This model is spatial and stochastic like our SRI model, but has a completely different architecture, so this is a strong test of the robustness of our conclusions. The SCI model replicates the qualitative findings of the SRI model, including a high probability that *Leptospira* could invade successfully if introduced, and average delays of 12 months under achievable sampling schemes.
- Finally, our investigation of the population decline of San Nicolas Island foxes found no evidence that the SNI foxes are infected with the same strain of *Leptospira* that is causing the outbreak in SRI foxes. There is evidence that exposure of SNI foxes to some strain of *Leptospira* has increased in the last decade, and some hints that this could be associated with SNI fox mortalities. Further study would be needed to confirm this link, and happily the SNI population has since rebounded.

*Conclusion:* *Leptospira* has become established in the SRI ecosystem, and our model simulations show that it is likely to persist long-term under a broad range of future potential demographic and environmental conditions. This persistence is governed largely by the lengthy duration of shedding by infected foxes, which enables the pathogen to maintain unbroken transmission despite the small size of the island fox population. The on-going outbreak is driven primarily by fox-to-fox transmission, and heavy precipitation seasons lead to elevated infection risk in ensuing years. Fortunately the demographic impact of *Leptospira* is sufficiently moderate that the fox population has continued to grow, despite widespread exposure of SRI foxes to the pathogen. However, the impact on island spotted skunks (now in decline) is unknown, as is the potential interaction with other stressors. Our models show that the pathogen could readily invade other island fox populations, if introduced, and that current monitoring programs would be unlikely to detect the pathogen before it establishes endemic spread.

### **Implications for future research/implementation**

Our project vastly increased our understanding of *Leptospira* ecology in the California coastal ecosystem, revealing new insights and unprecedented phenomena in the long-studied CSL/*Leptospira* system, and shedding important light on the newly discovered island fox/*Leptospira* system. In addition to this new knowledge, our work has clear implications for the management of these systems, as well as broader lessons for population management and public health.

### ***Management implications: Santa Rosa Island***

We discovered that *Leptospira* is not a recent introduction to the SRI ecosystem. Our serologic analyses show that it was present in SRI foxes in the 1980s and that the last surviving wild foxes had anti-*Leptospira* antibodies when they were taken into captivity. Our genomic analyses indicate that the *Leptospira* lineage on SRI diverged from any other known lineage decades ago. Furthermore, we showed that the pathogen has established robust endemic circulation in the reintroduced fox population on SRI, with direct evidence of sustained presence in SRI foxes from 2005 to present.

All available evidence indicates that the on-going SRI outbreak is driven by fox-to-fox transmission. The foxes are abundant and urinary shedding of the pathogen is highly prevalent (4-21% over the last decade) and long-lasting (often 1-3 years post-infection). In contrast, the skunks have declined sharply in abundance and we have never detected high prevalence of shedding in them, and there is no evidence that island deer mice, the only other terrestrial mammal present on SRI, get infected by *Leptospira*. Our mathematical model for *Leptospira* transmission on SRI was able to reproduce the initial outbreak and transition to endemic circulation without any contribution from skunks after 2006, and predicts long-term *Leptospira* persistence under foreseeable future conditions. We thus conclude that while another host species – almost certainly skunks – played a crucial role in sparking the outbreak in foxes, the on-going disease dynamics on the island are governed by the fox/*Leptospira* interaction and any external sources of infection are inconsequential.

In 2016, after a decade and a half of heroic efforts by land managers and biologists, the island fox subspecies on SRI was delisted (along with island fox subspecies on three other islands). However, the island has been proposed for federal designation as a wilderness, and is already managed as such by NPS, which would ensure continued protection of island foxes

under NPS wilderness Management Policies 2006 ([Section 6 Wilderness Preservation and Management](#)) requiring “preservation of wilderness character and wilderness resources in an unimpaired condition”. Given that *Leptospira* has been present on SRI for decades, and that its fox population recovered rapidly post-reintroduction despite widespread *Leptospira* transmission, there is no imminent need for active management of the disease. However, should future non-stationarities cause new stresses on the fox population, the additional impacts of *Leptospira* on fox health and demography may pose a conservation challenge. Therefore, ongoing monitoring and study of *Leptospira* on SRI is warranted, to ensure a rapid response should a significant decline occur, and also to address several remaining knowledge gaps.

The most important research needed to guide management on SRI is to gain more insight into possible conservation risks from this pathogen. Our project was able to demonstrate that some premature deaths of island foxes are associated with *Leptospira*, but our work to resolve the precise effects of the pathogen on fox survival and reproduction is on-going. It appears that *Leptospira* exerts subtle demographic costs, which on their own, and under the current climatic conditions, are not severe enough to prevent population growth, but do constitute a burden on the population that might interact with other future stressors. Population viability analyses have emphasized that island fox populations are naturally small and prone to fluctuations due to interactions between density dependence and environmental variability (chiefly rainfall) (Bakker et al., 2009; Bakker & Doak, 2008). We have shown that *Leptospira* incidence fluctuates in response to the same cues. Understanding the joint effects of disease and environmental stress on island fox demography would aid in anticipating conservation challenges. One major tool to aid this effort is the spatial, stochastic transmission model we have developed and fit to data for *Leptospira* on SRI. This model provides a platform to integrate new information and predict consequences of changing extrinsic factors including climate change, drought, or new biotic interactions such as a novel parasite or return of predation by golden eagles. Importantly, this model can also be adapted readily to understand the possible invasion and transmission dynamics of other pathogens of conservation concern for island foxes, such as canine distemper virus (Timm et al., 2009), complementing the capabilities of existing models that are non-spatial or have not been calibrated to real-world epidemic data (Doak et al., 2013; Sanchez & Hudgens, 2019).

Another issue, of increasing concern on SRI, is the possible impact of *Leptospira* on the island skunk population. While current abundance estimates are approximate, the endemic island spotted skunk population on SRI is clearly in decline, and our team members have joined a Working Group to investigate this issue (Island Spotted Skunk Working Group, 2020). Note that we have concluded (based on indirect evidence) that island skunks maintained circulation of *Leptospira* while the foxes were in captivity, and skunk abundance soared during this time, so it appears unlikely that *Leptospira* has severe impacts on skunk demography. This is reassuring, but as a practical matter it should be a priority to resolve the conflicting results on skunk serology from the two diagnostic labs we used, in order to have a reliable metric of *Leptospira* exposure to support monitoring of this declining endemic species.

Understanding the routes by which *Leptospira* transmits on SRI would bolster any future efforts to manage the pathogen and would clarify risks to other species including island skunks, marine mammals, and humans. SRI is a National Park that welcomes many members of the general public to camp and explore its natural splendors, and *Leptospira* is a zoonotic agent that can cause severe or fatal disease. Our findings indicate that infection risk to foxes is influenced by precipitation over the preceding two years, which is consistent with *Leptospira*'s known

ability to transmit via surface water or soil in other settings, and with emerging evidence that heavy rains can disperse infectious leptospires that have survived in soil for 6 months or more (Bierque et al., 2020). Investigation of possible environmental reservoirs of *Leptospira*, via PCR, metagenomic analysis, or culture of environmental samples, would yield valuable insight into the distribution of infection risk. Priority sites for sampling include standing water, moist soils, and fox or skunk latrine sites, particularly near campgrounds, picnic areas, and areas where CSL or elephant seals haul out on the island. These investigations into transmission routes and environmental reservoirs would yield valuable information to mitigate transmission risk to susceptible hosts, including human visitors to SRI.

### ***Management implications: other Channel Islands***

Our work has demonstrated that the strain of *Leptospira* associated with the SRI outbreak is well-adapted to circulate in island fox populations. The pathogen infects foxes efficiently and sheds for an extended duration, enabling persistence even at low population sizes. We built and analyzed two distinct transmission models, representing *Leptospira* in island foxes on SRI and San Clemente Island (SCL). Notably both models showed that *Leptospira* has a high probability of invading and developing into a large-scale outbreak if introduced to a naïve island fox population. Despite limited demographic impacts on SRI foxes thus far, introduction of a novel pathogen to a species of concern on a fragile island ecosystem, and under uncertain future conditions, is clearly undesirable. In addition, beyond its impact on island foxes, *Leptospira* has a broad host range that includes humans, and could cause more severe consequences in other hosts. Thus preventing introduction and establishment of *Leptospira* in their unique island fox subspecies should be a priority of land managers on the other Channel Islands.

With this in mind, the first important question is where such an introduction might come from. Our initial hypothesis that the SRI outbreak was sparked by spillover from sea lions proved false, as we learned that the pathogen had existed on SRI for decades before the fox population crash. However, our project still yielded valuable new insights into cross-species and cross-ecosystem transmission of *Leptospira*, and the possible sources of risk to other islands. Namely:

- Spillover from sea lions remains plausible, since CSL are infected in high numbers and have major rookeries and haulouts throughout the Channel Islands, and scavenging of CSL carcasses by island foxes has been reported. However, while we did document one instance of terrestrial-to-marine transmission (via genomic evidence that a *Leptospira* isolate from a sea lion nested clearly within the SRI outbreak clade), we have seen no evidence suggesting marine-to-terrestrial transmission. Our years of sampling CSL on San Miguel Island revealed low to zero prevalence of active infection on the rookery. Furthermore, it is important to note that *Leptospira* has circulated in CSL almost continuously since 1984, and has not yet successfully invaded the fox population on any other island, including those with major rookeries (SMI, SNI, and SCL). Altogether, we assess the risk of introduction from sea lions to be low, but not zero.
- The original source of infection for SRI is likely to remain unknown. *Leptospira* has been present on the island for decades or possibly centuries, and over this timespan the island was home to many introduced species such as pigs and sheep that are known hosts for the serovar involved in this outbreak (*Leptospira interrogans* serovar Pomona). We unearthed historic serum samples from SRI pigs that showed high seroprevalence to serovar Pomona in the 1980s, which demonstrates their past involvement but does not

implicate them as the source. All livestock species were removed from the island long ago, and no further biological specimens remain.

- Our analyses show evidence of multiple introductions of *Leptospira* from an unidentified reservoir to species in the California coastal ecosystem. We analyzed the genome sequences of *Leptospira* isolates obtained from SRI foxes and CSL before, during and after the 2013-2017 *Leptospira* fadeout from sea lions, as well as isolates from elephant seals on the California coast. Multiple lineages in marine mammals, in addition to the lineage from SRI foxes and skunks, share a common ancestor at the root of the phylogeny. We have evidence of 3-4 separate introductions of *Leptospira* to CSL and elephant seals in just the last decade, indicating that cross-species/cross-ecosystem transmission is common and has macroscopic impacts on *Leptospira* circulation in the California coastal ecosystem.
- Determining the reservoir responsible for these introductions would shed valuable light on sources of potential risk to other island fox populations. The strain of *Leptospira* involved in this system (*Leptospira interrogans* serovar Pomona) has a broad host range including raccoons, foxes, coyotes, and pigs. In separate research conducted at UCLA, we have found high seroprevalence of antibodies against *L. interrogans* serovar Pomona and urinary leptospire shedding in several wildlife species in Los Angeles County, including raccoons (*Procyon lotor*). Raccoons have been observed to ‘stow away’ on ferries and other vessels, and are suspected to have sparked the 1999 canine distemper epidemic on Catalina Island (Timm et al., 2009). Dogs can also be infected by *Leptospira*, so introduction via recreational boaters who violate the prohibition on dogs is also possible. Thus, there are plausible routes of introduction from mainland reservoirs of *Leptospira* to island fox populations on current unaffected islands.

Identifying the unknown reservoir of *Leptospira* in the California coastal ecosystem would enable an informed, holistic assessment of risks posed to DoD lands in the Channel Islands and elsewhere on the coast. Research to sample candidate wildlife hosts, including raccoons, possums, striped skunks, coyotes, and feral pigs, would yield important insights into the circulation of this zoonotic pathogen in California. Systematic sampling from wildlife rehabilitation centers and veterinary clinics would also produce valuable information. It is essential that such efforts include bacterial culture, since isolates are required for definitive typing of *Leptospira*, and we have now shown that whole genome sequencing can establish transmission connections between host species and ecosystems.

The second key question is how island managers can prevent establishment of *Leptospira* in their island’s fox population, if it is introduced. Here the crucial factor is how quickly the introduction is detected, since our work has shown that *Leptospira* can establish endemic circulation if allowed to spread unchecked for a year or more. Our reconstruction of the SRI outbreak’s origins indicated that the first cases occurred in mid-2005, and the pathogen was widespread by September 2006 when the first broad serosurvey was conducted -- although notably the SRI fox population was still small and unsettled at that time. Our modeling analyses mapped out the expected delay before the first case was detected under a range of invasion scenarios and sampling designs (see Figure 6.3.4.8 and Figure 6.3.5.1). While the quantitative results differ by scenario, and for our SRI and SCL models, the take-home finding is that under sampling schemes presently in place on the Channel Islands (i.e. sampling 40-100 foxes per year for serology, once per year), delays of 12-24 months are expected before passive surveillance

detects a seropositive individual. For serosurveillance to yield faster detection times, sampling would need to be more frequent than annual (which is logistically unsustainable) or perhaps could be focused in regions of greatest concern for pathogen introductions (e.g. near piers and other boat landing sites) or periods of greatest concern (e.g. during and immediately after major outbreaks in CSL). The work on this project was intended as a proof of concept that modeling could aid surveillance design; we would welcome the opportunity to conduct further work with interested island managers to analyze surveillance designs of interest.

Another key strategy is the maintenance of a sentinel population of foxes that are monitored actively via telemetry, so fox deaths can be investigated in a timely manner. From our experience on SRI and SNI, the limiting factor is carcass condition and whether biological samples can be salvaged for diagnostics. Thus, rapid detection and recovery must be prioritized, highlighting the irreplaceable role of frequent ground or aerial telemetry surveys. It was a cluster of fox deaths in 2010 that ultimately led to the discovery of the *Leptospira* outbreak on SRI. Notably, however, our retrospective work has shown that a large cluster of ‘unknown-cause’ deaths in 2006-7 was likely caused by the initial wave of the *Leptospira* outbreak. At the time there were many other pressing concerns, including on-going eagle predation, but this highlights the importance of building and maintaining awareness of pathogens present on the landscape, and on comparable landscapes. Our investigations of *Leptospira* on SRI lay a firm foundation for investigating mortality clusters on other Channel Islands, as shown in our investigation of the SNI fox population decline.

In summary, based on current knowledge the best practices to reduce risk of *Leptospira* invasion on the other Channel Islands would involve intensive biosecurity measures at mainland ports and island landing sites to prevent introduction by terrestrial wildlife or pet dogs, routine surveillance and (minimally) annual serologic screening for exposure to *L. interrogans* serovar Pomona, and maintenance of collared sentinel fox populations with frequent telemetry ‘life checks’. Based on our findings from SRI, this surveillance should be intensified for several years following heavy rain seasons. These strategies could be made stronger and more precise by additional research to identify the unknown reservoir of *Leptospira* that is seeding outbreaks throughout the coastal ecosystem, and by further modeling analyses to optimize surveillance design in response to managers’ needs. If the unknown reservoir can be found, then further gains would come from monitoring *Leptospira* dynamics in the reservoir, so periods of peak prevalence -- and hence highest risk for spillover -- can be identified and preventive measures can be stepped up.

### ***Management implications: CSL population***

Over the past 50 years, aided by the Marine Mammal Protection Act, the US stock of CSL has grown to a robust population of roughly 300,000 individuals. Much of this growth has taken place despite on-going circulation of *Leptospira*, which has caused repeated deadly outbreaks in CSL since 1984. Therefore it is apparent that, under current conditions, the CSL population is not threatened and there is no need for active management of *Leptospira* for conservation purposes. However, there are compelling reasons why it is important to monitor the health of the CSL population and its on-going interactions with *Leptospira*. CSL are a federally protected species, and mass stranding events due to leptospirosis or other causes raise concerns in the general public. The Marine Mammal Protection Act defines an unusual mortality event (UME) as “a stranding that is unexpected; involves a significant die-off of any marine mammal population; and demands immediate response.” Identifying and responding to UMEs requires

baseline data and scientific knowledge to assess their cause and what threat they may pose to the subject species. Furthermore, as large-bodied and long-lived apex predators that occupy the near-shore environment, CSL act as an important sentinel species for ocean health and its connections to environmental conservation and public health (Hazen et al., 2019; Randhawa et al., 2015). Finally, *Leptospira* has a wide host range and leptospirosis outbreaks in CSL can pose a direct risk to humans and animals that share the sea lion's coastal habitat.

Our project extended long-term data sets that describe CSL population ecology and *Leptospira* dynamics over several decades. Such long-term time series, and the scientific knowledge that can be gained from them, are irreplaceable assets for understanding current and future fluctuations in demography or disease impacts. In our work, we have developed new insight into the factors driving leptospirosis outbreak intensity, and their underlying mechanisms. We developed a semi-parametric model that can predict the risk of a major seasonal outbreak in CSL each year in real time, if input data-streams are maintained. This predictive capability would provide valuable information to marine mammal stranding and rehabilitation networks, allowing them to more effectively and humanely respond to leptospirosis-related strandings. Such predictions could also provide advance warning to land managers, including those responsible for island foxes, enabling them to modify pathogen surveillance efforts in species of concern according to current risk (e.g. stepping up surveillance near major CSL haulouts or rookeries). Finally, advance warning of CSL outbreaks would help coastal land managers and public health officials to prepare ahead and provide important public health messages regarding infection risk to humans and their pets that share the coastal environment with sea lions during major stranding events.

Opportune timing and the long-term nature of our broader study enabled us to observe, confirm, and investigate the unprecedented fadeout of *Leptospira* from the CSL population in 2013, followed by its re-emergence in 2017 and the largest outbreak on record in 2018. This surprising series of events typified the extreme dynamics that our model predicts will occur with increasing frequency, as global change leads to more severe oceanographic and climatic anomalies. We leveraged the depth of scientific study of CSL to understand the key drivers of this fadeout and re-emergence, but the broader lesson was that past patterns are not a full guide to what is possible in a changing world. In these complex ecological systems centered on nonlinear species interactions, correlational analyses and extrapolation of descriptive statistical models will not provide reliable projections to guide decision making.

To support more robust understanding and predictive ability for the CSL/*Leptospira* system and comparable systems, future research should focus on connecting population-level patterns to the underlying organismal dimension of response to environmental stressors. Most research on marine infectious disease -- and particularly on the impacts of climate change on marine disease -- has focused on marine invertebrates and fish, and often on direct impacts of temperature on these ectothermic hosts (Burge et al., 2014; Vega Thurber et al., 2020). For marine mammals, as endotherms and apex predators, changes in ocean and climate conditions will act via their physiology, trophic ecology, and behavior. These factors in turn will depend on the ecology and changing distributions of their prey species, and on the connections between nutrient and energy intake and CSL immune competence and survival. Our work made some inroads on understanding these complex pathways of causation, but there is much more to do. Well-designed studies that link the health and physiology of individual animals to the patterns observed at population scales could illuminate these questions, particularly if this work is sustained long enough to characterize baseline patterns plus the response to one or more

environmental perturbations. In parallel, supporting further work to link and analyze relevant large-scale datasets, for instance by collaborating with fisheries scientists to map changes in CSL prey distribution, could yield great benefits with modest investments.

### **Summary**

This project has illuminated the ecology of *Leptospira* in the California coastal ecosystem, via deep and multidisciplinary investigation of two focal systems: the recently-emerged *Leptospira* outbreak in island foxes and spotted skunks on Santa Rosa Island, and the long-standing endemic circulation of *Leptospira* in California sea lions. Both systems yielded surprises: the ‘novel’ outbreak on SRI turned out to be the re-emergence of a pathogen that had been present on the island for decades, and the ‘endemic’ pathogen in CSL disappeared for four years in the midst of our study. Both systems also revealed underlying structures where intrinsic processes (host demography and population immunity) interact with extrinsic non-stationarities (changing climate, ocean, and ecological conditions) to govern the dynamics of disease spread and resulting impacts on host population ecology.

One unifying theme, with repercussions across species monitoring and disease surveillance programs everywhere but especially for long-lived and protected species, is the extraordinary value of long-term studies with systematic surveillance and sample archiving. Our project benefited from decades of foundational work laid by government scientists and non-profit organizations, whose efforts produced priceless long-term time series data and freezers full of banked samples. These long-term investments have an irreplaceable role in understanding how complex ecological systems are responding to our changing world. These systems are non-linear, and for long-lived species the timescales of perturbation and response can be many years. Similarly, and obviously, responses to slow shifts in environmental conditions (e.g. global temperature) require long-term data, particularly for wildlife species of concern where experimental studies are not an option. Simply stated, for dynamic nonlinear systems, we can’t learn about impacts of a changing world from snapshots. Instead, we need to be able to characterize the dynamics over time, including shifts in dynamical behavior, which requires investment in sustained long-term studies with consistent methodology.

In addition to their clear benefits for tracking long-term trends and establishing baselines for what is normal (and what is a normal amount of variation), these long-term studies can pay off in unexpected ways. In our project, the banked serum and tissue samples from the first cohorts of foxes reintroduced to SRI helped us to reconstruct the origins of an outbreak that was occurring undetected at the time. Banked samples from decades before helped to prove that the pathogen had actually been present on the island all along. Even more vividly, our on-going intensive surveillance of *Leptospira* in CSL enabled us to nail down the fact that the pathogen faded out spontaneously from the CSL population. Without our intensive study, the absence of leptospirosis for a few years might have gone unnoted or been attributed to the vagaries of passive surveillance (via the adage ‘absence of evidence is not evidence of absence’). But in the context of our long-term, systematic study of the system, we have strong evidence that the pathogen actually was absent from the system.

Long-term monitoring programs are priceless assets in our efforts to understand the impacts of climate change and other non-stationarities on wildlife species of concern. These programs should be supported with stable funding, and with facilities for archiving precious biological samples. These investments can be leveraged further by supporting targeted additional field studies to gain deeper insights into particular challenges or mechanisms, and by teaming

with quantitative biologists and modelers who can help to extract maximum value from the data. Collaboration between agency scientists and academics can also maximize return on investment, by providing concrete and actionable guidance to species managers while also identifying conceptual themes that may help to generalize the findings to other systems. Through this integrative and interdisciplinary program of research, we can build scientific knowledge and produce evidence-based guidance to promote environmental conservation and resilience in our changing world.

## 8. Literature Cited

- Adler, B. (Ed.). (2015). *Leptospira and Leptospirosis*. Springer. <https://doi.org/10.1007/978-3-662-45059-8>
- Adler, B., & de la Peña Moctezuma, A. (2010). *Leptospira* and leptospirosis. *Veterinary Microbiology*, *140*(3–4), 287–296. <https://doi.org/10.1016/j.vetmic.2009.03.012>
- Aguilar, A., Roemer, G., Debenham, S., Binns, M., Garcelon, D., & Wayne, R. K. (2004). High MHC diversity maintained by balancing selection in an otherwise genetically monomorphic mammal. *Proceedings of the National Academy of Sciences*, *101*(10), 3490–3494.
- Ahmed, A., Grobusch, M. P., Klatser, P. R., & Hartskeerl, R. A. (2012). Molecular approaches in the detection and characterization of *Leptospira*. *Journal of Bacteriology & Parasitology*, *03*(02). <https://doi.org/10.4172/2155-9597.1000133>
- Ahmed, N., Devi, S. M., Machang'u, R. S., Ellis, W. A., & Hartskeerl, R. A. (2006). Multilocus sequence typing method for identification and genotypic classification of pathogenic *Leptospira* species. *Annals of Clinical Microbiology and Antimicrobials*, *10*.
- Anderson, R. M., & May, R. M. (1992). *Infectious diseases of humans: Dynamics and control*. Oxford university press.
- Antia, A., Ahmed, H., Handel, A., Carlson, N. E., Amanna, I. J., Antia, R., & Slifka, M. (2018). Heterogeneity and longevity of antibody memory to viruses and vaccines. *PLOS Biology*, *16*(8), e2006601. <https://doi.org/10.1371/journal.pbio.2006601>
- Bakker, V. J., & Doak, D. F. (2008). Population viability management: Ecological standards to guide adaptive management for rare species. *Frontiers in Ecology and the Environment*, *7*(3), 158–165.

- Bakker, V. J., Doak, D. F., Roemer, G. W., Garcelon, D. K., Coonan, T. J., Morrison, S. A., Lynch, C., Ralls, K., & Shaw, R. (2009). Incorporating ecological drivers and uncertainty into a demographic population viability analysis for the island fox. *Ecological Monographs*, *79*(1), 77–108. <https://doi.org/10.1890/07-0817.1>
- Bakun, A., Black, B. A., Bograd, S. J., García-Reyes, M., Miller, A. J., Rykaczewski, R. R., & Sydeman, W. J. (2015). Anticipated Effects of Climate Change on Coastal Upwelling Ecosystems. *Current Climate Change Reports*, *1*(2), 85–93. <https://doi.org/10.1007/s40641-015-0008-4>
- Bankevich, A., Nurk, S., Antipov, D., Gurevich, A. A., Dvorkin, M., Kulikov, A. S., Lesin, V. M., Nikolenko, S. I., Pham, S., Prjibelski, A. D., Pyshkin, A. V., Sirotkin, A. V., Vyahhi, N., Tesler, G., Alekseyev, M. A., & Pevzner, P. A. (2012). SPAdes: A New Genome Assembly Algorithm and Its Applications to Single-Cell Sequencing. *Journal of Computational Biology*, *19*(5), 455–477. <https://doi.org/10.1089/cmb.2012.0021>
- Barth, J. A., Menge, B. A., Lubchenco, J., Chan, F., Bane, J. M., Kirincich, A. R., McManus, M. A., Nielsen, K. J., Pierce, S. D., & Washburn, L. (2007). Delayed upwelling alters nearshore coastal ocean ecosystems in the northern California current. *Proceedings of the National Academy of Sciences of the United States of America*, *104*(10), 3719–3724. <https://doi.org/10.1073/pnas.0700462104>
- Begon, M., Telfer, S., Burthe, S., Lambin, X., Smith, M. J., & Paterson, S. (2009). Effects of abundance on infection in natural populations: Field voles and cowpox virus. *Epidemics*, *1*(1), 35–46. <https://doi.org/10.1016/j.epidem.2008.10.001>
- Bergh, C. van den, Venter, E. H., Swanepoel, R., & Thompson, P. N. (2019). High seroconversion rate to Rift Valley fever virus in cattle and goats in far northern KwaZulu-

- Natal, South Africa, in the absence of reported outbreaks. *PLOS Neglected Tropical Diseases*, 13(5), e0007296. <https://doi.org/10.1371/journal.pntd.0007296>
- Bharadwaj, R., Bal, A. M., Joshi, S. A., Kagal, A., Pol, S. S., Garad, G., Arjunwadkar, V., & Katti, R. (2002). An Urban Outbreak of Leptospirosis in Mumbai, India. *Jpn J Infect Dis*, 55, 194–196.
- Bierque, E., Thibeaux, R., Girault, D., Soupé-Gilbert, M.-E., & Goarant, C. (2020). A systematic review of *Leptospira* in water and soil environments. *PLOS ONE*, 15(1), e0227055. <https://doi.org/10.1371/journal.pone.0227055>
- Bishara, J., Amitay, E., Barnea, A., Yitzhaki, S., & Pitlik, S. (2002). Epidemiological and Clinical Features of Leptospirosis in Israel. *European Journal of Clinical Microbiology and Infectious Diseases*, 21(1), 50–52. <https://doi.org/10.1007/s10096-001-0660-6>
- Bivand, R., Keitt, T., & Rowlingson, B. (2018). *rgdal: Bindings for the “Geospatial” Data Abstraction Library* (R package version 1.3-6).
- Bjørnstad, O. N., Finkenstädt, B. F., & Grenfell, B. T. (2002). Dynamics of measles epidemics: Estimating scaling of transmission rates using a time series SIR model. *Ecological Monographs*, 72(2), 169–184.
- Bjørnstad, O. N., & Grenfell, B. T. (2001). Noisy clockwork: Time series analysis of population fluctuations in animals. *Science*, 293, 638–463. <https://doi.org/10.1126/science.1062226>
- Bograd, S. J., Schroeder, I., Sarkar, N., Qiu, X., Sydeman, W. J., & Schwing, F. B. (2009). Phenology of coastal upwelling in the California Current. *Geophysical Research Letters*, 36(1), 1–5. <https://doi.org/10.1029/2008GL035933>
- Bolin, C. A., & Zuerner, R. L. (1996). Correlation between DNA restriction fragment length polymorphisms in *Leptospira interrogans* serovar pomona type kennewicki and host

- animal source. *Journal of Clinical Microbiology*, 34(2), 424–425.  
<https://doi.org/10.1128/jcm.34.2.424-425.1996>
- Bolker, B. M. (2008). *Ecological Models and Data in R*. Princeton University Press.
- Boni, M. F., Mølbak, K., & Krogfelt, K. A. (2019). Inferring the Time of Infection from Serological Data. In *Handbook of Infectious Disease Data Analysis* (pp. 287–303). Chapman and Hall/CRC.
- Boonsilp, S., Thaipadungpanit, J., Amornchai, P., Wuthiekanun, V., Bailey, M. S., Holden, M. T. G., Zhang, C., Jiang, X., Koizumi, N., Taylor, K., Galloway, R., Hoffmaster, A. R., Craig, S., Smythe, L. D., Hartskeerl, R. A., Day, N. P., Chantratita, N., Feil, E. J., Aanensen, D. M., ... Peacock, S. J. (2013). A Single Multilocus Sequence Typing (MLST) Scheme for Seven Pathogenic *Leptospira* Species. *PLoS Neglected Tropical Diseases*, 7(1), e1954. <https://doi.org/10.1371/journal.pntd.0001954>
- Borremans, B., Gamble, A., Prager, K., Helman, S. K., McClain, A. M., Cox, C., Savage, V., & Lloyd-Smith, J. O. (2020). Quantifying antibody kinetics and RNA detection during early-phase SARS-CoV-2 infection by time since symptom onset. *ELife*, 9, e60122. <https://doi.org/10.7554/eLife.60122>
- Borremans, B., Hens, N., Beutels, P., Leirs, H., & Reijnders, J. (2016). Estimating Time of Infection Using Prior Serological and Individual Information Can Greatly Improve Incidence Estimation of Human and Wildlife Infections. *PLOS Computational Biology*, 12(5), e1004882. <https://doi.org/10.1371/journal.pcbi.1004882>
- Borremans, B., Leirs, H., Gryseels, S., Günther, S., Makundi, R., & de Belloq, J. G. (2011). Presence of Mopeia Virus, an African Arenavirus, Related to Biotope and Individual

- Rodent Host Characteristics: Implications for Virus Transmission. *Vector-Borne and Zoonotic Diseases*, 11(8), 1125–1131. <https://doi.org/10.1089/vbz.2010.0010>
- Borremans, B., Vossen, R., Becker-Ziaja, B., Gryseels, S., Hughes, N., Van Gestel, M., Van Houtte, N., Günther, S., & Leirs, H. (2015). Shedding dynamics of Morogoro virus, an African arenavirus closely related to Lassa virus, in its natural reservoir host *Mastomys natalensis*. *Scientific Reports*, 5, 10445. <https://doi.org/10.1038/srep10445>
- Brady, R. X., Alexander, M. A., Lovenduski, N. S., & Rykaczewski, R. R. (2017). Emergent anthropogenic trends in California Current upwelling. *Geophysical Research Letters*, 44(10), 5044–5052. <https://doi.org/10.1002/2017GL072945>
- Brookmeyer, R., & Gail, M. H. (1988). A Method for Obtaining Short-Term Projections and Lower Bounds on the Size of the AIDS Epidemic. *Journal of the American Statistical Association*, 83(402), 301–308. <https://doi.org/10.1080/01621459.1988.10478599>
- Brooks, S. P., & Gelman, A. (1998). General Methods for Monitoring Convergence of Iterative Simulations. *Journal of Computational and Graphical Statistics*, 7(4), 434–455. <https://doi.org/10.1080/10618600.1998.10474787>
- Brownie, C., & Robson, D. S. (1983). Estimation of Time-Specific Survival Rates from Tag-Resighting Samples: A Generalization of the Jolly-Seber Model Author ( s ): C. Brownie and D. S. Robson Published by: International Biometric Society Stable URL : <http://www.jstor.org/stable/2531015>. *Biometrics*, 39(2), 437–453.
- Buhnerkempe, M., Prager, K. C., Strelhoff, C. C., Greig, D. J., Laake, J. L., Melin, S. R., DeLong, R. L., Gulland, F. M., & Lloyd-Smith, J. O. (2017). Detecting signals of chronic shedding to explain pathogen persistence: *Leptospira interrogans* in California sea lions. *Journal of Animal Ecology*, 86(3), 460–472. <https://doi.org/10.1111/1365-2656.12656>

- Buhnerkempe, M., Prager, K., Gulland, F., & Lloyd-Smith, J. (2013). *Maximizing the potential of serology data: A model of Leptospira antibody dynamics in California sea lions*.
- Burge, C. A., Mark Eakin, C., Friedman, C. S., Froelich, B., Hershberger, P. K., Hofmann, E. E., Petes, L. E., Prager, K. C., Weil, E., Willis, B. L., Ford, S. E., & Harvell, C. D. (2014). Climate Change Influences on Marine Infectious Diseases: Implications for Management and Society. *Annual Review of Marine Science*, 6(1), 249–277.  
<https://doi.org/10.1146/annurev-marine-010213-135029>
- Burnham, K. P., & Anderson, D. R. (2002). Model selection and multimodel inference: A practical information-theoretic approach. In *Ecological Modelling* (Vol. 172). Springer.  
<https://doi.org/10.1016/j.ecolmodel.2003.11.004>
- Burnstein, T., & Baker, J. A. (1954). Leptospirosis in swine caused by *Leptospira pomona*. *Journal of Infectious Diseases*, 94(1), 53–64.
- Caley, P., & Hone, J. (2004). Disease transmission between and within species, and the implications for disease control. *Journal of Applied Ecology*, 41(1), 94–104.  
<https://doi.org/10.1111/j.1365-2664.2004.00867.x>
- Campagnolo, E. R., Warwick, M. C., Marx Jr., H. L., Cowart, R. P., Donnell Jr., H. D., Bajani, M. D., Bragg, S. L., Esteban, J. E., Alt, D. P., Tappero, J. W., Bolin, C. A., & Ashford, D. A. (2000). Analysis of the 1998 outbreak of leptospirosis in Missouri in humans exposed to infected swine. *J Am Vet Med Assoc*, 216(5), 676–682.  
<https://doi.org/10.2460/javma.2000.216.676>
- Campbell, K. R., Juarez-Colunga, E., Grunwald, G. K., Cooper, J., Davis, S., & Gralla, J. (2019). Comparison of a time-varying covariate model and a joint model of time-to-event outcomes in the presence of measurement error and interval censoring: Application to

- kidney transplantation. *BMC Medical Research Methodology*, 19(1), 130.  
<https://doi.org/10.1186/s12874-019-0773-1>
- Carretta, J. V., Forney, K. A., Muto, M. M., Barlow, J., Baker, J., Hanson, B., & Lowry, M. S. (2006). U. S. Pacific marine mammal stock assessments: 2005. In *NOAA Technical Memorandum NMFS*.
- Carretta, J. V., Forney, K. A., Oleson, E. M., Martien, K. K., Muto, M., Lowry, M. S., Barlow, J., Baker, J. D., Hanson, B., Lynch, D., Carswell, L., Brownell, R. L., Robbins, J., Mattila, D. K., Ralls, K., & Hill, M. C. (2012). *U.S. Pacific marine mammal stock assessments, 2011* (noaa:4506). <https://repository.library.noaa.gov/view/noaa/4506>
- Chavez, F. P., Pennington, J. T., Castro, C. G., Ryan, J. P., Michisaki, R. P., Schlining, B., Walz, P., Buck, K. R., McFadyen, A., & Collins, C. A. (2002). Biological and chemical consequences of the 1997-1998 El Niño in central California waters. *Progress in Oceanography*, 54(1–4), 205–232. [https://doi.org/10.1016/S0079-6611\(02\)00050-2](https://doi.org/10.1016/S0079-6611(02)00050-2)
- Chavez, F. P., Ryan, J., Lluch-cota, S. E., C, M. Ñ., & C, M. N. (2003). From anchovies to sardines and back: Multidecadal change in the Pacific ocean. *Science*, 299(5604), 217–221. <https://doi.org/10.1126/science.1075880>
- Chirathaworn, C., Inwattana, R., Poovorawan, Y., & Suwancharoen, D. (2014). Interpretation of microscopic agglutination test for leptospirosis diagnosis and seroprevalence. *Asian Pacific Journal of Tropical Biomedicine*, 4(Suppl 1), S162–S164.  
<https://doi.org/10.12980/APJTB.4.2014C580>
- Cilia, G., Fratini, F., Buona, E. della, & Bertelloni, F. (2020). Preliminary Evaluation of In Vitro Bacteriostatic and Bactericidal Effect of Salt on *Leptospira* spp. *Veterinary Sciences*, 7(4), 154. <https://doi.org/10.3390/vetsci7040154>

- Clark, R. K., Jessup, D. A., Hird, D. W., Ruppanner, R., & Meyer, M. E. (1983). Serologic survey of California wild hogs for antibodies against selected zoonotic disease agents. *Journal of the American Veterinary Medical Association*, *183*(11), 1248–1251.
- Clifford, D. L., Mazet, J. A. K., Dubovi, E. J., Garcelon, D. K., Coonan, T. J., Conrad, P. A., & Munson, L. (2006). Pathogen exposure in endangered island fox (*Urocyon littoralis*) populations: Implications for conservation management. *Biological Conservation*, *131*(2), 230–243. <https://doi.org/10.1016/j.biocon.2006.04.029>
- Colagross-Schouten, A. M., Mazet, J. A. K., Gulland, F. M. D., Miller, M. A., & Hietala, S. (2002). Diagnosis and seroprevalence of leptospirosis in California sea lions from coastal California. *Journal of Wildlife Diseases*, *38*(1), 7–17. <https://doi.org/10.7589/0090-3558-38.1.7>
- Collins, P. W. (1980). Food habits of the Island fox (*Urocyon littoralis littoralis*) on San Miguel Island, California. *Proceedings of the Second Conference on Scientific Research in the National Parks*, *12*, 152–164.
- Coonan, T. J., Bakker, V., Hudgens, B., Boser, C. L., Garcelon, D. K., & Morrison, S. A. (2014). On the Fast Track to Recovery: Island Foxes on the Northern Channel Islands. *Monographs of the Western North American Naturalist*, *7*(1), 9,373-381.
- Coonan, T. J., Guglielmino, A., & Shea, R. (2015). *Island Fox Recovery Program: Channel Islands National Park 2014 annual report* (pp. 1–52). Nat. Resour. Rep. NPS/MEDN/NRR.
- Coonan, T. J., Schwemm, C. A., & Garcelon, D. K. (2010). *Decline and Recovery of the Island Fox: A Case Study for Population Recovery*. Cambridge University Press. <https://doi.org/10.1017/CBO9780511781612>

- Corwin, A. L., Ryan, A., Bloys, W., Thomas, R., Deniega, B., & Watts, D. (1990). A waterborne outbreak of leptospirosis among United States military personnel in Okinawa, Japan. *International Journal of Epidemiology*, *19*(3), 743–748.
- Coulson, T., Rohani, P., & Pascual, M. (2004). Skeletons, noise and population growth: The end of an old debate? *Trends in Ecology and Evolution*, *19*(7), 359–364.  
<https://doi.org/10.1016/j.tree.2004.05.008>
- Craft, M. E. (2015). Infectious disease transmission and contact networks in wildlife and livestock. *Philosophical Transactions of the Royal Society B: Biological Sciences*, *370*(1669), 20140107. <https://doi.org/10.1098/rstb.2014.0107>
- Crooks, K. R., & Van Vuren, D. (1995). Resource utilization by two insular endemic mammalian carnivores, the island fox and island spotted skunk. *Oecologia*, *104*(3), 301–307.
- Cumberland, P., Everard, C. O., & Levett, P. N. (1999). Assessment of the efficacy of an IgM-elisa and microscopic agglutination test (MAT) in the diagnosis of acute leptospirosis. *The American Journal of Tropical Medicine and Hygiene*, *61*(5), 731–734.  
<https://doi.org/10.4269/ajtmh.1999.61.731>
- Cumberland, P., Everard, C. O., Wheeler, J. G., & Levett, P. N. (2001). Persistence of anti-leptospiral IgM, IgG and agglutinating antibodies in patients presenting with acute febrile illness in Barbados 1979-1989. *European Journal of Epidemiology*, *17*(7), 601–608.  
<https://doi.org/10.1023/a:1015509105668>
- Cypher, B. L., Madrid, A. Y., Van Horn Job, C. L., Kelly, E. C., Harrison, S. W. R., & Westall, T. L. (2014). Multi-population comparison of resource exploitation by island foxes: Implications for conservation. *Global Ecology and Conservation*, *2*, 255–266.  
<https://doi.org/10.1016/j.gecco.2014.10.001>

- Cypher, B. L., Madrid, A. Y., Van Horn Job, C. L., Kelly, E., Harrison, S. W. R., & Westall, T. L. (2011). *Resource Exploitation by Island Foxes: Implications for Conservation* (C. D. of F. and Game, Ed.; Vols. 2011–01).
- de Graaf, W. F., Kretzschmar, M. E. E., Teunis, P. F. M., & Diekmann, O. (2014). A two-phase within-host model for immune response and its application to serological profiles of pertussis. *Epidemics*, *9*, 1–7. <https://doi.org/10.1016/j.epidem.2014.08.002>
- DeLong, R. L., Antonelis, G. A., Oliver, C. W., Stewart, B. S., Lowry, M. C., & Yochem, P. K. (1991). *Effects of the 1982–83 El Niño on Several Population Parameters and Diet of California Sea Lions on the California Channel Islands*. 166–172.  
[https://doi.org/10.1007/978-3-642-76398-4\\_18](https://doi.org/10.1007/978-3-642-76398-4_18)
- DeLong, R. L., Melin, S. R., Laake, J. L., Morris, P., Orr, A. J., & Harris, J. D. (2017). Age- and sex-specific survival of California sea lions (*Zalophus californianus*) at San Miguel Island, California. *Marine Mammal Science*, *33*(4), 1097–1125.  
<https://doi.org/10.1111/mms.12427>
- Dierauf, L. A., Vandenbroek, D. J., Roletto, J., Koski, M., Amaya, L., & Gage, L. J. (1985). An epizootic of leptospirosis in California sea lions. *Journal of the American Veterinary Medical Association*, *187*(11), 1145–1148.
- Dikken, H., & Kmety, E. (1978). Chapter VIII Serological Typing Methods of Leptospire. *Methods in Microbiology*, *11*, 259–307.
- Doak, D. F., Bakker, V. J., & Vickers, W. (2013). Using Population Viability Criteria to Assess Strategies to Minimize Disease Threats for an Endangered Carnivore. *Conservation Biology*, *27*(2), 303–314. <https://doi.org/10.1111/cobi.12020>

- Drummond, A. J., Ho, S. Y. W., Phillips, M. J., & Rambaut, A. (2006). Relaxed Phylogenetics and Dating with Confidence. *PLoS Biology*, *4*(5), e88.  
<https://doi.org/10.1371/journal.pbio.0040088>
- Ellis, W. A. (2015). Animal Leptospirosis. In B. Adler (Ed.), *Current Topics in Microbiology and Immunology* (Vol. 387, pp. 99–137). Springer Berlin Heidelberg.  
[https://doi.org/10.1007/978-3-662-45059-8\\_6](https://doi.org/10.1007/978-3-662-45059-8_6)
- Epstein, J. H., Baker, M. L., Zambrana-Torrel, C., Middleton, D., Barr, J. A., DuBovi, E., Boyd, V., Pope, B., Todd, S., Crameri, G., Walsh, A., Pelican, K., Fielder, M. D., Davies, A. J., Wang, L.-F., & Daszak, P. (2013). Duration of Maternal Antibodies against Canine Distemper Virus and Hendra Virus in Pteropid Bats. *PLOS ONE*, *8*(6), e67584.  
<https://doi.org/10.1371/journal.pone.0067584>
- Faine, S., Adler, B., Bolin, C., & Perolat, P. (1999). *“Leptospira” and leptospirosis* (2nd ed.). MediSci. <https://research.monash.edu/en/publications/leptospira-and-leptospirosis>
- Feldkamp, S. D., DeLong, R. L., & Antonelis, G. A. (1991). Effects of El Niño 1983 on the Foraging Patterns of California Sea Lions (*Zalophus californianus*) near San Miguel Island, California. In F. Trillmich & K. A. Ono (Eds.), *Pinnipeds and El Niño: Responses to Environmental Stress* (pp. 146–155). Springer Berlin Heidelberg.  
[https://doi.org/10.1007/978-3-642-76398-4\\_16](https://doi.org/10.1007/978-3-642-76398-4_16)
- Fieberg, J., & DelGiudice, G. D. (2009). What time is it? Choice of time origin and scale in extended proportional hazards models. *Ecology*, *90*(6), 1687–1697.  
<https://doi.org/10.1890/08-0724.1>

- Finkenstädt, B. F., & Grenfell, B. T. (2000). Time series modelling of childhood diseases: A dynamical systems approach. *Applied Statistics*, 49, 187–205.  
<https://doi.org/10.1111/1467-9876.00187>
- Fischer, R. J., Morris, D. H., van Doremalen, N., Sarchette, S., Matson, M. J., Bushmaker, T., Yinda, C. K., Seifert, S. N., Gamble, A., Williamson, B. N., & others. (2020). Effectiveness of N95 respirator decontamination and reuse against SARS-CoV-2 virus. *Emerging Infectious Diseases*.
- Fisheries, N. (2020, May 12). *Frequent Questions: 2013-2016 California Sea Lion Unusual Mortality Event | NOAA Fisheries (West Coast)*. NOAA.  
<https://www.fisheries.noaa.gov/national/marine-life-distress/frequent-questions-2013-2016-california-sea-lion-unusual-mortality>
- Fisheries, N. (2021, May 19). *2013-2016 California Sea Lion Unusual Mortality Event in California | NOAA Fisheries (West Coast)*. NOAA.  
<https://www.fisheries.noaa.gov/national/marine-life-distress/2013-2016-california-sea-lion-unusual-mortality-event-california>
- Fouts, D. E., Matthias, M. A., Adhikarla, H., Adler, B., Amorim-Santos, L., Berg, D. E., Bulach, D., Buschiazzi, A., Chang, Y.-F., Galloway, R. L., Haake, D. A., Haft, D. H., Hartskeerl, R., Ko, A. I., Levett, P. N., Matsunaga, J., Mechaly, A. E., Monk, J. M., Nascimento, A. L. T., ... Vinetz, J. M. (2016). What makes a bacterial species pathogenic?: Comparative genomic analysis of the genus *Leptospira*. *PLOS Neglected Tropical Diseases*, 10(2), e0004403. <https://doi.org/10.1371/journal.pntd.0004403>

- Galloway, R. L., & Levett, P. N. (2008). Evaluation of a modified pulsed-field gel electrophoresis approach for the identification of *Leptospira* serovars. *The American Journal of Tropical Medicine and Hygiene*, 78(4), 628–632.
- Garcelon, D. K., Wayne, R. K., & Gonzales, B. J. (1992). A serologic survey of the island fox (*Urocyon littoralis*) on the Channel Islands, California. *Journal of Wildlife Diseases*, 28(2), 223–229. <https://doi.org/10.7589/0090-3558-28.2.223>
- Gearin, P. J., Melin, S. R., DeLong, R. L., Gosho, M. E., & Jeffries, S. J. (2017). Migration patterns of adult male California sea lions (*Zalophus californianus*). *NOAA Technical Memorandum NMFS-AFSC-346*, 29. <https://doi.org/10.7289/V5/TM-AFSC-346>
- Gelman, A., & Hill, J. (2007). *Data Analysis Using Regression and Multilevel/Hierarchical Models*. Cambridge University Press.
- Gerber, J. A., Roletto, J., Morgan, L. E., Smith, D. M., & Gage, L. J. (1993). Findings in pinnipeds stranded along the central and northern California coast, 1984-1990. *Journal of Wildlife Diseases*, 29(3), 423–433.
- Gilbert, A. T., Fooks, A. R., Hayman, D. T. S., Horton, D. L., Müller, T., Plowright, R., Peel, A. J., Bowen, R., Wood, J. L. N., Mills, J., Cunningham, A. A., & Rupprecht, C. E. (2013). Deciphering Serology to Understand the Ecology of Infectious Diseases in Wildlife. *EcoHealth*, 10(3), 298–313. <https://doi.org/10.1007/s10393-013-0856-0>
- Gostic, K., Gomez, A. C., Mummah, R. O., Kucharski, A. J., & Lloyd-Smith, J. O. (2020). Estimated effectiveness of symptom and risk screening to prevent the spread of COVID-19. *ELife*, 9, e55570.
- Grassly, N. C., Fraser, C., & Garnett, G. P. (2005). Host Immunity and Synchronized Epidemics of Syphilis. *Nature*, 433(27), 417–421. <https://doi.org/10.1038/nature03212.1>

- Greig, D. J., Gulland, F. M. D., & Kreuder, C. (2005). A Decade of Live California Sea Lion (*Zalophus californianus*) Strandings Along the Central California Coast: Causes and Trends, 1991-2000. *Aquatic Mammals*, 31(1), 11–22.  
<https://doi.org/10.1578/am.31.1.2005.11>
- Grenfell, B. T., & Bjørnstad, O. N. (2005). Epidemic cycling and immunity. *Nature*, 433, 366–367.
- Grenfell, B. T., & Dobson, A. P. (Eds.). (1995). *Ecology of infectious diseases in natural populations*. Cambridge University Press.
- Gu, Z., Eils, R., & Schlesner, M. (2016). Complex heatmaps reveal patterns and correlations in multidimensional genomic data. *Bioinformatics (Oxford, England)*, 32(18), 2847–2849.  
<https://doi.org/10.1093/bioinformatics/btw313>
- Gulland, F. M. D., Koski, M., Lowenstine, L. J., Colagross, A., Morgan, L., & Spraker, T. (1996). Leptospirosis in California sea lions (*Zalophus californianus*) stranded along the central California coast, 1981-1994. *Journal of Wildlife Diseases*, 32(4), 572–580.  
<https://doi.org/10.7589/0090-3558-32.4.572>
- Haake, D. A., & Levett, P. N. (2015). Leptospirosis in Humans. In *Leptospira and Leptospirosis* (pp. 65–97). Springer.
- Handel, A., & Rohani, P. (2015). Crossing the scale from within-host infection dynamics to between-host transmission fitness: A discussion of current assumptions and knowledge. *Philosophical Transactions of the Royal Society B: Biological Sciences*, 370(1675), 20140302. <https://doi.org/10.1098/rstb.2014.0302>

- Hardestam, J., Karlsson, M., Falk, K. I., Olsson, G., Klingström, J., & Lundkvist, Å. (2008). *Puumala Hantavirus Excretion Kinetics in Bank Voles (Myodes glareolus)*. *14*(8), 1209–1215. <https://doi.org/10.3201/eid1408.080221>
- Hardin, J. W., & Hilbe, J. M. (2002). *Generalized estimating equations* (1st ed.). Chapman and Hall/CRC.
- Hasegawa, M., Kishino, H., & Yano, T. (1985). Dating of the human-ape splitting by a molecular clock of mitochondrial DNA. *Journal of Molecular Evolution*, *22*(2), 160–174. <https://doi.org/10.1007/BF02101694>
- Hathaway, S. C., Little, T. W. A., Jones, T. W. H., Stevens, H., & Butland, R. W. (1984). Infection by leptospire of the Pomona serogroup in cattle and pigs in south west England. *Veterinary Record*, *115*(10), 246–248.
- Hawley, D. M., Grodio, J., Jr, S. F., Kirkpatrick, L., & Ley, D. H. (2011). Experimental infection of domestic canaries (*Serinus canaria domestica*) with *Mycoplasma gallisepticum*: A new model system for a wildlife disease. *Avian Pathology*, *40*(3), 321–327. <https://doi.org/10.1080/03079457.2011.571660>
- Hazen, E. L., Abrahms, B., Brodie, S., Carroll, G., Jacox, M. G., Savoca, M. S., Scales, K. L., Sydeman, W. J., & Bograd, S. J. (2019). Marine top predators as climate and ecosystem sentinels. *Frontiers in Ecology and the Environment*, *17*(10), 565–574. <https://doi.org/10.1002/fee.2125>
- Heath, S. E., & Johnson, R. (1994). Leptospirosis. *Journal of the American Veterinary Medical Association*, *205*(11), 1518–1523.

- Heisey, D. M., Joly, D. O., & Messier, F. (2006). The fitting of general force-of-infection models to wildlife disease prevalence data. *Ecology*, *87*(9), 2356–2365.  
[https://doi.org/10.1890/0012-9658\(2006\)87\[2356:tfogfm\]2.0.co;2](https://doi.org/10.1890/0012-9658(2006)87[2356:tfogfm]2.0.co;2)
- Held, L., Hens, N., O’Neill, P., & Wallinga, J. (Eds.). (2019). *Handbook of Infectious Disease Data Analysis*. Chapman and Hall/CRC. <https://doi.org/10.1201/9781315222912>
- Isaac, N. J. B., Jarzyna, M. A., Keil, P., Dambly, L. I., Boersch-Supan, P. H., Browning, E., Freeman, S. N., Golding, N., Guillera-Aroita, G., Henrys, P. A., Jarvis, S., Lahoz-Monfort, J., Pagel, J., Pescott, O. L., Schmucki, R., Simmonds, E. G., & O’Hara, R. B. (2020). Data Integration for Large-Scale Models of Species Distributions. *Trends in Ecology & Evolution*, *35*(1), 56–67. <https://doi.org/10.1016/j.tree.2019.08.006>
- Island Spotted Skunk Working Group. (2020). *Island Spotted Skunk Conservation Plan*.  
<http://www.californiaislands.net/skunks>
- Johnston, J. H., Lloyd, J., McDonald, J., & Waitkins, S. (1983). Leptospirosis—an occupational disease of soldiers. *Journal of the Royal Army Medical Corps*, *129*(2), 111–114.
- Kahle, D., & Wickham, H. (2013). ggmap: Spatial Visualization with ggplot2. *The R Journal*, *5*(1), 144–161.
- Katz, A. R., Sasaki, D. M., Mumm, A. H., Escamilla, J., Middleton, C. R., & Romero, S. E. (1997). Leptospirosis on Oahu: An outbreak among military personnel associated with recreational exposure. *Military Medicine*, *162*(2), 101–104.
- Kingscote, B. F. (1986). Leptospirosis in red foxes in Ontario. *Journal of Wildlife Diseases*, *22*(4), 475–478.
- Kinlan, B., Graham, M., & Erlandson, J. (2003). *Late Quaternary Changes in the Size and Shape of the California Channel Islands: Implications for Marine Subsidies to Terrestrial*

*Communities. In Proceedings of the Sixth California Islands Symposium, edited by D. Garcelon and C. Schwemm.*

- Knowlton, J. L., Josh Donlan, C., Roemer, G. W., Samaniego-Herrera, A., Keitt, B. S., Wood, B., Aguirre-Muñoz, A., Faulkner, K. R., & Tershy, B. R. (2007). Eradication of non-native mammals and the status of insular mammals on the California Channel Islands, USA, and Pacific Baja California Peninsula Islands, Mexico. *The Southwestern Naturalist*, 52(4), 528–540.
- Ko, A. I., Goarant, C., & Picardeau, M. (2009). Leptospira: The dawn of the molecular genetics era for an emerging zoonotic pathogen. *Nature Reviews Microbiology*, 7(10), 736–747. <https://doi.org/10.1038/nrmicro2208>
- Koelle, K., Rodó, X., Pascual, M., Yunus, M., & Mostafa, G. (2005). Refractory periods and climate forcing in cholera dynamics. *Nature*, 436(7051), 696–700. <https://doi.org/10.1038/nature03820>
- Kullback, S., & Leibler, R. A. (1951). On Information and Sufficiency. *The Annals of Mathematical Statistics*, 22(1), 79–86. <https://doi.org/10.1214/aoms/1177729694>
- Laake, J. L. (2013). *RMark: An R Interface for analysis of capture-recapture data with MARK* (noaa:4372). <https://repository.library.noaa.gov/view/noaa/4372>
- Laake, J. L. (2020). *MarkedTMB*. <https://github.com/jlaake/MarkedTMB>
- Laake, J. L., Lowry, M. S., DeLong, R. L., Melin, S. R., & Carretta, J. V. (2018). Population growth and status of California sea lions. *The Journal of Wildlife Management*, 82(3), 583–595. <https://doi.org/10.1002/jwmg.21405>
- Lafferty, K. (2009). The ecology of climate change and infectious diseases. *Ecology*, 90(4), 888–900.

- Laughrin, L. L. (1977). *The island fox: A field study of its behavior and ecology* [PhD Thesis].  
University of California, Santa Barbara.
- Leggat, P. A. (2010). Tropical diseases of military importance: A Centennial Perspective.  
*Journal of Military and Veterans Health, 18*(4), 25.
- Levett, P. N. (2001). Leptospirosis. *Clinical Microbiology Reviews, 14*(2), 296–326.  
<https://doi.org/10.1128/CMR.14.2.296-326.2001>
- Levett, P. N. (2003). Usefulness of Serologic Analysis as a Predictor of the Infecting Serovar in  
Patients with Severe Leptospirosis. *Clinical Infectious Diseases, 36*(4), 447–452.  
<https://doi.org/10.1086/346208>
- Lloyd-Smith, J. O., George, D., Pepin, K. M., Pitzer, V. E., Pulliam, J. R. C., Dobson, A. P.,  
Hudson, P. J., & Grenfell, B. T. (2009). Epidemic Dynamics at the Human-Animal  
Interface. *Science, 326*(5958), 1362–1367.
- Lloyd-Smith, J. O., Greig, D. J., Hietala, S., Ghneim, G. S., Palmer, L., St Leger, J., Grenfell, B.  
T., & Gulland, F. M. (2007). Cyclical changes in seroprevalence of leptospirosis in  
California sea lions: Endemic and epidemic disease in one host species? *BMC Infectious  
Diseases, 7*, 125–136. <https://doi.org/10.1186/1471-2334-7-125>
- Lowry, M. S., & Forney, K. A. (2005). Abundance and distribution of California sea lions  
(*Zalophus californianus*) in central and northern California during 1998 and summer  
1999. *Fishery Bulletin, 103*(2), 331–343.
- Lowry, M. S., Melin, S., & Laake, J. L. (2017). Breeding season distribution and population  
growth of California sea lions, *Zalophus californianus*, in the United States during 1964-  
2014. *NOAA Technical Memorandum NMFS-SWFSC-574*, 66.  
<https://doi.org/10.7289/V5/TM-SWFSC-5>

- Mackenzie, R. B., Reiley, C. G., Alexander, A. D., Bruckner, E. A., Diercks, F. H., & Beye, H. K. (1966). An Outbreak of Leptospirosis among US Army Troops in the Canal Zone I. Clinical and Epidemiological Observations. *The American Journal of Tropical Medicine and Hygiene*, *15*(1), 57–63.
- Maniscalco, J. M., Wynne, K., Pitcher, K. W., Hanson, M. B., Melin, S. R., & Atkinson, S. (2004). The Occurrence of California Sea Lions (*Zalophus californianus*) in Alaska. *Aquatic Mammals*, *30*(3), 427–433. <https://doi.org/10.1578/AM.30.3.2004.427>
- Manly, B. F. J. (2017). *Randomization, Bootstrap and Monte Carlo Methods in Biology* (3rd ed.). Chapman and Hall/CRC. <https://doi.org/10.1201/9781315273075>
- McCrum, F. R., Stockard, J. L., Robinson, C. R., Turner, L. H., Levis, D. G., Maisey, C. W., Kelleher, M. F., Gleiser, C. A., & Smadel, J. E. (1957). Leptospirosis in Malaya I. Sporadic cases among military and civilian personnel. *The American Journal of Tropical Medicine and Hygiene*, *6*(2), 238–256.
- Melin, S. R., DeLong, R. L., & Siniff, D. B. (2008). The effects of El Niño on the foraging behavior of lactating California sea lions (*Zalophus californianus californianus*) during the nonbreeding season. *Canadian Journal of Zoology*, *86*, 192–206. <https://doi.org/10.1139/Z07-132>
- Melin, S. R., DeLong, R. L., & Thomason, J. R. (2000). Attendance patterns of California sea lion (*Zalophus californianus*) females and pups during the non-breeding season at San Miguel island. *Marine Mammal Science*, *16*(1), 169–185.
- Melin, S. R., Laake, J. L., DeLong, R. L., & Siniff, D. B. (2012). *Age-specific recruitment and natality of California sea lions at San Miguel Island, California*. *28*(4), 776.

- Melin, S. R., Orr, A. J., Harris, J. D., Laake, J. L., & DeLong, R. L. (2012). California sea lions: An indicator for integrated ecosystem assessment of the California current system. *California Cooperative Oceanic Fisheries Investigations Reports*, 53, 140–152.
- Melin, S. R., Orr, A. J., Harris, J. D., Laake, J. L., DeLong, R. L., Gulland, F. M. D., & Stoutd, S. (2010). Unprecedented mortality of California sea lion pups associated with anomalous oceanographic conditions along the central California coast in 2009. *California Cooperative Ocean and Fisheries Investigations Report 2009*, 51, 182–194.
- Meng, X. J., Lindsay, D. S., & Sriranganathan, N. (2009). Wild boars as sources for infectious diseases in livestock and humans. *Philosophical Transactions of the Royal Society B: Biological Sciences*, 364(1530), 2697–2707. <https://doi.org/10.1098/rstb.2009.0086>
- Menge, B., & Menge, D. (2013). Dynamics of coastal meta-ecosystems: The intermittent upwelling hypothesis and a test in rocky intertidal regions. *Ecological Monographs*, 83(3), 283–310. <https://doi.org/10.1890/07-1861.1>
- Meredith, M., & Krushke, J. (2018). *HDInterval: Highest (posterior) density intervals*. <https://rdrr.io/cran/HDInterval/man/hdi.html>
- Metcalf, C. J. E., Bjørnstad, O. N., Grenfell, B. T., & Andreasen, V. (2009). Seasonality and comparative dynamics of six childhood infections in pre-vaccination Copenhagen. *Proceedings of the Royal Society B: Biological Sciences*, 276(1676), 4111–4118. <https://doi.org/10.1098/rspb.2009.1058>
- Mittlböck, M., & Heinzl, H. (2002). Measures of explained variation in gamma regression models. *Communications in Statistics - Simulation and Computation*, 31(1), 61–73. <https://doi.org/10.1081/sac-9687282>

- Moore, S. M., Gilbert, A., Vos, A., Freuling, C. M., Ellis, C., Kliemt, J., & Müller, T. (2017). Rabies Virus Antibodies from Oral Vaccination as a Correlate of Protection against Lethal Infection in Wildlife. *Tropical Medicine and Infectious Disease*, 2(3), 31. <https://doi.org/10.3390/tropicalmed2030031>
- Morris, D. H., Yinda, K. C., Gamble, A., Rossine, F. W., Huang, Q., Bushmaker, T., Fischer, R. J., Matson, M. J., Van Doremalen, N., Vikesland, P. J., Marr, L. C., Munster, V. J., & Lloyd-Smith, J. O. (2021). Mechanistic theory predicts the effects of temperature and humidity on inactivation of SARS-CoV-2 and other enveloped viruses. *ELife*, 10, e65902. <https://doi.org/10.7554/eLife.65902>
- Mummah, R. O., Hoff, N. A., Rimoin, A. W., & Lloyd-Smith, J. O. (2020). Controlling emerging zoonoses at the animal-human interface. *One Health Outlook*, 2(1), 17. <https://doi.org/10.1186/s42522-020-00024-5>
- Nams, V. O. (1990). *Locate II* [Pacer Comput. Software].
- Nettles, V. F., Corn, J. L., Erickson, G. A., & Jessup, D. A. (1989). A survey of wild swine in the United States for evidence of hog cholera. *Journal of Wildlife Diseases*, 25(1), 61–65. <https://doi.org/10.7589/0090-3558-25.1.61>
- Odell, D. K. (1981). California sea lion, *Zalophus californianus* (Lesson, 1828). In S. H. Ridgeway & R. J. Harrison (Eds.), *Handbook of marine mammals. Vol. 1. The walrus, sea lions, fur seals, and sea otter* (pp. 67–97). Academic Press, London.
- Page, A. J., Cummins, C. A., Hunt, M., Wong, V. K., Reuter, S., Holden, M. T. G., Fookes, M., Falush, D., Keane, J. A., & Parkhill, J. (2015). Roary: Rapid large-scale prokaryote pan genome analysis. *Bioinformatics*, 31(22), 3691–3693. <https://doi.org/10.1093/bioinformatics/btv421>

- Panaphut, T., Domrongkitchaiporn, S., & Thinkamrop, B. (2002). Prognostic factors of death in leptospirosis: A prospective cohort study in Khon Kaen, Thailand. *Int J Infect Dis*, 6, 52–59.
- Pedersen, K., Pabilonia, K. L., Anderson, T. D., Bevins, S. N., Hicks, C. R., Kloft, J. M., & Deliberto, T. J. (2015). Widespread detection of antibodies to *Leptospira* in feral swine in the United States. *Epidemiology and Infection*, 143(10), 2131–2136.  
<https://doi.org/10.1017/S0950268814003148>
- Pedersen, T. L. (2019). *patchwork: The composer of plots*. <https://patchwork.data-imaginist.com/reference/index.html>
- Pedersen, T., & Robinson, D. (2019). *gganimate: A grammar of animated graphics* (R package version 1.0.3).
- Pepin, K. M., Kay, S. L., Golas, B. D., Shriner, S. S., Gilbert, A. T., Miller, R. S., Graham, A. L., Riley, S., Cross, P. C., Samuel, M. D., Hooten, M. B., Hoeting, J. A., Lloyd-Smith, J. O., Webb, C. T., & Buhnerkempe, M. G. (2017). Inferring infection hazard in wildlife populations by linking data across individual and population scales. *Ecology Letters*, 20(3), 275–292. <https://doi.org/10.1111/ele.12732>
- Pepin, K. M., Pedersen, K., Wan, X.-F., Cunningham, F. L., Webb, C. T., & Wilber, M. Q. (2019). Individual-Level Antibody Dynamics Reveal Potential Drivers of Influenza A Seasonality in Wild Pig Populations. *Integrative and Comparative Biology*, 59(5), 1231–1242. <https://doi.org/10.1093/icb/icz118>
- Peterson, R. S., & Bartholomew, G. A. (1967). *The natural history and behavior of the California sea lion*. The American Society of Mammologists.
- Plummer, M. (2019). *rjags: Bayesian Graphical Models using MCMC*. <https://rdrr.io/cran/rjags/>

- Pollock, K. H., Winterstein, S. R., Bunck, C. M., & Curtis, P. D. (1989). Survival Analysis in Telemetry Studies: The Staggered Entry Design. *The Journal of Wildlife Management*, 53(1), 7–15. <https://doi.org/10.2307/3801296>
- Pothin, E., Ferguson, N. M., Drakeley, C. J., & Ghani, A. C. (2016). Estimating malaria transmission intensity from Plasmodium falciparum serological data using antibody density models. *Malaria Journal*, 15(1), 79. <https://doi.org/10.1186/s12936-016-1121-0>
- Prager, K. C., Alt, D. P., Buhnerkempe, M. G., Greig, D. J., Galloway, R. L., Wu, Q., Gulland, F. M. D., & Lloyd-Smith, J. O. (2015). Antibiotic Efficacy in Eliminating Leptospiruria in California Sea Lions (*Zalophus californianus*) Stranding with Leptospirosis. *Aquatic Mammals*, 41(2), 203–212. <https://doi.org/doi:10.1578/AM.41.2.2015.203>
- Prager, K. C., Buhnerkempe, M. G., Greig, D. J., Orr, A. J., Jensen, E. D., Gomez, F., Galloway, R. L., Wu, Q., Gulland, F. M. D., & Lloyd-Smith, J. O. (2020). Linking longitudinal and cross-sectional biomarker data to understand host-pathogen dynamics: *Leptospira* in California sea lions (*Zalophus californianus*) as a case study. *PLOS Neglected Tropical Diseases*, 14(6), e0008407. <https://doi.org/10.1371/journal.pntd.0008407>
- Prager, K. C., Greig, D. J., Alt, D. P., Galloway, R. L., Hornsby, R. L., Palmer, L. J., Soper, J., Wu, Q., Zuerner, R. L., Gulland, F. M., & Lloyd-Smith, J. O. (2013). Asymptomatic and chronic carriage of *Leptospira interrogans* serovar Pomona in California sea lions (*Zalophus californianus*). *Veterinary Microbiology*, 164(1–2), 177–183. <https://doi.org/10.1016/j.vetmic.2013.01.032>
- R Core Team. (2018). *R: A language and environment for statistical computing*. R Foundation for Statistical Computing.

- R Core Team. (2019). *R: A language and environment for statistical computing*. R Foundation for Statistical Computing. <http://www.r-project.org>
- R Core Team. (2021). *R: A language and environment for statistical computing*. R Foundation for Statistical Computing. <https://www.R-project.org/>
- Racine, J. (2000). Consistent cross-validators model-selection for dependent data: Hv-block cross-validation. *Journal of Econometrics*, *99*, 39–61. [https://doi.org/10.1016/S0304-4076\(00\)00030-0](https://doi.org/10.1016/S0304-4076(00)00030-0)
- Ralls, K., Sanchez, J. N., Savage, J., Coonan, T. J., Hudgens, B. R., & Cypher, B. L. (2013). Social relationships and reproductive behavior of island foxes inferred from proximity logger data. *Journal of Mammalogy*, *94*(6), 1185–1196. <https://doi.org/10.1644/13-MAMM-A-057.1>
- Rambaut, A., Drummond, A. J., Xie, D., Baele, G., & Suchard, M. A. (2018). Posterior Summarization in Bayesian Phylogenetics Using Tracer 1.7. *Systematic Biology*, *67*(5), 901–904. <https://doi.org/10.1093/sysbio/syy032>
- Randhawa, N., Gulland, F., Ylitalo, G. M., DeLong, R., & Mazet, J. A. K. (2015). Sentinel California sea lions provide insight into legacy organochlorine exposure trends and their association with cancer and infectious disease. *One Health*, *1*, 37–43. <https://doi.org/10.1016/j.onehlt.2015.08.003>
- Robinson, J. A., Ortega-Del Vecchyo, D., Fan, Z., Kim, B. Y., vonHoldt, B. M., Marsden, C. D., Lohmueller, K. E., & Wayne, R. K. (2016). Genomic Flatlining in the Endangered Island Fox. *Current Biology: CB*, *26*(9), 1183–1189. <https://doi.org/10.1016/j.cub.2016.02.062>

- Rodo, X., Pascual, M., Fuchs, G., & Faruque, A. (2002). ENSO and cholera: A nonstationary link related to climate change? *Proceedings of the National Academy of Sciences of the United States of America*, *99*(20), 12901–12906. <https://doi.org/10.1073/pnas.182203999>
- Roemer, G. W. (1999). *The ecology and conservation of the island fox (Urocyon littoralis)*. UCLA.
- Roemer, G. W., Coonan, T. J., Garcelon, D. K., Bascompte, J., & Laughrin, L. (2001). Feral pigs facilitate hyperpredation by golden eagles and indirectly cause the decline of the island fox. *Animal Conservation*, *4*, 307–318.
- Roemer, G. W., Donlan, C. J., & Courchamp, F. (2002). Golden eagles, feral pigs, and insular carnivores: How exotic species turn native predators into prey. *Proceedings of the National Academy of Sciences*, *99*(2), 791–796.
- Roemer, G. W., Smith, D. A., Garcelon, D. K., & Wayne, R. K. (2001). The behavioural ecology of the island fox (*Urocyon littoralis*). *Journal of Zoology*, *255*(1), 1–14.
- Rogers, D. J., Randolph, S. E., Snow, R. W., & Hay, S. I. (2002). Satellite imagery in the study and forecast of malaria. *Nature*, *415*(6872), 710–715. <https://doi.org/10.1038/415710a>
- Röltgen, K., Powell, A. E., Wirz, O. F., Stevens, B. A., Hogan, C. A., Najeeb, J., Hunter, M., Wang, H., Sahoo, M. K., Huang, C., Yamamoto, F., Manohar, M., Manalac, J., Otrelo-Cardoso, A. R., Pham, T. D., Rustagi, A., Rogers, A. J., Shah, N. H., Blish, C. A., ... Boyd, S. D. (2020). Defining the features and duration of antibody responses to SARS-CoV-2 infection associated with disease severity and outcome. *Science Immunology*, *5*(54), eabe0240. <https://doi.org/10.1126/sciimmunol.abe0240>
- Russell, K. L., Gonzalez, M. A. M., Watts, D. M., Lagos-Figueroa, R. C., Chauca, G., Ore, M., Gonzalez, J. E., Moron, C., Tesh, R. B., & Vinetz, J. M. (2003). An outbreak of

- leptospirosis among Peruvian military recruits. *The American Journal of Tropical Medicine and Hygiene*, 69(1), 53–57.
- Sanchez, J. N., & Hudgens, B. R. (2019). Impacts of heterogeneous host densities and contact rates on pathogen transmission in the Channel Island fox (*Urocyon littoralis*). *Biological Conservation*, 236, 593–603. <https://doi.org/10.1016/j.biocon.2019.05.045>
- Sanchez, J. N., & Hudgens, B. R. (2020). Vaccination and monitoring strategies for epidemic prevention and detection in the Channel Island fox (*Urocyon littoralis*). *PLOS ONE*, 15(5), e0232705. <https://doi.org/10.1371/journal.pone.0232705>
- Santos, R. F. dos, Silva, G. C. P. da, Assis, N. A. de, & Mathias, L. A. (2016). Agglutinins to *Leptospira* spp. in equines slaughtered in the southern region of Brazil. *Semina: Ciências Agrárias*, 37(2), 841. <https://doi.org/10.5433/1679-0359.2016v37n2p841>
- Schwing, F. B., Bond, N. A., Bograd, S. J., Mitchell, T., Alexander, M. A., & Mantua, N. (2006). Delayed coastal upwelling along the U.S. West Coast in 2005. *Geophysical Research Letters*, 33, L22S01.
- Sehgal, S., Murhekar, M., & Sugunan, A. (1995). Outbreak of leptospirosis with pulmonary involvement in north Andaman. *Indian J Med Res*, 102, 9–12.
- Simonsen, J., Mølbak, K., Falkenhorst, G., Krogfelt, K. A., Linneberg, A., & Teunis, P. F. M. (2009). Estimation of incidences of infectious diseases based on antibody measurements. *Statistics in Medicine*, 28(14), 1882–1895. <https://doi.org/10.1002/sim.3592>
- Smith, C., Skelly, C., Kung, N., Roberts, B., & Field, H. (2014). Flying-Fox Species Density—A Spatial Risk Factor for Hendra Virus Infection in Horses in Eastern Australia. *PLOS ONE*, 9(6), e99965. <https://doi.org/10.1371/journal.pone.0099965>

- Smith, M. J., Telfer, S., Kallio, E. R., Burthe, S., Cook, A. R., Lambin, X., & Begon, M. (2009). Host–pathogen time series data in wildlife support a transmission function between density and frequency dependence. *Proceedings of the National Academy of Sciences*, *106*(19), 7905–7909.
- Stewart, B., Yochem, P., & Francis, J. (1991). Seasonal and Annual Variability in the Diet of California Sea Lions *Zalophus californianus* at San Nicolas. *Fishery Bulletin*, *89*.
- Streltsoff, C. C., Vijaykrishna, D., Riley, S., Guan, Y., Peiris, J. S. M., & Lloyd-Smith, J. O. (2013). Inferring patterns of influenza transmission in swine from multiple streams of surveillance data. *Proceedings of the Royal Society B: Biological Sciences*, *280*(1762), 20130872. <https://doi.org/10.1098/rspb.2013.0872>
- Sturtz, S., Ligges, U., & Gelman, A. (2005). R2WinBUGS: A Package for Running WinBUGS from R. *Journal of Statistical Software*, *12*(1), 1–16. <https://doi.org/10.18637/jss.v012.i03>
- Suchard, M. A., Lemey, P., Baele, G., Ayres, D. L., Drummond, A. J., & Rambaut, A. (2018). Bayesian phylogenetic and phylodynamic data integration using BEAST 1.10. *Virus Evolution*, *4*(1). <https://doi.org/10.1093/ve/vey016>
- Sun, J. (2006). *The statistical analysis of interval-censored failure time data*. Springer.
- Szeredi, L., & Haake, D. A. (2006). Immunohistochemical identification and pathologic findings in natural cases of equine abortion caused by leptospiral infection. *Veterinary Pathology*, *43*(5), 755–761. <https://doi.org/10.1354/vp.43-5-755>
- Tabel, H., & Karstad, L. (1967). The renal carrier state of experimental *Leptospira pomona* infections in skunks (*Mephitis mephitis*). *American Journal of Epidemiology*, *85*(1), 9–16.

- Tersago, K., Crespin, L., Verhagen, R., & Leirs, H. (2012). Impact of Puumala virus infection on maturation and survival in bank voles: A capture-mark-recapture analysis. *Journal of Wildlife Diseases*, *48*(1), 148–156. <https://doi.org/10.7589/0090-3558-48.1.148>
- Teunis, P. F. M., Eijkeren, J. van, Ang, C. W., Duynhoven, Y. van, Simonsen, J. B., Strid, M. A., & Pelt, W. van. (2012). Biomarker dynamics: Estimating infection rates from serological data. *Statistics in Medicine*, *31*(20), 2240–2248. <https://doi.org/10.1002/sim.5322>
- Teunis, P. F. M., van der Heijden, O. G., de Melker, H. E., Schellekens, J. F. P., Versteegh, F. G. A., & Kretzschmar, M. E. E. (2002). Kinetics of the IgG antibody response to pertussis toxin after infection with *B. pertussis*. *Epidemiology and Infection*, *129*(3), 479–489. <https://doi.org/10.1017/s0950268802007896>
- Teunis, P. F. M., van Eijkeren, J. C. H., de Graaf, W. F., Marinović, A. B., & Kretzschmar, M. E. E. (2016). Linking the seroresponse to infection to within-host heterogeneity in antibody production. *Epidemics*, *16*, 33–39. <https://doi.org/10.1016/j.epidem.2016.04.001>
- Therneau, T. (2021). *A Package for Survival Analysis in R* (R package version 3.2-11) [Computer software]. <https://CRAN.R-project.org/package=survival>
- Timm, S. F., Munson, L., Summers, B. A., Terio, K. A., Dubovi, E. J., Rupprecht, C. E., Kapil, S., & Garcelon, D. K. (2009). A suspected canine distemper epidemic as the cause of a catastrophic decline in Santa Catalina Island foxes (*Urocyon littoralis catalinae*). *Journal of Wildlife Diseases*, *45*(2), 333–343. <https://doi.org/10.7589/0090-3558-45.2.333>
- Traggiai, E., Puzone, R., & Lanzavecchia, A. (2003). Antigen dependent and independent mechanisms that sustain serum antibody levels. *Vaccine*, *21 Suppl 2*, S35-37. [https://doi.org/10.1016/s0264-410x\(03\)00198-1](https://doi.org/10.1016/s0264-410x(03)00198-1)

- Trillmich, F., Ono, K., Costa, D., DeLong, R., Feldkamp, S., Francis, J., Gentry, R. L., Heath, C., LeBoeuf, B., & Majluf, P. (1991). The effects of El Nino on pinniped populations in the eastern Pacific. *Ecological Studies*, *88*, 247–270.
- Trueba, G., Zapata, S., Madrid, K., Cullen, P., & Haake, D. (2004). Cell aggregation: A mechanism of pathogenic *Leptospira* to survive in fresh water. *International Microbiology*, *7*(1), 35–40.
- Tunbridge, A., Dockrell, D., Channer, K., & McKendrick, M. (2002). A breathless triathlete. *The Lancet*, *359*(9301), 130. [https://doi.org/10.1016/S0140-6736\(02\)07372-5](https://doi.org/10.1016/S0140-6736(02)07372-5)
- Van Doremalen, N., Bushmaker, T., Morris, D. H., Holbrook, M. G., Gamble, A., Williamson, B. N., Tamin, A., Harcourt, J. L., Thornburg, N. J., Gerber, S. I., & others. (2020). Aerosol and surface stability of SARS-CoV-2 as compared with SARS-CoV-1. *New England Journal of Medicine*, *382*(16), 1564–1567.
- Vandormael, A., Tanser, F., Cuadros, D., & Dobra, A. (2020). Estimating trends in the incidence rate with interval censored data and time-dependent covariates. *Statistical Methods in Medical Research*, *29*(1), 272–281. <https://doi.org/10.1177/0962280219829892>
- Varni, V., Ruybal, P., Lauthier, J. J., Tomasini, N., Brihuega, B., Koval, A., & Caimi, K. (2014). Reassessment of MLST schemes for *Leptospira* spp. Typing worldwide. *Infection, Genetics and Evolution*, *22*, 216–222. <https://doi.org/10.1016/j.meegid.2013.08.002>
- Vaughn, D. W., Green, S., Kalayanarooj, S., Innis, B. L., Nimmannitya, S., Suntayakorn, S., Endy, T. P., Raengsakulrach, B., Rothman, A. L., Ennis, F. A., & Nisalak, A. (2000). Dengue Viremia Titer, Antibody Response Pattern, and Virus Serotype Correlate with Disease Severity. *The Journal of Infectious Diseases*, *181*(1), 2–9. <https://doi.org/10.1086/315215>

- Vedros, N. A., Smith, A. W., Schonewald, J., Migaki, G., & Hubbard, R. C. (1971).  
Leptospirosis Epizootic among California Sea Lions. *Science*, 172(3989), 1250–1251.  
<https://doi.org/10.1126/science.172.3989.1250>
- Vega Thurber, R., Mydlarz, L. D., Brandt, M., Harvell, D., Weil, E., Raymundo, L., Willis, B. L., Langevin, S., Tracy, A. M., Littman, R., Kemp, K. M., Dawkins, P., Prager, K. C., Garren, M., & Lamb, J. (2020). Deciphering Coral Disease Dynamics: Integrating Host, Microbiome, and the Changing Environment. *Frontiers in Ecology and Evolution*, 8, 402.  
<https://doi.org/10.3389/fevo.2020.575927>
- Vehtari, A., Gabry, J., Magnusson, M., Yao, Y., Bürkner, P.-C., Paananen, T., & Gelman, A. (2020). *loo: Efficient leave-one-out cross-validation and WAIC for Bayesian models*.  
<https://mc-stan.org/loo/>
- Vehtari, A., Gelman, A., & Gabry, J. (2017). Practical Bayesian model evaluation using leave-one-out cross-validation and WAIC. *Statistics and Computing*, 27(5), 1413–1432.  
<https://doi.org/10.1007/s11222-016-9696-4>
- Venables, W. N., & Ripley, B. D. (2002). *Modern Applied Statistics with S* (4th ed.). Springer-Verlag. <https://doi.org/10.1007/978-0-387-21706-2>
- Vespignani, A., Tian, H., Dye, C., Lloyd-Smith, J. O., Eggo, R. M., Shrestha, M., Scarpino, S. V., Gutierrez, B., Kraemer, M. U., Wu, J., & others. (2020). Modelling covid-19. *Nature Reviews Physics*.
- Weise, M. J., Costa, D. P., & Kudela, R. M. (2006). Movement and diving behavior of male California sea lion (*Zalophus californianus*) during anomalous oceanographic conditions of 2005 compared to those of 2004. *Geophysical Research Letters*, 33(22).  
<https://doi.org/10.1029/2006gl027113>

- Weitz, J. S., Beckett, S. J., Coenen, A. R., Demory, D., Dominguez-Mirazo, M., Dushoff, J., Leung, C.-Y., Li, G., Măgălie, A., Park, S. W., Rodriguez-Gonzalez, R., Shivam, S., & Zhao, C. Y. (2020). Modeling shield immunity to reduce COVID-19 epidemic spread. *Nature Medicine*, 26(6), 849–854. <https://doi.org/10.1038/s41591-020-0895-3>
- Wickham, H. (2016). *ggplot2: Elegant Graphics for Data Analysis* (2nd ed.). Springer International Publishing. <https://doi.org/10.1007/978-3-319-24277-4>
- Wickham, H., François, R., Henry, L., & Müller, K. (2019a). *dplyr: A grammar of data manipulation* (R package version 0.8.1).
- Wilber, M. Q., Webb, C. T., Cunningham, F. L., Pedersen, K., Wan, X.-F., & Pepin, K. M. (2020). Inferring seasonal infection risk at population and regional scales from serology samples. *Ecology*, 101(1), e02882. <https://doi.org/10.1002/ecy.2882>
- Wilke, C. O. (2020). *ggridges: Ridgelines plots in “ggplot2.”* <https://cran.r-project.org/web/packages/ggridges/vignettes/introduction.html>
- Wood, J. E. (1958). Age Structure and Productivity of a Gray Fox Population. *Journal of Mammalogy*, 39(1), 74–86. <https://doi.org/10.2307/1376612>
- Wood, S. (2011). Fast stable restricted maximum likelihood and marginal likelihood estimation of semiparametric generalized linear models. *Journal of the Royal Statistical Society (B)*, 73(1), 3–36.
- Wood, S. N. (2017). *Generalized additive models: An introduction with R*. CRC press.
- Wood, S. N., Pya, N., & Säfken, B. (2016). Smoothing Parameter and Model Selection for General Smooth Models. *Journal of the American Statistical Association*, 17.
- World Health Organization. (2011). *Report of the second meeting of the leptospirosis burden epidemiology reference group.* (p. 37).

- Wu, Q., Prager, K. C., Goldstein, T., D.P., A., Galloway, R. L., Zuerner, R. L., Lloyd-Smith, J., & Schwacke, L. (2014). Development of a real-time PCR for the detection of pathogenic *Leptospira* spp. In California sea lions. *Diseases of Aquatic Organisms*, *110*(3), 165–172. <https://doi.org/10.3354/dao02752>
- Zhang, Z., Reinikainen, J., Adeleke, K. A., Pieterse, M. E., & Groothuis-Oudshoorn, C. G. M. (2018). Time-varying covariates and coefficients in Cox regression models. *Annals of Translational Medicine*, *6*(7), 121–121. <https://doi.org/10.21037/atm.2018.02.12>
- Zuerner, R. L., & Alt, D. P. (2009). Variable Nucleotide Tandem-Repeat Analysis Revealing a Unique Group of *Leptospira interrogans* Serovar Pomona Isolates Associated with California Sea Lions. *Journal of Clinical Microbiology*, *47*(4), 1202–1205. <https://doi.org/10.1128/JCM.01639-08>
- Zuerner, R. L., & Bolin, C. A. (1997). Differentiation of *Leptospira interrogans* isolates by IS1500 hybridization and PCR assays. *Journal of Clinical Microbiology*, *35*(10), 2612–2617. <https://doi.org/10.1128/jcm.35.10.2612-2617.1997>

## 9. Appendices

### Appendix A. Supporting Data

#### *Supporting data for 5.1.2. and 6.1.2.*

Location data for seven foxes with time of infection estimates before 2006. Data and metadata can be found at: <https://github.com/rileyo/foxserdp/blob/master/spatialdata2004-06.csv>.

#### *Supporting data for 5.1.3. and 6.1.3.*

Sample Name	Batch	Year	Host	Sample tissue	Included in tree
CSL06-048_S14	3	1988	CSL	Kidney	x
CSL06-048_S22	2	1988	CSL	Kidney	
CSL10029_S4	1	2011	CSL	Urine	x
CSL10039_S5	1	2011	CSL	Kidney	x
CSL10040_S15	3	2011	CSL	Kidney	x
CSL10040_S6	1	2011	CSL	Kidney	
CSL10052_S8	1	2011	CSL	Kidney	x
CSL10082_S9	1	2011	CSL	Kidney	x
CSL10082K-1_S23	3	2011	CSL	Kidney	
CSL10082K-2_S24	3	2011	CSL	Kidney	
CSL10083_S10	1	2011	CSL	Kidney	
CSL10083_S7	2	2011	CSL	Urine	x
CSL10083K_S22	3	2011	CSL	Kidney	
CSL10083U_S21	3	2011	CSL	Urine	
CSL10084_S11	1	2011	CSL	Kidney	
CSL10084_S8	2	2011	CSL	Urine	x
CSL10087_S12	1	2011	CSL	Kidney	
CSL10087_S9	2	2011	CSL	Urine	x
CSL10097_S16	1	2011	CSL	Kidney	x
CSL10101_S10	2	2011	CSL	Urine	x
CSL10101_S13	1	2011	CSL	Kidney	
CSL10113_S14	1	2011	CSL	Kidney	x
CSL10120_S15	1	2011	CSL	Kidney	x
CSL10442_S11	3	2012	CSL	Urine	x
CSL11-224_S19	2	2011	CSL	Kidney	x
CSL209-11_S18	1	2011	CSL	Urine	x
CSL215-11_S19	1	2011	CSL	Urine	x

CSL31_S17	1	2010	CSL	Urine	
CSL31U_S18	3	2010	CSL	Urine	x
CSL5651-11_S20	1	2011	CSL	Urine	x
CSL6175_S1	1	2004	CSL	Kidney	x
CSL6187_S11	2	2004	CSL	Kidney	x
CSL6210_S17	3	2004	CSL	Kidney	x
CSL6210_S18	2	2004	CSL	Kidney	
CSL6434-11_S3	3	2011	CSL	Urine	x
CSL7091_S12	2	2006	CSL	Kidney	x
CSL7108_S13	2	2006	CSL	Kidney	x
CSL7374-12_S24	2	2011	CSL	Urine	x
CSL7522_S14	2	2007	CSL	Unknown	x
CSL7522_S20	2	2007	CSL	Unknown	
CSL7525_S16	2	2007	CSL	Kidney	x
CSL7533_S15	2	2007	CSL	Kidney	x
CSL7703-12_S10	3	2012	CSL	Urine	x
CSL7905_S17	2	2008	CSL	Unknown	x
CSL7905_S21	2	2008	CSL	Unknown	
CSL9784_S7	1	2011	CSL	Kidney	x
CSL9887_S2	1	2010	CSL	Kidney	
CSL9887_S19	3	2010	CSL	Kidney	x
CSL9979_S3	1	2011	CSL	Kidney	x
ES077_S16	3	2011	ES	Kidney	x
ES077_S24	1	2011	ES	Kidney	
ES3197_S21	1	2011	ES	Kidney	x
ES3197_S22	1	2011	ES	Urine	
ES3208_S23	1	2011	ES	Urine	x
Fox23850_S1	3	2015	Fox	Urine	x
Fox24024_S4	3	2017	Fox	Urine	x
Fox24072_S23	2	2015	Fox	Urine	x
Fox32256_S3	2	2011	Fox	Urine	x
Fox36401_S2	2	2011	Fox	Urine	x
Fox86076_S8	3	2013	Fox	Urine	x
Fox87536_S2	3	2013	Fox	Urine	x
FoxC0D60_S4	2	2011	Fox	Urine	x
FoxC6561_S9	3	2013	Fox	Urine	x
FoxE6D47_S1	2	2011	Fox	Urine	x
SkunkA0451_S5	2	2011	Spotted skunk	Urine	x
SkunkE7B4A_S20	3	2011	Spotted skunk	Urine	
SkunkE7B4A_S6	2	2011	Spotted skunk	Urine	x

**Table A.1. Sequenced genomes from four host species in the Coastal California Ecosystem.**

MLST Scheme	ST	Allele ID												
		glmU	pntA	sucA	tpiA	pfkB	mreA	caiB	adk	icdA	LipL32	LipL41	rrs2	secY
Scheme #1 [Boonsilp 2013]	140	3	3	3	3	4	5	16						
Scheme #2 [Varni 2014]	52	2	3				1		3	2	10	4		
Scheme #3 [Ahmed 2006]	58								2	2	3	4	2	6

**Table A.2. Multi-locus strain typing (MLST) results.** Isolates were analyzed against the three published MLST schemes and all resulted in the same strain type and allele reference numbers for each scheme.

***Supporting data for 5.3.2.4. and 6.3.2.4.***

Intervals of time-at-risk for 1226 foxes for analyzing risk factors for infections. Data and metadata can be found at: <https://github.com/rileyo/foxserdp/blob/master/survivalIntervals.csv>

***Supporting data for 5.3.4. and 6.3.4.***

The data and metadata for the fox transmission model can be found at:  
[https://github.com/bennyborremans/fox\\_lepto\\_data](https://github.com/bennyborremans/fox_lepto_data)

The data for the CSL outbreak model can be found at:  
[https://github.com/bennyborremans/CSL\\_lepto\\_outbreak\\_model](https://github.com/bennyborremans/CSL_lepto_outbreak_model)

## Appendix B. List of Scientific/Technical Publications

1. Articles in peer-reviewed journals
  - a. In print
    - i. Becker, D. J., Washburne, A. D., Faust, C. L., Pulliam, J. R. C., Mordecai, E. A., Lloyd-Smith, J. O., & Plowright, R. K. (2019). Dynamic and integrative approaches to understanding pathogen spillover. *Philosophical Transactions of the Royal Society B: Biological Sciences*, 374(1782), 20190014. <https://doi.org/10.1098/rstb.2019.0014>
    - ii. Borremans, B., Faust, C., Manlove, K. R., Sokolow, S. H., & Lloyd-Smith, J. O. (2019). Cross-species pathogen spillover across ecosystem boundaries: Mechanisms and theory. *Philosophical Transactions of the Royal Society B: Biological Sciences*, 374(1782), 20180344. <https://doi.org/10.1098/rstb.2018.0344>
    - iii. Borremans, B., Gamble, A., Prager, K., Helman, S. K., McClain, A. M., Cox, C., Savage, V., & Lloyd-Smith, J. O. (2020). Quantifying antibody kinetics and RNA detection during early-phase SARS-CoV-2 infection by time since symptom onset. *ELife*, 9, e60122. <https://doi.org/10.7554/eLife.60122>
    - iv. Buhnerkempe, M. G., Prager, K. C., Strelhoff, C. C., Greig, D. J., Laake, J. L., Melin, S. R., DeLong, R. L., Gulland, F. M., & Lloyd-Smith, J. O. (2017). Detecting signals of chronic shedding to explain pathogen persistence: *Leptospira interrogans* in California sea lions. *Journal of Animal Ecology*, 86(3), 460–472. <https://doi.org/10.1111/1365-2656.12656>
    - v. DeRango, E. J., Prager, K. C., Greig, D. J., Hooper, A. W., & Crocker, D. E. (2020). Climate variability and life history impact stress, thyroid, and immune markers in California sea lions (*Zalophus californianus*) during El Niño conditions. *Conservation Physiology*, 7(1). <https://doi.org/10.1093/conphys/coz010>
    - vi. Fischer, R. J., Morris, D. H., van Doremalen, N., Sarchette, S., Matson, M. J., Bushmaker, T., Yinda, C. K., Seifert, S. N., Gamble, A., Williamson, B. N., & others. (2020). Effectiveness of N95 respirator decontamination and reuse against SARS-CoV-2 virus. *Emerging Infectious Diseases*.
    - vii. Gamble, A., Bazire, R., Delord, K., Barbraud, C., Jaeger, A., Gantelet, H., Thibault, E., Lebarbenchon, C., Lagadec, E., Tortosa, P., Weimerskirch, H., Thiebot, J.-B., Garnier, R., Tornos, J., & Boulinier, T. (2020). Predator and scavenger movements among and within endangered seabird colonies: Opportunities for pathogen spread. *Journal of Applied Ecology*, 57(2), 367–378. <https://doi.org/10.1111/1365-2664.13531>

- viii. Gamble, A., Fischer, R. J., Morris, D. H., Yinda, K. C., Munster, V. J., & Lloyd-Smith, J. O. (2021). Heat-treated virus inactivation rate depends strongly on treatment procedure: Illustration with SARS-CoV-2. *BioRxiv*, 2020.08.10.242206. <https://doi.org/10.1101/2020.08.10.242206>
- ix. Gostic, K., Gomez, A. C., Mummah, R. O., Kucharski, A. J., & Lloyd-Smith, J. O. (2020). Estimated effectiveness of symptom and risk screening to prevent the spread of COVID-19. *ELife*, 9, e55570.
- x. Gostic, K. M., Bridge, R., Brady, S., Viboud, C., Worobey, M., & Lloyd-Smith, J. O. (2019). Childhood immune imprinting to influenza A shapes birth year-specific risk during seasonal H1N1 and H3N2 epidemics. *PLOS Pathogens*, 15(12), e1008109. <https://doi.org/10.1371/journal.ppat.1008109>
- xi. Gostic, K. M., Wunder, E. A., Bisht, V., Hamond, C., Julian, T. R., Ko, A. I., & Lloyd-Smith, J. O. (2019). Mechanistic dose–response modelling of animal challenge data shows that intact skin is a crucial barrier to leptospiral infection. *Philosophical Transactions of the Royal Society B: Biological Sciences*, 374(1782), 20190367. <https://doi.org/10.1098/rstb.2019.0367>
- xii. Helman, S. K., Mummah, R. O., Gostic, K. M., Buhnerkempe, M. G., Prager, K. C., & Lloyd-Smith, J. O. (2020). Estimating prevalence and test accuracy in disease ecology: How Bayesian latent class analysis can boost or bias imperfect test results. *Ecology and Evolution*, 10(14), 7221–7232. <https://doi.org/10.1002/ece3.6448>
- xiii. Island Spotted Skunk Working Group. (2020). Island Spotted Skunk Conservation Plan. <http://www.californiaislands.net/skunks>
- xiv. Jaeger, A., Gamble, A., Lagadec, E., Lebarbenchon, C., Bourret, V., Tornos, J., Barbraud, C., Lemberger, K., Delord, K., Weimerskirch, H., Thiebot, J.-B., Boulinier, T., & Tortosa, P. (2020). Impact of Annual Bacterial Epizootics on Albatross Population on a Remote Island. *EcoHealth*, 17(2), 194–202. <https://doi.org/10.1007/s10393-020-01487-8>
- xv. Morris, D. H., Yinda, K. C., Gamble, A., Rossine, F. W., Huang, Q., Bushmaker, T., Fischer, R. J., Matson, M. J., & van Doremalen, N. (2020). The effect of temperature and humidity on the stability of SARS-CoV-2 and other enveloped viruses. *BioRxiv*, 33.
- xvi. Morris, D. H., Yinda, K. C., Gamble, A., Rossine, F. W., Huang, Q., Bushmaker, T., Fischer, R. J., Matson, M. J., Van Doremalen, N., Vikesland, P. J., Marr, L. C., Munster, V. J., & Lloyd-Smith, J. O. (2021). Mechanistic theory predicts the effects of temperature and humidity on inactivation of SARS-CoV-2 and other enveloped viruses. *ELife*, 10, e65902. <https://doi.org/10.7554/eLife.65902>

- xvii. Mummah, R. O., Hoff, N. A., Rimoin, A. W., & Lloyd-Smith, J. O. (2020). Controlling emerging zoonoses at the animal-human interface. *One Health Outlook*, 2(1), 17. <https://doi.org/10.1186/s42522-020-00024-5>
- xviii. Neely, B. A., Prager, K. C., Bland, A. M., Fontaine, C., Gulland, F. M., & Janech, M. G. (2018). Proteomic Analysis of Urine from California Sea Lions (*Zalophus californianus*): A Resource for Urinary Biomarker Discovery. *Journal of Proteome Research*, 17(9), 3281–3291. <https://doi.org/10.1021/acs.jproteome.8b00416>
- xix. Plowright, R. K., Parrish, C. R., McCallum, H., Hudson, P. J., Ko, A. I., Graham, A. L., & Lloyd-Smith, J. O. (2017). Pathways to zoonotic spillover. *Nature Reviews Microbiology*, 15(8), 502–510. <https://doi.org/10.1038/nrmicro.2017.45>
- xx. Prager, K. C., Buhnerkempe, M. G., Greig, D. J., Orr, A. J., Jensen, E. D., Gomez, F., Galloway, R. L., Wu, Q., Gulland, F. M. D., & Lloyd-Smith, J. O. (2020). Linking longitudinal and cross-sectional biomarker data to understand host-pathogen dynamics: *Leptospira* in California sea lions (*Zalophus californianus*) as a case study. *PLOS Neglected Tropical Diseases*, 14(6), e0008407. <https://doi.org/10.1371/journal.pntd.0008407>
- xxi. Sura, S. A., Smith, L. L., Ambrose, M. R., Amorim, C. E. G., Beichman, A. C., Gomez, A. C. R., Juhn, M., Kandlikar, G. S., Miller, J. S., Mooney, J., Mummah, R. O., Lohmueller, K. E., & Lloyd-Smith, J. O. (2019). Ten simple rules for giving an effective academic job talk. *PLOS Computational Biology*, 15(7), e1007163. <https://doi.org/10.1371/journal.pcbi.1007163>
- xxii. Van Doremalen, N., Bushmaker, T., Morris, D. H., Holbrook, M. G., Gamble, A., Williamson, B. N., Tamin, A., Harcourt, J. L., Thornburg, N. J., Gerber, S. I., & others. (2020). Aerosol and surface stability of SARS-CoV-2 as compared with SARS-CoV-1. *New England Journal of Medicine*, 382(16), 1564–1567.
- xxiii. Vega Thurber, R., Mydlarz, L. D., Brandt, M., Harvell, D., Weil, E., Raymundo, L., Willis, B. L., Langevin, S., Tracy, A. M., Littman, R., Kemp, K. M., Dawkins, P., Prager, K. C., Garren, M., & Lamb, J. (2020). Deciphering Coral Disease Dynamics: Integrating Host, Microbiome, and the Changing Environment. In *Frontiers in Ecology and Evolution* (Vol. 8). <https://www.frontiersin.org/article/10.3389/fevo.2020.575927>
- xxiv. Vespignani, A., Tian, H., Dye, C., Lloyd-Smith, J. O., Eggo, R. M., Shrestha, M., Scarpino, S. V., Gutierrez, B., Kraemer, M. U., Wu, J., & others. (2020). Modelling covid-19. *Nature Reviews Physics*.

- xxv. Whitmer, E. R., Borremans, B., Duignan, P. J., Johnson, S. P., Lloyd-Smith, J. O., McClain, A. M., Field, C. L., & Prager, K. C. (2021). Classification and Regression Tree Analysis For Predicting Prognosis In Wildlife Rehabilitation: A Case Study Of Leptospirosis In California Sea Lions (*Zalophus Californianus*). *Journal of Zoo and Wildlife Medicine*, 52(1), 38–48. <https://doi.org/10.1638/2020-0111>
- xxvi. Zhang, T., Dai, L., Barton, J. P., Du, Y., Tan, Y., Pang, W., Chakraborty, A. K., Lloyd-Smith, J. O., & Sun, R. (2020). Predominance of positive epistasis among drug resistance-associated mutations in HIV-1 protease. *PLOS Genetics*, 16(10), e1009009. <https://doi.org/10.1371/journal.pgen.1009009>
- b. Conference or symposium abstracts
- i. Borremans, B., Pepin, K., Prager, K. C., Greig, D., Gomez, A. C., Melin, S. R., Laake, J. L., Lowry, M., DeLong, R. L., Grenfell, B., Gulland, F. M., & Lloyd-Smith, J. O. (2019). Environment and immunity drive disease outbreaks in California sea lions (*Zalophus californianus*). *Ecology and Evolution of Infectious Diseases*, Princeton, NJ.
  - ii. Guglielmino, A., Mummah, R. O., Borremans, B., Galloway, R. L., Hornsby, R. L., Alt, D. P., Coonan, T. J., Prager, K. C., & Lloyd-Smith, J. O. (2019). Leptospirosis in the Channel Island Fox: A Long-Term Study to Assess the Origin, Spread and Impact of *Leptospira interrogans* serovar Pomona in an Endangered Island Fox Population. *Wildlife Disease Association Annual Conference*, Lake Tahoe, CA.
  - iii. Guglielmino, A., Prager, K. C., Alt, D. P., Borremans, B., Buhnerkempe, M. G., Coonan, T., Galloway, R. L., Greig, D. J., Gomez, A. C. R., Harris, J. D., Helman, S. K., Laake, J. L., Melin, S. R., Mummah, R., Orr, A. J., Wu, Q., DeLong, R. L., Gulland, F. M. D., & Lloyd-Smith, J. O. (2018). Leptospirosis in the California coastal ecosystem. Department of Defense (DoD) Strategic Environmental Research and Development Program (SERDP) and Environmental Security Technology Certification Program (ESTCP) Symposium. Department of Defense (DoD) Strategic Environmental Research and Development Program (SERDP) and Environmental Security Technology Certification Program (ESTCP) Symposium, Washington DC.
  - iv. Mummah, R. O., Guglielmino, A., Borremans, B., Alt, D. P., Galloway, R. L., Hornsby, R. L., Lefler, J., Matthias, M. A., Zuerner, R. L., Prager, K. C., & Lloyd-Smith, J. O. (2019). Investigating cross-species transmission of *Leptospira interrogans* in coastal California mammals using genome

- sequence analysis. 11th Meeting of the International Leptospirosis Society, Vancouver, Canada.
- v. Mummah, R. O., Guglielmino, A., Borremans, B., Alt, D. P., Prager, K. C., & Lloyd-Smith, J. O. (2018a). Comparative genomics of *Leptospira interrogans* in coastal California mammals. 16th Annual Ecology and Evolution of Infectious Diseases, Glasgow, UK.
  - vi. Mummah, R. O., Guglielmino, A., Borremans, B., Alt, D. P., Prager, K. C., & Lloyd-Smith, J. O. (2018b). Comparative genomics of *Leptospira interrogans* in coastal California mammals. Gordon Research Seminar on Biology of Spirochetes, Ventura, CA.
  - vii. Mummah, R. O., Guglielmino, A., Borremans, B., Galloway, R., Prager, K. C., & Lloyd-Smith, J. O. (2019). Reconstructing the origins of a leptospirosis outbreak in Channel Island Foxes. Ecology and Evolution of Infectious Diseases, Princeton, NJ.
  - viii. Prager, K. C. (2019a). Infectious Disease in Wildlife. Invited Talk - Western University College of Veterinary Medicine.
  - ix. Prager, K. C. (2019b). *Leptospira* ecology in mammals of the California coastal ecosystem. Invited Talk - The Keck Science Department of Claremont Colleges.
  - x. Prager, K. C. (2021a). *Leptospira* in California sea lions fade-out (and re-emergence) of an endemically circulating pathogen. Invited Talk - NOAA Alaska Fisheries Science Center, Marine Mammal Laboratory.
  - xi. Prager, K. C. (2021b). Leptospirosis in the California Ecosystem. Invited Talk - Western University College of Veterinary Medicine Zoo and Wildlife Symposium.
  - xii. Prager, K. C., Borremans, B., Alt, D. P., Buhnerkempe, M. G., DeLong, R. L., Duignan, P. J., Field, C., Galloway, R. L., Gomez, A. C. R., Greig, D. J., Harris, J. D., Helman, S., Hornsby, R. L., Johnson, S., Melin, S. R., Mummah, R., Orr, A. J., Wu, Q., Gulland, F. M. D., & Lloyd-Smith, J. O. (2019). Fade-out and re-emergence of *Leptospira interrogans* serovar Pomona in a wildlife reservoir host – California sea lion (*Zalophus californianus*). 11th Meeting of the International Leptospirosis Society. 11th Meeting of the International Leptospirosis Society, Vancouver, Canada.
  - xiii. Prager, K. C., Borremans, B., Alt, D. P., Buhnerkempe, M. G., DeLong, R. L., Duignan, P. J., Hornsby, R. L., Johnson, S., Melin, S. R., Mummah, R., Orr, A. J., Wu, Q., Gulland, F. M. D., & Lloyd-Smith, J. O. (2019). Fade-Out and Re-Emergence of *Leptospira interrogans* serovar Pomona in a Wildlife Reservoir Host – California sea lions (*Zalophus californianus*). Ecology and Evolution of Infectious Diseases.

- xiv. Prager, K. C., Borremans, B., Buhnerkempe, M. G., Fontaine, C., Galloway, R. L., Gomez, A. C. R., Harris, J., Helman, S. K., Melin, S. R., Mummah, R., Orr, A., Greig, D. J., Wu, Q., Gulland, F. M. D., & Lloyd-Smith, J. O. (2018). Fade-Out of an Endemic Pathogen in a Wildlife Host: Did Environmental Stress Cause Apparent Disappearance of *Leptospira* from the California Sea Lion Population (*Zalophus californianus*)? International Association for Aquatic Animal Medicine. International Association for Aquatic Animal Medicine, San Diego, CA.
- xv. Prager, K. C., Borremans, B., Galloway, R. L., Helman, S. K., Orr, A. J., Greig, D. J., Wu, Q., Gulland, F. M. D., & Lloyd-Smith, J. O. (2018). Fade-Out of an Endemic Pathogen in a Wildlife Host: Did Environmental Stress Cause *Leptospira* to Disappear from the California Sea Lion (*Zalophus californianus*) Population? Wildlife Disease Association. Wildlife Disease Association, Saint Augustine, Florida.
- xvi. Prager, K. C., Borremans, B., Gomez, A. C. R., Buhnerkempe, M. G., Fontaine, C., Galloway, R. L., Harris, J., Helman, S. K., Melin, S. R., Mummah, R., Orr, A. J., Greig, D. J., Wu, Q., Gulland, F. M. D., & Lloyd-Smith, J. O. (2018). Fade-Out of an Endemic Pathogen in a Wildlife Host: Did Environmental Stress Cause *Leptospira* to Disappear from the California Sea Lion (*Zalophus californianus*) Population? Ecology and Evolution of Infectious Disease. Ecology and Evolution of Infectious Disease, University of Glasgow, Scotland.
- xvii. Prager, K. C., Guglielmino, A., Mummah, R., Borremans, B., Alt, D. P., Buhnerkempe, M. G., Coonan, T., Galloway, R. L., Greig, D. J., Gomez, A. C. R., Harris, J. D., Helman, S. K., Laake, J. L., Melin, S. R., Orr, A. J., Suchard, M., Wu, Q., DeLong, R. L., Gulland, F. M. D., & Lloyd-Smith, J. O. (2019). Leptospirosis in the California coastal ecosystem. Department of Defense (DoD) Strategic Environmental Research and Development Program (SERDP) and Environmental Security Technology Certification Program (ESTCP) Symposium. Department of Defense (DoD) Strategic Environmental Research and Development Program (SERDP) and Environmental Security Technology Certification Program (ESTCP) Symposium, Washington DC.
- xviii. Prager, K. C., Guglielmino, A., Mummah, R., Borremans, B., Alt, D. P., Buhnerkempe, M. G., Coonan, T., Renee L. Galloway, Greig, D. J., Gomez, A. C. R., Harris, J. D., Helman, S. K., Laake, J. L., Melin, S. R., Orr, A. J., Suchard, M., Wu, Q., DeLong, R. L., Gulland, F. M. D., & Lloyd-Smith, J. O. (2020). Leptospirosis in Endangered Island Foxes and California Sea Lions: Outbreak Prediction and Prevention in a Changing World. SERDP ESTCP Symposium 2020.

- xix. Prager, K. C., Neely, B., Fontaine, C., Gulland, F. M. D., & Janech, M. (2019). Proteomic Analysis of Urine from California Sea Lions (*Zalophus californianus*) With and Without Leptospirosis. Wildlife Disease Association. Wildlife Disease Association, Tahoe, California.
- xx. Prager, K. C., Neely, B., Fontaine, C., Lloyd-Smith, J. O., & Janech, M. (2018). Proteomic Analysis of Urine from California Sea Lions (*Zalophus californianus*) with and without Leptospirosis. International Association for Aquatic Animal Medicine. International Association for Aquatic Animal Medicine, San Diego, CA.

## Appendix C. Other Supporting Material

### *Supplementary information for 5.2.3.1. and 6.2.3.1.*

#### *Environment and body condition*

Here we present statistical analyses for the effects of comorbidities (i.e. having been diagnosed with pneumonia, domoic acid toxicity, or malnutrition) on the correlation between BMI and spring transition. Sea lions diagnosed with pneumonia stranded during years with a significantly later spring transition ( $0.12 \pm 0.02$  vs  $0.02 \pm 0.01$ , F-value = 15.6, df = 8759, P-value < 0.0001). There was no significant effect of pneumonia diagnosis on the correlation between spring transition and BMI, except for yearlings, where the negative correlation was only statistically significant for those diagnosed with pneumonia (effect est. =  $-0.63 \pm 0.17$ , F-value = 13.5, df = 819, P-value = 0.0003). Sea lions diagnosed with domoic acid stranded during years with a significantly earlier spring transition ( $-0.41 \pm 0.02$  vs  $0.11 \pm 0.01$ , F-value = 296, df = 8759, P-value < 0.0001). For yearlings and juveniles not diagnosed with domoic acid toxicity, but not for other age classes or for yearlings/juveniles diagnosed with domoic acid toxicity, there was a significant negative correlation between BMI and spring transition (yearlings: effect est. =  $-0.30 \pm 0.09$ , F-value = 10.5, df = 3589, P-value = 0.001; juveniles: effect est. =  $-0.72 \pm 0.14$ , F-value = 28.1, df = 1469, P-value < 0.0001). Sea lions diagnosed with malnutrition stranded during years with a significantly earlier spring transition ( $-0.35 \pm 0.02$  vs  $0.19 \pm 0.01$ , F-value = 533, df = 8759, P-value < 0.0001). There was a significant effect of malnutrition diagnosis on the correlation between spring transition and BMI, where the correlation was less strong for sea lions not diagnosed with malnutrition (Pups malnutrition: no significant correlation; Pups non-malnutrition: effect est. =  $-2.7 \pm 0.6$ , F-value = 20.1, df = 87, P-value < 0.0001; Yearlings malnutrition: effect est. =  $-0.3 \pm 0.1$ , F-value = 10.0, df = 1513, P-value = 0.002; Yearlings non-malnutrition: effect est. =  $-1.3 \pm 0.1$ , F-value = 85.3, df = 2165, P-value < 0.0001; Juveniles malnutrition: no significant correlation. Juveniles non-malnutrition: effect est. =  $-1.0 \pm 0.1$ , F-value = 50.1, df = 1399, P-value < 0.0001; Subadults malnutrition: effect est. =  $-1.7 \pm 0.7$ , F-value = 6.7, df = 134, P-value = 0.01; Subadults non-malnutrition: effect est. =  $-0.9 \pm 0.2$ , F-value = 20.3, df = 1181, P-value < 0.0001; Adults malnutrition: effect est. =  $-2.4 \pm 1.0$ , F-value = 6.3, df = 124, P-value = 0.01; Adults non-malnutrition: no significant correlation). Taken together, these results indicate that the effects of comorbidities are inconsistent and only seen for some age classes.

#### *Environment and sea lion movement*

Variation in sea lion movement patterns was another important potential mechanism linking environment and *Leptospira* transmission. As *Leptospira interrogans* serovar Pomona is not expected to survive long in salt water (Trueba et al., 2004), successful transmission requires close contacts between sea lions, which means that mixing patterns are likely to be crucial. Unfortunately, while there is some qualitative information on how and when different demographic groups move, there are no data available that can be used to parameterize even rudimentary movement models needed to test hypotheses on how environment affects population mixing. Answering these questions properly would require a thorough study of sea lion movement patterns in relation to life history and environment, which is outside the scope of this article. However, as a first attempt at gaining more insight into the relationship between environment and movement, we analyzed TMMC strand counts over time as a rough proxy for how many sea lions of different age and sex classes were in the central sea lion range at a given

time (35°59'N, 121°30'W to 37°42'N, 123°05'W), and test the correlation between this proxy and environmental variables SST and upwelling. Only strand counts in the northern half of the TMMC range (north of Monterey, 36.6N) were chosen in order to maximize the signal contained in movement in the central sea lion range, as we expect that there will be less variation in movement in the southern range due to the obligatory link of pups and lactating females to the rookeries in the Channel Islands (Melin et al., 2000)

The number of stranded sea lions in the northern half of the TMMC range was counted for young sea lions (male and female yearlings, male juveniles, female subadults), male adults, and female adults, as these three demographic groups are known to exhibit highly different movement patterns throughout the year (Gearin et al., 2017; Melin et al., 2000; Peterson & Bartholomew, 1967). Importantly, in order to produce a measure of sea lion location and not just a measure of how many stranded in a given year, all strand counts were normalized by the respective estimated population sizes for each group. A downside of using stranding data as a proxy for the movement patterns of the wild population is that each cause of stranding can affect age/sex classes differently, resulting in biased estimates of sea lions present in the TMMC range. In an attempt to avoid this bias, the causes that are known to be strongly age/sex were filtered out of the dataset prior to movement analyses. These causes are leptospirosis, domoic acid toxicity, cancer, and malnutrition (Greig et al., 2005). Despite this filtering however it is likely that there are still unknown biases influencing strand counts, and we must stress that the use of stranding data within the TMMC range only is a far from ideal way to characterize movement and mixing throughout the sea lion range. Nevertheless, we believe it is worth investigating these data in case a strong pattern emerges that can be used as a basis for future research.

Annual strand counts are calculated for three periods corresponding with candidate environmental variables: (1) June through October, (2) June and July, (3) August through October. Correlations between the top selected environmental variables (Table 6.2.3.3) and the strand counts corresponding with the time in the year (June-October for Spring Transition, June-July for SST, August-October for SST and Upwelling) are tested using ANOVA of the fitted linear regression with strand counts as outcome variable and environmental variable as independent variable.

There is a significant positive correlation between number of strands and SST for young animals and for male adults (Table A.3). There are no significant correlations for any of the other environmental variables (Table A.3). Increased strands at high SST in the center of the sea lion range may indicate farther foraging due to bad conditions (Feldkamp et al., 1991; Melin et al., 2008), or perhaps earlier migration northward for male adults. While the absence of a similar significant effect for female adults may be due to the fact there really is none, it may also be due to the fact that a large proportion of female adults are constrained to feeding areas near the rookeries in the south of the range (Melin et al., 2000). The consequence of farther movement and earlier migration would be that in bad years with high SST there would be less mixing, resulting in lower transmission rates in the period leading up to the outbreak season, and smaller outbreaks.

Age & Sex Class	Environmental variable	Effect estimate	Effect est. standard error	F value	P value
Yearling + Male Juvenile + Female Subadult	South ST	0.30	0.18	2.60	0.12
	Central SST Jun-Jul	0.63	0.24	7.10	0.01
	South Upw Aug-Oct	-0.08	0.38	0.05	0.83
Female Adult	South ST	0.06	0.21	0.08	0.78
	Central SST Jun-Jul	0.34	0.30	1.29	0.28
	South Upw Aug-Oct	0.23	0.54	0.18	0.68
Male Adult	South ST	0.01	0.20	0.00	0.97
	Central SST Jun-Jul	0.77	0.23	10.70	0.01
	South Upw Aug-Oct	0.38	0.43	0.79	0.38

**Table A.3. ANOVA statistics for the linear regression of environmental variables vs. number of strands (normalized by dividing by population size of the corresponding demographic groups) in the TMMC range.**

*Supplementary information for 5.3.1 and 6.3.1*

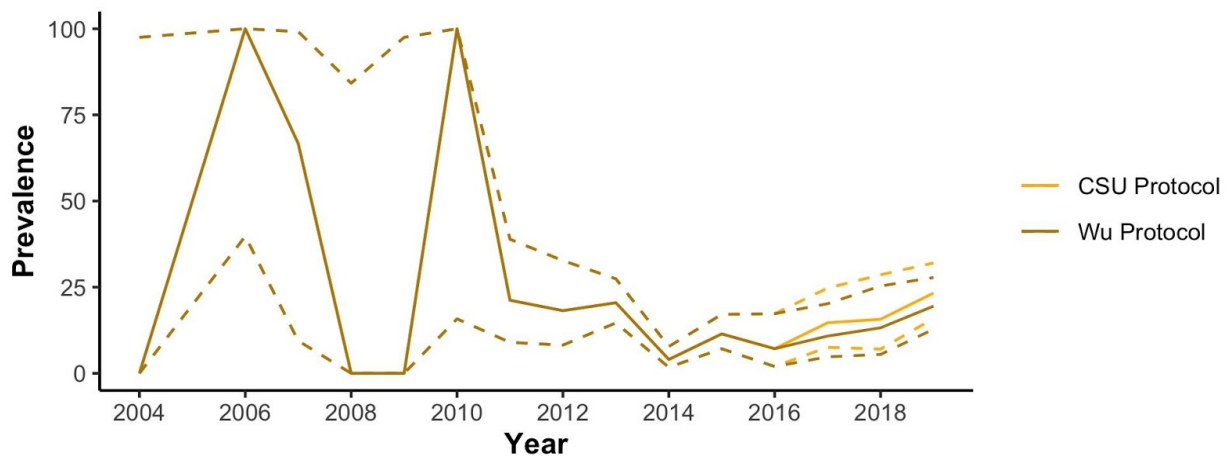


**Figure A.1. Island fox infection prevalence on SRI, 2010-2019, comparing the two PCR protocols.** The Wu protocol for PCR (solid yellow) was used throughout the study, and the more sensitive CSU protocol (solid gold) was added beginning in 2016. 95% confidence intervals are shown with dashed lines.

Fox Year	All		Adult		Pup	
	POS/N (SP)	95% CI	POS/N (SP)	95% CI	POS/N (SP)	95% CI
2004	0/1 (0)	0-98%	0/1 (1)	0-98%	NA	NA
2005	NA	NA	NA	NA	NA	NA
2006	4/4 (1)	40-100%	4/4 (1)	40-100%	NA	NA
2007	2/3 (0.67)	9-99%	1/2 (0.5)	1-99%	1/1 (1)	3-100%
2008	0/2 (0)	0-84%	0/2 (0)	0-84%	NA	NA
2009	0/1 (0)	0-98%	0/1 (0)	0-98%	NA	NA
2010	2/2 (1)	16-100%	2/2 (1)	16-100%	NA	NA
2011	7/33 (0.21)	9-39%	7/29 (0.24)	10-44%	0/4 (0)	0-60%
2012	8/44 (0.18)	8-33%	7/38 (0.18)	8-34%	1/6 (0.17)	0-64%
2013	34/166 (0.2)	15-27%	32/144 (0.22)	16-30%	2/22 (0.09)	1-29%
2014	8/199 (0.04)	2-8%	7/176 (0.04)	2-8%	1/23 (0.04)	0-22%
2015	20/175 (0.11)	7-17%	17/141 (0.12)	7-19%	3/34 (0.09)	2-24%
2016	4/56 (0.07)	2-17%	3/47 (0.06)	1-18%	1/9 (0.11)	0-48%
2017	11/75 (0.15)	5-20%	10/67 (0.15)	4-21%	1/8 (0.13)	0-53%
2018	8/51 (0.16)	5-25%	8/44 (0.18)	7-30%	0/7 (0)	0-34%
2019	27/116 (0.23)	13-28%	25/107 (0.23)	12-28%	2/9 (0.22)	3-60%

**Table A.4. Prevalence of infection with *Leptospira* in SRI island foxes over time, showing results from the CSU protocol.** Positive results (POS), sample size (N), infection prevalence and 95% confidence intervals (CI) for all foxes, adult foxes, and pups, based on positive PCR or IHC results per fox year. Numbers shown in grey were obtained using the Wu protocol, and are identical to numbers in Table 6.3.1.2. Numbers shown in black were obtained using the CSU protocol, and differ from Table 6.3.1.2. One sample per individual fox was used per fox year. If a fox had both positive and negative samples within a fox year, it was treated as positive for this calculation. Culture results were not included, as no fox tested positive for culture without also testing positive via PCR.

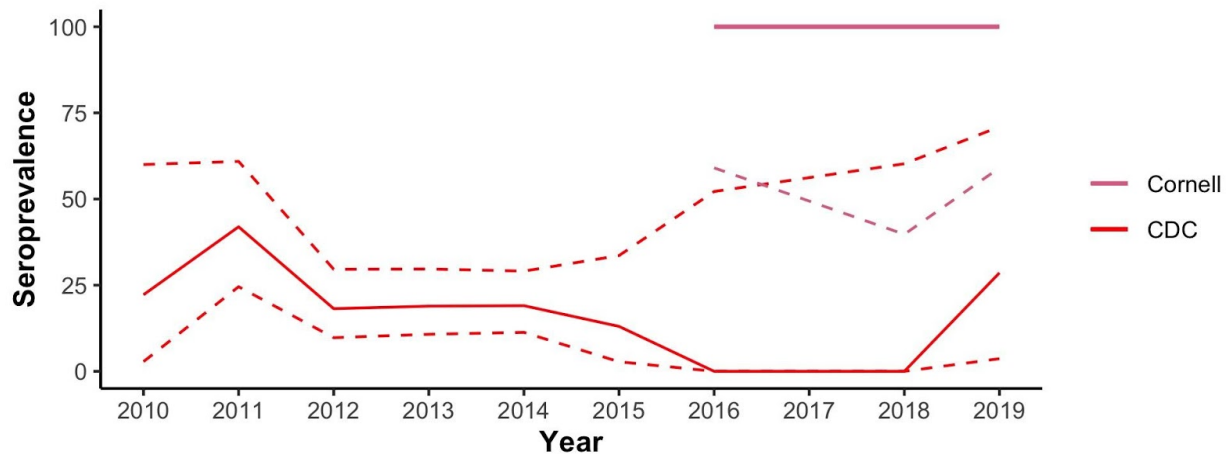


**Figure A.2. Skunk prevalence and seroprevalence over time, showing lab differences.** Longitudinal skunk seroprevalence (solid red) from MAT results tested at CDC throughout the study, and skunk seroprevalence for 2016-2019 based on results from AHDC (solid pink). 95% confidence intervals are shown with dashed lines.

Fox Year	CDC		ADHC	
	POS/N (SP)	95% CI	POS/N (SP)	95% CI
2010	2/9 (0.22)	3-60%	NA	NA
2011	13/31 (0.42)	25-61%	NA	NA
2012	12/66 (0.18)	10-30%	NA	NA
2013	14/74 (0.19)	11-30%	NA	NA
2014	17/84 (0.2)	12-30%	NA	NA
2015	3/23 (0.13)	3-34%	NA	NA
2016	0/5 (0)	0-52%	7/7 (1)	59-100%
2017	NA	NA	NA	NA
2018	0/4 (0)	0-60%	4/4 (1)	40-100%
2019	2/7 (0.29)	4-71%	7/7 (1)	59-100%

**Table A.5. Seroprevalence of anti-*Leptospira* antibodies in island spotted skunks, comparing results from CDC and ADHC.** Positive results (POS), sample size (N), infection prevalence and 95% confidence intervals (CI) intervals for skunks, using MAT results per fox year. One sample per individual skunk was used per fox year. If a skunk had both positive and negative samples within a fox year, it was treated as positive for this calculation.

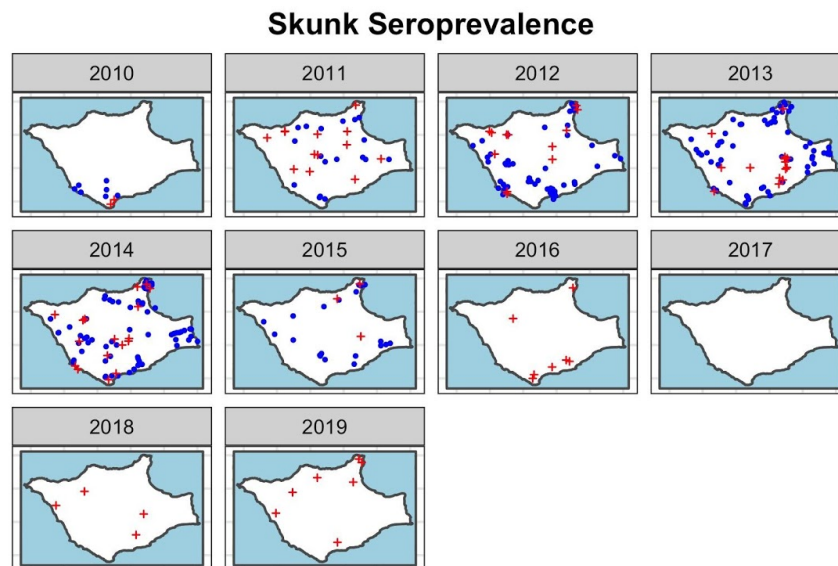


**Figure A.3. Spatiotemporal patterns of seroprevalence in island spotted skunks (CDC results 2010-2015, ADHC results 2016-2019).** Spatial distribution of MAT positive (red pluses) and negative samples (blue circles) in island spotted skunks for each year. This figure is the analogue of Figure 6.3.1.7, except the ADHC results are shown from 2016-2019 in place of CDC results.

### Supplementary information for 5.3.2.2 and 6.3.2.2

#### Prior distribution of peak antibody level

A subset of recently negative individuals was used to provide information about what the possible distribution of peak antibody levels could be. Antibody levels were assumed to have peaked during the interval between the last negative timepoint preceding the first positive one. Here, a negative timepoint could be either a negative sample or an animal's birth date. After data exploration, a subset of individuals was selected for which the maximum time between the last negative and first positive timepoints was 250 days. This resulted in a dataset of 54 individuals. Although a period of 250 days is still a relatively long interval, selecting a smaller interval would have resulted in a much smaller dataset due to the seasonality of sampling. In order to take this into account we used a prior distribution with a slightly larger mean than the distribution fitted to the observed data, but with a broader standard deviation. This resulted in a prior distribution that is weakly informative, thus allowing a large influence of the data on the posterior likelihood. Figure S1 shows the distribution of observed antibody levels and the fitted normal distributions. The distribution was fitted using the function `fitdistr` of R package MASS (Venables & Ripley, 2002). Using simulated data, we found that the effect of the prior distribution specifications was not large, and that the mean peak antibody level could be estimated well (Figure A.4 and Table A.6).

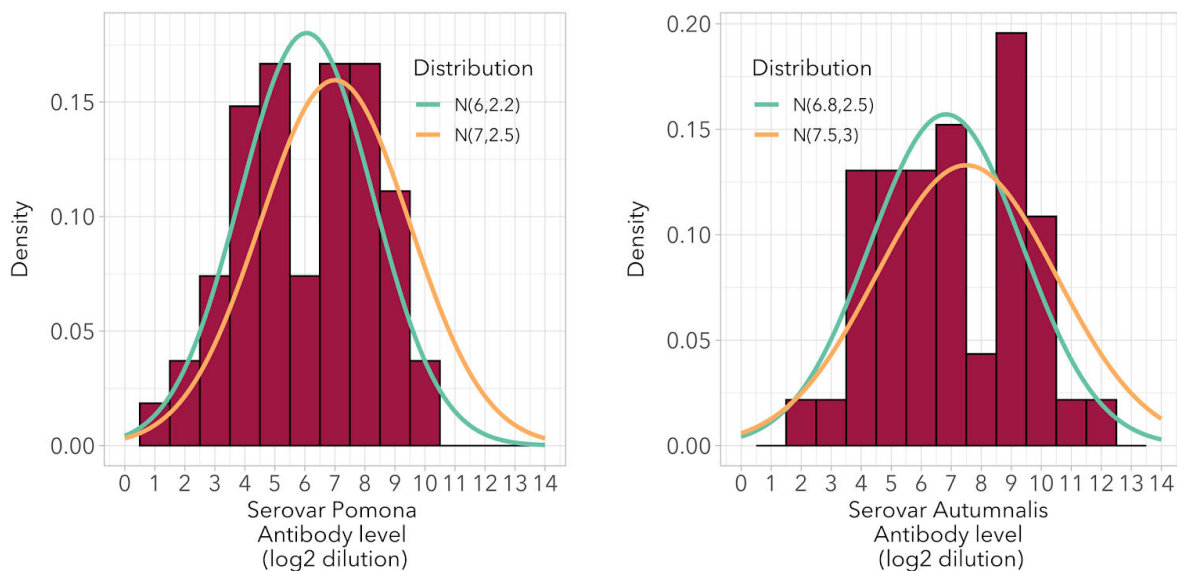


**Figure A.4. Antibody levels for a subset of individual foxes that tested negative relatively recently.** (Left: serovar Pomona, right: serovar Autumnalis). Fitted distributions are shown in teal, and distributions used as priors are shown in orange.

Parameter	Prior distribution
$\beta_{0,Pomona}$ , $\beta_{0,Autumnalis}$	$p(\log(\beta_0)) \sim N(\beta_0^h, \Sigma_{\beta_0}^h)$ , multivariate normal distribution with mean vector $\beta_0^h = [7 \ 7.5]$ and covariance matrix $\sigma_{\beta_0}^h = [2 \ 0 \ 0 \ 2]$ .
$\sigma_{\beta_{0,Pomona}}$ , $\sigma_{\beta_{0,Autumnalis}}$	$p(\sigma_{\beta_0}) \sim Wishart(V, df)$ , Wishart distribution with scale matrix $V = [2.5 \ 0 \ 0 \ 3]$ and degrees of freedom $df = 2$ .
$\lambda_0$	$p(\lambda_0) \sim Gamma(1, 20)$ , Gamma distribution with the same parameters for serovars Pomona and Autumnalis.
$\sigma_{\lambda_0}$	$p(\sigma_{\lambda_0}) \sim Gamma(2, 3)$ , Gamma distribution with the same parameters for serovars Pomona and Autumnalis.
$r_0$	$p(r_0) \sim N(\log(0.5), 0.1)$ , Normal distribution with the same parameters for serovars Pomona and Autumnalis.
$v_0$	$p(v_0) \sim N(\log(0.0005), 1)$ , Normal distribution with the same parameters for serovars Pomona and Autumnalis.

**Table A.6. Hyperpriors for the different parameters.**

### *Simulations and sensitivity analysis*

The model fitting approach was tested using simulated data for 75 individuals, using the double exponential function (see 5.3.2.2). For each individual a peak antibody level representing serovar Pomona was randomly generated from a certain normal distribution that depended on the simulated scenario (see section 1 below). A second peak antibody level representing serovar Autumnalis was generated from a different distribution of which the mean was  $0.84 \log_2$  units higher, and with an additional standard deviation of 0.5 to add realistic variation. Next, a decay rate was randomly generated from a certain distribution (see section 2 below), where the mean of the distribution for serovar Autumnalis was 20% higher than that for serovar Pomona. Using those parameters, between two and five samples (the number was randomly chosen with equal probability) were generated for each individual at random times after the peak antibody time, with a maximum time of 2000 days. A negative sample preceding the first positive sample was also generated to inform the maximum peak antibody interval size, where the time was randomly generated up to a maximum of 500 days prior to the peak antibody time. Last, noise was randomly added to the data where each sample had a probability of 5% to decrease by one  $\log_2$  unit, 90% to remain the same, and 5% to increase by one  $\log_2$  unit. This represents variation resulting from the microscopic agglutination assay in two-fold dilution units. Each individual's peak time sample was removed from the dataset prior to model fitting, to represent reality.

Simulations were done for two scenarios:

1. **Effect of peak antibody level prior specification.** In order to test the effect of the

specifications of the prior distribution of peak antibody level on the posterior estimate, we fitted the same simulated data using different prior specifications of peak antibody. Peak antibody levels (serovar Pomona) were generated from normal distribution  $N(7,1)$ , and decay rates from  $N(0.0008, 0.0002)$ . Model parameters were fit for six prior distributions of peak antibody level, to assess the effect of the mean and the standard deviation on the posterior estimates:  $N(6,1)$ ,  $N(8,1)$ ,  $N(10,1)$ ,  $N(8,2)$ ,  $N(8,3)$ ,  $N(8,4)$ . For all prior distributions the posterior estimates accurately estimated mean peak antibody level at the population level (Figure A.5). Individual-level estimates of peak antibody time were good overall (Figure A.6, Figure A.7), but when the “real” (i.e. simulated) peak antibody level was at the extremes of the population-level distribution the estimates became less accurate.

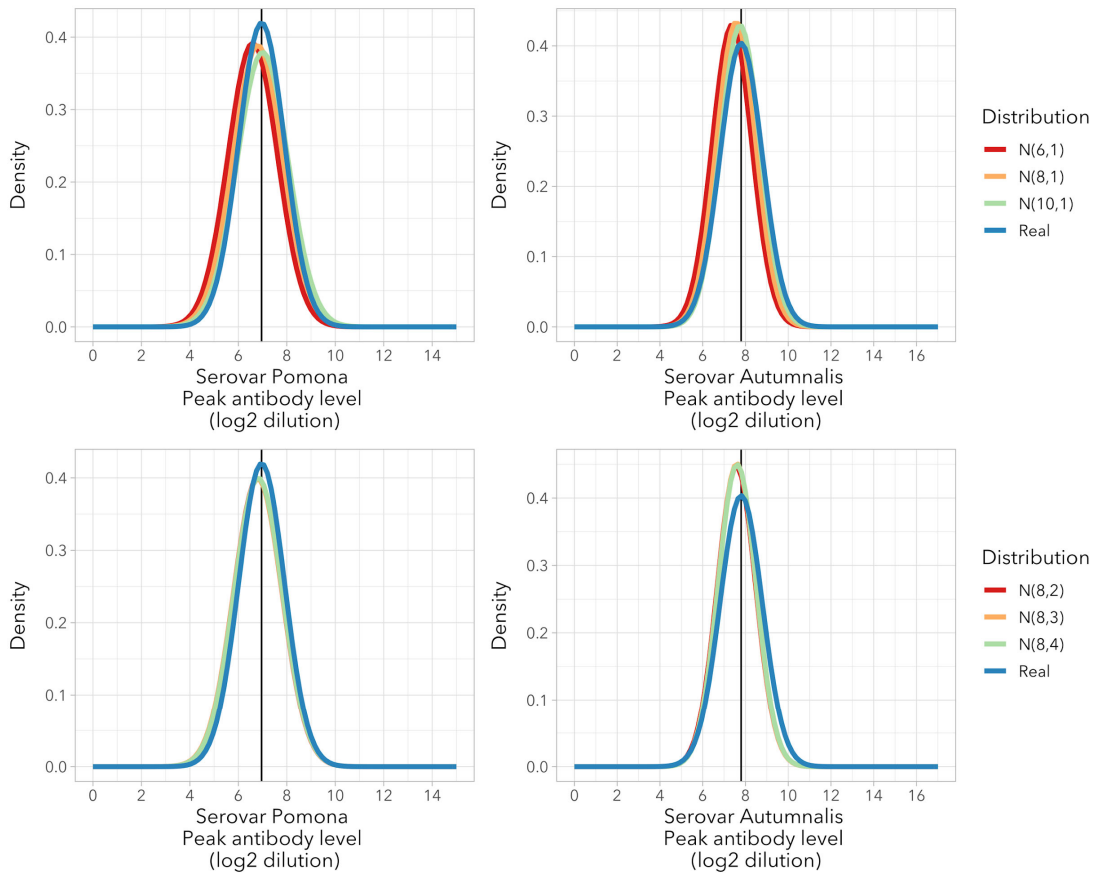


**Figure A.5. Posterior estimates of peak antibody level for different prior distributions.** Real = generated distributions with means 7 (SD 1) and 7.8 (SD 1) for serovars Pomona and Autumnalis, respectively.

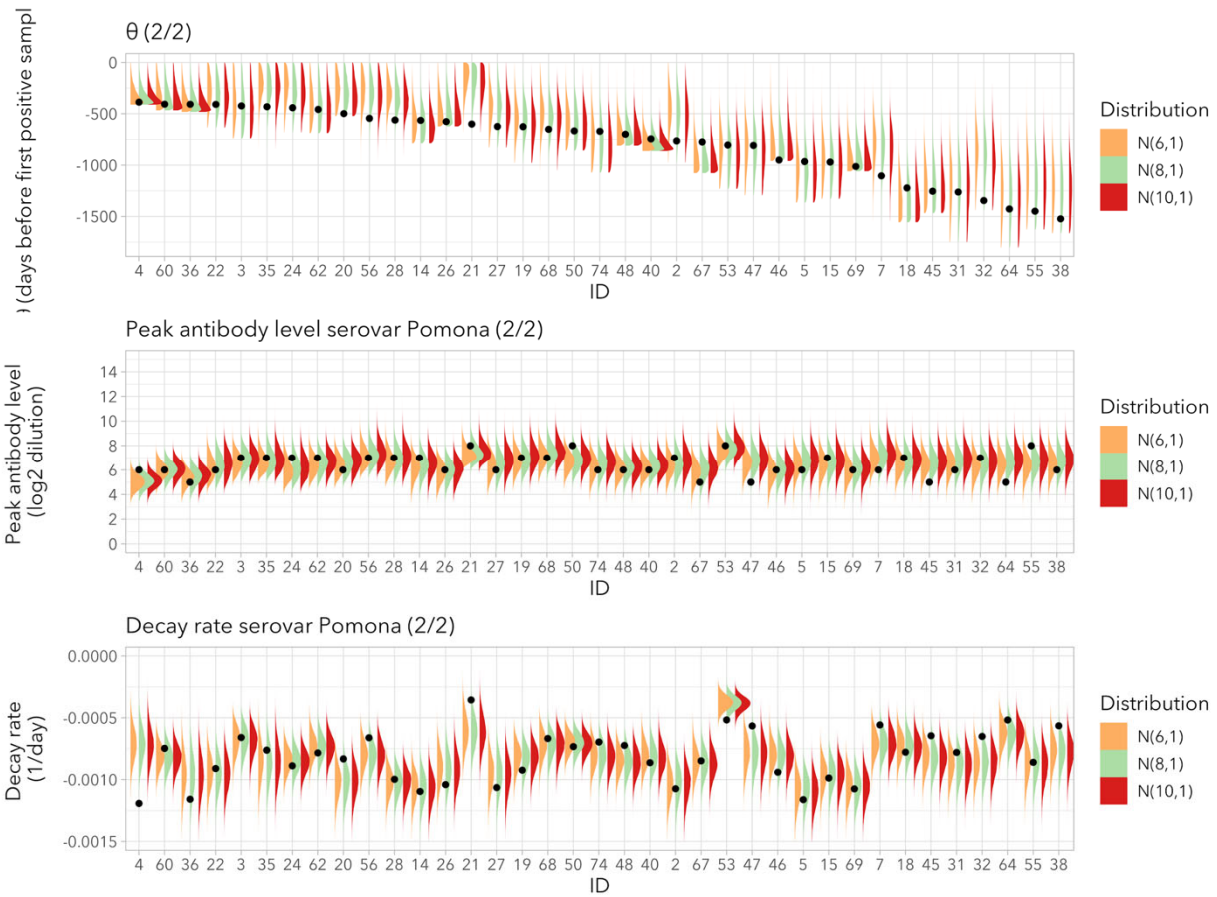


**Figure A.6. Effect of prior peak antibody level means.** Posterior densities of peak antibody time, peak antibody level, and decay rate for the first half of the 75 simulated individuals. Dots indicate the “real” simulated value, distributions are posterior densities flipped vertically

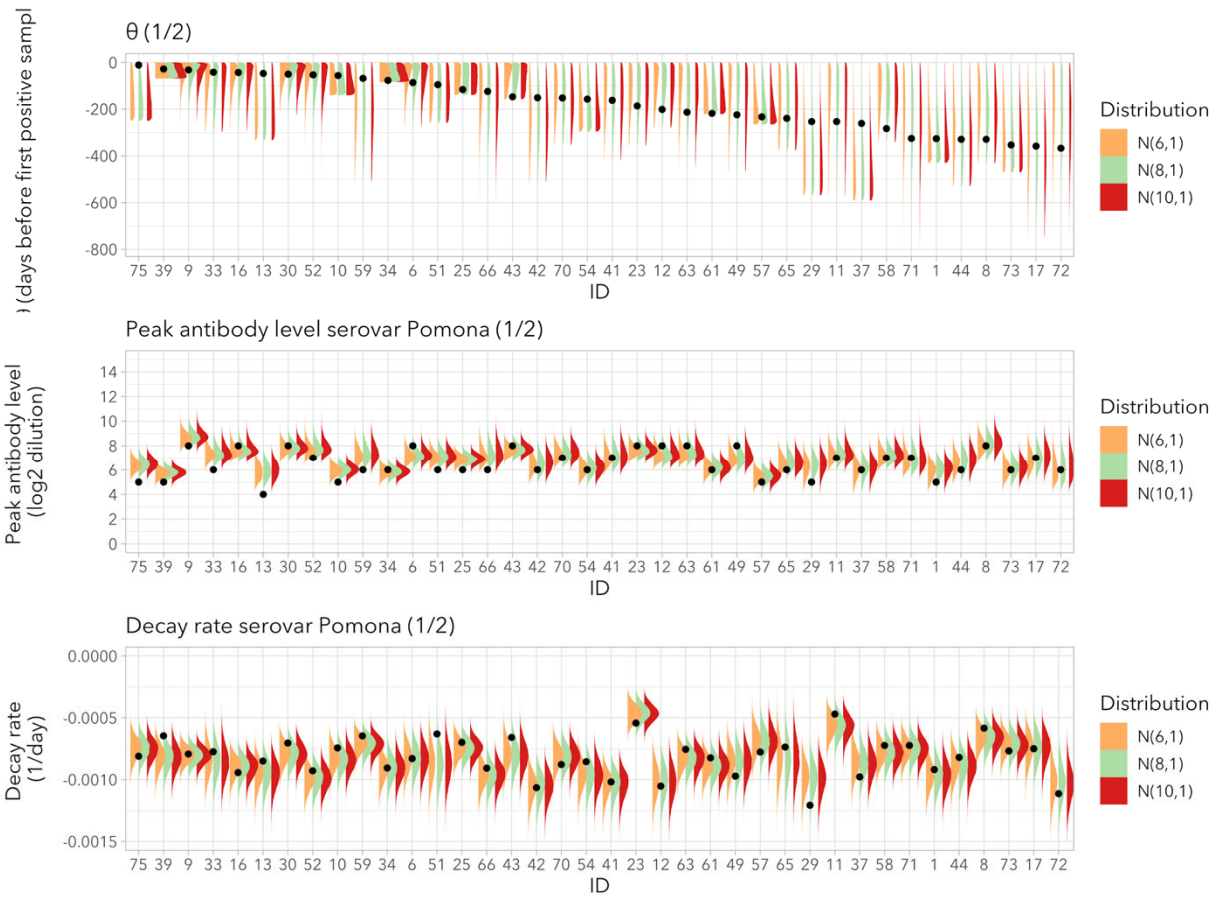


**Figure A.7. Effect of prior peak antibody level standard deviations.** Posterior densities of peak antibody time, peak antibody level, and decay rate for the first half of the 75 simulated individuals. Dots indicate the “real” simulated value, distributions are posterior densities flipped vertically.

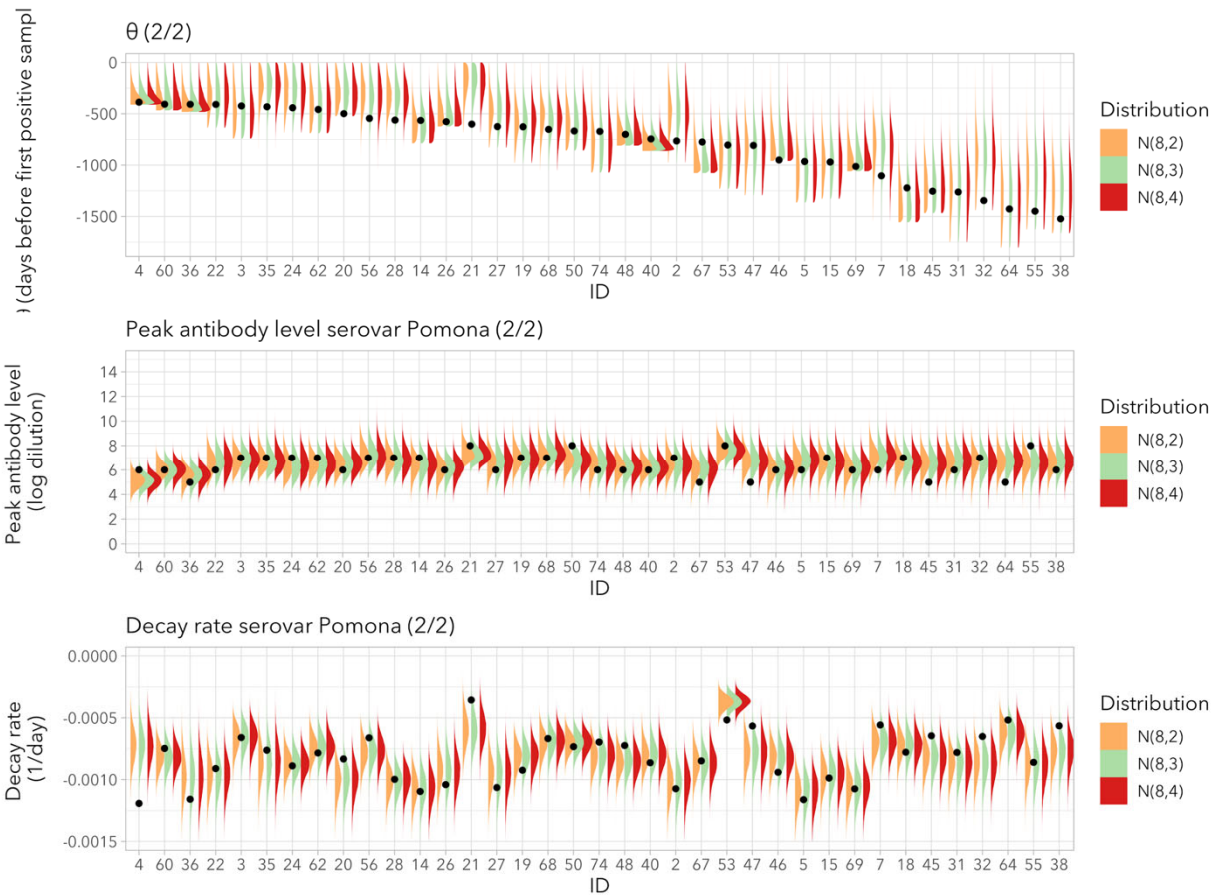


**Figure A.8. Effect of prior peak antibody level standard deviations.** Posterior densities of peak antibody time, peak antibody level, and decay rate for the second half of the 75 simulated individuals. Dots indicate the “real” simulated value, distributions are posterior densities flipped vertically.

- Effect of the magnitude of peak antibody level and decay rate.** Mean peak antibody level as well as decay rate are expected to have a strong effect on how well the models will be able to estimate peak antibody time. In order to quantify this, we fitted models to a series of datasets simulated using a range of peak antibody levels and decay rates. The effect of the different function shapes was then quantified as the mean reduction in the peak antibody interval time. Peak antibody levels (serovar Pomona) were generated from distributions with mean 7 and standard deviations 0.5, 1, 2 and 3. Decay rates (serovar Pomona) were generated from normal distributions with means 0.005, 0.001, 0.0005, 0.0001 and standard deviation 0.0002. Figure A.9 shows antibody decay for the different decay rates. Model parameters were fit for each combination of peak antibody level and decay rate distributions. Model performance was clearly dependent on the characteristics of antibody decay, where smaller variation in peak antibody level and/or faster decay resulted in more accurate estimates of peak antibody time, and larger gains of the posterior distribution of peak antibody times relative to the prior uniform interval (Table A.7).

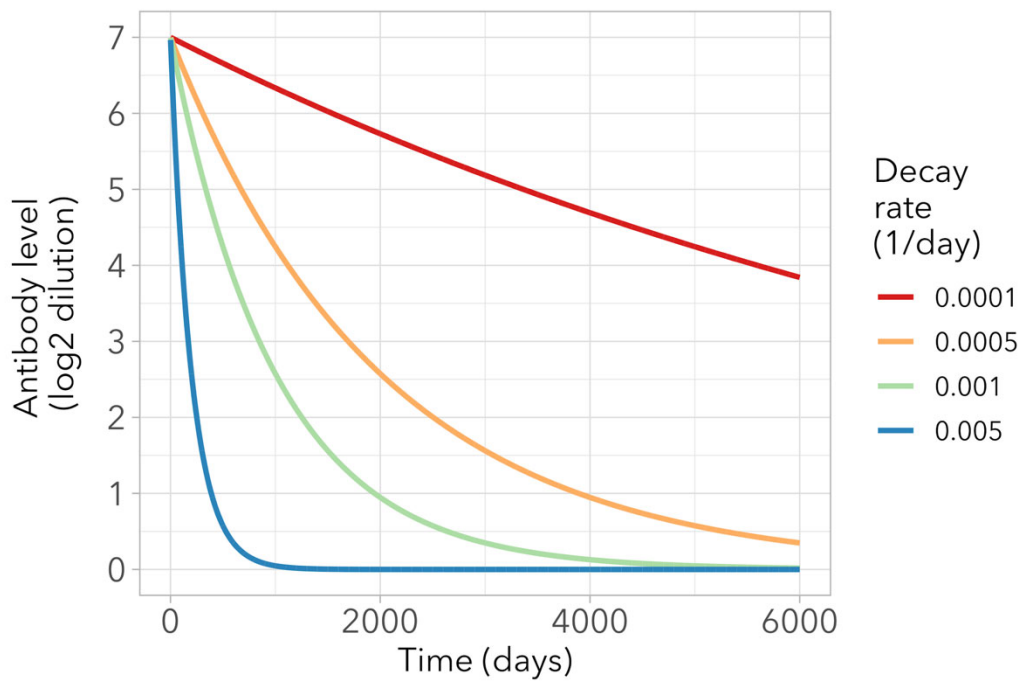


**Figure A.9. Antibody decay curves for different decay rates.**

Last, in order to quantify the effect of decay rate on how well the method can be expected to estimate peak antibody time, we calculated the time needed to decay from antibody level 8 to 6 log<sub>2</sub> dilution units for a range of decay rates (Figure A.10). A larger time window will result in a less precise estimate of peak antibody time, and Figure A.10 clearly illustrates that decay rate will be a major determinant of how well a time-of-infection estimation method can be expected to perform.

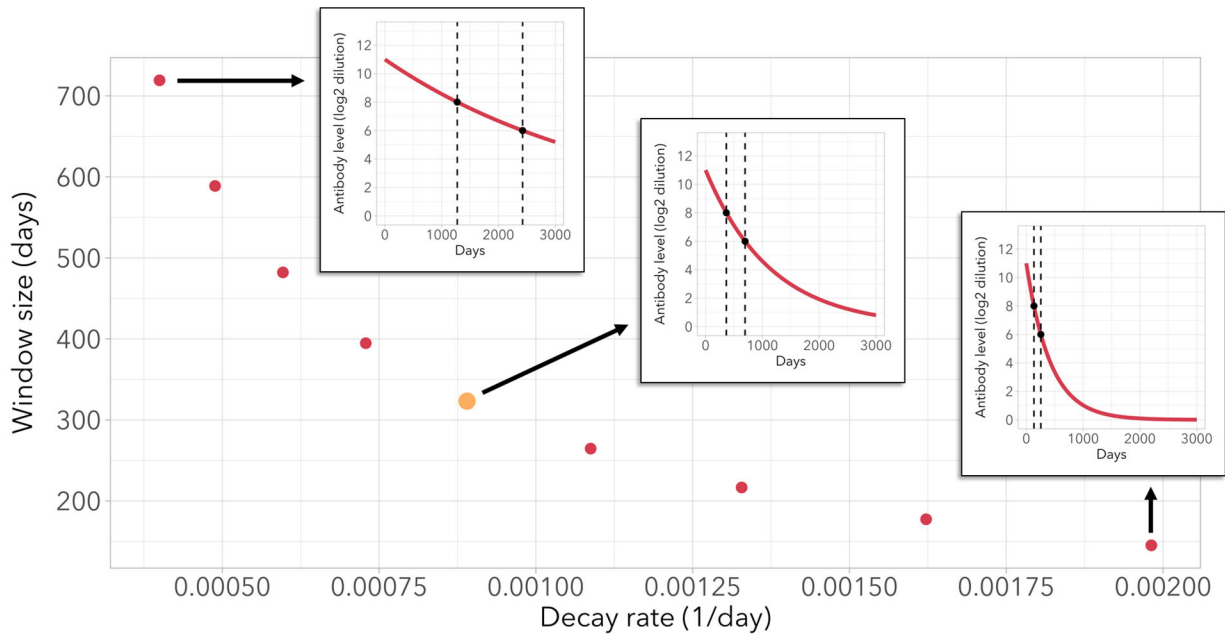


**Figure A.10.** The number of days (window size) it takes for antibodies to decay from 8 to 6  $\log_2$  dilution units, for a range of biologically realistic decay rates. The yellow dot marks a decay rate close to the one estimated for serovar Pomona. Inset figures show the decay function for selected decay rates, with the window between antibody levels 8 and 6 indicated with dotted lines.

Peak antibody interval reduction (%)					Relative entropy (bits)				
Peak Ab SD ( $\log_2$ units)	Decay rate ( $\log_2$ units/day)				Peak Ab SD ( $\log_2$ units)	Decay rate ( $\log_2$ units/day)			
	0.005	0.001	0.0005	0.0001		0.005	0.001	0.0005	0.0001
<b>0.5</b>	49	52	39	10	<b>0.5</b>	1.04	1.07	0.71	0.11
<b>1.0</b>	48	40	27	8	<b>1.0</b>	1.01	0.75	0.44	0.07
<b>2.0</b>	41	30	17	7	<b>2.0</b>	0.75	0.51	0.23	0.05
<b>3.0</b>	37	21	13	6	<b>3.0</b>	0.66	0.33	0.17	0.04

**Table A.7. Model performance on individual seroconversion time ( $\theta_i$ ).** Gained information on seroconversion time relative to the prior knowledge, a uniform interval bound by the last negative and first positive samples. Left: the percentage by which the seroconversion interval size was reduced, where the 95% CrI of the posterior distribution was taken as the new interval. Right: the information gained by the posterior distribution, expressed as relative entropy, where a higher value indicates a larger information gain expressed in ‘bits’ units.

### *Correlations between peak antibody level and covariates*

We tested whether observed peak antibody level correlated with certain variables, as such a correlation could be integrated into a model of peak antibody time and improve the posterior estimate. Peak antibody level was approximated by the level of the first positive sample for the subset of 54 individuals that had been infected recently (see 5.3.2.1). Variables tested were: sex,

body weight, a body condition score, age class, reproductive status, birth year and sample collection month. Correlations were tested for each variable using a linear model with normal error distribution, using  $\log_2$  antibody level as outcome variable. The linear models were fitted using rjags (Plummer 2019), with uninformative normal prior  $N(0,100)$  for the effect estimates.

There were no variables for which the 95% credible intervals did not include 0.

The same analysis was performed using peak antibody levels estimates from the models instead of observed values for recently negative individuals. Similarly, no significant effects were observed.

### *Peak antibody levels of serovars Pomona and Autumnalis*

Because a preliminary analysis of the antibody levels for serovars Pomona and Autumnalis suggested a linear correlation, we explicitly incorporated this into the Bayesian model to test whether this was indeed the case. This was done using a multivariate normal distribution for the peak antibody levels of both serovars. The model indeed found a strong correlation between the two (Figure A.11). where peak antibody levels for serovar Pomona are on average 0.67  $\log_2$  units lower than those for serovar Autumnalis, with a slope of 0.99 (95% CrI 0.90 to 1.14) and an  $R^2$  value of 0.99 (95% CrI 0.94 to 1.00).

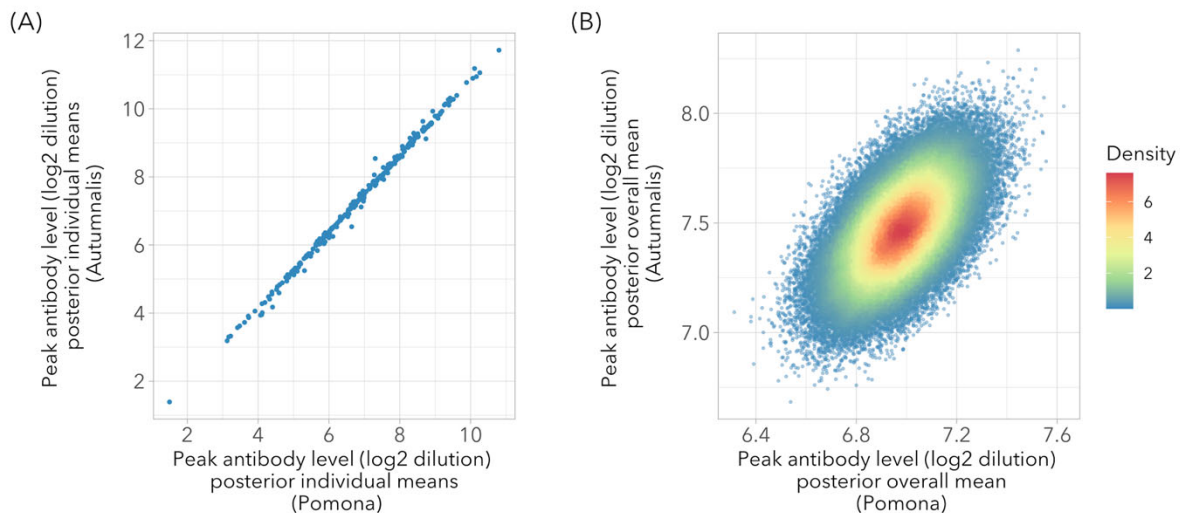


**Figure A.11. Correlation between peak antibody levels for serovars Pomona and Autumnalis.** (A) Posterior means of each individual. (B) Posterior MCMC samples of the overall means of peak antibody level for the last 20,000 iterations

### *Predictors of model performance*

We tested whether any variables correlated with an individual's reduction in the peak antibody interval size. Candidate variables were prior peak antibody interval size, number of samples, time range covered by the samples, estimated peak antibody level and estimated decay rate for serovar Pomona. Correlations were tested using linear models with a log-transformed interval reduction outcome variable. Results are shown in Table A.8, Table A.9, and Figure A.4.

Variable	Effect estimate	F value (df)	P value	AIC
Prior peak antibody interval size	0.14	36.9 (305)	< 0.0001	298
Number of samples	-0.04	2.3 (305)	0.13	331
Time range of samples	-0.01	0.2 (305)	0.63	333
Peak antibody level posterior mean	0.08	10.6 (305)	0.001	323
Decay rate posterior mean	0.19	81.4 (305)	< 0.0001	260
Antibody level of the first positive sample	0.05	5.4 (305)	0.02	328

**Table A.8. Statistics for the correlations between outcome variable ‘% peak antibody interval reduction’ and candidate variables.**

Variable	AIC
Peak level + decay rate + interval size	156
Decay rate + interval size	210
Decay rate + peak level	230
Peak level + decay rate + number of samples	231
Decay rate + first positive level	248
Decay rate posterior mean	260
Peak level + interval size	282
Prior peak antibody interval size	298
Peak antibody level posterior mean	323
Peak level + number of samples	323
Antibody level of the first positive sample	328
Number of samples	331
Time range of samples	333

**Table A.9. AIC values for linear regression models including single and multiple variables fitted to outcome variable ‘% peak antibody interval reduction’.**

Sorted by AIC value

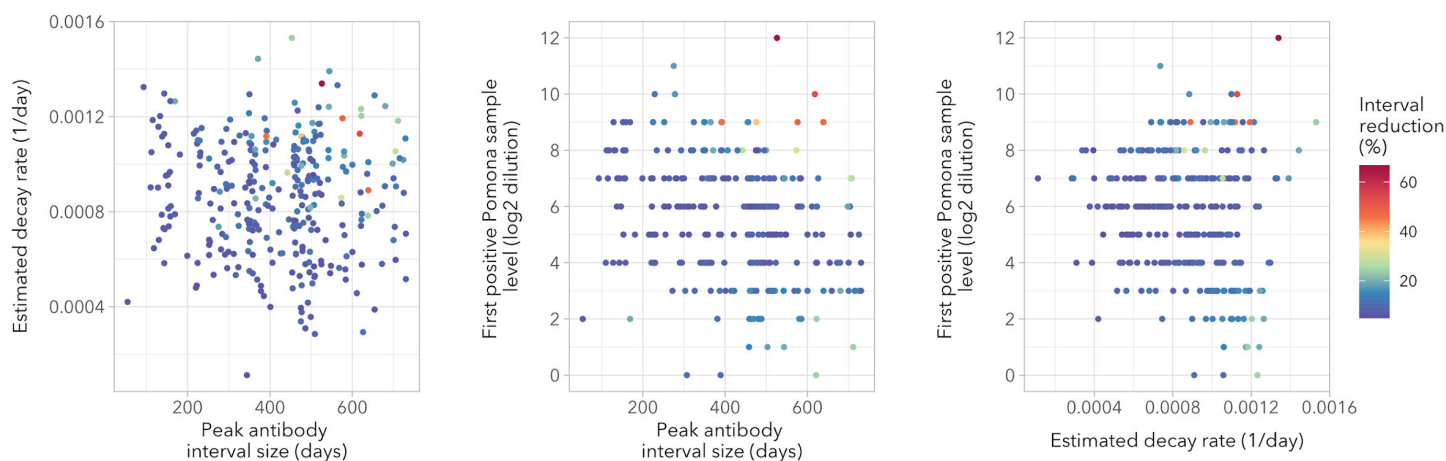


**Figure A.12. Peak antibody interval reduction (heatmap colors) for key correlates decay rate, peak antibody interval size, and level of the first positive sample.**

### JAGS code

JAGS code for the double exponential model.

```
# priors
for(j in 1:length(neg.int)){

  # multivariate distribution for pomona and autumnalis peak antibody levels
  mu_pom_aut[j,1:2] ~ dnorm(mu_pom_aut_mean,mu_pom_aut_precision)

  # extract mean peak levels for pomona and autumnalis
  mu_pomona[j] <- mu_pom_aut[j,1]
  mu_aut[j] <- mu_pom_aut[j,2]

  # decay rates pomona and autumnalis
  decay_pomona[j] ~ dnorm(decay_overall_pomona,decay_tau_overall_pomona)
  decay_aut[j] ~ dnorm(decay_overall_aut,decay_tau_overall_aut)

  # time between peak level and first positive, shared between pomona and autumnalis
  theta[j] ~ dunif(neg.int[j],0)
}

sigma_pomona ~ dunif(0,50)
tau_pomona <- 1/(sigma_pomona*sigma_pomona)

sigma_aut ~ dunif(0,50)
tau_aut <- 1/(sigma_aut*sigma_aut)

lab_effect ~ dnorm(0,0.01)

#hyper priors

# multivariate pomona autumnalis mean and sd
mu_pom_aut_mean ~ dnorm(mu_means,tau_means)
```

```

mu_pom_aut_precision ~ dwish(omega,wishdf)

# extract individual means peak level
mu_overall_pomona <- mu_pom_aut_mean[1]
mu_overall_aut <- mu_pom_aut_mean[2]

# multivariate precision matrix
inverse_mu_pom_aut_precision <- inverse(mu_pom_aut_precision)
sigma_overall_pomona <- inverse_mu_pom_aut_precision[1,1]^(1/2)
sigma_overall_aut <- inverse_mu_pom_aut_precision[2,2]^(1/2)

# decay rates
decay_overall_pomona ~ dgamma(decay.rate.mean.prior.shape.pomona,decay.rate.mean.prior.rate.pomona)
decay_sigma_overall_pomona ~ dgamma(decay.rate.sd.prior.shape.pomona,decay.rate.sd.prior.rate.pomona)
decay_tau_overall_pomona <- 1/(decay_sigma_overall_pomona*decay_sigma_overall_pomona)

decay_overall_aut ~ dgamma(decay.rate.mean.prior.shape.aut,decay.rate.mean.prior.rate.aut)
decay_sigma_overall_aut ~ dgamma(decay.rate.sd.prior.shape.aut,decay.rate.sd.prior.rate.aut)
decay_tau_overall_aut <- 1/(decay_sigma_overall_aut*decay_sigma_overall_aut)

# likelihood
for(i in 1:length(time)){
  # predicted level pomona
  titer_pred_pomona[i] <- lab_effect*lab[i] + mu_pomona[id[i]]*exp(-decay_pomona[id[i]]*(time[i]-
theta[id[i]]))
  true_titer_pomona[i] ~ dnorm(titer_pred_pomona[i],tau_pomona)

  # interval censoring
  titer_pomona[i] ~ dinterval(true_titer_pomona[i], c(1,2,3,4,5,6,7,8,9,10,11,12,13))

  # predicted level autumnalis
  titer_pred_aut[i] <- lab_effect*lab[i] + mu_aut[id[i]]*exp(-decay_aut[id[i]]*(time[i]-theta[id[i]]))
  true_titer_aut[i] ~ dnorm(titer_pred_aut[i],tau_aut)

  # interval censoring
  titer_aut[i] ~ dinterval(true_titer_aut[i], c(1,2,3,4,5,6,7,8,9,10,11,12,13))

  # store sum loglikelihood as parameter for WAIC calculation
  LogLik[i] = log(dnorm(titer_pomona[i], true_titer_pomona[i],tau_pomona)) + log(dnorm(titer_aut[i],
true_titer_aut[i],tau_aut))
}

```

**Supplementary information for 5.3.2.4. and 6.3.2.4**

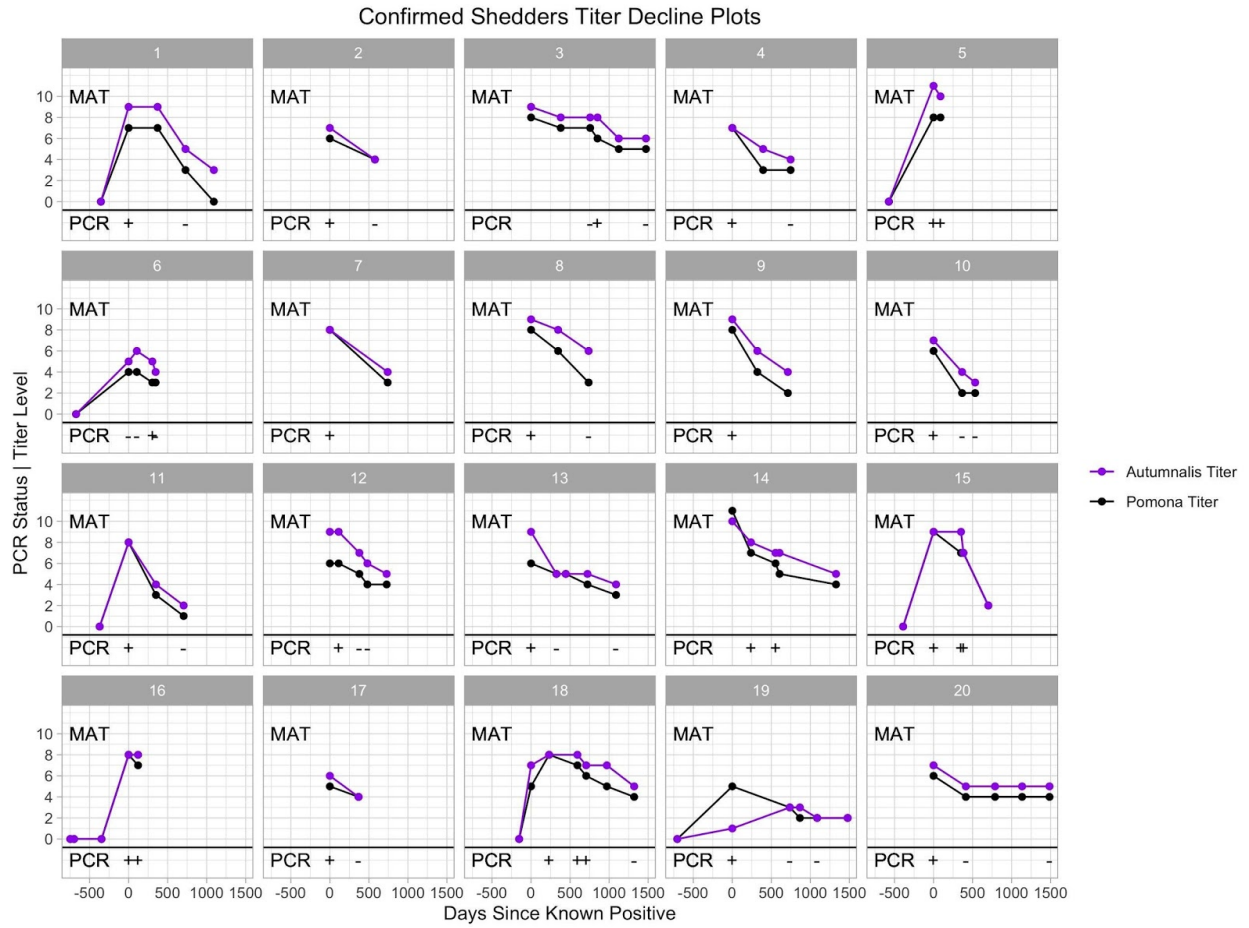


**Figure A.13. Longitudinal antibody titer dynamics in Channel Island foxes.**

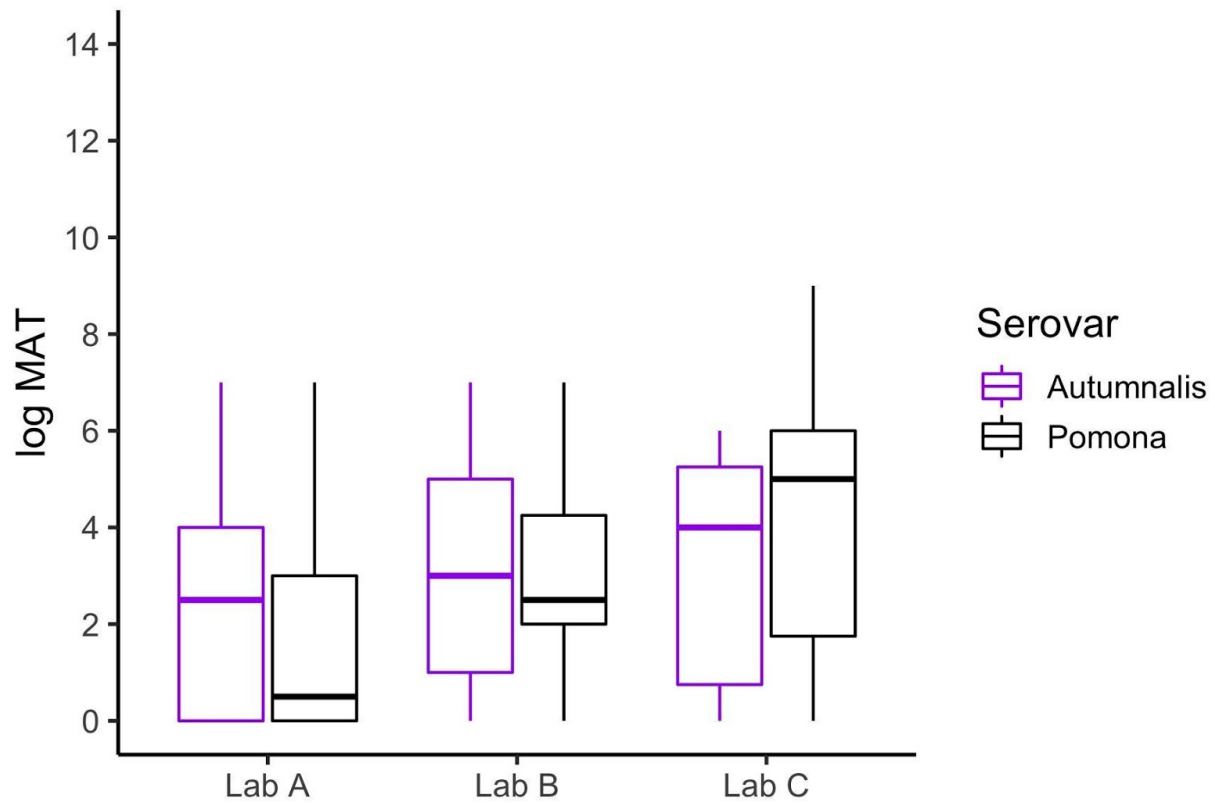


**Figure A.14. Differences in antibody titer magnitude for a subset (n=32) of samples that were run to endpoint for serovars Autumnalis and Pomona at all three labs**

Serovar Pomona titer level at Lab A	0	1:100	1:200	1:400	1:800	1:1600	1:3200	1:6400	1:12800	1:25600	1:51200	0 (but pos against Aut)
# Samples chosen for comparison	10	3	3	3	3	3	3	3	4	2	3	6

**Table A.10. The number of samples chosen per serovar Pomona titer level at Lab A for inter-lab titer comparison.**

*Supplementary information for 5.3.4. and 6.3.4.*

This information can be found at: [https://github.com/bennyborremans/CSL\\_lepto\\_outbreak\\_model](https://github.com/bennyborremans/CSL_lepto_outbreak_model)